Wolfson College
University of Oxford

ROLE OF PPARα IN THE CARDIAC METABOLIC ADAPTATION TO CHRONIC HYPOXIA

Amira Hajirah Abd Jamil

Cardiac Metabolism Research Group
Department of Physiology, Anatomy and Genetics

Submitted for the degree of Doctor of Philosophy
Trinity Term 2012

Supervisors:
Prof. Kieran Clarke
Dr. Mark Cole

ACKNOWLEDGEMENT

I would like to express my deepest gratitude to Professor Kieran Clarke, and Dr Mark Cole for their remarkable supervision, guiding me to completion. For their wealth of knowledge and expertise, immeasurable amount of support and advice, and most importantly, for having faith in me, I am forever grateful.

I owe my sincere thanks to Dr Lisa Heather, who has been an integral part of my DPhil right from the beginning; intellectually, experimentally and socially (poker face!). I'm indebted to Dr Carolyn Carr and Dr Rhys Evans, for their invaluable insights in accomplishing this thesis. Special recognition to Lucy Ambrose, Dr Suat Cheng Tan, and Dr Renata Gomes, for contributing their technical expertise, and to all that have assisted me along the way, including Elizabeth Sutton, Emma Carter, Dr Mary Slingo, Dr Kar Kheng Yeoh and Dr Dunja Aksentijevic.

I would like to extend my appreciation to Yvonne, and all other members of CMRG, Dr Tyler, Dr Cochlin, Mike, Dan, Lydia, Vicki, Arne, Latt and Filipo for all their kind help and advice. CMRG moments are not complete without their daily laughter, smiles and friendship (topped with a lot of cakes!); I thank every one of them for making my 4 years here memorable.

I thank the Malaysian Ministry of Higher Education for funding my DPhil.

My heartfelt thanks go to all my friends, especially Mas, Bab, Anna, Rui and Kim for their devoted friendship throughout this demanding journey. Kudos to my special cheer leaders, my two little brothers and sisters for never failing to make home feel so near. And lastly, to my parents, you are the real strength behind all my work and accomplishments, I dedicate this thesis to you.

ABSTRACT

ROLE OF PPARα IN THE CARDIAC METABOLIC ADAPTATION TO CHRONIC HYPOXIA

Amira Hajirah Abd Jamil

Wolfson College, University of Oxford, Trinity Term 2012

The principal substrate used by the normal adult human heart is free fatty acids, the remainder being, predominantly, carbohydrate. During failure, the heart becomes less reliant on fatty acid metabolism, possibly as a result of tissue hypoxia. Therefore, understanding hypoxic adaptation may explain the metabolic changes that occur during the development of heart failure. As peroxisome proliferator activated receptor alpha (PPARα) modulates cardiac fatty acid metabolism, the work in this thesis focused on the role of PPARα in cardiac metabolic adaptation to chronic hypoxia. It was found that isolated hearts from chronically hypoxic (11% O_2 for 3 weeks) mice were more glycolytic, had reduced PPARα expression and decreased fatty acid metabolism, but had normal function, determined using *in vivo* cine-MRI. ^{31}P MRS of isolated perfused mouse hearts showed a drop in PCr with hypoxia, but ΔG_{ATP} was not altered, indicating that metabolic reprogramming was sufficient to maintain ATP production and contractile function. Increased or decreased PPARα expression, using a high fat diet or PPARα null mice, respectively, prevented metabolic adaptation to hypoxia and caused cardiac dysfunction. Hypoxia with high fat feeding was particularly deleterious, reducing ejection fraction by 9%, possibly due to increased mitochondrial uncoupling. PPARβ/δ and γ were not involved in the adaptation to hypoxia, and none were modified by PPARα stimulation or ablation. Cardiac VEGF and PDK1, prominent hypoxia-inducible factor (HIF) targets, were increased by hypoxia, indicating that HIF may have been involved in metabolic adaption. However, high fat feeding prevented VEGF accumulation during hypoxia, suggesting that impaired HIF signalling may have contributed to the maladaptive response to hypoxia. In order to determine the relationship between HIF and PPARα, HIF was stabilised pharmacologically using FG2216/BIC in HL-1 cardiomyocytes, to show decreased PPARα expression and caused similar metabolic changes to those seen in the *in vivo* hypoxic heart. In conclusion, this study demonstrated that HIF downregulation of PPARα is crucial for metabolic adaptation and maintenance of cardiac function during chronic hypoxia. Similar metabolic changes that occur in end-stage heart failure may also be a response to increasing hypoxia.

TABLE OF CONTENTS

ABREVIATIONS

2-OG	2-oxoglutarate
α-KGDH	alpha-ketoglutarate dehydrogenase
ACC	acetyl-CoA carboxylase
ACS	acyl-CoA synthethase
ADP	adenosine diphosphate
ANOVA	analysis of variance
ATP	adenosine triphosphate
BIC	2-(1-chloro-4-hydroxyisoquinoline-3-carboxamido) acetic acid
BW	body weight
CAT	carnitine acyl-transferase
CI	cardiac index
CO	cardiac output
CPT	carnitine palmitoyltransferase
Cr	creatine
CS	citrate synthase
DMOG	dimethyloxalylglycine
EDV	end-diastolic volume
ESV	end-systolic volume
EPO	erythropoietin
ETC	electron transport chain
FABP	fatty acid binding protein
FAD	flavin adenine dinucleotide
FBS	fetal bovine serum
FFA	free fatty acids

FIH	factor inhibiting HIF
HIF	hypoxia inducible factor
GLUT	glucose transporters
GWW	gram wet weight
KH	Krebs Henseleit
LDH	lactate dehydrogenase
LV	left ventricle
MCD	malonyl-CoA decarboxylase
MCAD	medium chain acyl-CoA dehydrogenase
MTE1	mitochondrial thioesterase 1
NAD	nicotinamide adenine dinucleotide
NEFA	non-esterified free fatty acids
p-VHL	von Hippel Lindau protein
PBS	phosphate buffered saline
PCr	phosphocreatine
PDH	pyruvate dehydrogenase
PDK	pyruvate dehydrogenase kinase
PGC1	peroxisome proliferator-activated receptor gamma coactivator 1
PHD	prolyl-4-hydroxylase
PGK	phosphoglycerate kinase
PPAR	peroxisome proliferator activated receptor
PPRE	peroxisome proliferator response element
qRT-PCR	real-time quantitative reverse transcription polymerase chain reaction
RXR	retinoid X receptor
SIRT	silent mating-type information regulation two

TAC	transverse aortic constriction
TAG	triacylglycerol
TCr	total creatine
UCP	uncoupling protein
VEGF	vascular endothelial growth factor

CHAPTER 1

GENERAL INTRODUCTION

1.1 HEART FAILURE

The heart consumes more energy than any other organ in the body, contracting approximately 100,000 times a day to pump blood to all parts of the body, supplying nutrients and oxygen to the tissues and removing waste products [1]. Heart failure is defined as the inability of the heart to pump sufficient blood to peripheral tissues to meet the energy requirement of the body [2, 3]. It is characterised by reduced cardiac output, ejection fraction, increased pulmonary and systemic venous pressures, pulmonary and peripheral oedema, resulting from severe loss of cardiac contractile function [4] and serves as the final manifestation of many cardiac diseases [5]. Ventricular hypertrophy, increased sympathetic drive and activation of the renin-angiotensin system compensate for the haemodynamic overloading of the heart, but when these compensatory mechanisms are insufficient to meet the metabolic demand of the body, cardiac failure ensues [4, 6].

Despite pharmacological inhibition of the sympathetic nervous system [7-9] and the renin angiotensin system [10, 11] being of significant benefit, the prognosis and quality of life of chronic heart failure patients remain poor. In the UK, heart failure is associated with an annual mortality rate of 10 to 50%, affecting at least one in 100 people [12] and more than 2% of the US population, or almost 5 million people, are affected [13].

Chronic heart failure is multifactorial [14] but evidence suggests that the progression of heart failure is associated with metabolic remodelling [15-18] and altered energetics [19, 20]. For this reason, metabolic interventions may provide an important adjuvant therapy for heart failure. Knowledge of the factors regulating cardiac metabolism in the

healthy heart will aid in the understanding of changes that occur in the failing heart, and the development of new treatments.

1.2 CARDIAC ENERGY METABOLISM

In order to maintain ceaseless contractile activity, the heart requires a constant source of energy, supplied in the form of ATP. Each day, the human heart must synthesise approximately 30 kg of ATP [21, 22] generated almost exclusively via mitochondrial oxidative phosphorylation [23]. The heart is a metabolic omnivore, capable of metabolising various exogenous substrates including fatty acids, glucose, pyruvate and lactate to satisfy its energy demands [24, 25] (Figure 1.1). The fuels are broken down to the 2 carbon compound acetyl-CoA, which feeds into the mitochondrial Krebs cycle, generating $NADH+H^+$ and $FADH_2$. These reducing equivalents donate electrons that are shuttled between complexes I to IV of the respiratory electron transport chain (ETC) in the inner mitochondrial membrane. The electrons are accepted by an oxygen molecule at complex IV of the ETC, producing H_2O as a by-product. Concomitantly, complexes I, III and IV of the ETC use the energy released in this redox reaction to pump protons into the mitochondrial intermembrane space, generating an electrochemical gradient across the inner membrane. This gradient is the driving force for the phosphorylation of ADP to ATP by facilitating the re-entry of protons into the mitochondrial matrix via the by the F_1F_o ATP synthase [23, 26, 27].

Since ATP synthesis and contractile work are tightly coupled to the supply of oxygen and the rate of oxidative phosphorylation, the heart is highly selective in its fuel utilisation. The heart is able to switch its substrate preference, and the relative

contribution of the different substrates for energy production is largely determined by their availability, coronary blood flow, oxygen supply, hormone levels and cardiac workload [28, 29]. Palmitate yields more ATP per carbon atom than glucose, pyruvate or lactate. Glucose, however is a more oxygen efficient fuel source, yielding 11% more ATP per oxygen atom consumed during oxidation than fatty acids. This means that the healthy heart preferentially uses fatty acid as a fuel source yielding 105 ATP molecules per palmitate molecule oxidised, compared with 32 from glucose (Table 1.1) [21].

Table 1.1: Stochiometrically derived ATP yields of different substrates

Substrate	ATP yield per molecule	ATP yield per carbon atom	ATP yield per oxygen atom
Glucose	32	5.2	2.58
Lactate	15	4.9	2.46
Pyruvate	12	4.1	2.50
Palmitate	105	6.7	2.33

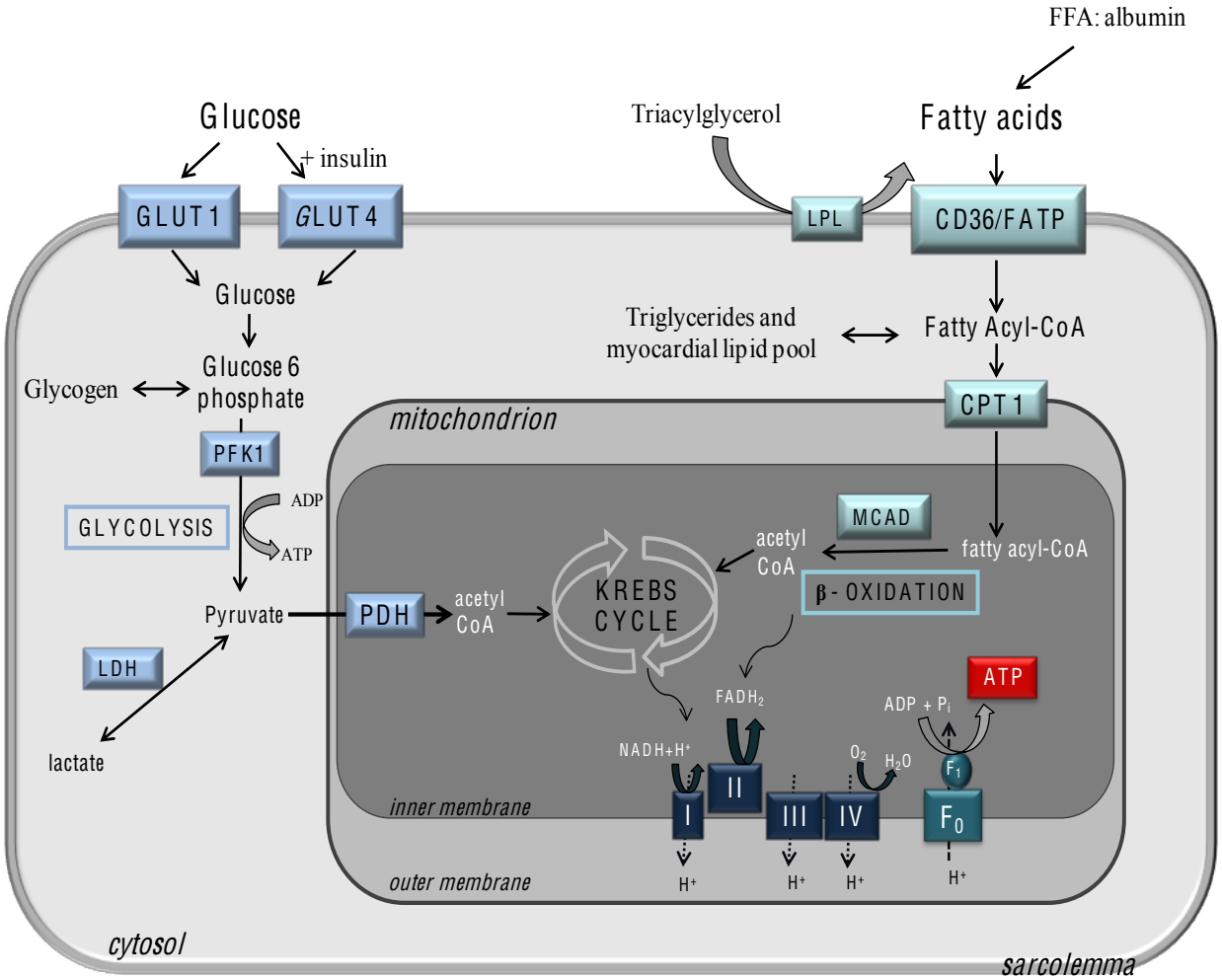

Figure 1.1: Major energy producing pathway and mitochondrial energy metabolism in the heart. The respiratory chain consists of four complexes: I-IV. NADH derived from glycolysis, the Krebs cycle and fatty acid oxidation is oxidised by complex I, and $FADH_2$ is oxidised at complex II. Electrons are transferred through the electron transport chain to the final acceptor O_2. The free energy available from the electron transfer is used to pump out H^+ and generate an electrochemical gradient across the inner mitochondrial membrane. This gradient is the driving force for ATP synthesis by the F_1F_o ATP synthase.

1.2.1 Fatty acid uptake and metabolism

The rate of myocardial fatty acid uptake is primarily determined by circulating levels of free fatty acids, which can range approximately from 0.2 to 0.8 mM in healthy humans over the course of a day [30, 31]. In the healthy heart, long chain fatty acids (LFCA) are the predominant metabolic substrate, accounting for approximately 70-

80% of mitochondrial oxidative phosphorylation [21, 31, 32] LCFA are hydrophobic and insoluble in aqueous environments, so they are transported to the heart bound to albumin as non-esterified fatty acids (NEFAs) or esterified to triacylglycerol and incorporated into lipoproteins, such as chylomicrons [33, 34]. Non-esterified fatty acids, complexed to albumin, are the predominant source of fatty acid used by the heart with endogenous triacylglycerol acting as reserve when circulating levels are low [35, 36].

The uptake of FFAs into myocardial cells can occur passively across cell membranes, but primarily uptake is mediated by transporter mechanisms involving fatty acid translocase (FAT/CD36), plasma membrane fatty acid binding protein (FABPPM) and fatty acid transport proteins (FATP1 and 6). After uptake, cytosolic FFAs are activated by acyl-CoA synthetase (ACS) to form fatty acyl-CoA derivatives [37]. The mitochondrial membrane is impermeable to acyl-CoA molecules, thus long chain fatty acyl moiety is transferred from the cytosol into the matrix by a carnitine-dependent transport system. First, the CoA moiety is removed from the acyl-CoA and replaced by carnitine, catalysed by carnitine palmitoyltransferase-1 (CPT1) in the compartment between the inner and the outer mitochondrial membranes. Next, carnitine acyltranslocase (CAT) transport this long chain acylcarnitine across the inner mitochondrial membrane in exchange for free carnitine. Lastly, CPTII regenerates long-chain acyl-CoA in the mitochondrial matrix. CPTI serves the key regulatory role in controlling the rate of fatty acid metabolism, being inhibited by malonyl-CoA from the carboxylation of acetyl-CoA by acetyl-CoA carboxylase (ACC), thus suppressing β-oxidation when glucose is the principal substrate metabolised [30, 38, 39] (Figure 1.2b).

Following cellular uptake, long-chain acyl-CoAs are oxidised via the β-oxidation pathway, a sequential cycle where, at each turn, acetyl-CoA, $NADH+H^+$ and $FADH_2$ are generated, feeding into the Krebs cycle and the respiratory chain [30]. Transcriptional and translational mechanisms influence the concentration of β-oxidation enzymes, such as medium-chain acyl-CoA dehydrogenase (MCAD), thereby regulating the rate of fatty acid metabolism [40].

1.2.2 Glucose uptake and metabolism

In the healthy heart, 20-30% of energy produced is derived from the oxidation of glucose. Glucose metabolism can be separated into 2 processes –cytosolic glycolysis and mitochondrial glucose oxidation, which are partitioned according to the heart's energy demand. During normal oxidative metabolism, glycolytically produced pyruvate is decarboxylated to acetyl-CoA within the mitochondria prior to entry into the Krebs cycle for glucose oxidation.

The sarcolemma is relatively impermeable to glucose, the uptake of glucose from the circulation is facilitated by glucose transporters GLUT1 and GLUT4 [41]. GLUT1 is responsible for basal glucose uptake and constitutively present in the sarcolemma [42], whereas GLUT4 cycles between the sarcolemma and intracellular vesicles in response to insulin, exercise and hypoxia, and is the predominant regulator of glucose uptake [43].

When glucose is taken up in cardiomyocytes, it is phosphorylated by the enzyme hexokinase to glucose-6-phosphate, which cannot be exported from the myocytes and therefore is either directed to glycogen synthesis, pentose phosphate shunt or to

glycolysis. Glycolysis is the conversion of glucose-6-phosphate to pyruvate via a series of enzyme-controlled stages. Phosphofructokinase-1 (PFK-1) is a key regulatory enzyme in the glycolytic pathway, allosterically regulated by the cellular energy status and metabolite concentrations [21, 27, 32]. The end product of glycolysis, pyruvate, can either enter the mitochondria for oxidation or be reduced to lactate in the cytosol. Glycolysis is the conversion of cytosolic glucose to pyruvate, which is converted to acetyl-CoA within the mitochondria prior to entry into the Krebs cycle for glucose oxidation. Under aerobic conditions, pyruvate is converted to acetyl-CoA within the mitochondria prior to entry into the Krebs cycle for glucose oxidation. Mitochondrial pyruvate dehydrogenase (PDH) catalyses the oxidative decarboxylation of pyruvate, and is the key regulated enzyme complex in glucose metabolism [32]. When fatty acids are the predominant fuels being utilised, PDH is phosphorylated and inhibited by pyruvate dehydrogenase kinase (PDK) enzymes 1–4, as they are activated by the NADH and acetyl-CoA being generated when the energy status of the cardiomyocyte is high. In contrast, PDH is dephosphorylated and activated by pyruvate dehydrogenase phosphatase (PDP), which is activated by insulin and calcium [44, 45] (Figure 1.2a).

a)

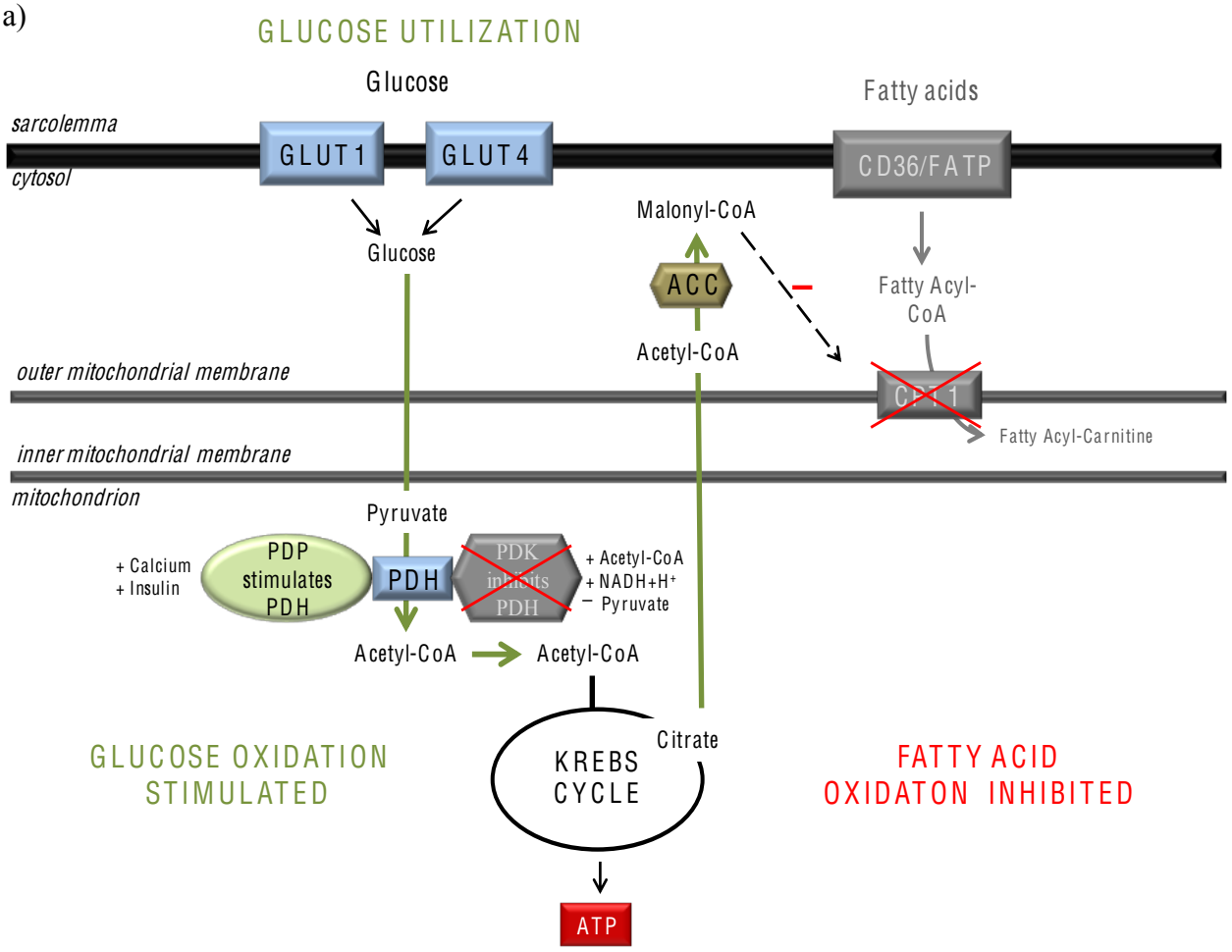

Figure 1.2a: The key role of pyruvate dehydrogenase (PDH) in regulating the balance between glucose and fatty acid metabolism in the heart. Glucose utilisation predominates: Glucose is converted to pyruvate, which inhibits pyruvate dehydrogenase kinase (PDK). In addition, insulin stimulates pyruvate dehydrogenase phosphatase (PDP). The overall effect on PDH is a dephosphorylation and activation, converting pyruvate to acetyl-CoA, which can enter the Krebs cycle for oxidation. Because of isocitrate dehydrogenase inhibition, mitochondrial citrate accumulates and is exported across the inner and outer mitochondrial membrane to the cytosol, where it is cleaved to form cytosolic acetyl-CoA. This is used by acetyl-CoA carboxylase (ACC) to synthesise malonyl-CoA, a strong inhibitor of CPT1, resulting in inhibition of mitochondrial fatty acid uptake and oxidation

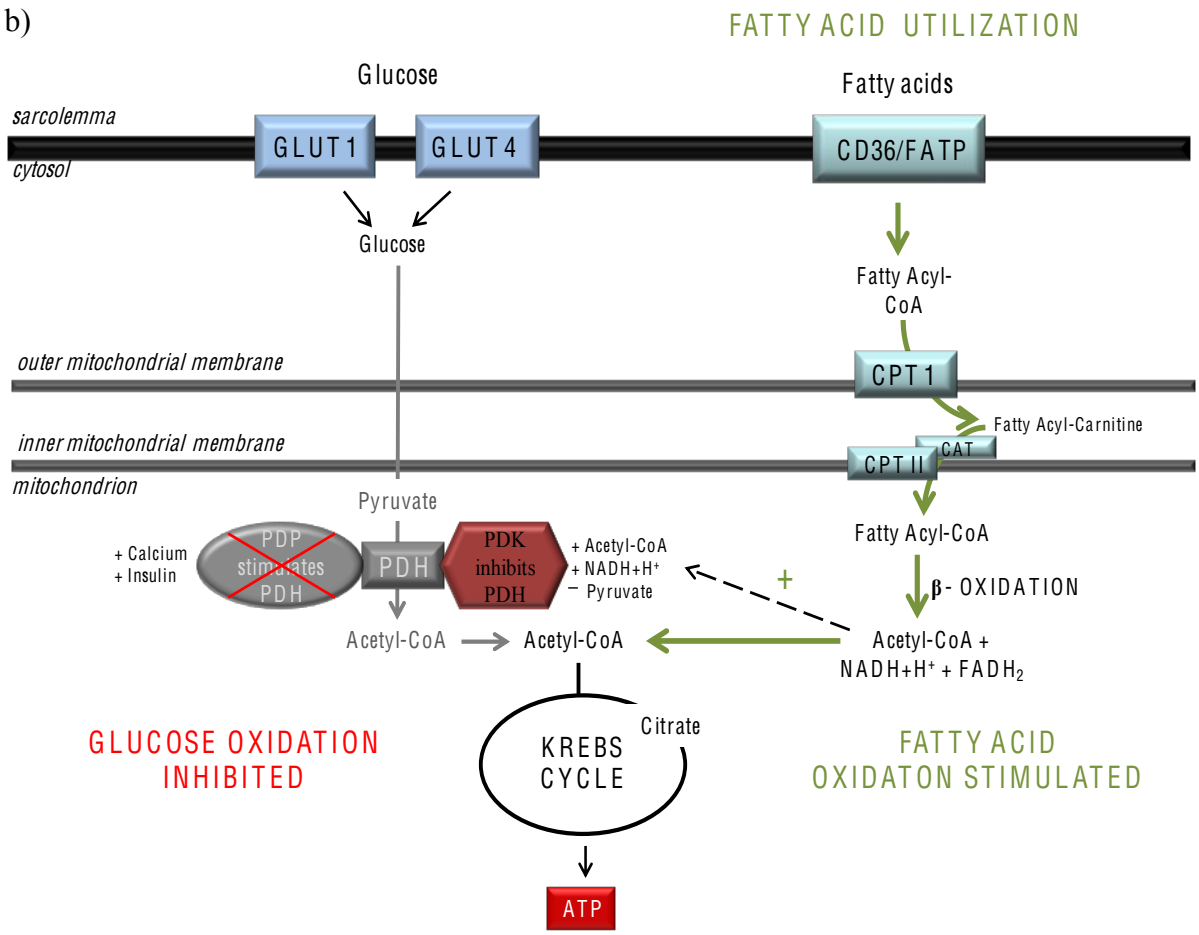

Figure 1.2b: The key role of pyruvate dehydrogenase (PDH) in regulating the balance between glucose and fatty acid metabolism in the heart. Fatty acid oxidation predominates: In the absence of malonyl-CoA, mitochondrial fatty acid uptake by CPT1 is active, resulting in β-oxidation of fatty acids and the generation of acetyl-CoA and $NADH+H^+$. These two mitochondrial coenzymes stimulate PDK, which phosphorylates and inactivates PDH, preventing subsequent glucose oxidation. Fatty acid-derived acetyl-CoA enters the Krebs cycle for ATP generation.

1.3 PPARs AND CARDIAC ENERGY METABOLISM

Recent studies have focused on a class of ligand activated transcription factors, known as peroxisome proliferator-activated receptors (PPARs) due to their extensive involvement in metabolic disorders [46, 47]. PPARs possess domain structure consisting of a NH_2-terminal region with a ligand-independent transactivation domain (AF-1), followed by a DNA-binding domain (two zinc fingers) and, at the COOH-terminus, a ligand and dimerization domain and a ligand-dependent activation domain (AF-2) (Figure 1.3a). Ligand activation of PPARα leads to the heterodimerisation with 9-*cis* retinoic acid-activated receptors (RXRs), and the recruitment of several co-activators, including peroxisome proliferator-activated receptor gamma coactivator 1 alpha (PGC1α) [48] and subsequent binding to the DNA consensus binding sequence (AGGTCAnAGGTCA), referred to as the peroxisome proliferator response element (PPRE) [49, 50] (Figure 1.3b). In the heart, functional PPREs have been identified in many genes encoding proteins involved in lipid metabolism [51-53].

The first member of the PPAR family, PPARα, was cloned as a novel murine nuclear receptor that mediates the transcriptional effects of peroxisome proliferators [54]. Other closely related receptors encoded by different genes were subsequently cloned and named PPARβ/δ, and PPARγ [53, 55]. In the intact heart, PPARβ/δ is the most abundant, having an almost 70% mRNA expression, followed by PPARα, which had an expression of 25%, and PPARγ was the least expressed of the three [56, 57].

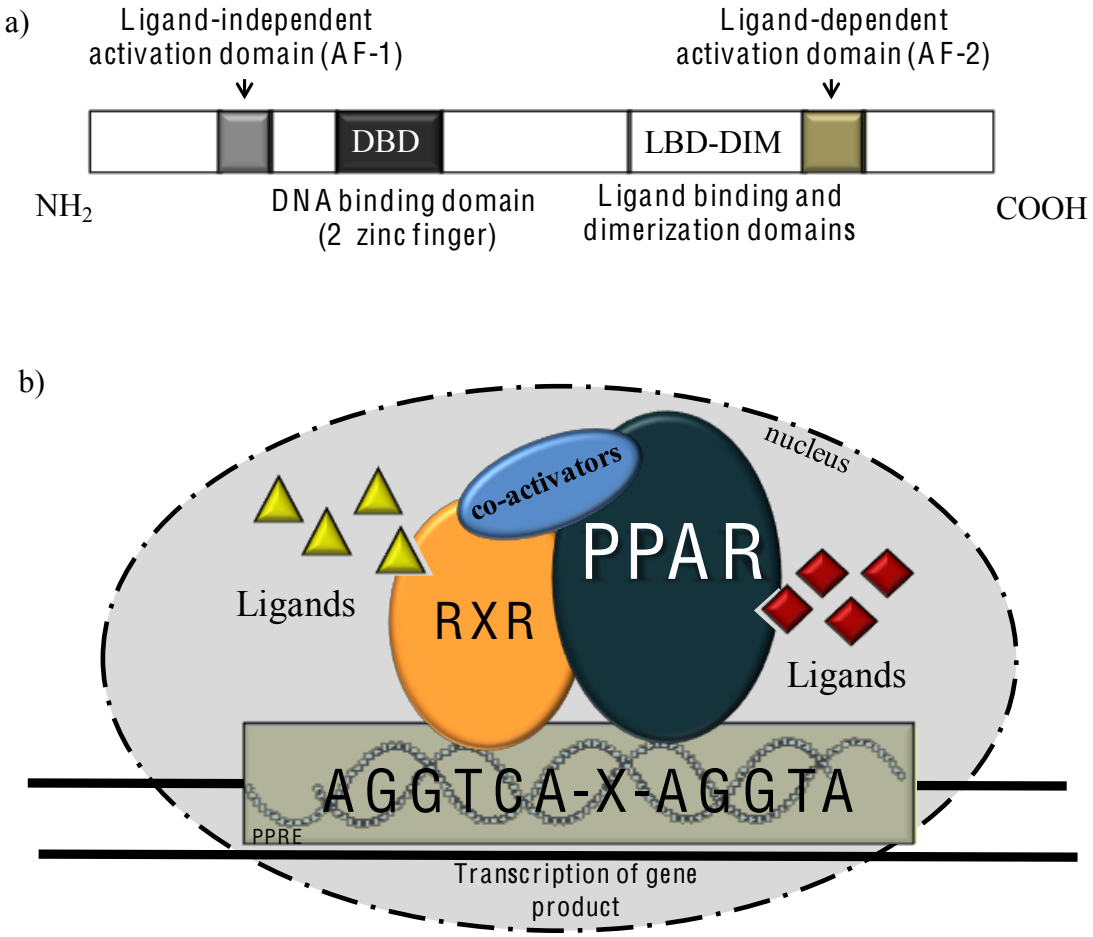

Figure 1.3: a) General structure [58] and b) proposed mechanism of peroxisome proliferator-activated receptor (PPARs) activation leading to metabolic remodelling.

PPARα is the best characterised isoforms and has been identified as the transcriptional regulator of fatty acid metabolism [53, 59] thus, highly enriched in tissues with high capacity for fatty acid oxidation such as the heart, brown adipose tissues, slow-twitch skeletal muscle and liver [57, 60]. Endogenous ligands for PPARα include long chain fatty acids and their metabolites [61-63]; a high fat diet, rich in very-long-chain fatty acids and polyunsaturated fatty acid such as docosahexaenoic acid and eicosapentaenoic acids have been shown to activate PPARα [64, 65]. Activation of PPARα increases cardiac expression of genes involved in three major steps in the cellular fatty acid utilisation pathway: 1) fatty acid

transport and esterification [66-68], 2) fatty acid mitochondrial import [52, 69] and 3) mitochondrial β-oxidation [68, 70] (Summarized in Table 1.2). Other cardiac transporter proteins shown to have PPARα response element in its promoter region are the mitochondrial uncoupling protein, UCP3 [71, 72], and mitochondrial thioesterase, MTE1 [73]. Increasing long chain, but not medium chain, fatty acid supply up regulates UCP3 mRNA and protein levels in both skeletal and cardiac muscle, with greatest effect being seen in cardiac muscle [74]. Therefore, PPARα is proposed to act as a lipid sensor in the heart, increasing capacity for fatty acid oxidation in response to elevated levels of intracellular lipid [59]. PPARα also regulates the transcription of cardiac pyruvate dehydrogenase kinase, PDK4 [75, 76], suggesting that it may control both fatty acid and glucose balance in the heart.

Table 1.2: Transcriptional regulation of genes encoding proteins involved in fatty acid metabolism by PPARα

Metabolic pathway proposed to be **regulated by PPARα**	Proteins
Fatty acid transport and utilisation	FATP, FAT/CD36, FABP, ACS, [66-68]
Fatty acid mitochondrial import	M-CPT1 [52, 69]
Mitochondrial β-oxidation	MCAD, LCAD, VLCAD [68, 70]
Mitochondrial uncoupling protein	UCP3 [71, 72]
Mitochondrial thioesterase	MTE1 [73]
Glucose metabolism	PDK4 [75]

Although the expression of cardiac PPARβ/δ is highest relative to PPARα and PPARγ, its cardiac effects are not well established. Studies in cardiac myocytes demonstrated that overexpression of PPARβ/δ increased the expression of classic PPARα target genes such as those involved in fatty acid oxidation [77, 78],

suggesting that PPARα and PPARβ/δ have overlapping targets and function in the heart. The PPAR isoform least expressed in the heart, PPARγ, appears to have an indirect role in cardiac fatty acid metabolism, secondary to its peripheral effect [79, 80]. PPARγ is highly expressed in white adipose tissue [57], where it triggers the differentiation of adipocytes and is activated by oxidised fatty acids [81]. PPARγ activation increases fatty acid uptake into adipose tissue, due to induction of lipoprotein lipase and fatty acid transporter proteins, favouring the removal of NEFAs and TAG from plasma and increase peripheral glucose utilisation [82]. Thus, PPARγ activation can reduce myocardial fatty acid uptake and oxidation by decreasing plasma free fatty acid content by sequestering fatty acids in adipocytes [83].

1.3.1 Role of uncoupling protein 3

Pharmacological stimulation of PPARα upregulated UCP3 in the heart [84, 85] and skeletal muscle [86] at both gene and protein level, identifying UCP3 as one of PPARα downstream targets [87]. It is expressed on the inner mitochondrial membrane and has been shown to uncouple mitochondrial respiration from ATP synthesis. The UCPs allow protons to re-enter the mitochondrial matrix via an alternative route to the ATP synthase, thus dissipating the proton gradient independent of ATP synthesis [88]. This results in decreased mitochondrial efficiency, as the same oxygen utilisation generates decreased concentration of ATP [89].

A number of physiological roles for UCP3 have been hypothesised. The gene locus that encompass UCP3 are strongly linked to resting metabolism rate energy expenditure [90], and although the process of mitochondrial uncoupling is

thermogenic, the low expression suggests that they would not make a significant contribution to overall body temperature [91]. The UCPs are induced by fatty acid and upregulated when plasma free fatty acids are elevated, such as fasting [85, 92]. It is possible that UCPs may be involved in fatty acid transport, transferring excess fatty acids out of the mitochondrial matrix. It has been proposed that UCP3 shuttles long chain fatty acids out of the mitochondria [93]. Once inside the mitochondria, excess long-chain fatty acyl-CoA can be converted to a free fatty acid anion, (FFA-) and a free CoA by the action of MTE1 [94, 95]. The FFA- anion is then transported out of the mitochondria into the cytosol by UCP3, when it can be re-esterified by FACS to long-chain fatty acly-CoA in a process that requires 2 ATP [93]. Proton transfer and uncoupling is potentially a secondary effect of this action as once in the intramembraneous space, the FFA- anion can associate with a proton and move back into the mitochondrial matrix and relinquish the proton [96, 97]. Alternatively, when the proton gradient is high the UCPs may act as a release valve, to prevent the formation of reactive oxygen species (ROS) by the respiratory chain intermediaries [98].

1.4 METABOLIC ABNORMALITIES IN HEART FAILURE

The chronically failing heart has been shown to be metabolically abnormal, in both animal models and patients. The failing heart has long been associated with depleted high energy phosphate reserves [99], associated with reduced PCr/ATP ratio [100, 101]. During the relatively hypoxic foetal period, the developing heart utilises glucose as the chief energy source but switches to long-chain fatty acid oxidation after birth [102]. During end-stage heart failure, it is believed that the heart reverts to foetal metabolic gene profile by regulating adult gene transcripts [15, 23, 103, 104]

which may serve to reduce ATP requirements and oxygen consumption, but at a cost of diminished contractile reserve [105]. Evidence suggests that substrate switch away from fatty acids towards glucose utilisation is an end-stage heart failure phenomenon, and in the early stages of heart failure, there is a normal or elevated rate of fatty acid oxidation [23].

In humans, measurements of myocardial substrate utilisation in heart failure provided somewhat conflicting data. Early studies have indirectly assessed myocardial metabolism and suggested that during the development of heart failure, the heart switches its metabolism away from fatty acids to carbohydrate metabolism for energy production [106, 107]. Indirect calorimetry measurements in patients with congestive heart failure revealed 3-fold increase in myocardial uptake and oxidation of fatty acids and a 35% decrease in glucose uptake and oxidation compared to age-matched healthy individuals [108]. A more recent direct measurement of substrate utilisation in humans obtained by PET analysis in congestive heart failure patients with ejection fraction of no more than 35%, revealed an increase in labelled myocardial fatty acid uptake and a decrease in deoxyglucose uptake compared to healthy subjects [109]. However, a PET study conducted in patients with idiopathic cardiomyopathy with similar ejection fraction indicated a 49% increase in myocardial glucose uptake and 35% reduction in fatty acid uptake and oxidation compared to healthy individuals [110].

Conversely, animal studies have provided additional insight into the changes in cardiac metabolism that accompany heart failure. In a dog model of moderate coronary microembolization-induced heart failure, isotopic tracers were used to

directly measure substrate oxidation, and showed no differences in myocardial glucose, lactate or fatty acid metabolism compared to healthy dogs [111]. Conversely, in dog models of terminal pacing-induced heart failure, fatty acid oxidation was decreased by at least 35% while glucose oxidation increased by 40% [40, 112], suggesting that down-regulation of fatty acid oxidation occurs only in more severe or late-stage heart failure. Isolated hearts from rat infarct models of heart failure reveal that after 8 weeks of infarction, there was a significant increase in glucose oxidation with no change in fatty acid oxidation [113], suggesting that in the early stages of HF there is increased glucose metabolism but not a reduction in exogenous fatty acid metabolism.

Although the mechanism responsible for the downregulation of the fatty acid oxidation pathway in the failing heart is not clear, changes at the molecular level are in agreement with a decreased fatty acid flux. Decreased expression of PPARα and/or RXRα have been reported, and may play a key role in the myocardial substrate switch observed in the failing hearts [103, 114, 115]. In addition, mRNA and protein levels of CPT1, MCAD, LCAD are reduced in explanted failed hearts and transplant recipients compared with unused donor hearts [103], and in biopsies of patients with end-stage heart failure (ejection fraction less than 20%). Decreased GLUT4, and GLUT1 mRNA expression in animals [112] and patients with end-stage heart failure have also been reported [104, 116]. It is unknown whether this reversion to foetal metabolism is an adaptive or maladaptive response, but it has been proposed that the metabolic switch occurs as the hearts to increasing hypoxia [117, 118].

1.5 MYOCARDIAL HYPOXIA

The heart is an aerobic organ, consuming approximately 8-15mL O_2/min/100g of tissues at a resting pulse rate: 5-10mL O_2/min/100g tissues more than the brain [117]. Chronic myocardial hypoxia results when there is a disproportion between oxygen supply and demand at tissue level [119-121], caused by a drop by in arterial pO2 matched to an adequate perfusion.

Hypoxic states of the heart have been recognised as the most 'frequent and dangerous diseases of modern time' [121] contributing to various forms of cardiac diseases, including congenital heart disease, chronic cor pulmonale [119, 122, 123] and the most common, being ischaemic heart diseases [124-127]. It is reported that approximately two-thirds of all patients with heart failure have a history of myocardial ischaemia [23]. Although these diseases are multifactorial, distinguishing the contribution of hypoxia by understanding cellular adaptation to decreased oxygen supply will provide an insight into these hypoxia-associated cardiac diseases.

1.5.1 Hypoxia inducible factor

Since a constant supply of oxygen is critical to sustain cardiac function, slight alterations in oxygen tension elicit important physiological responses at the cellular level [128]. One of the pivotal mediators of the cellular response to hypoxia is hypoxia-inducible factor (HIF), a key modulator of the transcriptional response to hypoxic stress (Figure 1.4) [129, 130]. HIF regulates the expression of multiple genes; together these genes control cellular process, including a switch from oxidative to glycolytic metabolism [131], and stimulation of oxygen delivery through erythropoiesis and angiogenesis [132, 133]. Therefore, their target genes include

erythropoietin (EPO) [133], vascular endothelial growth factor (VEGF) [132, 134], GLUT1 [135, 136] and PDK1 [137, 138]. Besides its essential role in oxygen homeostasis, HIF has been implicated as a critical factor for pathogenesis of ischaemic heart disease, stroke, cancer and chronic lung disease [139].

The transcription factor HIF is a heterodimer, consisting of two basic helix-loop-helix PAS proteins, oxygen labile α subunit and a stable β subunit, also known as ARNT (aryl hydrocarbon receptor nuclear translocator). There are three known members of the HIF family (HIF-1, HIF-2 and HIF-3) and all are α/β heterodimeric proteins. HIF-1 was the first factor to be cloned and is the best understood isoform [127]. HIF-2 is closely related to HIF-1 and HIF-3 is a distant relative of HIF-1 and little is currently known about its function and involvement in oxygen homeostasis [140]. HIF-1α is expressed ubiquitously in all cells, whereas HIF-2α and HIF-3α are selectively expressed in certain tissues, including vascular endothelial cells, liver parenchymal cells, and cells of the myeloid lineage [141-144]. Under normoxic conditions, HIF-α is constitutively degraded. HIF-α is regulated at the level of protein turnover by prolyl hydroxylation by prolyl-4-hydroxylases (PHDs) and at the level of coactivator recruitment by asparaginyl hydroxylation, with both of these hydroxylation reactions linked to oxygen availability [145] (Figure 1.4).

PHDs are dioxygenase enzymes that split molecular oxygen (named PHD1, PHD2, and PHD3), of which PHD2 and PHD3 are predominantly expressed in the heart [144]. One oxygen atom is inserted into the HIFα peptide at the prolyl residue in the oxygen-dependent degradation domain (ODDD) (hydroxylation of HIF-α) while the other converts 2-oxoglutarate (2OG) to succinate, yielding CO_2 as a by-product. This

pathway can only occur in the presence of oxygen with 2-OG as co-substrate. Upon hydroxylation of the prolyl residue in ODDD, HIF-α is recognized by von Hippel Lindau protein (pVHL) and targets the protein to the ubiquitinylation machinery, leading to proteasomal degradation [127, 140, 145] (Figure 1.4).

Factor inhibiting HIF (FIH) is an asparaginyl hydroxylase which catalyses the splitting of molecular oxygen, using one oxygen atom for hydroxylation of the target asparagine (Asn) within the C-terminal transactivation domain (CAD) of HIF-α, and the other for oxidising the co-substrate 2-OG as above. The CAD recruits CBP/p300 (Creb-binding protein/protein 300), which is essential to link HIF-α to the hypoxia response element (HRE) transcriptional factor and initiate the transcriptional machinery of the HIF system. Hydroxylation of this single asparagine residue was found to be sufficient to prevent the interaction of the CAD with the essential transcriptional coactivator CBP/p300, thus silencing the HIF-α transcriptional ability [127, 140, 145] (Figure 1.4). Under hypoxia, PHDs and FIHs are inhibited, allowing HIF-α to translocate into the nucleus and dimerise with HIF-β at the Per ARNT SIM (PAS) domain to form functional heterodimeric HIF. Activated HIF then binds to the hypoxia response elements (HREs), leading to a transcriptionally active complex which activates the expression of its target genes (Figure 1.4).

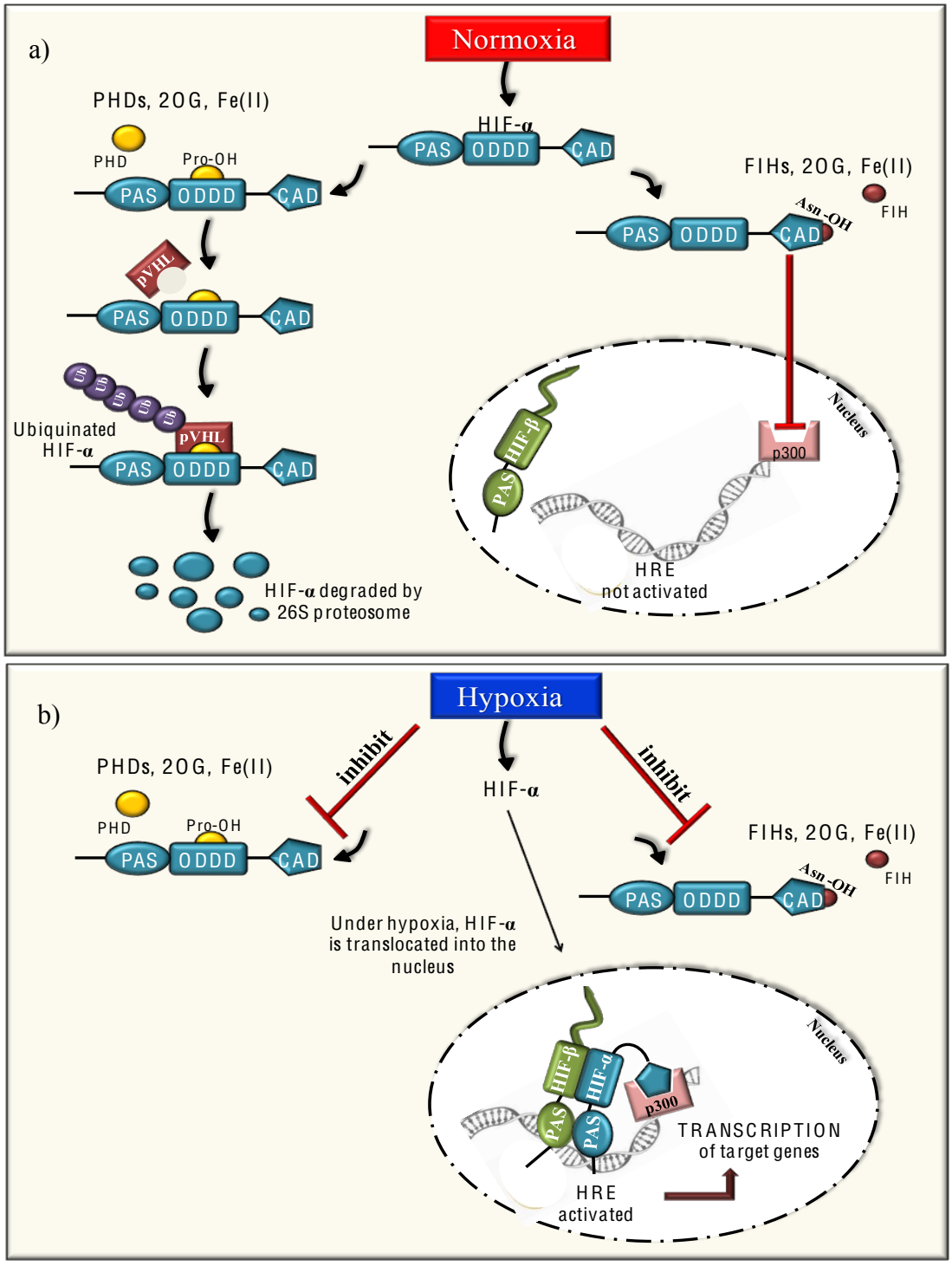

Figure 1.4: a) Regulation of HIF-α via two pathways under normoxia. PHDs hydroxylate proline residue of HIF-α in ODDD domain, in the presence of 2-OG and Fe (II). Hydroxylated HIF-α is recognised by pVHL which targets the protein for proteasomal degradation by ubiquitin protein. FIHs hydroxylate asparagine residue of HIF-α in the CAD domain, in the presence of 2-OG and Fe (II). Hydroxylated HIF-α is blocked to interact with the essential transcriptional coactivator CBP/p300, thus silencing the HIF transcriptional ability. b) Under hypoxia, both pathways are inhibited, HIF-α translocates to nucleus, dimerise with HIF-β and activates the HIF system.

1.5.2 Cardiac substrate utilisation following myocardial hypoxia

The most frequently used experimental model in research on hypoxia simulated under laboratory condition is in a normobaric or hypobaric chamber. Hypobaric and normobaric hypoxia in animal models have been employed commonly to a simulated altitude of approximately 5500 metres (11% oxygen). However, most of the animal models were immediately placed in the chamber, exposing them to severe hypoxic insult, inducing pathological hypoxia, associated with ventricular hypertrophy [146-150].

Molecular findings from these studies indicated that hypoxia altered cardiac substrate metabolism towards glucose metabolism in a similar way to advanced heart failure. In rats, cardiac glucose uptake is increased by at least 52% [151] while the glycolytic enzyme hexokinase was 2.5-fold higher after 2 weeks of chronic hypoxic exposure [147], parallel to *in vitro* studies reporting augmented glycolytic capacity in various mammalian cells in response to hypoxia [131, 136], including HL-1 cardiomyocytes [152]. Similarly in humans, high altitude tolerant natives, such as Himalayan Sherpas and Andean Quechuas, have enhanced glucose uptake [153]. Findings on glucose transporters are inconclusive; mRNA expression of cardiac GLUT1 and GLUT4 in rats was not altered after 4 weeks of chronic hypoxia [146] but GLUT1 proteins increased 1.5-fold after 2 weeks of hypoxia, while GLUT4 protein levels remained unchanged [150].

In contrast, many genes controlling fatty acid metabolism are downregulated with chronic hypoxia [120]. PPARα protein levels, along with *in vivo* cardiac MCAD gene promoter activity in mice are downregulated as early as 7 days in moderate (14% O_2)

hypoxic exposure [148]. Other models of systemic hypoxia, induced by chemical induction (cobalt chloride treatment and iso-volaemic dilution) showed 50% decrease in PPARα expression and its target genes, including PDK4 and CPT1 [154]. The activity of cardiac enzymes metabolising fatty acid, β-hydroxy-acyl-CoA dehydrogenase and CPT1 were also reduced with chronic hypoxia [147, 155, 156]. While it is apparent that the transcriptional profile of cardiac metabolic genes in response to chronic hypoxia is consistent with increased reliance on glucose metabolism, information on glucose and fatty acid utilisation, though glycolysis and β-oxidation, respectively, are lacking.

Decreased PCr/ATP ratio was observed in Sherpa hearts [157], supporting the increased reliance of glucose for myocardial ATP production, which may be detrimental as anaerobic glycolysis can only provide limited amounts of energy in the form of ATP [21]. This is in agreement to lowland subjects, exposed to 20 hours of normobaric hypoxia in a purpose-built hypoxic chamber [158], and acclimatised to 11 days of altitude at 5300 m (Everest Base Camp) [159]. NMR spectroscopy studies in rodents are limited, but decreased cardiac PCr/ATP ratio has been reported in isolated mouse hearts exposed to 3 weeks of 11% hypoxia [160, 161], albeit with carbohydrate as the sole perfusate and similarly, this was measured in hypoxic mouse hearts that were hypertrophied. Therefore, it is very difficult to assess whether the metabolic phenotype is translated into a functional adaptation, raising the need to establish a hypoxia protocol which induces a physiological hypoxia. Indeed, the decrease in PCr/ATP ratio is an indicator of impaired metabolic status in cardiac disease [101]; the switch to glucose metabolism may serve to decrease ATP requirement, but at the cost of a diminished contractile reserve [105].

1.5.3 **Interaction between HIF and PPARα**

In 2001, Narravula and Colgan suggested that PPARα bears a DNA consensus motif for HIF-1α. This was the first study which reported a direct interaction between HIF and PPARα, leading to reduced PPARα protein levels following HIF activation in hypoxic epithelial cells. In the same year, Huss *et al.* suggested that the reduction of PPARα in hypoxic rat cardiomyocytes was independent of the HIF pathway, but as a result of deceased levels of its obligate partner, RXR. This finding was refuted by the recent findings of Belanger *et al.*, as they showed that the reduction in PPARα/RXR binding in hypoxic rat cardiomyocyte was HIF-1α dependent. In cancer cells, HIF-2α was shown to form complexes with PPARα, thereby reducing the activity of PPARα in hypoxia. The upstream mechanism responsible for reduced PPARα and/or RXRα levels in response to hypoxia remains ambiguous.

It is possible that the downregulation of PPARα by HIF may underlie the metabolic switch away from fatty acid oxidation in the failing heart. Indeed, recent studies have shown that HIF-1α levels are elevated in rat model of volume-overload heart failure [162] and in hearts of patients with ischaemic cardiomyopathy [163], consistent with increased PHD2 and PHD3 proteins in hypoxic and infarcted rat hearts [144]. Conversely, cardiac myocyte specific HIF-1α deletion reduced contractile function and cardiac ATP, PCr and lactate levels [164]. Given the essential role of HIF-1α in coordinating gene expression during limited oxygen supply, these data suggest that hypoxia is an intrinsic element of chronic heart failure and activation of HIF is possibly an adaptive response.

1.6 THESIS AIMS

Following from above, the main objective of this thesis was to understand the cardiac metabolic response to chronic, physiological hypoxia. Given its key role in cardiac substrate utilisation and recent association with HIF, PPARα is hypothesised to be involved in the hypoxic response. Moreover, current findings linking hypoxia mediated metabolic alterations to PPARα were established at the molecular level, without measurement of metabolic flux and whether these results were representative of the intact heart under physiological hypoxic conditions had not been investigated. Cardiac functional data coupled with metabolic and energetics data following chronic hypoxia are also lacking. A systematic approach has been outlined in this thesis to address this issue. First, chapter 3 characterised cardiac hypoxic response in a mouse model of physiological hypoxia, generated by a novel chronic hypoxia protocol. This chapter provides an extensive overview of substrate fluxes in the chronically hypoxic mouse hearts, linking the subsequent effect of fuel selection to cardiac energetics and ultimately cardiac function. This was complemented by a molecular profiling of the hypoxic heart, establishing a molecular mechanism by measuring tissue mRNA expression and protein levels. Second, to establish the involvement of PPARα in the hypoxic response, PPARα expression was modified by high fat feeding or genetic ablation, as described in chapter 4 and 5 respectively. Similarly, the functional and metabolic consequences of PPARα stimulation and ablation following chronic hypoxia were examined. PPARα$^{-/-}$ mice were subjected to both hypoxia and high fat feeding, isolating any changes that were independent of the PPARα pathway. Finally, chapter 6 aimed to explore the relationship between PPARα and HIF in HL-1 cells: a cardiac cell line derived from mouse atrial cardiomyocytes. This chapter described the temporal metabolic changes in HL-1 cells upon exposure to hypoxia and the

effect of HIF stabilisation using a commercial non-specific inhibitor and a novel specific PHD inhibitor on the different cardiac PPAR isoforms.

CHAPTER 2

MATERIALS AND METHODS

General materials and methods are presented here, with specific methods applicable to the individual studies presented in the relevant results chapters.

2.1 ANIMAL CARE

Fourteen month-old male EvSv129 control and PPARα$^{-/-}$ mice were housed on a 12hr light/dark cycle and kept under controlled conditions of temperature, light and humidity, with *ad libitum* access to chow and water. Mice were a kind gift of Dr Frank J. Gonzalez (National Cancer Institute, Bethesda, MD, USA). All animal procedures were in accordance with the UK Home Office guidelines under The Animals (Scientific Procedures) Act, 1986.

2.2 GENERATION OF CHRONICALLY HYPOXIC MOUSE MODEL

2.2.1 Normobaric hypoxic chamber

Chronic hypoxic exposure was performed in a 400 litre glass-fronted chamber (Biospherix, USA) (Figure 2.1), which allowed free diffusion of ambient air via ventilation holes. Oxygen concentration was controlled by active flow of gaseous nitrogen, and an oxygen sensor inside the chamber. Chamber oxygen and carbon dioxide content was monitored continuously, with carbon dioxide not exceeding 0.5% by controlling chamber ventilation. Humidity was maintained inside the chamber at ambient levels, between 40 and 60%.

2.2.2 Adaptation period

Mice were initially exposed to a seven day hypoxic acclimatisation period, during which chamber oxygen content was lowered on a daily basis, 2% per day down to 15% O_2, then 1% per day until a minimum of 11%. Thereafter oxygen level was maintained at 11% for 12 days (Figure 2.1). Mice were weighed on a daily basis, involving a brief return to normoxia (< 30 seconds). Following hypoxic housing, all mice were exposed to 1 hour of room air, to discount short term effects of re-oxygenation on cardiac function [165]. Thus all results represent long term adaptation to hypoxic conditions.

a)

b)

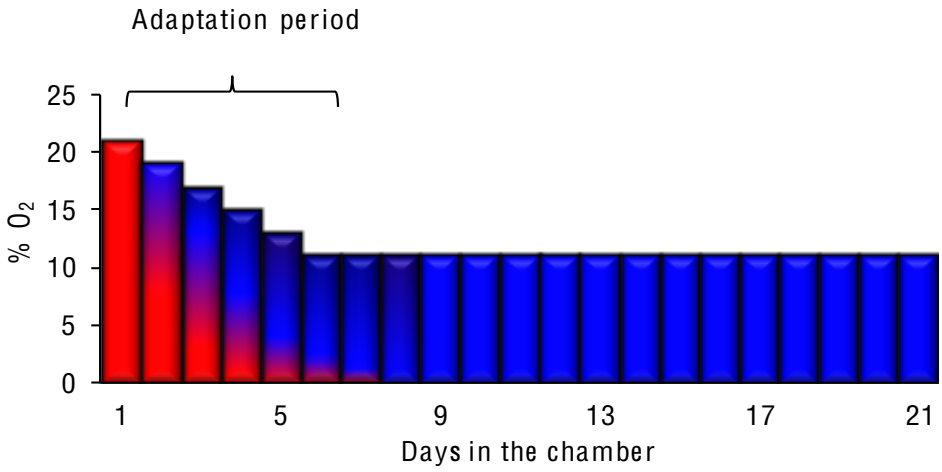

Figure 2.1: a) Normobaric hypoxic chamber and b) acclimatization period with hypoxia protocol.

2.2.3 Measurements of blood haemoglobin and haematocrit

Post heart excision, blood was immediately collected from the chest cavity. Blood haematocrit was measured using a microhaematocrit reader (Hawksley, UK) and blood haemoglobin was measured using ABL 700 series blood gas analyser (Radiometer, UK), as specified by the manufacturer's instruction.

2.2.4 Enzyme-linked immunosorbent assay (ELISA) for VEGF

Approximately 30 mg of powdered frozen heart tissues was added to 300 µl of ELISA buffer (Appendix 1) and homogenized using a Polytron homogenizer for 30 seconds. Supernatant was saved and aliquots were removed for determination of protein concentration (BCA protein assay kit, Perbio, UK). A 96-well plate was coated with 100 µl/well VEGF capture antibody (R&D System, UK) overnight. ELISA assay was performed on the samples according to the manufacturer's instruction.

2.3 MAGNETIC RESONANCE IMAGING

Mice underwent *in vivo* cine MRI to characterize cardiac morphology and function. Mice were anesthetized with 1.5% isoflourane in O_2 and positioned supine in a purpose-built cradle. ECG electrodes were inserted into the forepaws and a respiration loop was taped across the chest. The cradle was lowered into a vertical-bore, 11.7 T MR system (Magnex Scientific, Oxon, United Kingdom) with a 40 mm birdcage coil (Rapid Biomedical, Wu¨rzburg, Germany) and a Bruker console running Paravision 2.1.1 (Bruker Medical, Ettlingen, Germany). A stack of contiguous 1 mm thick true short-axis ECG and respiration-gated cine-FLASH

images were acquired to cover the entire left and right ventricles of the mice. Image data were segmented using Image J program (NIH Image, Bethesda, MD) [166]. Left ventricular end-diastole (ED) and end-systole (ES), corresponding to the frames of maximal and minimal ventricular volume, respectively, were identified. The epicardial and endocardial borders were outlined using the free hand drawing tool. From these segments volumes, characteristics of cardiac function including stroke volume (SV =EDV-ESV), ejection fraction (EF= SV/EDV), cardiac output (CO= SV x heart rate) and cardiac index (CI =CO/ body mass) were calculated (Figure 2.2).

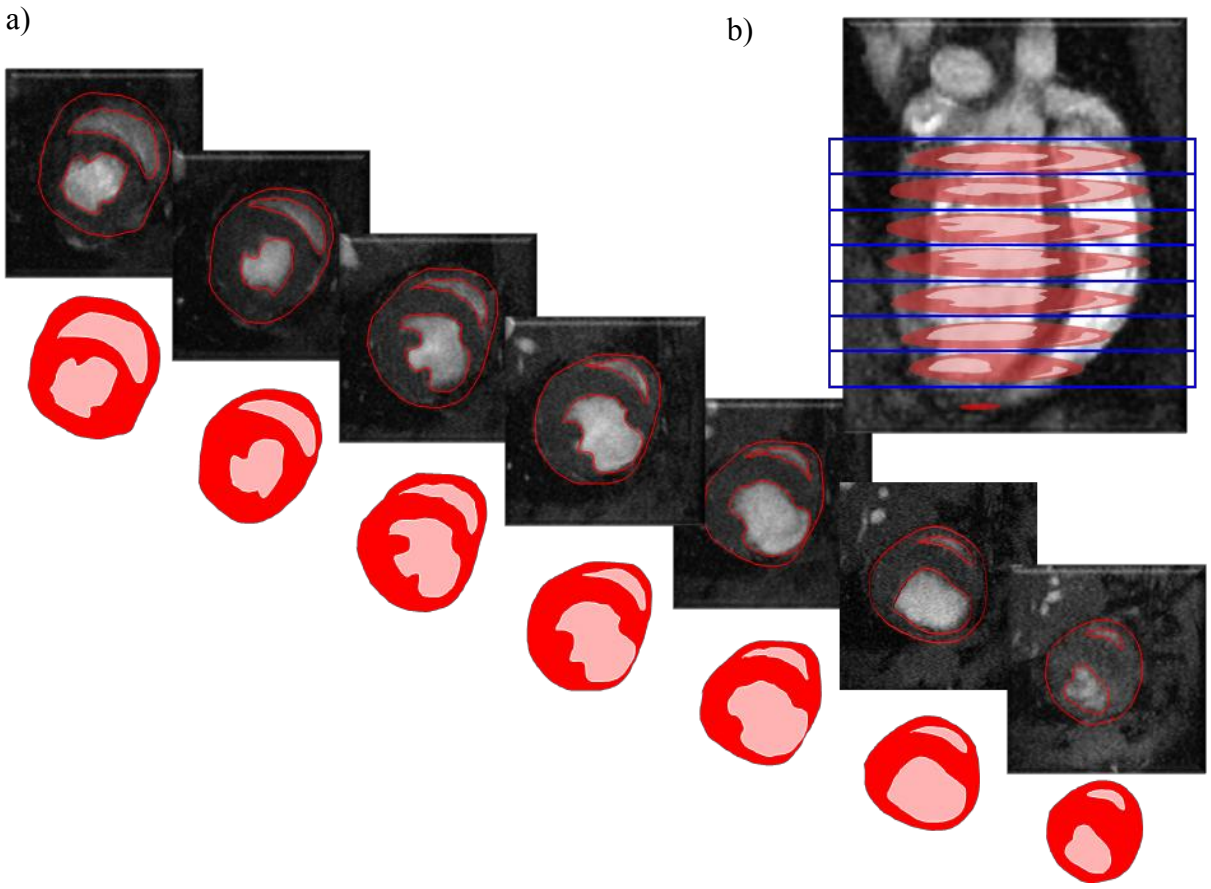

Figure 2.2: a) End- systolic and end- diastolic short axis images of hearts showing the outlined epicardial and endocardial borders of the left ventricle b) Long axis view of the rat heart showing seven contiguous slices of 1.5 mm thickness covering the entire left ventricle.

2.4 ISOLATED HEART PERFUSION

2.4.1 Preparation of Krebs-Henseleit buffer

1.5% fatty acid-free bovine serum albumin (Sigma, UK) and 0.4 mM palmitate were added to Krebs-Henseleit (KH) buffer (Appendix 1). This solution was placed in dialysis tubing and left to equilibrate overnight with KH buffer, to allow lowering of free calcium due to calcium chelation by albumin. Immediately prior to use, the free calcium concentration was measured using a radiometer blood gas analyser adjusted if necessary, to a final concentration between 1.8-1.9 mM.

2.4.2 *Ex vivo* Langendorff heart perfusion

Mice were anaesthetised using pentobarbitone and hearts were rapidly excised and arrested in ice-cold KH buffer. Hearts were weighed prior to perfusion. Hearts were cannulated via the aorta, and perfused in Langendorff mode with KH buffer (gassed 95% O_2, 5% CO_2) at 37^{o}C, at a constant perfusion pressure of 100 mmHg (Figure 2.3). The left atrium was opened and a fluid-filled, PVC balloon was inserted into the left ventricle and inflated to an end-diastolic pressure (EDP) of 4-8 mmHg (Figure 2.4). This was connected by polyethylene tubing to a blood pressure transducer, and the signal acquired via a bridge amplifier to a PowerLab data acquisition system (ADInstruments, Oxfordshire, UK). This system measured pressure development within the left ventricle, with the peak and nadir of the wave representing the systolic and end-diastolic pressure (Figure 2.5). Heart rates were determined by trigger points on the ascending limb of the pressure waveform. Left ventricular developed pressure (LVDP) was determined as systolic pressure minus EDP. Rate pressure product (RPP) was calculated as the product of LVDP and heart rate.

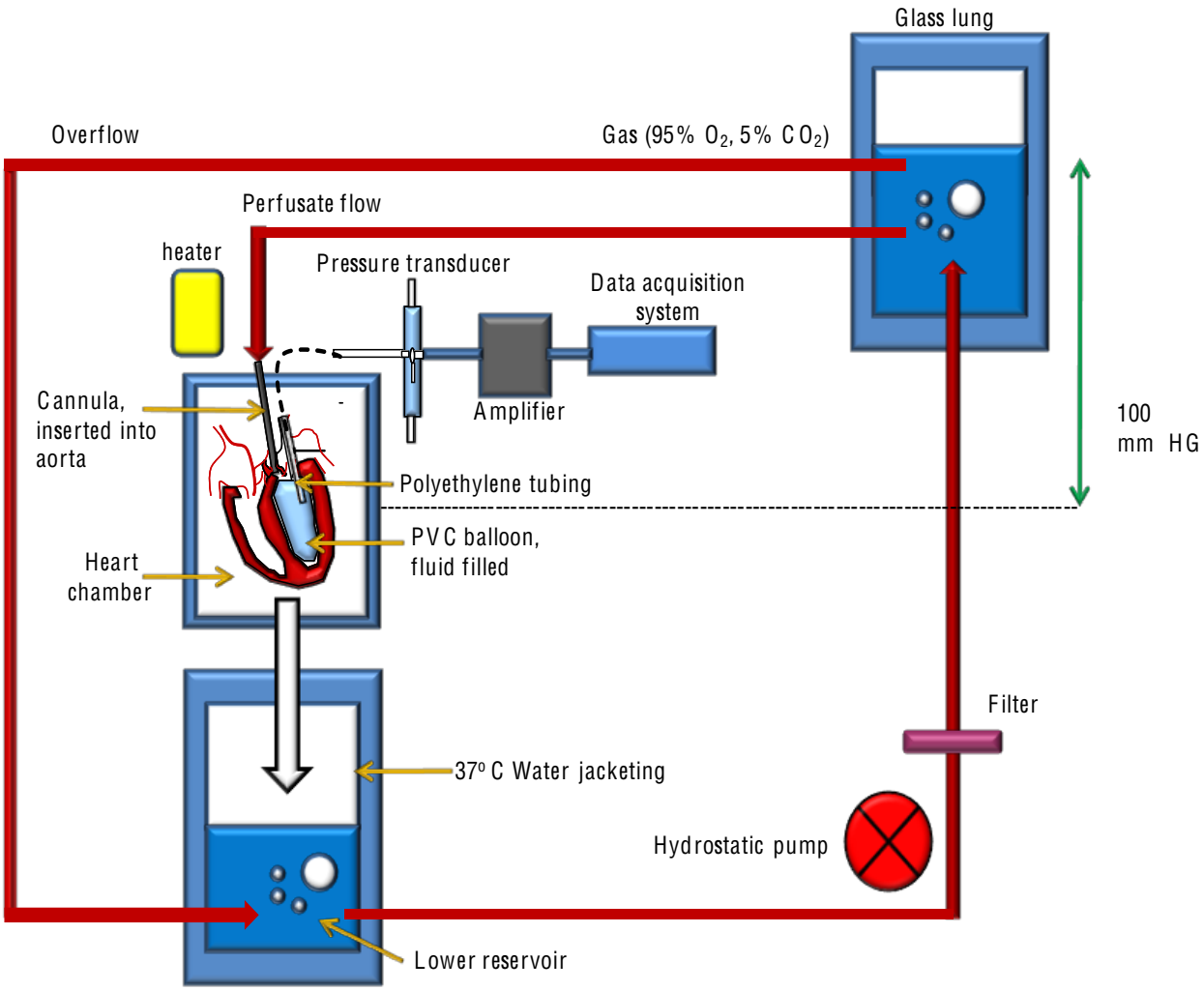

Figure 2.3: Representation of the Langendorff heart perfusion setup. Perfusion buffer was filtered through 5.0 µm filters (Millipore, UK) and oxygenated using a glass lung located above the heart, at a height equivalent to a perfusion pressure of 100 mmHG. Buffer was heated to a constant temperature of 37°C by a heater directly above the heart and the water jacketed glass wear. The heart was perfused via a cannula inserted into the aorta. Coronary effluent was collected in a chamber directly below the heart, and recirculated to the buffer reservoir.

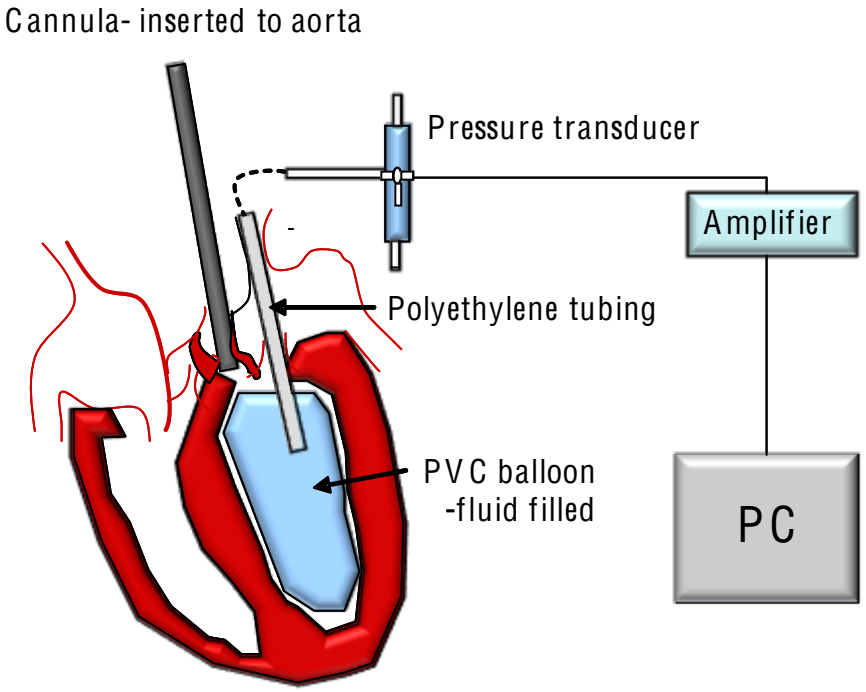

Figure 2.4: Diagrammatic representation of the isolated, perfused heart technique. Hearts were cannulated via the aorta, and the coronary arteries were perfused in Langendorff retrograde-mode. A PVC, fluid filled balloon was inserted into the left ventricle, and connected to a pressure transducer and data acquisition system, allowing for measurement of cardiac function.

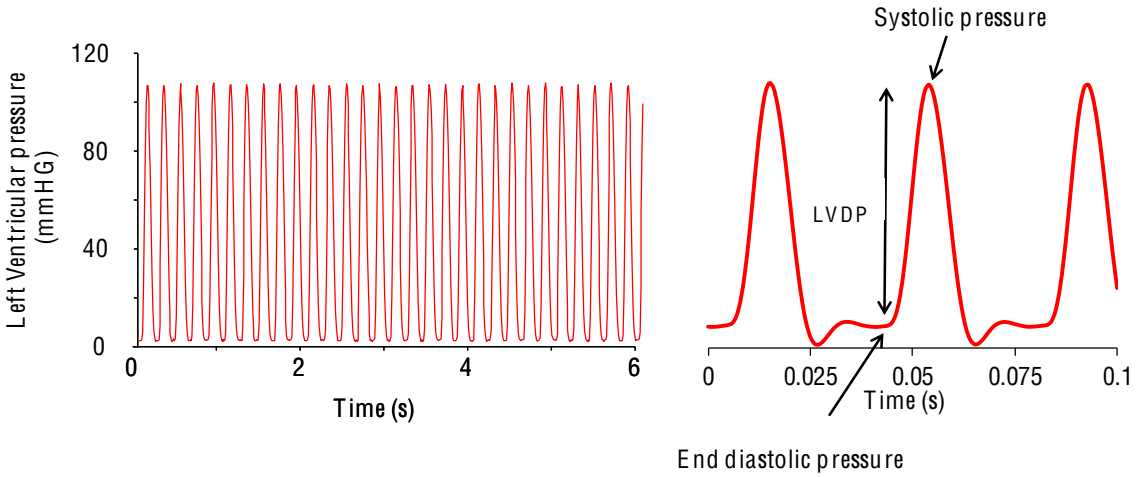

Figure 2.5: Pressure changes were measured in real-time, and allowed for determination of systolic and end-diastolic pressure. Heart rate was calculated by setting trigger points within the ascending portion of the pressure wave.

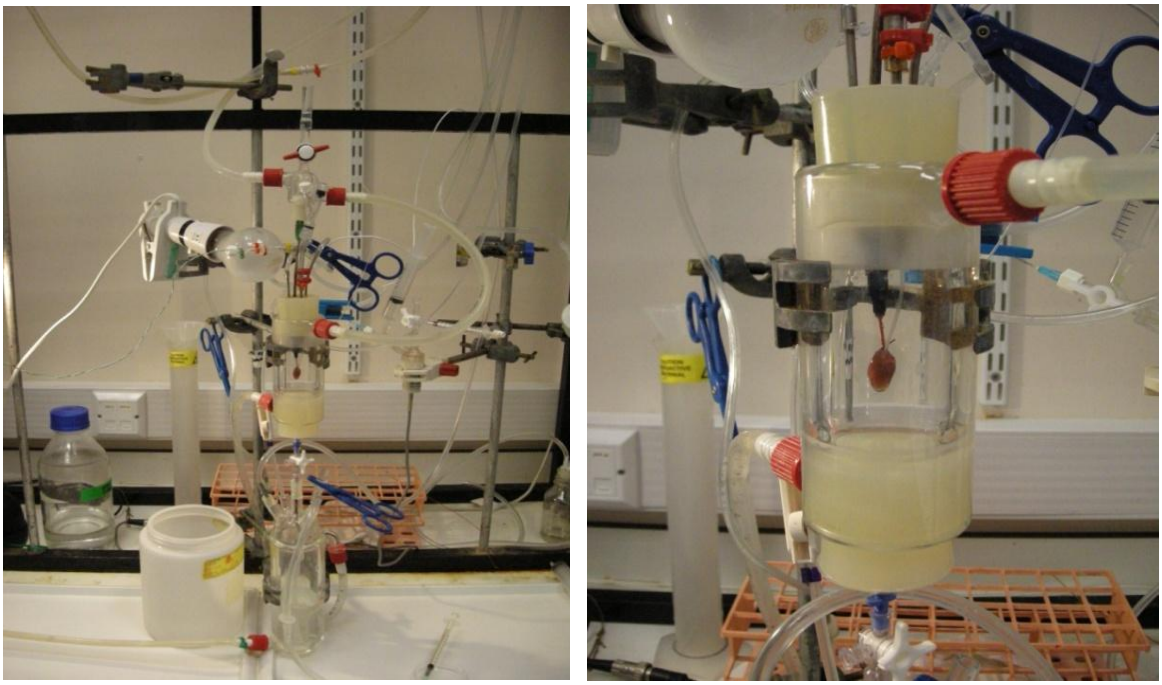

Figure 2.6: Langendorff heart perfusion setup

2.4.3 Determination of glycolytic flux

Hearts were perfused with 100 ml recirculating KH buffer containing 11 mM glucose and 0.4 mM palmitate bound to 1.5% fatty acid-free bovine serum albumin (Sigma, UK) and 25μCi of D[5-^{3}H]-glucose (Amersham, Bucks, UK). Following a 10 minute stabilisation period, basal glycolytic rates were determined by collecting 1mL of aliquots of recirculating buffer every 5 minutes for 30 minutes. Insulin-stimulated glycolytic rates were determined after addition of 500 $\mu U.L^{-1}$ insulin to the recirculating buffer and 1 ml of aliquots were collected again every 5 minutes for a further 30 minutes. Glycolytic rates were determined in perfusion aliquots, as the conversion of ^{3}H-glucose to $^{3}H_2O$ [35]. $^{3}H_2O$ was separated from ^{3}H-glucose using a Dowex anion exchange column (Sigma, UK).

For each aliquot sample, glycolytic rates were calculated using the equations:-

$$\text{Total glycolytic flux per heart } (\mu mol.heart^{-1}) = \frac{[\text{sample cpm} - \text{sample time 0 cpm}] \times \text{recirculating buffer volume (ml)}}{[\text{specific activity}.ml^{-1} - \text{sample time 0 cpm}] / \text{glucose (mM)}}$$

$$\text{Total glycolytic flux per gram wet weight } (\mu mol.gww^{-1}) = \frac{\text{Total glycolytic flux } (\mu mol.heart^{-1})}{\text{Heart weight (g)}}$$

As 0.2 ml aliquots were diluted in scintillation fluid and counted for radioactivity, to normalise to counts per ml values are multiplied by 5. The glycolytic rates per gww ($\mu mol.gww^{-1}.min^{-1}$) were calculated by plotting the total glycolytic flux for all samples against time. A minimum of 5 data points were fitted with linear regression and the gradient was equal to the glycolytic rate. Insulin-stimulated glycolytic rates were calculated as the glycolytic rate in the presence of insulin minus the basal glycolytic rate.

2.4.4 Determination of lactate efflux

1 ml lactate assay buffer containing 1% nicotinamide adenine dinucleotide (NAD) was added with distilled water to varying volumes of a 0.0022% lactate solution to generate ten solutions with different lactate concentrations, from 0 to 100 mM. 10 µl lactate dehydrogenase (Sigma, UK) was added to each solution, and following a 20 minute incubation, absorbance was determined at 340 nm to give a standard curve. This method is based on the fact that conversion of lactate to pyruvate by lactate dehydrogenase also converts NAD^+ to NADH, which absorbs at 340 nm while NAD^+ does not.

Lactate concentrations in the aliquots collected during perfusion were determined by adding 0.1 ml of each aliquot to 1 ml lactate assay buffer and 0.9 ml of water. 10µl lactate dehydrogenase was added to each solution, and absorbance at 340 nm was measured before and after 20 minute incubation. Lactate concentrations were calculated from the differences in absorbance using the equation of the linear regression line fitting the standard curve.

2.4.5 Determination of palmitate oxidation rates

A separate set of hearts were perfused with 100 ml recirculating KH buffer containing 11 mM glucose and 0.4 mM palmitate bound to 1.5% fatty acid-free bovine serum albumin (Sigma, UK) and containing 25µCi [9,10-^{3}H]-palmitate (Amersham, Bucks, UK). Following a 10 min stabilisation period, aliquots of recirculating buffer were collected every 5 to 10 minutes during the perfusion protocol. Palmitate oxidation rates were determined by the conversion of ^{3}H-palmitate to $^{3}H_2O$ [35].

In addition, a 0.5 ml aliquot of the unextracted time 0 aliquot was counted to determine the specific activity of the buffer. For each aliquot sample, palmitate oxidation rates were calculated using the equations:-

$$\text{Total palmitate oxidation per heart } (\mu mol.heart^{-1}) = \frac{[\text{sample cpm} - \text{sample time 0 cpm}] \times 8.26 \times \text{recirculating buffer volume}}{[\text{specific activity}.ml^{-1} - \text{sample time 0 cpm}] / \text{palmitate (mM)}}$$

$$\text{Total palmitate oxidation per gram wet weight } (\mu mol.gww^{-1}) = \frac{\text{Total palmitate oxidation } (\mu mol.heart^{-1})}{\text{Heart weight (g)}}$$

The dilution factor of 8.26 was due to the dilution of the buffer aliquot during the extraction protocol. As 0.5 ml aliquots were diluted in scintillation fluid and counted for radioactivity, to normalise to counts per ml values are multiplied by 2. The rates of palmitate oxidation per gram wet weight (gww) ($\mu mol.gww^{-1}.min^{-1}$) were calculated by plotting total palmitate oxidation for all samples against time. A minimum of 5 data points were fitted with linear regression and the gradient was equal to the palmitate oxidation rate. The palmitate oxidation rates obtained using this technique with the optimised Langendorff conditions were comparable to those published for the working heart perfusion technique [35].

2.5 Measurement of high-energy phosphate metabolism

Isolated mouse hearts were perfused in the Langendorff mode as described above. Isolated mouse hearts perfused with KH buffer containing 11 mM glucose and 0.4 mM palmitate were inserted into an 11.7 Tesla vertical bore magnet (Magnex Scientific, Oxon, United Kingdom) using a Bruker Avance console (Bruker Medical, Ettlingen, Germany) with a 10 mm I.D probe containing concentric ^{1}H and ^{21}P sensitive coils. The heart was centralised in these coils using acquisition of a brief ^{1}H image. Fully relaxed ^{31}P spectra was collected using pulse-and-collect sequence at a repetition time of 10s and a flip angle of 90^{o}. Six ^{31}P MR spectra of 192 averages (each 32 per spectrum) were acquired and quantified for PCr, ATP and Pi. Intracellular pH was determined from the chemical shift between the Pi and phosphocreatine (PCr) peaks using the equation: $pH= 6.72- \log (\delta - 5.72)/ (3.17-\delta)$ [167]. Mouse hearts were freeze clamped at the temperature of liquid nitrogen at the end of experiments (Assisted by Dr Mark Cole).

2.5.1 Calculations of high-energy phosphate concentration

Intracellular absolute ATP concentration was determined by high-pressure liquid chromatography. Frozen heart tissue was crushed under liquid nitrogen. Approximately 25 mg crushed tissue was homogenised in 550 µl 60% perchloric acid and 100 µl of homogenate removed and added to 100 µl 4% NaOH for protein determination using the Lowry method [168]. KOH was added to the remaining homogenate to bring the pH to 7, before centrifugation at 5500 rpm for 5 minutes. Phosphorus metabolite concentrations were measured in the supernatant using high-pressure liquid chromatography with JASCO gradient pump, Sigma column (length 25 cm, diameter 5 mm) and JASCO UC detector. Phosphorus metabolite concentration was expressed as nmol per mg protein. To calculate the intracellular concentration, total heart protein content was assumed to be 0.17 g protein per gram wet weight and the intracellular volume was assumed to be 0.5 ml per gram wet weight [169]. The absolute ATP concentration was then multiplied by PCr/ATP ratio to calculate [PCr]. HPLC also determined total creatine concentration, which allowed calculation of free creatine, and determination of cytosolic ADP from the creatine kinase reaction: $[ADP] = ([ATP]\,[\text{free creatine}]/\,[PCr]\,[H^+]\,K_{ck})$ using a K_{ck} of 1.66 x $10^9 m^{-1}$. The free energy from ATP hydrolysis (ΔG_{ATP}) was calculated using the equation: $\Delta G_{ATP} = \Delta G°' + RT\ln([ADP]\,[Pi]/[ATP])$, where $\Delta G°'$ is the value for ATP hydrolysis at 37°C, taken to be -30.5 $kJmol^{-1}$ and R is the gas constant, taken to be 8.31 $Jmol^{-1}.K^{-1}$.

2.6 HL-1 CELL CULTURE

HL-1 murine cardiomyocytes were a kind gift from Dr William C. Claycomb (New Orleans, USA). The cells were cultured on 6-well plates precoated with 5 μg/ml fibronectin and 0.02% gelatin, and maintained in Claycomb medium (Sigma). The cells were supplemented with 10% foetal bovine serum, ascorbic acid (0.3 mM), norepinephrine (0.1 mM), L- glutamine (4 mM) and 1% penicillin-streptomycin and incubated in 5% CO_2 at 37°C and 95% humidity. The medium was changed daily and after treatments (as specified in chapter 6), all cells were aspirated with PBS and harvested for protein analysis and RNA extraction. All experiments were performed on confluent beating cells.

2.7 WESTERN BLOTTING

Whole heart and skeletal tissue lysates and cell lysates were used in this study. A general description of the technique is outlined below, with variations for the specific proteins supplied in Appendix 2.

2.7.1 Tissue lysate preparation

Approximately 30 mg of powdered frozen tissues was added to 300 μl of lysis buffer (Appendix 1) and homogenized using a Polytron homogenizer for 30 seconds. The lysates were boiled for 5 minutes and centrifuged at 13,000 rpm for 10 min, the supernatant was saved and aliquots were removed for determination of protein concentration (BCA protein assay kit, Perbio, UK). To the remaining supernatant, 5% β-mercaptoethanol (v/v) was added, followed by boiling for 5 min and storing at -80^{o}C.

2.7.2 Cell lysate preparation

To remove cell culture medium, confluent HL-1 cells in 6-well plates were washed twice with PBS. 150µl lysis buffer containing protease inhibitor was added to wells and cells were scraped from wells into Eppendorfs and immediately frozen in liquid nitrogen. Cells in lysis buffer were homogenised using a 21G needle, boiled for 5 minutes and centrifuged at 13,000 rpm for 10 minutes. The supernatant was saved and aliquots were removed for determination of protein concentration (BCA protein assay kit, Perbio, UK). To the remaining supernatant, 5% β-mercaptoethanol (v/v) was added, followed by boiling for 5 minutes and storing at -80 ^{o}C.

2.7.3 Polyacrylamide gel electrophoresis and protein transfer

Equal amounts of protein (20 - 40µg) were diluted in Laemmli loading buffer (Appendix 1) and loaded onto 12% polyacrylamide gels. Gels were run at 120 V for approximately 2 hours. A piece of Immobilon-P membrane (Millipore, UK) and two pieces of extra thick chromatography paper (BioRad, UK) were cut to the same size as the gel. These were soaked with the gel for 30 min in sodium dodecyl sulphate (SDS) transfer buffer (Appendix 1), layered onto the semi-dry transfer apparatus (Biorad, UK) and transferred at 0.07 A per gel for 1 hour. The membranes were stained with Ponceau S stain (Sigma, UK) to determine successful protein transfer and even protein loading. Blots were washed in TBS-Tween (Appendix 1) and blocked in 5% (w/v) dried milk in TBS-Tween (25 ml per blot) for at least 1 hour.

2.7.4 Immunoblotting detection and band quantification

The membrane was washed for 1 hour in TBS-Tween, with the solution changed every 15 minutes. The specific primary antibody was diluted in 5% (w/v) dried milk

in TBS-Tween (12 ml per blot), and incubated on the membrane. The membranes were then washed for 2 hour in TBS-Tween, with the solution changed every 15 minutes. The appropriate horseradish peroxidase-conjugated secondary antibody (Santa Cruz, USA) was diluted in 5% (w/v) dried milk in TBS-Tween (12 ml per blot), and incubated on the membrane. Membranes were washed for a further hour in TBS-Tween, with the solution changed every 15 min. The membrane was covered in enhanced chemiluminescence (ECL) detection solution (Amersham, UK) and sandwiched between sheets of acetate. Membranes were exposed to X-ray film and developed using a Compact X4 automatic X-ray film processor (X-ograph Imaging systems, UK). Protein bands were quantified using Un-Scan-It, Version 6.1 (Silk Scientific, USA).

2.8 REAL-TIME QUANTITATIVE REVERSE-TRANSCRIPTION POLYMERASE CHAIN REACTION (qRT-PCR)

2.8.1 Primer specificity and efficacy

Primers were designed using Primer3 software based on interpretation of GenBank or Ensembl Genome Browser search results and were obtained from Eurofins MWG Operon (UK) (please refer to Appendix 3 for primer sequence). Primer specificity was enhanced by designing a primer pair that flanked the exon–exon border of the gene of interest, to avoid the primers amplifying genomic DNA that may be contained in samples. Primer specificity was confirmed by blasting the primer sequence against genomic databases available at NCBI. No significant homology sequence should be found, to ensure gene specific amplification rather than amplification of several transcripts with one primer pair. For primer efficiency test, a series of 2-fold

dilutions of cDNA were prepared and amplified with consistent concentration of primer using the qRT-PCR machine. The threshold cycle (Ct) value was obtained after the PCR procedure and plotted against log cDNA dilution. Primer amplification efficiency was calculated as $E = (\exp{-1/m} - 1)$ X 100% where E is the amplification efficiency and m is the slope of the dilution curve.

2.8.2 RNA extraction

Total RNA was extracted and purified from 30 mg of powdered frozen heart tissues using Qiagen® RNeasy Fibrous Tissue Kit (QIAGEN, UK) according to manufacturer's instruction. For cells, total RNA was extracted and purified from ≤5 x 10^6 confluent HL1 cells using Qiagen® RNeasy Mini Kit (QIAGEN, UK) according to manufacturer's instruction. RNA concentration and purity was determined by measuring the absorbance at A230, A260 and A280 using a NanoDrop® Spectrophotometer (NanoDrop Technologies). A ratio of A260/A280 ~ 2.0 indicates that the RNA is protein-free pure RNA and a ratio of a260/230 ~2.0 indicates that the RNA was phenol and ethanol free.

2.8.3 Reverse transcription (complementary DNA synthesis)

Complementary DNA (cDNA) was synthesised from the RNA template using the AB high capacity transcriptase kit (Applied Biosystem). Every 1 µg RNA sample was reverse transcribed using 1 µl reverse transcriptase, 2 µl random primer, 0.8 µl dNTPs (10 mM each), and 2 µl buffer and topped up by RNase free water to a total volume of 20 µl. The reaction mixture was subjected to incubation for 10 mins at 25°C, 120 minutes at 37°C and 5 seconds at 85°C. Real time PCR amplification was performed using the Applied Biosystems StepOnePlus Real-Time PCR System (AB

International, CA). The real-time PCR mastermix was prepared by adding 10 µl AB Sybrgreen PCR mastermix (AB International, CA), 1 µl reverse primer, 1 µl forward primer, 1 µl cDNA and 7 µl distilled water. The total volume for each real-time PCR reaction was 20 µl. The PCR program was set up with an initial heat activation step at 95^{o}C for 10 minutes. Forty cycles of thermocycling were performed with a denaturation step at 95 ^{o}C for 15 seconds, an annealing and extension step at 60^{o}C for 1 minute. Fluorescence was measured at the end of each extension step. After amplification, a melting curve was acquired and melting curves were used to determine the specificity of PCR products.

2.8.4 qRT-PCR data analysis

Relative quantification of target gene expression normalized to the housekeeping gene, β-actin was performed using the $2^{-\Delta\Delta Ct}$ method [170, 171].

2.9 GLYCOLYTIC ENZYME ASSAY

Total enzyme activities of the glycolytic enzymes, pyruvate kinase and phosphoglycerate kinase were measured in heart extracts. The activity of pyruvate kinase was measured in media containing 50 mM imidazole (pH 7.6), 20 mM KCl, and 2 mM MgCl2, 0.1 mM EDTA, 0.1 mM NADH, 1 mM ADP, and 4.5 U/ml lactate dehydrogenase. The reaction was started by addition of 1 mM phosphoenolpyruvate. A decrease in absorbance was registered at 340 nm. The activity of 3-phosphoglycerate kinase was measured using a reaction mixture containing 50 mM imidazole buffer (pH7.6), 2 mM MgCl2, 0.1 mM EDTA, 1mM MATP, 5 mM 3-phosphoglycerate, 0.2 mM NADH and 5 U/ml of glyceraldehyde-3-phosphate

dehydrogenase. The reaction was started by addition of 40 µl of heart extract. Changes in absorbance were recorded at 340 nm (performed by Dunja Aksentijevic).

2.10 Myocardial triacylglycerol and fatty acid assay

Cardiac lipids were extracted from freeze clamped tissue (25-50 mg) using 10 ml of 2:1 chloroform:methanol solution. After thorough mixing and phase separation, the lower phase was air dried at 50^{o}C and resuspended with 200 µl ethanol. Using an assay kit (RANDOX, UK), cardiac triglyceride (TRIGS, RANDOX UK) and fatty acid content (NEFA, RANDOX UK) of this solution was measured spectrophotometrically at 500 nm, and normalized to gww of heart tissue.

2.11 Plasma metabolites

Following heart excision, blood was immediately collected from the chest cavity and plasma was separated by centrifugation and stored at -80^{o}C. Analysis of plasma glucose and triacylglycerol were carried out using an automated spectrophotometric analyser (Monarch Laboratories, USA). Aliquots of plasma were stored in the presence of 2% lipoprotein lipase inhibitor (Xenical, Roche, USA), to prevent breakdown of plasma triglycerides by endothelial-derived lipoprotein lipase, and assayed for FFA (NEFA assay kit, Wako Chemicals, Germany).

2.12 Statistical analysis

Results are expressed as means ± standard error of the mean (SEM). Data were analyzed using two way analysis of variance (ANOVA) with post-hoc t-testing. $p < 0.05$ was taken as the level of statistical significance.

CHAPTER 3

EFFECT OF CHRONIC HYPOXIA ON CARDIAC FUNCTION AND METABOLISM

3.1 ABSTRACT

The principal substrate used by the normal adult human heart is free fatty acids, the remainder being predominantly carbohydrate. In hypoxia, the heart switches from fatty acid towards glucose metabolism. As hypoxia may be a component of cardiac disease, understanding hypoxic adaptation could play an essential role in understanding the metabolic changes during the development of heart failure. The aim of the work in this chapter is to characterise the cardiac response to chronic hypoxia by assessing cardiac function, substrate fluxes and the molecular mechanism underlying any changes. The hypoxia protocol consisted of incremental reduction in oxygen content in the first week of housing, followed by 2 weeks at 11% oxygen. Control mice were housed in normoxic conditions within the same room. *In vivo* cardiac function was measured using multi-slice cardiac cine MRI. Hearts were isolated and perfused in the Langendorff mode with ^{3}H-labeled substrates for measurements of glycolytic flux and palmitate oxidation. High-energy phosphate metabolites were measured in isolated perfused hearts using ^{31}P MRS. Despite a reduction in LV mass, cardiac index and ejection fraction were maintained following hypoxic exposure. Hypoxia increased basal glycolytic flux 2-fold ($p < 0.01$) and decreased palmitate oxidation by 27% ($p < 0.05$). This was associated with a 36% ($p < 0.01$) reduction in PPARα mRNA expression, which decreased protein levels of PPARα downstream targets; MCAD by 24% ($p < 0.05$), UCP3 by 52% ($p < 0.05$), MTE1 by 39% ($p < 0.01$) and PDK4 by 28% ($p < 0.05$). PPARβ/δ and PPARγ mRNA expression was unaltered by chronic hypoxia. PCr/ATP ratio fell in chronically hypoxic hearts, but the driving force of ATP hydrolysis, ΔG_{ATP}, was not significantly altered by hypoxia, indicating that in this particular protocol, metabolic reprogramming was sufficient to maintain ATP production and contractile function. Hypoxia altered the downstream markers of HIF; cardiac VEGF and PDK1 protein levels increased 3-fold ($p < 0.01$) and 79% ($p < 0.01$) respectively, suggesting a HIF-dependent mechanism. In conclusion, cardiac metabolic adaptation to chronic hypoxia was associated with the downregulation of PPARα and its downstream targets, which was essential for the maintenance of cardiac function.

3.2 INTRODUCTION

Under aerobic conditions, the principal substrate used by the normal adult human heart is free fatty acids, the remainder being predominantly carbohydrate. In animal models of pressure overload hypertrophy [172], chronically infarcted hearts [173], and end-stage human heart failure [174], the heart shifts away from fatty acid utilisation towards glycolysis for producing ATP [25], with many mitochondrial β-oxidative enzymes, such as CPT1 and MCAD, being reduced [103]. This switch decreases the oxygen requirement of the heart for ATP production, which is higher per mole of fatty acid substrate oxidised than for glucose [21]. However, in the long term, this switch may become detrimental, as less ATP is generated per mole of glucose metabolised, resulting in lower ATP content, as observed in patients with severe heart failure [19, 20, 101]. Whether this metabolic switch plays an adaptive or maladaptive role in the pathogenesis of end-stage heart failure is unknown. It is possible that the metabolic switch occurs as the hearts adapts to increasing hypoxia [117, 118], as emerging molecular evidence suggests that hypoxia alters cardiac substrate metabolism towards glucose utilisation in a similar way as occurs in cardiac diseases [120].

While it is apparent that the transcriptional profile of cardiac metabolic genes in response to chronic hypoxia is consistent with increased reliance on glucose metabolism, information on glucose and fatty acid utilisation, through glycolysis and β-oxidation, respectively, are lacking. The increase reliance on anaerobic metabolism during hypoxia may also be detrimental in the long term as glycolysis can only provide limited amounts of energy in the form of ATP [21], as hypoxia in humans was shown to decrease PCr/ATP ratio [158, 159], raising the need to measure cardiac

energetics following chronic hypoxia. Moreover, *in vivo* functional data in combination with metabolic flux have not been reported, making it difficult to assess whether the hypoxic metabolic phenotype is an adaptive or maladaptive response.

3.2.2 Study aim

Despite evidence of a similarity between cardiac changes in hypoxia with cardiac diseases, conclusive mechanistic studies, examining metabolism in combination with function in an intact hypoxic heart, are lacking. Additional studies are also needed to determine gene/protein expression and enzyme activities in combination with substrate flux measurements in the same hearts, allowing a greater understanding of the mechanisms regulating substrate metabolism following hypoxic exposure. Thus the specific aim of this chapter was to establish a novel physiological chronic hypoxia protocol for mouse model to allow the direct determination of cardiac function and metabolism in the hypoxic heart, with the molecular alterations underlying the changes.

3.3 METHODS

Methods are described in Chapter 2. Briefly, mice were housed in a normobaric hypoxic chamber for 3 weeks and control mice were placed in the same room. Body weight and food intake was monitored daily. Mice were anaesthetized and *in vivo* cardiac morphology and function were measured using multi-slice cardiac MRI. Hearts were excised and perfused in the Langendorff mode. Glycolytic flux and palmitate oxidation rates were measured using ^{3}H labeled substrates. Using ^{31}P MRS, high energy phosphate metabolites were also measured in isolated perfused hearts.

Following perfusion, hearts were freeze-clamped in liquid nitrogen for further molecular analysis. Whole cell lysates from powdered frozen heart were used to measure protein levels of MCAD, UCP3, MTE1, GLUT1, GLUT4, PDK1, PDK4, RXRα, SIRT1, mitochondrial proteins (PGC1α, αKGDH, citrate synthase) and electron transport chain proteins (Complex I, II and IV) by western blotting. mRNA expression of PPARα, PPARβ/δ and PPARγ was analyzed using qRT-PCR. VEGF protein levels were quantified using ELISA. Cardiac lipids were extracted from freeze-clamped tissue, using a chloroform:methanol solution, for the measurement of cardiac TAG and FFA content.

3.4 RESULTS

3.4.1 Effect of chronic hypoxia on mouse physiology

Mice housed in normoxia consumed 2.77 ± 0.38 g of pelleted chow daily, consistent with food consumption data in healthy mice [175] (Figure 3.1). Hypoxia did not alter food intake, as mice housed in hypoxia consumed 3.04 ± 0.23 g of food daily. During the acclimatization period, a small number of mice (average of 1 mouse per hypoxic run) displayed symptoms of altitude sickness and lost more than 10% of body weight after 3 consecutive days, and were removed from the chamber. In general, hypoxic mice were able to maintain body weight throughout the duration of the protocol. Whole blood haemoglobin and haematocrit increased by 52% and 50%, respectively ($p < 0.01$), in chronically hypoxic mice compared with normoxic controls ($p < 0.01$) (Figure 3.1).

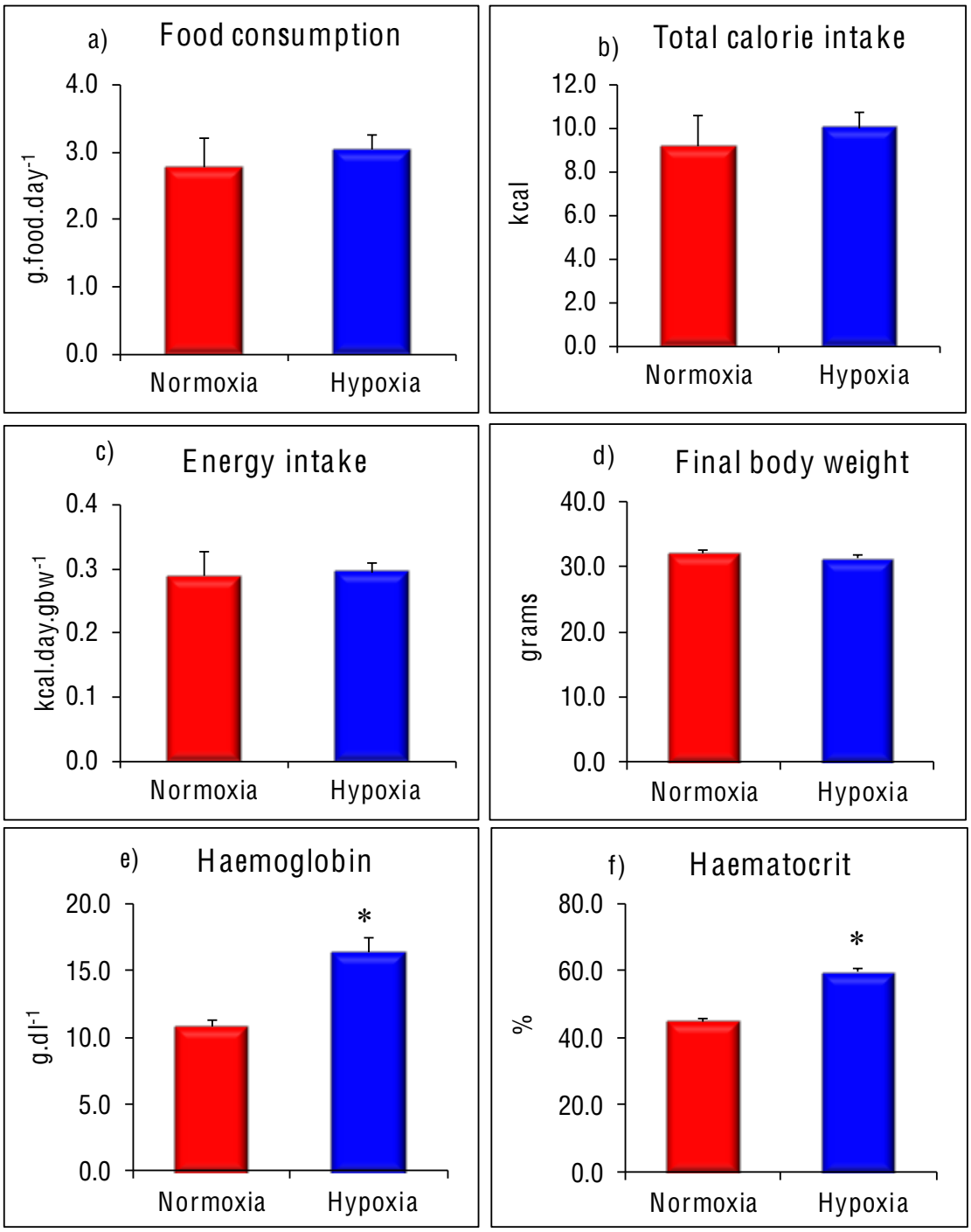

Figure 3.1 Effect of chronic hypoxia on mouse physiology: a) Food consumption, b) total calorie intake, c) energy intake, d) final body weight, e) haemoglobin and f) haematocrit in mice following 3 weeks of chronic hypoxia. *$p < 0.05$ relative to normoxic mice. n = 5-22 per group.

3.4.2. *In vivo* cardiac morphology and function

Cardiac LV mass, determined using *in vivo* cine MRI, was 19% lower ($p < 0.01$) in hypoxic mice. As there was no difference between normoxic and hypoxic body weights, chronically hypoxic mouse hearts were hypotrophic, having heart/body weight ratios 17% lower than normoxic mice ($p < 0.01$) (Figure 3.2). Cardiac output and ejection factions were unaffected by 3 weeks of hypoxia (Figure 3.3), despite an 18% lower stroke volume in hypoxic mice, resulting from 17% lower ($p < 0.05$) end-diastolic volumes. End-systolic volumes were unchanged by hypoxia (Table 3.1).

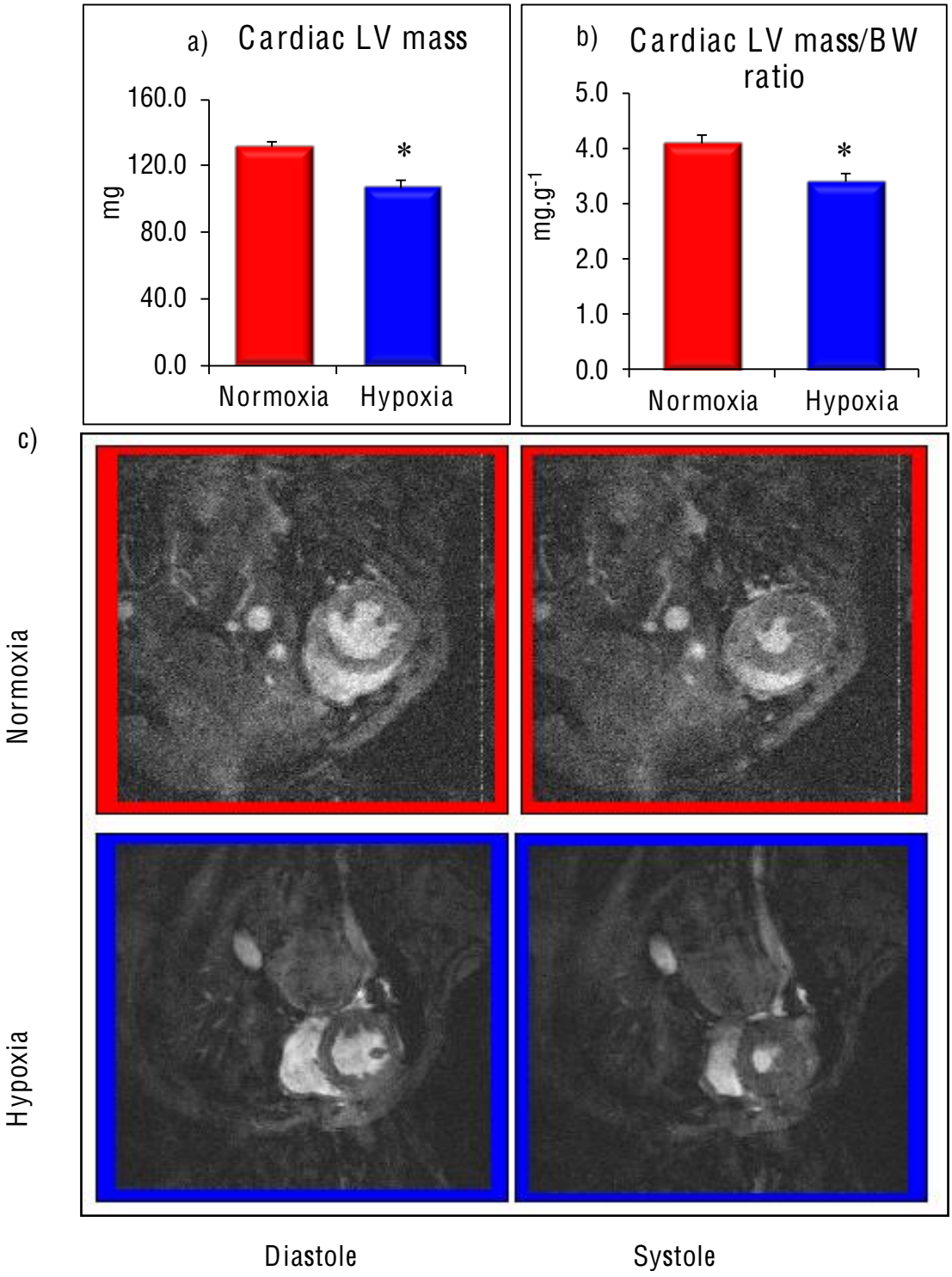

Figure 3.2 Effect of chronic hypoxia on cardiac morphology: a) Cardiac LV mass, b) Cardiac LV mass/body weight (BW) ratio and c) representative MR short axis heart images at end diastole and systole in mice following 3 weeks of chronic hypoxia. *$p < 0.05$ relative to normoxic mice. n = 16-22 per group.

Table 3.1: *In vivo* cardiac function following 3 weeks of chronic hypoxia. Data are means ± SEM. *p < 0.05 relative to normoxic mice.

	Normoxia n=22	Hypoxia n=16
End diastolic volume (µl)	64.2 ± 2.8	53.5 ± 4.0*
End systolic volume (µl)	24.6 ± 1.7	21.1 ± 2.8
Heart rate (bpm)	444 ± 10.0	495 ± 25.0
Stroke volume (µl)	39.6 ± 1.8	32.4 ± 2.5*
Cardiac output ($ml.min^{-1}$)	17.4 ± 0.7	16.1 ± 1.6

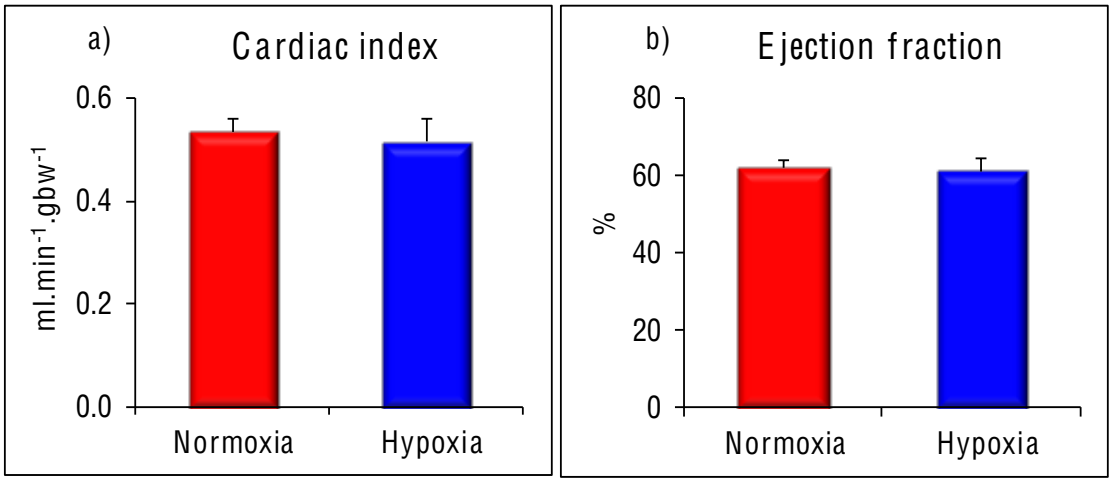

Figure 3.3 Effect of chronic hypoxia on cardiac function: a) Cardiac index and b) ejection fraction in mice following 3 weeks of chronic hypoxia. No statistically significant differences. n = 16-22 per group.

3.4.3 Plasma metabolites

Plasma glucose, triacylglycerol and free fatty acid concentrations were not altered by 3 weeks of hypoxia (Figure 3.4).

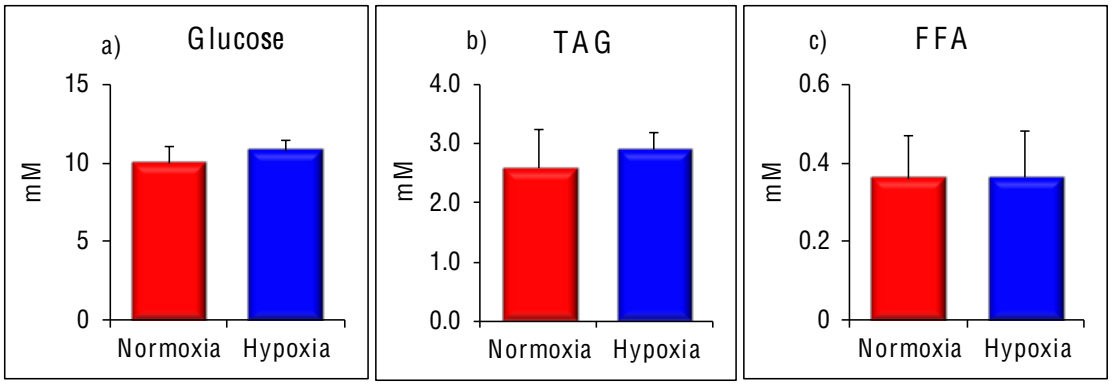

Figure 3.4 Plasma metabolites: Plasma concentration of a) glucose, b) triacylglycerol (TAG) and c) free fatty acids (FFA) in mice following 3 weeks of chronic hypoxia. No statistically significant differences. n = 6 per group.

3.4.4 Cardiac substrate metabolism

Cardiac substrate metabolism was significantly modified by hypoxia, which increased cardiac glycolysis 2.3-fold ($p < 0.01$) and lactate efflux 2.2-fold ($p < 0.01$) compared to normoxic mice. Insulin-stimulated glycolytic flux was unchanged by hypoxia. Fatty acid oxidation was 27% lower in hypoxic mouse hearts compared to normoxic mice ($p < 0.05$) (Figure 3.5). Myocardial TAG content was 31% higher in hypoxic mice ($p < 0.05$), and myocardial FFA content was unaltered by hypoxia (Figure 3.5).

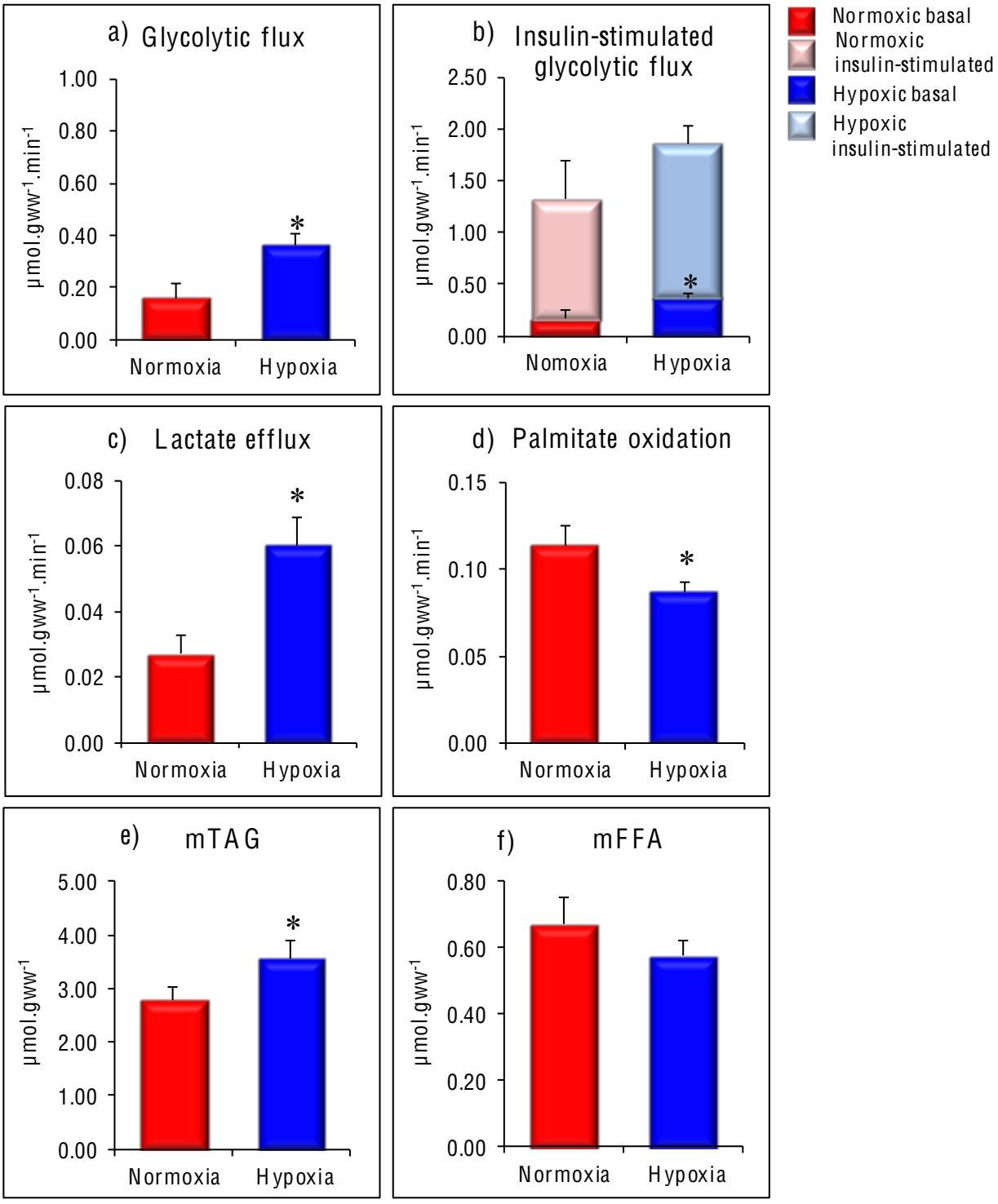

Figure 3.5 Cardiac substrate metabolism: a) Glycolytic flux, b) insulin-stimulated glycolytic flux, c) lactate efflux, d) palmitate oxidation, e) myocardial TAG (mTAG) content and f) myocardial FFA (mFFA) content in mice following 3 weeks of chronic hypoxia. *$p < 0.05$ relative to normoxic mice. n = 6 per group.

3.4.5 Cardiac high-energy phosphate metabolism

Cardiac high energy phosphate metabolism was assessed in the isolated perfused heart by ^{31}P NMR spectroscopy and HPLC. There was a mean cardiac PCr/ATP ratio of 1.96 ± 0.25 in normoxic mouse hearts, consistent with studies reporting PCR/ATP ratio measured by ^{31}P NMR at physiological heart rates in mice [176] and healthy human [101]. Cardiac phosphate metabolism was impaired following hypoxia. PCr/ATP ratio was reduced by 29% ($p < 0.01$). Cardiac phosphocreatine concentration, [PCr] was reduced by 31% ($p < 0.01$), with [ATP] unaltered. Total creatine, [TCr] was reduced by 28% ($p < 0.05$) and cytosolic free [ADP] was doubled ($p < 0.05$). However, the driving force of ATP hydrolysis, ΔG_{ATP}, was unchanged (Figure 3.6).

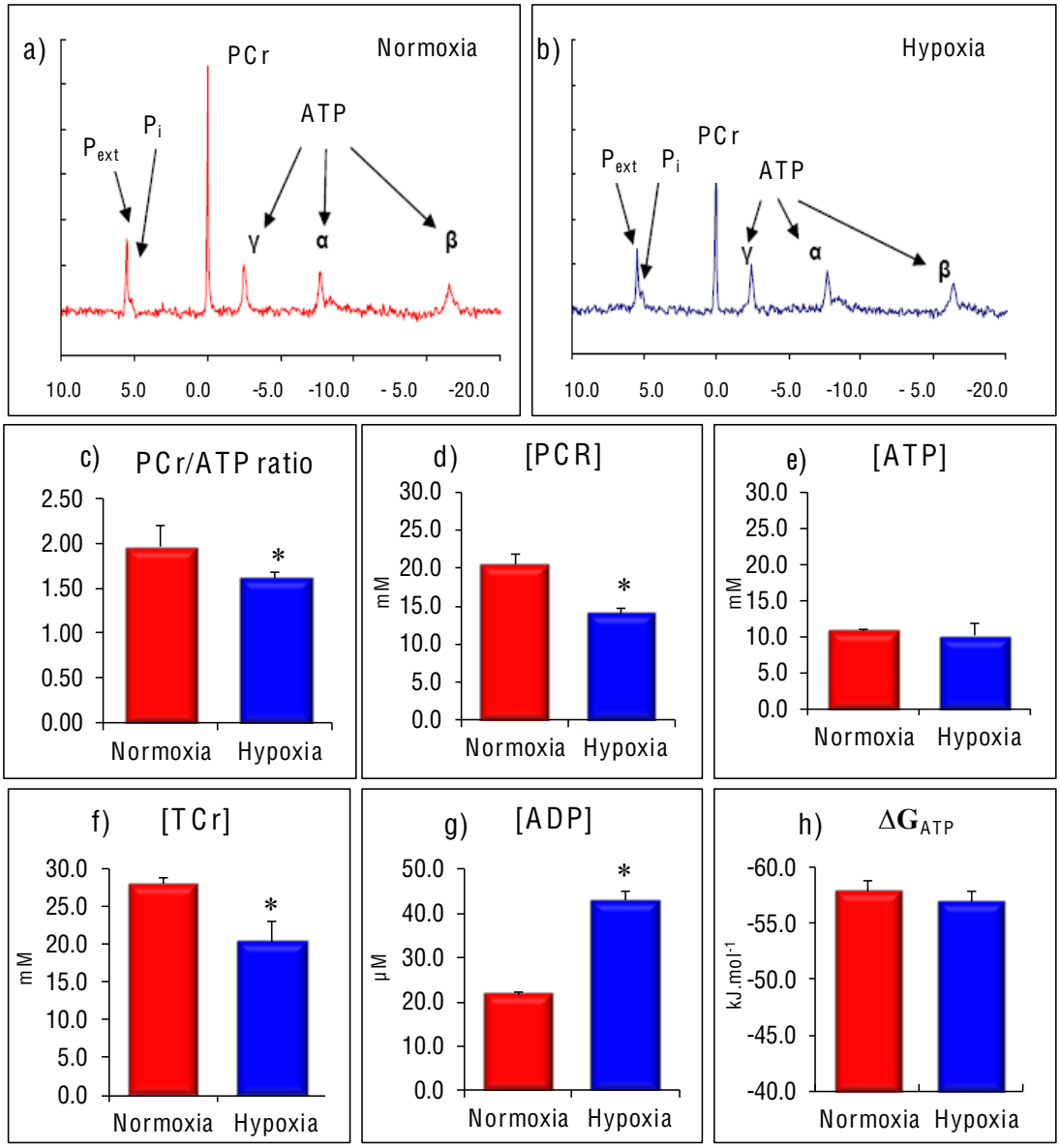

Figure 3.6 Cardiac high energy phosphate metabolism: Representative MR spectra in a) normoxic and b) hypoxic wild type mice. Cardiac c) PCr/ATP ratio, concentration of d) PCR, e) ATP, f) TCr, g) ADP and h) ΔG_{ATP} in mice following 3 weeks of chronic hypoxia. *$p < 0.05$ relative to normoxic mice. n = 5-7 per group.

3.4.6 Cardiac molecular profile

Please refer to Appendix 4 for western blot images (where applicable).

3.4.6.1 Hypoxia markers

Hypoxia increased cardiac VEGF protein levels 2.5-fold ($p < 0.05$) as a result of 46% ($p < 0.05$) increase in cardiac VEGF mRNA expression, and decreased SIRT1 protein levels by 31% in ($p < 0.05$).

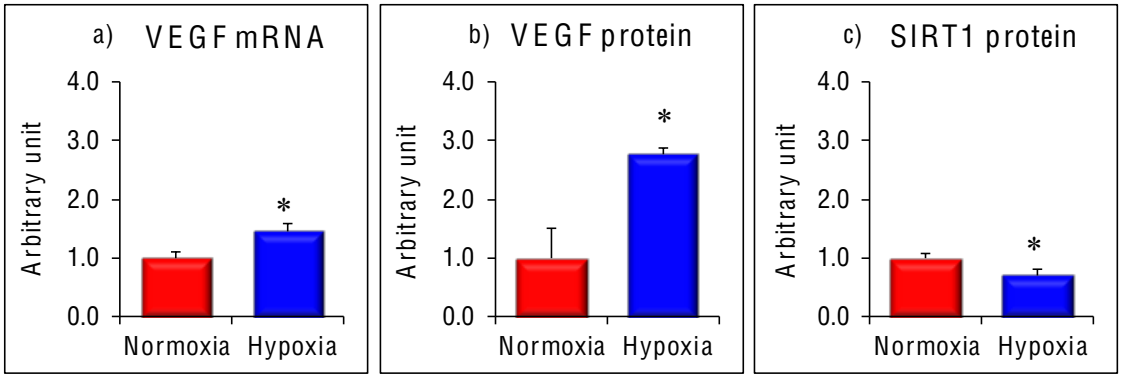

Figure 3.7 Cardiac hypoxia markers: a) VEGF mRNA expression, protein levels of b) VEGF and c) SIRT1 in mice following 3 weeks hypoxia. mRNA expression in cardiac tissues was normalized to the geometric mean of β-actin (housekeeping gene). *$p < 0.05$ relative to normoxic mice. $n = 6$ per group.

3.4.6.2 Glucose metabolism

Cardiac glucose transporter protein levels, GLUT1 and GLUT4, were unchanged by chronic hypoxia (Figure 3.8). Hypoxia increased PDK1 protein levels by 79% ($p < 0.05$) and conversely, decreased PDK4 protein levels by 28% ($p < 0.05$) (Figure 3.8). The activities of 2 glycolytic enzymes, pyruvate kinase and PGK1, were not affected by chronic hypoxia (Figure 3.8).

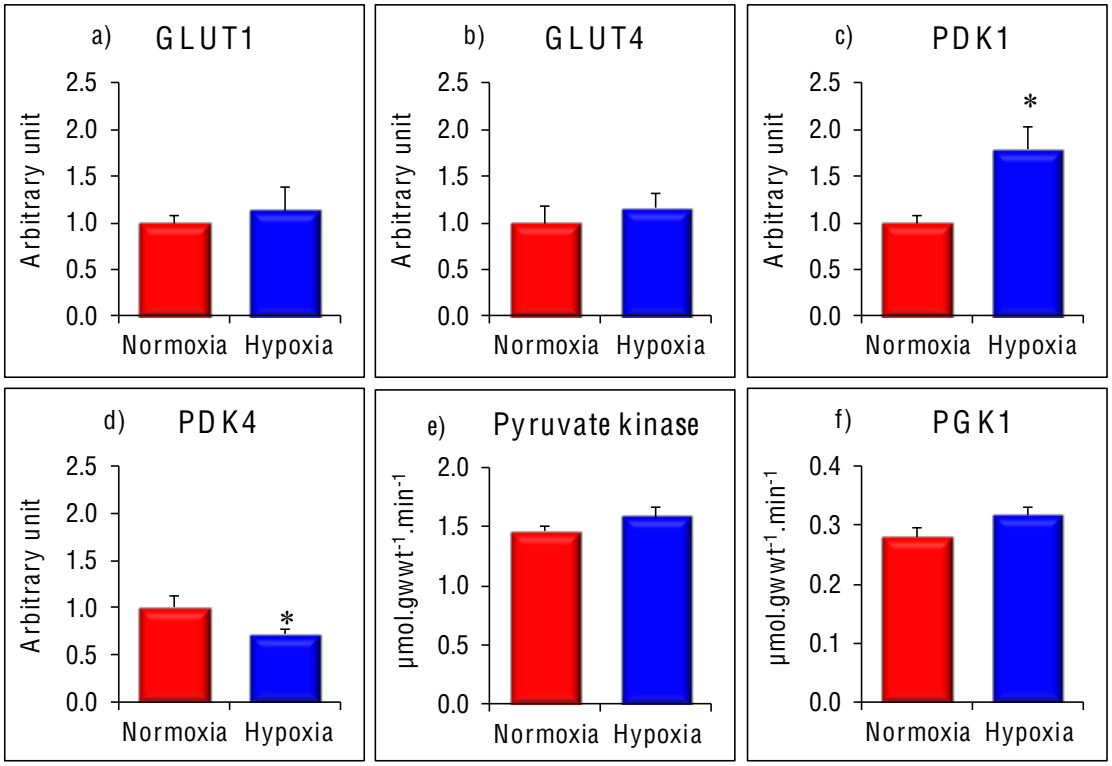

Figure 3.8 Glucose metabolism: Cardiac protein levels of glucose transporters, a) GLUT1, b) GLUT4, and pyruvate dehydrogenase kinase isoforms c) PDK1, d) PDK4 in normoxic and hypoxic mice. Cardiac glycolytic enzyme activities of d) pyruvate kinase and e) phosphoglycerate kinase 1(PGK1) in mice following 3 weeks of chronic hypoxia. *$p < 0.05$ relative to normoxic mice. n = 5-6 per group.

3.4.6.3 Mitochondrial proteins

Cardiac mitochondrial proteins, including PGC1α, citrate synthase and αKGDH were not affected by hypoxia (Figure 3.9). Similarly, hypoxia did not alter protein levels of complex I, II and IV of the electron transport chain (Figure 3.9)

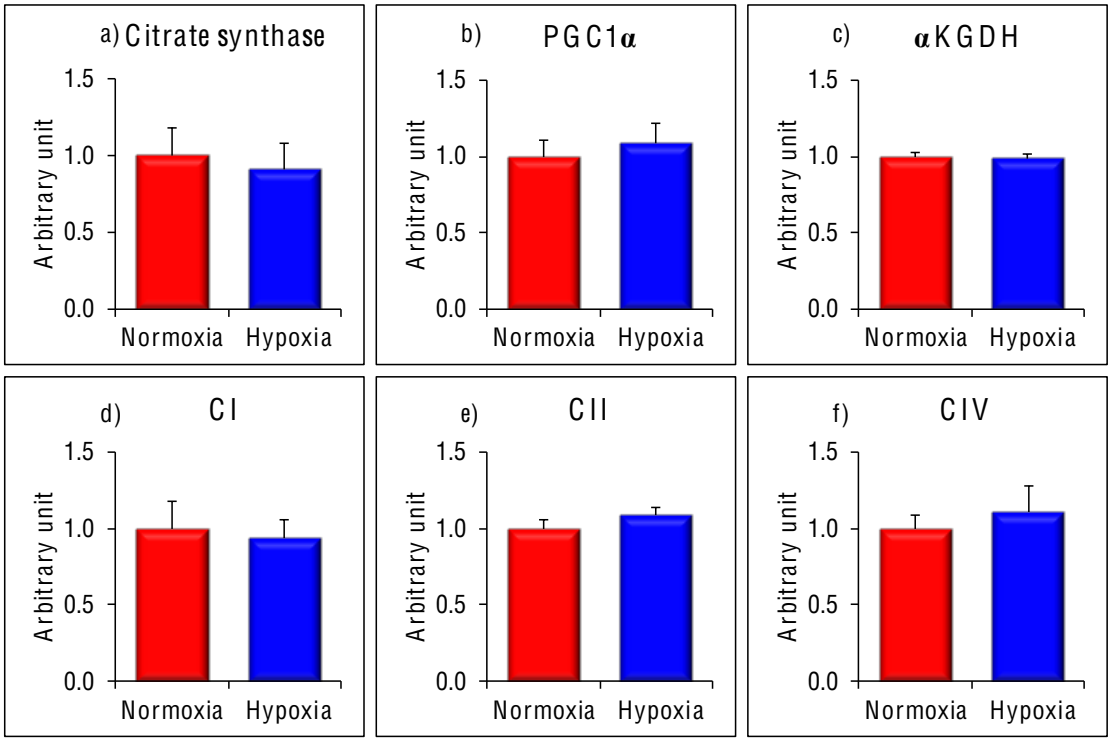

Figure 3.9 Cardiac mitochondrial proteins: a) Citrate synthase, b) PGC1α, c) αKGDH, d) CI, e) CII and f) CIV of the electron transport chain protein levels in mice following 3 of chronic hypoxia. No statistically significant differences. n = 5-6 per group.

3.4.6.4 Fatty acid metabolism

Protein levels of established downstream targets of PPARα involved in fatty acid metabolism were decreased with hypoxia. MCAD protein levels were 24% lower as a result of 33% reduction in its mRNA expression (Figure3.10). Hypoxia decreased cardiac UCP3 and MTE1 protein levels by 52% ($p < 0.05$) and 39% ($p < 0.01$), respectively (Figure3.10).

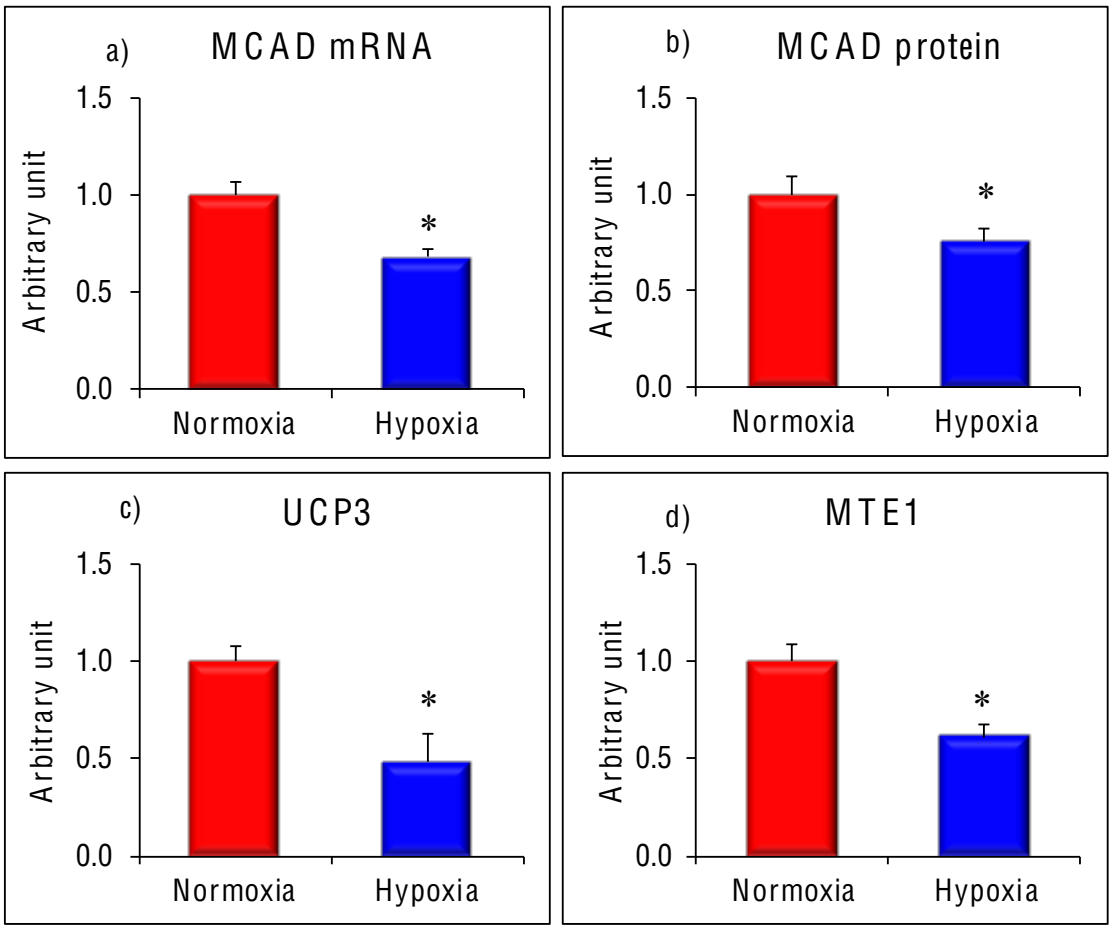

Figure 3.10 Fatty acid metabolism: Cardiac a) MCAD mRNA expression, protein levels of b) MCAD, c) UCP3, and d) MTE1 in mice following 3 weeks of chronic hypoxia. mRNA expression in cardiac tissues was normalized to the geometric mean of β-actin (housekeeping gene). *$p < 0.05$ relative to normoxic mice. n = 6-9 per group.

3.4.6.5 Cardiac PPARs activity

Hypoxic housing decreased cardiac PPARα mRNA expression by 36% ($p < 0.01$). However, protein levels of RXRα (PPARα obligate partner), were not significantly altered by hypoxia. PPARβ/δ and PPARγ mRNA expression was not altered by chronic hypoxia (Figure 3.11).

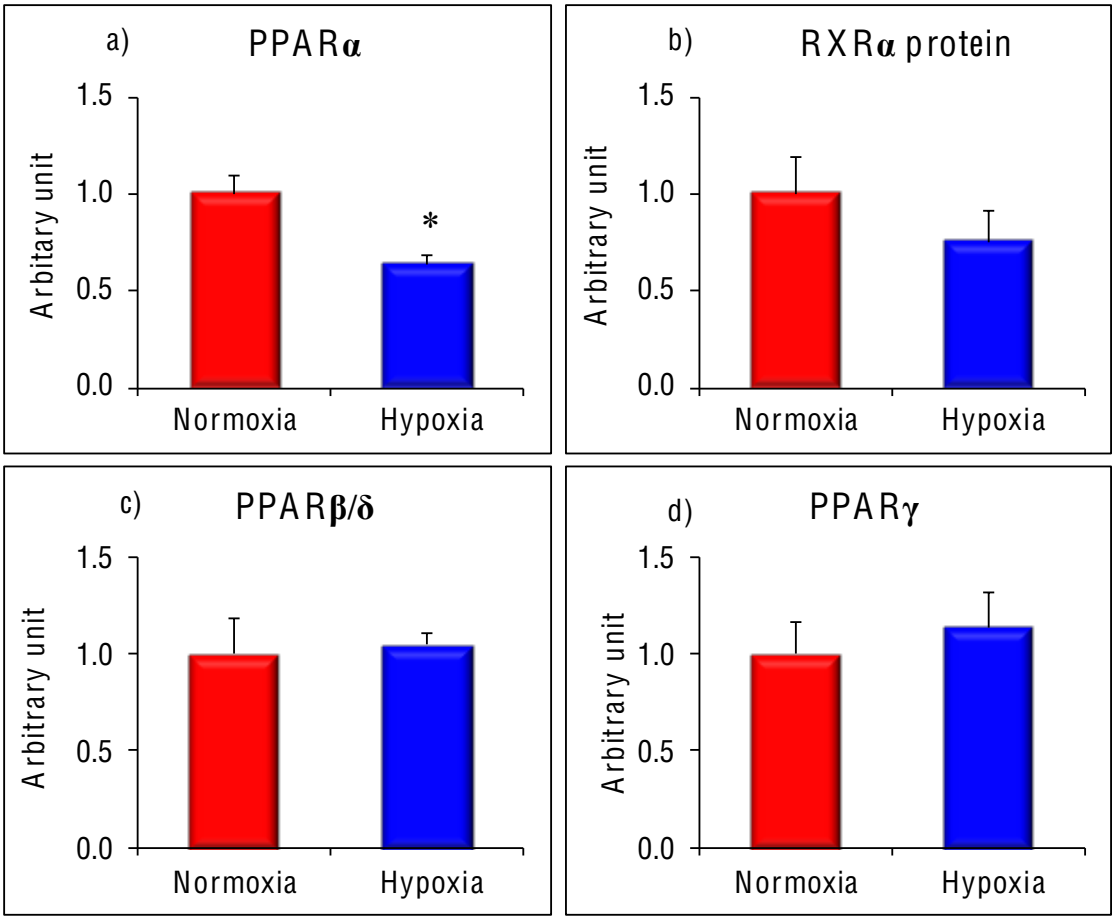

Figure 3.11 Cardiac PPAR isoforms: a) PPARα mRNA expression and its obligate partner b) RXRα protein levels, mRNA expression of c) PPARβ/δ and d) PPARγ in mice following 3 weeks of chronic hypoxia. mRNA expression in cardiac tissues was normalized to the geometric mean of β-actin (housekeeping gene). *$p < 0.05$ relative to normoxic mice. $n = 6$ per group.

Table 3.2: Summary of results

Data are means ± SEM. *p < 0.05 relative to normoxic wild type mice

	Normoxia	n	Hypoxia	n
Hypoxic physiology				
Food consumption (g.food.day^{-1})	2.76 ± 0.06	6	3.04 ± 0.23	5
Total calorie intake (kcal)	9.15 ± 1.44	6	10.0 ± 0.76	5
Energy intake (kcal.day.gbw^{-1})	0.29 ± 0.04	6	0.30 ± 0.01	5
Final body weight (g)	32.1 ± 0.60	22	31.3 ± 0.60	16
Haematocrit (%)	45.1 ± 0.70	22	60.4 ± 0.90*	16
Haemoglobin (g.dl^{-1})	11 .5± 0.40	22	16.7 ± 1.00*	16
Cardiac morphology and function				
LV mass (mg)	131.2 ± 3.50	22	106.4 ± 4.70 *	16
LVmass/body wt ratio (mg.g^{-1})	4.1 ± 0.20	22	3.4 ± 0.10 *	16
End-diastolic volume (µl)	64.2 ± 2.80	22	53.5 ± 4.00 *	16
End-systolic volume (µl)	24.6 ± 1.70	22	21.1 ± 2.80	16
Heart rate (bpm)	444 ± 10.0	22	495 ± 25.0	16
Stroke volume (µl)	39.6 ± 1.80	22	32.4 ± 2.10*	16
Cardiac output (ml.min^{-1})	17.4 ± 0.70	22	16.1 ± 1.60	16
Cardiac index (ml.min^{-1}.gbw^{-1})	0.54 ± 0.03	22	0.51 ± 0.04	16
Ejection fraction (%)	61.9 ± 1.90	22	61.1 ± 3.10	16
Plasma metabolites				
Glucose (mM)	9.93 ± 1.11	6	10.78 ± 0.89	6
TAG (mM)	2.59 ± 0.65	6	2.89 ± 0.30	6
FFA (mM)	0.36 ± 0.07	6	0.36 ± 0.05	6
Cardiac metabolism				
Glycolytic flux (µmol.gww.min^{-1})	0.16 ± 0.05	6	0.36 ± 0.04*	6
Insulin-stimulated glycolytic flux (µmol.gww.min^{-1})	1.15 ± 0.37	6	1.49 ± 0.18	6
Lactate efflux (µmol.gww.min^{-1})	0.03 ± 0.01	6	0.06 ± 0.01*	6
Palmitate oxidation (µmol.gww.min^{-1})	0.12 ± 0.01	6	0.09 ± 0.01*	6
Cardiac lipid content				
mTAG (µmol.gww^{-1})	2.78 0.25	6	3.63 ± 0.31*	6
mFFA (µmol.gww^{-1})	0.67 0.08	6	0.57 ± 0.44	6
Glycolytic enzymes				
Pyruvate kinase (µmol.gww^{-1}.min^{-1})	1.5 ± 0.04	6	1.58 ± 0.08	6
PGK1(µmol.gww^{-1}.min^{-1})	0.3 ± 0.01	6	0.32 ± 0.01	6
Cardiac high phosphate metabolites				
PCr/ATP ratio	1.96 ± 0.25	5	1.61 ± 0.07*	7
ATP (mM)	10.8 ± 0.11	5	10.0 ± 1.67	7
PCr (mM)	20.4 ± 1.48	5	14.0 ± 0.70*	7
TCr (mM)	28.0 ± 0.72	5	20.3 ± 2.71*	7
ADP (µM)	21.7 ± 0.61	5	43.0 ± 2.10*	7
ΔG_{ATP} (kJ.mol$^{-1)}$	1.96 ± 0.25	5	1.61 ± 0.07*	7

Table 3.2 (continued)

Cardiac mRNA expression (arbitrary unit)				
PPARα	1.00 ± 0.10	6	0.64 ± 0.05*	6
PPARβ/δ	1.00 ± 0.19	6	1.05 ± 0.06	6
PPARγ	1.00 ± 0.17	6	1.14± 0.18	6
MCAD	1.00 ± 0.07	6	0.67 ± 0.08*	6
VEGF	1.00 ± 0.10	5	1.46 ± 0.18*	5
Cardiac protein levels (arbitrary unit)				
SIRT1	1.00 ± 0.08	9	0.69 ± 0.10*	10
VEGF	1.00 ± 0.19	8	2.77 0.04	7
GLUT1	1.00 ± 0.09	5	1.13 ± 0.09	6
GLUT4	1.00 ± 0.18	6	1.15 ± 0.16	6
PDK1	1.00 ± 0.08	5	1.79 ± 0.20*	5
PDK4	1.00 ± 0.05	6	0.72 ± 0.05*	6
Citrate synthase	1.00 ± 0.18	5	0.91 ± 0.17	6
PGC1α	1.00 ± 0.11	5	1.09 ± 0.13	6
αKGDH	1.00 ± 0.03	5	0.99 ± 0.03	6
Complex I	1.00 ± 0.11	5	0.94 ± 0.11	6
Complex II	1.00 ± 0.06	5	1.08 ± 0.05	5
Complex IV	1.00 ± 0.09	5	1.11 ± 0.16	6
MCAD	1.00 ± 0.10	9	0.76 ± 0.07*	9
UCP3	1.00 ± 0.08	6	0.48 ± 0.14*	6
MTE1	1.00 ± 0.09	6	0.61 ± 0.06*	6
RXRα	1.00 ± 0.19	6	0.75 ± 0.17	5

3.5 DISCUSSION

3.5.1 Principal finding

In this study, a hypoxia protocol was developed of sufficient severity and duration to induce physiological hypoxia in mice. Chronic hypoxia resulted in metabolic adaptation in cardiac muscle, which maintained cardiac function, at least for the 3-week duration of the current study. Hypoxia shifted myocardial substrate preference towards glucose metabolism, with a concomitant decrease in fatty acid oxidation. At the molecular level, the metabolic adaptation appeared to be linked to a reduction in PPARα expression and subsequent reduction in protein levels of its downstream targets. This orchestrated metabolic strategy may have allowed the heart to maintain ATP production during chronic hypoxia.

3.5.2 Hypoxia protocol

The hypoxia protocol for mice induced adaptation period in the first week, as the oxygen level was decreased in daily steps from 21% to 11% before maintaining the oxygen concentration at 11%. During the initial period of acclimatisation, some mice experienced weight lost but eventually recovered after a week of hypoxic adaptation. In skeletal muscle, loss of muscle fibre and hence muscle mass is a component of hypoxic adaptation in order to reduce the diffusion distance for oxygen [177]. This is seen with increased capillary density [178] and stimulation of capillary growth from 3 weeks until 6 weeks of chronic exposure to 12% O_2 [179], hence increasing the capillary to fibre ratio in skeletal muscle. The reduction of body weight during the initial period is independent of food intake, as hypoxia in itself did not modify calorie intake. This is surprising considering the well-documented decrease in human

appetite and calorie consumption at high altitudes [180-182], but this was not observed in our study.

The work in this chapter was the first to investigate *in vivo* cardiac function and metabolism in intact mouse hearts, which incorporated an adaptation period in the hypoxia protocol. McClelland *et al.* [183, 184] adopted a similar hypoxia protocol, but looked at the effect of prolonged (8-10 weeks) high altitude acclimatisation on substrate metabolism in rat skeletal muscle. Rats exposed to chronic hypoxia (more than 2 weeks) in the absence of an adaptation period displayed right and left ventricular hypertrophy [146, 147, 149, 160]. Severe oxygen deprivation typically induces a functional overload of the right ventricle due to pulmonary hypertension, causing marked ventricular hypertrophy [185]. Our hypoxia protocol however, resulted in a reduction of left ventricular mass, consistent with human acclimatisation studies [186]. The hypoxic adaptation in the heart was similar to that observed in skeletal muscle, as increased capillary to fibre ratio has also been reported in hearts of rats subjected to 10% O_2 for 4 weeks [187].

Blood metabolite results indicated that the hypoxic mouse underwent the typical changes associated with chronic hypoxia. The hypoxia protocol raised haemoglobin and haematocrit levels comparable to the values reported in rodents [148, 149, 154] and humans [158], despite considerable variation in both duration (1-12 weeks) and severity (11%-14%) of hypoxia. Moreover, HIF upregulation was evident as cardiac VEGF, a prominent HIF downstream target [132, 188] was increased 3-fold at both mRNA and protein levels. Together, these data suggest that the protocol produced

graded hypoxia and morphological changes consistent with those in human hypoxia, in addition to being well tolerated by the mice.

3.5.3 Cardiac function and metabolism

Wild type mice had compensated cardiac function, and maintained cardiac output and ejection fraction following 3 weeks exposure to chronic hypoxia, consistent with other reports from more severe levels of oxygen restriction in the heart [186, 189]. In humans, post-hypoxic LV cardiac function is considered to scale to body mass [190]. This has shown that despite a reduction in left ventricular mass, cardiac index, a measure of the ability of the heart to supply blood to peripheral tissues, and LV ejection fraction, the amount of blood discharged with each cardiac cycle, were normal.

Experiments from the isolated heart found that hypoxia induced a metabolic switch away from fatty oxidation towards the glycolytic pathway of producing energy, consistent with the molecular evidence in current literature [120]. PPARα has been shown to negatively correlate with blood haemoglobin content in high altitude tolerant humans [191], hypoxic animal models [146, 148] and simulated chemical systemic hypoxia [154]. However none of these studies examined the consequences of this alteration to metabolic flux. Here, the reduction in fatty acid metabolism corresponded to the decrease in PPARα mRNA expression measured in hypoxic mouse hearts. Since PPARα activity is known to affect cardiac lipid metabolism [53] the reduction in PPARα seen with chronic hypoxia possibly decreased palmitate oxidation via its downstream control of MCAD protein [70]. Myocardial triglyceride was also elevated by hypoxia, possibly as a consequence of reduced fatty acid

utilisation through β-oxidation [23]. Therefore, PPARα may be involved in the partitioning of this lipid, by regulating the mobility of cardiac triglyceride stores as a source of β-oxidation [192] as well as controlling expression of β-oxidation genes.

This is the first report of increased glycolytic flux in mouse hearts exposed to chronic hypoxia, in agreement with *in vitro* studies reporting augmented glycolytic capacity in various mammalian cells [136, 193, 194]. The increase in net lactate efflux was proportional to the increase in glycolytic flux with hypoxia, showing that the ratio of lactate production to glucose intake was still maintained, suggesting unchanged glucose oxidation rate. The balance between glycolysis and glucose oxidation with hypoxia, *in vivo*, is not well established and the involvement of PDK isoforms in regulating PDH flux under limited oxygen supply are not well defined. There was a decrease in cardiac PDK4, in agreement with other hypoxia studies [146, 154], identifying PDK4 as a PPARα downstream target, as documented by others [75]. In contrast, HIF potentially mediated the increase in PDK1 with hypoxia *in vitro*, decreasing mitochondrial respiration [137, 195]. Here, increased cardiac PDK1 observed in the hypoxic mice was possibly as a result of HIF activation, but its direct effect on glucose oxidation in vivo is yet to be determined, which serves as a limitation to this study. Elevated HIF levels in the peri-infarct region in rats also increased GLUT1 and haemoxygenase-1 levels, both of which are known HIF regulated proteins [144]. Increased GLUT 1 and GLUT 4 with hypoxia were reported in some studies [150, 196]. However, in the present study, there were no significant difference in glucose transporters and glycolytic enzyme levels in the hypoxic mouse hearts. It is possible that the increase in glycolysis was mediated by an increase in translocation of GLUT4 vesicles to the sarcolemma. Translocation mechanism in

response to stimulation by insulin, or by AMP-activated protein kinase, has been suggested to act in hypoxia [197].

The benefit of increased glucose utilisation under hypoxic conditions may be limited; although the switch from fatty acids as an energy source to the exclusive use of glucose is calculated to increase the efficiency of ATP production by 12–14% [21], a complete substrate switch is unlikely to occur. Indeed, a larger fall of cardiac efficiency (20-40%) driven by increased in oxygen consumption has been attributed to increased mitochondrial uncoupling by UCP3 secondary to elevation of fatty acid [198, 199]. UCP3, via PPARα control [71, 85] was decreased by hypoxia, parallel to the metabolic shift away from fatty acid oxidation. Essop *et al.* demonstrated that the decrease in cardiac UPC3 levels following 11% hypoxic exposure for 7 days does not affect overall mitochondrial efficiency of oxidative phosphorylation, but decreased oxygen consumption in isolated left ventricular mitochondria by 16% [200]. The reduction in UCP3 with hypoxia may serve to increase mitochondrial efficiency of ATP production, assuming that respiration is reduced with hypoxia. MTE1 is proposed to act in concert with uncoupling protein UCP3 [73, 94]. Therefore, decreased mitochondrial uncoupling via decreased PPARα, is potentially a component of the hypoxic metabolic adaptation of the heart.

Despite apparent hypoxic adaptation, the PCr/ATP ratio was decreased in chronically hypoxic hearts as a result of reduced phosphocreatine levels, with a subsequent increase in cytosolic ADP. Phosphocreatine acts as a high-energy phosphate reserve to maintain ATP at levels sufficient to support contractile function [1], and in humans, the decrease in PCr/ATP ratio following hypoxic exposure did not appear to

have any long term detrimental effects [159]. Decreased PCr/ATP with hypoxic exposure has been reported previously in isolated perfused hearts [160, 161], but complete quantitative analysis of phosphate metabolism has not been coupled with cardiac ^{31}P NMR spectroscopy data with a physiological balance of substrates. Here, the fall in PCr/ATP is consistent with a shift away from fatty acid towards glucose utilisation as glycolysis can only provide limited amounts of energy, compared to fatty acid oxidation [21]. Despite the changes in phosphate metabolism, the driving force of ATP hydrolysis, ΔG_{ATP}, was not significantly altered with hypoxia. This is as a result of a large change in total creatine, the cause of which is unknown, but may reflect the changes in left ventricular morphology with chronic hypoxia. These data suggest, in this particular hypoxic protocol at least, metabolic reprogramming was sufficient to maintain ATP production and function.

Cardiac protein levels of electron transport chain (ETC) complexes in our study were not altered following chronic hypoxia. Previous work in our lab has shown that in rats exposed to 3 weeks of chronic hypoxia, the two distinct populations of mitochondria, SSM and IFM downregulated cardiac mitochondrial respiration and in SSM, this was as a result of decreased ETC complexes I, II and IV activities, but not at protein levels [201]. Moreover, the unchanged levels of integral mitochondrial proteins, citrate synthase, PGC1α and α-ketoglutarate dehydrogenase indicates that overall cardiac mitochondrial content was not modified following 3 weeks of hypoxia. Green *et al.* determined that muscle oxidative potential was lower in skeletal muscle of human subjects exposed extreme altitude simulation of 8300 metres[202]. This decline has also only been found following extreme hypobaric hypoxia in rodent studies; Cervos Navarro *et al.* reported myocardial mitochondrial mass was decreased

in rats exposed to 7% O_2 for 17 days [203], suggesting that only a severe hypoxic insult would result in distinct mitochondrial functional changes.

Neither PPARβ/δ or PPARγ were altered with chronic hypoxia. The relationship between PPAR β/δ and hypoxia has not been suggested, but in pathological cardiac hypertrophy, where hypoxia may be a component of metabolic remodelling, PPARγ is upregulated [204], but this was not implicated in our moderate hypoxia protocol. Reduced PPARα activity was observed in epithelial cells after 6 and 18 hours exposure to 5% O_2 [205] and in chemically-induced hypoxic cancer cells [206], without affecting PPARγ expression. Therefore, our data suggest that the cardiac metabolic adaptation during chronic hypoxia is regulated by PPARα, independent of other cardiac PPAR isoforms.

3.5.4 **Upstream regulation of PPARα**

Cardiac VEGF, an established downstream marker of HIF-1α stabilisation [132, 188] was elevated several-fold after 3 weeks of hypoxia. Together with the apparent increase in PDK1, the decrease in PPARα observed may indicate a HIF-mediated response; however, the data is not conclusive. It has been suggested that hypoxia decreased RXR via a HIF-independent mechanism [207], but cardiac RXRα was not significantly affected by hypoxic exposure in this study.

SIRT1 has also been recently implicated in mediating the hypoxic response in various tissues. Lim *et al.* found that HIF-1 signalling is repressed by SIRT1 in a range of mouse cells and tissues and such repression is relieved during chronic hypoxia, due to inhibition of SIRT1 by an increase in cellular NAD^+ levels [208]. Conversely,

increased expression of SIRT1 during hypoxia may selectively augment HIF-2α levels rather than affecting HIF-1α levels [209]. The exact role played by sirtuins in hypoxia is unclear. In addition, SIRT1 may act in association with PPARα to protect the heart from hypertrophy, metabolic dysregulation, and inflammation [210]. SIRT1 protein levels were significantly decreased with hypoxia, which may suggest that it acts as an intermediary regulator between PPARα and hypoxia.

In summary, the work in this chapter has shown that the heart metabolically adapted in response to chronic hypoxia. This was associated with changes in a series of proteins known to control cardiac metabolic flux and under PPARα control. The fall in PPARα expression, in the absence of changes of other PPAR isoforms, suggests that PPARα concerted the metabolic changes in response to chronic hypoxia. The net effect of the metabolic reprogramming was sufficient to maintain cardiac ATP production and thus normal contractile function. The extent of PPARα involvement in cardiac metabolic changes in chronic hypoxia was investigated in the following chapters.

CHAPTER 4

INVOLVEMENT OF PPARα IN CARDIAC ADAPTATION TO CHRONIC HYPOXIA

4.1 ABSTRACT

In chapter 3, it was implicated that PPARα, via its downstream control of cardiac metabolism, was involved in cardiac metabolic adaptation to hypoxia. The aim of this chapter was to further establish the link between hypoxia and PPARα. Fatty acids are natural ligands for PPARα - here, PPARα expression was stimulated using high fat feeding. *In vivo* cardiac function, substrate metabolism and high-energy phosphate metabolism were assessed in hearts exposed to high fat feeding with or without exposure to chronic hypoxia. Wild type animals were fed a high fat diet vs. ordinary chow pellets and exposed to 3 weeks of normoxia or hypoxia. High fat feeding under normoxia had no effect on cardiac function, but the combination of high fat feeding plus hypoxia decreased cardiac output by 25% ($p < 0.01$) and ejection fraction by 12% ($p < 0.05$) respectively, compared to normoxic chow fed mice. High fat feeding increased PPARα mRNA expression 1.5-fold ($p < 0.05$) irrespective of oxygen availability, overriding the fall in PPARα expression with hypoxia, while PPARβ/δ and PPARγ activity remained unchanged. This resulted in a 17% increase in palmitate oxidation ($p < 0.05$), with PPARα downstream targets, MCAD mRNA expression and protein levels increased 1.5-fold ($p < 0.05$), while both UCP3 and MTE1 protein levels doubled ($p < 0.05$) in all high fat fed mice hearts. Glycolytic flux and lactate efflux were unchanged with high fat feeding in both normoxia and hypoxia. Cardiac PCr/ATP ratio was not changed with high fat feeding relative to chow fed mice, but was decreased by 25% ($p < 0.01$) with hypoxia. ΔG_{ATP} was significantly lower with high fat feeding, irrespective of oxygen exposure ($p < 0.05$). Cardiac VEGF mRNA and protein levels were unaltered in hypoxia with high fat feeding, suggesting impaired HIF regulation. In conclusion, feeding a high fat diet under hypoxic conditions prevented metabolic adaptation to hypoxia, with cardiac substrate metabolism similar to that of normoxic high fat fed mice. With scarce oxygen supply, the increase in UCP3 may have decreased the efficiency of mitochondrial ATP synthesis and led to impaired cardiac function following chronic hypoxia.

4.2 INTRODUCTION

PPARα plays a central role in the regulation of cellular lipid metabolism in tissues with high capacity for fatty acid oxidation, such as heart, brown adipose tissue, slow-twitch skeletal muscle, and liver [57, 63, 70]. Alteration of cardiac metabolism may hence occur via modulation of PPARα expression. The observation that the failing heart displays cardiac metabolic abnormalities [16, 103] has sparked much interest on the effect of PPARα modulation on cardiac diseases. Due to PPARα's large hydrophobic ligand-binding sites, they can be activated by diverse compounds and pharmacological analogues [53]. The first recognised PPARα activators were synthetic agents, including clofibrate and pharmacological agonist, WY-14,643 [54] while fatty acids have been identified as the natural ligand for PPARα [61, 63].

Transgenic mice that overexpress PPARα in a cardiac-specific manner, under the control of the myosin heavy chain (MHC) promoter (MHC-PPARα mice) have impaired cardiac function [211, 212]. MHC-PPARα mice also have abnormal metabolism, with a 1.5-fold increase in myocardial fatty acid oxidation, 3-fold decrease in glucose uptake and exhibit triglyceride and ceramide accumulation, and cardiac hypertrophy that was exacerbated by high fat feeding [211, 212]. The abnormalities in cardiac metabolism appear to impair recovery of cardiac function when subjected to ischaemic-reperfusion injury [213]. These studies suggest that increased PPARα expression can be deleterious to cardiac metabolism and function.

The failing heart shows decreased expression of genes involved in fatty acid metabolism and transcriptional changes in PPARα at both mRNA and protein levels [103, 174]. These changes may potentially be adaptive, but this remains inconclusive.

PPARα expression was decreased by 26% in rat models of pressure overload-induced hypertrophy, and subsequent pharmacological reactivation of PPARα by WY-14,643 caused severe contractile dysfunction [214], suggesting that PPARα downregulation is essential for the maintenance of contractile function in the hypertrophied heart. This is consistent with studies that found beneficial effects of pharmacological inhibition of β-oxidation, through CPT1 inhibition with etomoxir in animals [215, 216] and in humans [217]. In contrast, pharmacological stimulation of PPARα had no adverse effect in a rat model of post-infarction heart failure; 12 weeks administration of the PPARα agonist fenofibrate upregulated fatty acid metabolic pathway and caused LV hypertrophy but did not worsen LV function [218].

Apart from pharmacological activation of PPARα, numerous studies have also investigated the effect of dietary manipulation of PPARα via high fat feeding on cardiac metabolism and function. High fat feeding (45% kcal from fat) for 5 weeks have been shown to increase palmitate oxidation by 33%, with a concomitant 50% decrease in glycolysis and increased the expression of PPARα target genes including, MCAD, UCP3, MTE1 and PDK4 [219]. Despite the apparent switch towards fatty acid metabolism, high fat feeding alone does not appear to affect cardiac morphology nor have detrimental effect on cardiac function after 3 weeks (55% kcal from fat) [199], 10 weeks (60% kcal from fat) [220], 12 weeks [221] and even up to 14 months of moderately high fat feeding (30% kcal from fat) [222]. The effect of high fat feeding on animal models of pressure overload hypertrophy and established heart failure however, are inconsistent. Chess *et al.* demonstrated that high fat feeding (60% kcal from fat) for a prolonged duration of 16 weeks did not exacerbate the hypertrophic response to transverse aortic constriction (TAC) or alter ejection fraction

compared to mice fed on low fat diet [223]. Similarly, high fat feeding (60% kcal from fat) for 8 weeks [224], 12 weeks (45% kcal from fat) [218] and 16 weeks [225] in rats subjected to coronary ligation (infarct models of heart failure) did not worsen LV dysfunction despite elevated plasma FFA and triglycerides. This is surprising as elevated plasma FFA is a strong predictor of sudden cardiac death in patients undergoing coronary angiography [226]. Similarly, accumulation of lipids and their derivatives in the heart is associated with cardiac dysfunction and 'lipotoxicity', which was described as a potential causative factor for the progression of heart failure [227]. In support, Raher *et al.* reported that mice subjected to TAC and high fat feeding (60% kcal from fat) for 4 weeks demonstrated greater hypertrophy, marked LV systolic and diastolic dysfunction, and decreased survival compared with chow fed mice subjected to TAC [228]. The exact mechanisms for these observations are still not well understood. The variation in cardiac outcomes may be related to temporal effects or the degree of cardiac dysfunction induced by various surgical procedures. It is possible that different aetiologies of heart failure, such as ischaemia, or pathological hypertrophy, differentially effect cardiac substrate metabolism and respond differently to pharmacological or dietary activation of PPARα. Given that hypoxia maybe a component of many cardiac diseases [139], this study aimed to investigate the link between the hypoxic myocardium and PPARα activity on cardiac metabolism and function, independent of cardiac diseases. In this chapter the role of PPARα during hypoxic adaptation is further defined by stimulating PPARα activity using high fat feeding.

4.2.2 Study aim

The work from the previous chapter demonstrated that PPARα was involved in maintaining the balance between glucose and fatty acid utilisation during chronic hypoxia, and preserved cardiac function. Since the alteration of cardiac metabolism may occur via modulation of PPARα expression, the goal of this study was to further define the role of PPARα in hypoxic adaptation by examining the changes in cardiac function, energetics and metabolism in high fat fed mice exposed to chronic hypoxia. Moreover, the effect of dietary manipulation targeting the PPARα pathway on cardiac metabolism, in combination with function in an intact hypoxic heart, is lacking. It is hypothesised that the high-fat diet would increase UCP3 levels, uncoupling respiration and impairing cardiac function in the hypoxic heart.

4.3 METHODS

Wild type mice were fed with high-fat diet or ordinary chow pellets and exposed to 3 weeks of normoxia and hypoxia. Standard laboratory chow had Atwater fuel energy (AFE) of 3.3 kcal/g, with 7.5% fat, 17.5% protein and 75% carbohydrate. The custom-produced high-fat diet had an AFE of 5.1 kcal/g, with 55% fat, 29% protein and 16% carbohydrate (Appendix 5). Food intake and body weights were monitored daily.

Methods have been described in Chapter 2. Briefly, *in vivo* cardiac morphology and function were measured using multi-slice cardiac MRI. Hearts were excised and perfused in Langendorff mode for measurement of glycolytic flux and palmitate oxidation rates using ^{3}H labeled substrates. High-energy phosphate metabolites were measured using ^{31}P MRS in isolated perfused hearts. Following perfusion, hearts were freeze-clamped in liquid nitrogen for molecular analysis. Whole cell lysates from powdered frozen heart were used to measure protein levels of MCAD, UCP3, MTE1, GLUT4, PDK4, RXR, and SIRT1. mRNA expression of VEGF, MCAD, PPARα, PPARβ/δ and PPARγ was quantified using qRT-PCR. VEGF protein levels were quantified using ELISA. Cardiac lipids were extracted from freeze clamped tissues, using chloroform: methanol solution, for the measurement of myocardial TAG and FFA content.

Whole cell lysates from powdered frozen gastrocnemius were used to measure protein levels of UCP3, MTE1, and PDK4.

4.4 RESULTS

Results for normoxic and hypoxic chow fed mice presented in Chapter 3, are shaded in grey to represent the control groups in this chapter.

4.4.1 Effect of chronic hypoxia and high fat feeding on mouse physiology

Food consumption was not modified by high fat feeding (Figure 4.1). However, due its higher calorie content, high fat diet resulted in a 30% increase in energy intake ($p < 0.05$). This did not result in an increase in body weight in normoxic mice, and body weight in hypoxic high fat fed mice was 11% lower than normoxic mice fed a chow diet ($p < 0.05$).

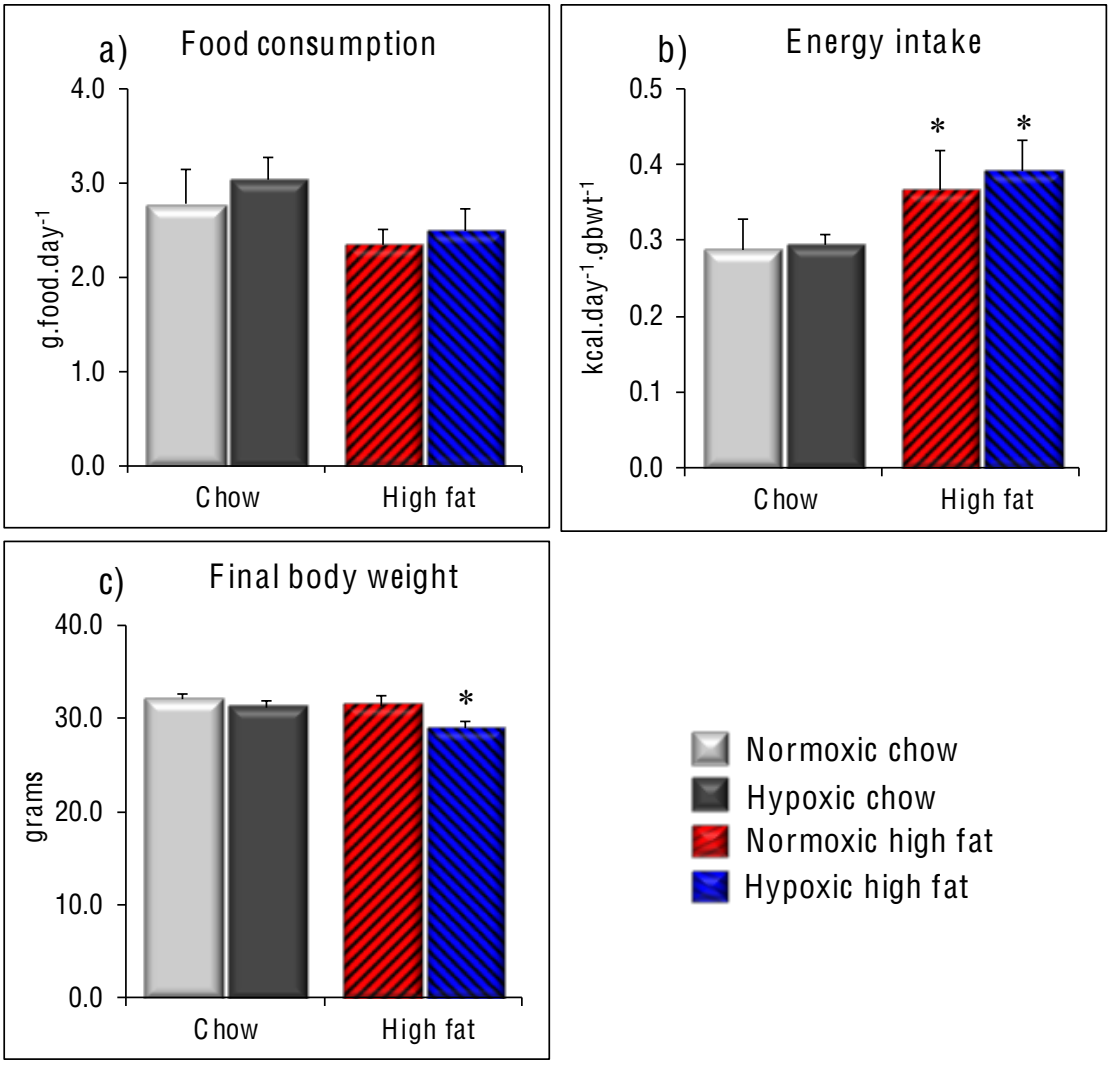

Figure 4.1 Effect of chronic hypoxia and high fat feeding on mouse physiology: a) Food consumption, b) energy intake and c) final body weight in chow and high fat fed mice following 3 weeks of chronic hypoxia. *$p < 0.05$ relative to normoxic chow fed mice. n = 6-22 per group

4.4.2. *In vivo* cardiac morphology

Hypoxia significantly reduced left ventricular mass in both chow and high fat fed mice ($p < 0.01$). However, when corrected for body weight, left ventricular mass was not changed by hypoxia in high fat fed mice (Figure 4.2).

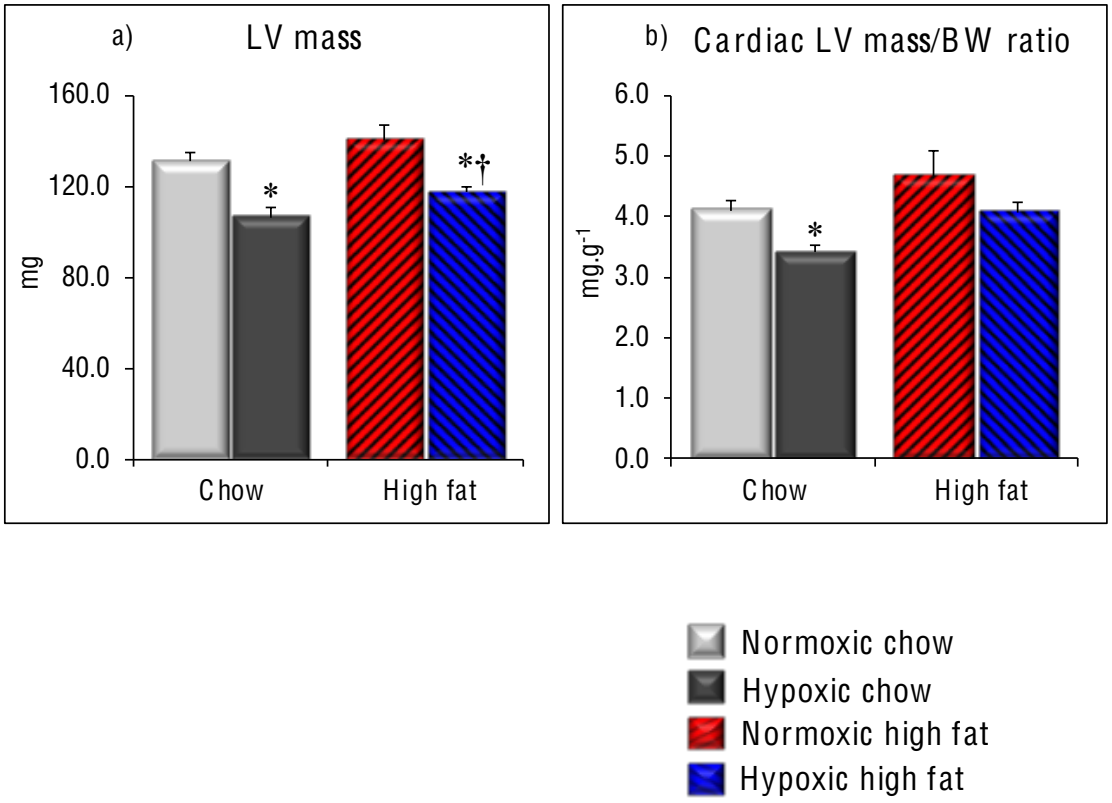

Figure 4.2 Effect of chronic hypoxia and high fat feeding on cardiac morphology: a) Cardiac LV mass and b) Cardiac LV mass / body weight (BW) ratio in chow and high fat fed mice following 3 weeks of chronic hypoxia. *$p < 0.05$ relative to normoxic chow fed mice, †< 0.05 relative to normoxic high fat fed mice. n = 6-22 per group.

4.4.3. *In vivo* cardiac function

High fat feeding under normoxic conditions had no effect on cardiac function. However, feeding a high fat diet under hypoxic conditions resulted in marked abnormalities in cardiac function. Despite a higher heart rate, cardiac output was reduced by 24% ($p < 0.05$) in hypoxic high fat fed mice relative to both normoxic chow, and high fat fed mice. This was as a consequence of 33% lower stroke volumes ($p < 0.01$) and a 25% reduction in EDV ($p < 0.01$) in hypoxic high fat fed mice (Figure 4.3.1). Hypoxia plus high fat feeding reduced cardiac index and ejection fraction by 15% ($p < 0.05$) and 12% ($p < 0.05$) respectively relative to normoxic chow fed mice (Figure 4.3.2).

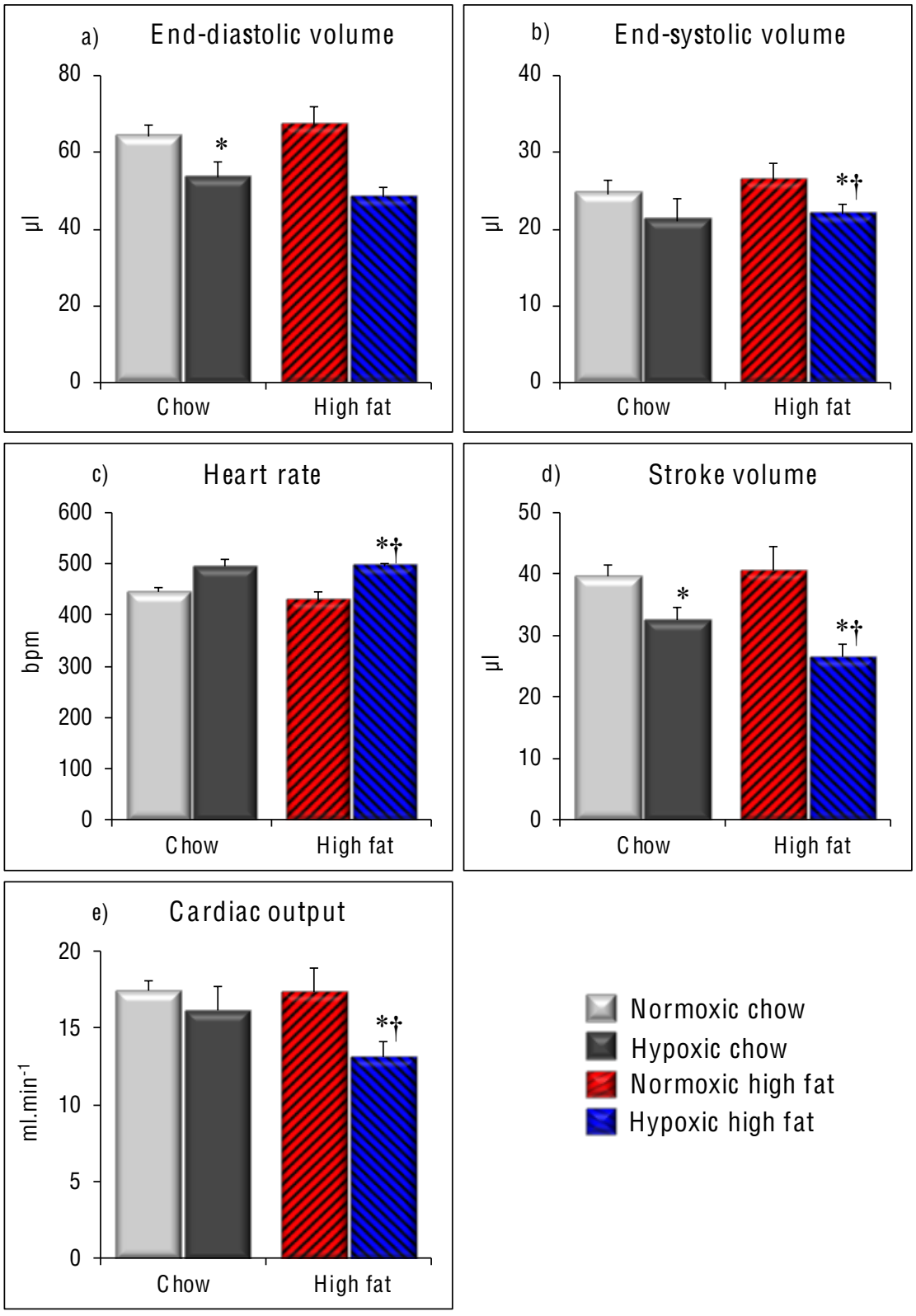

Figure 4.3.1 Effect of chronic hypoxia and high fat feeding on *in vivo* cardiac function: a) End-diastolic volume, b) end-systolic volume, c) heart rate, d) stroke volume and e) cardiac output in chow fed and high fat mice following 3 weeks of chronic hypoxia. *p < 0.05 relative to normoxic mice. † < 0.05 relative to normoxic high fat fed mice. n = 6-22 per group.

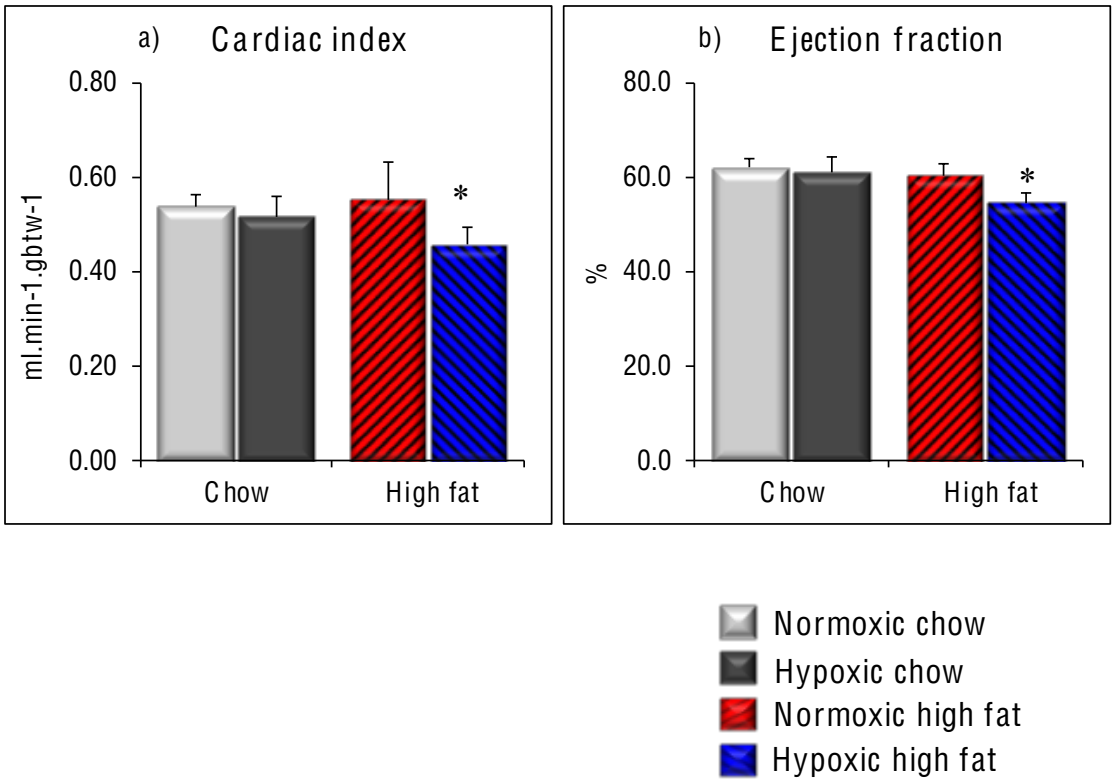

Figure 4.3.2 Effect of chronic hypoxia and high fat feeding on *in vivo* cardiac function: a) Cardiac index and b) ejection fraction in chow and high fat fed mice following 3 weeks of chronic hypoxia. *$p < 0.05$ relative to normoxic chow fed mice. n = 6-22 per group.

4.4.4 Plasma metabolites

The short duration of high fat feeding did not significantly alter plasma glucose, triacylglycerol and free fatty acids concentration in both normoxia and hypoxia (Figure 4.4).

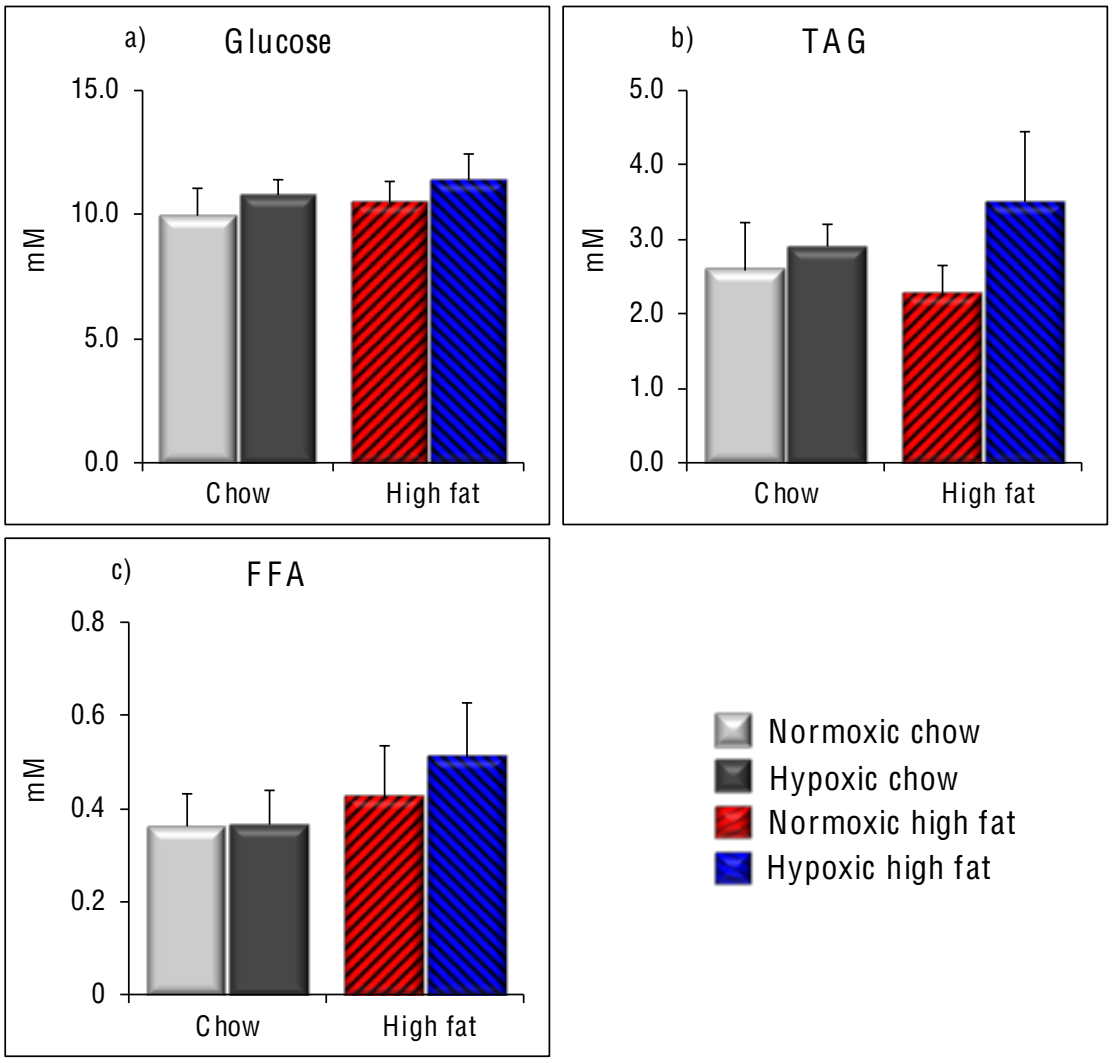

Figure 4.4 Plasma metabolites: Plasma concentration of a) glucose, b) triacylglycerol (TAG) and c) free fatty acids (FFA) in chow and high fat fed mice following 3 weeks of chronic hypoxia. No statistically significant differences. n = 6 per group.

4.4.5 Cardiac substrate metabolism

High fat feeding for 3 weeks in normoxia resulted in a 17% increase in fatty acid oxidation ($p < 0.02$), with unchanged glycolytic flux and net lactate efflux (Figure 4.5). Feeding a high fat diet under hypoxic conditions also increased fatty acid oxidation by 26% ($p < 0.02$) and similarly, did not alter glycolytic flux and lactate efflux. High fat feeding increased myocardial TAG by 1.8 fold ($p <0.01$) and 1.6-fold ($p < 0.02$) in normoxic and hypoxic mouse hearts respectively. Myocardial FFA was the same in all mouse hearts (Figure 4.5).

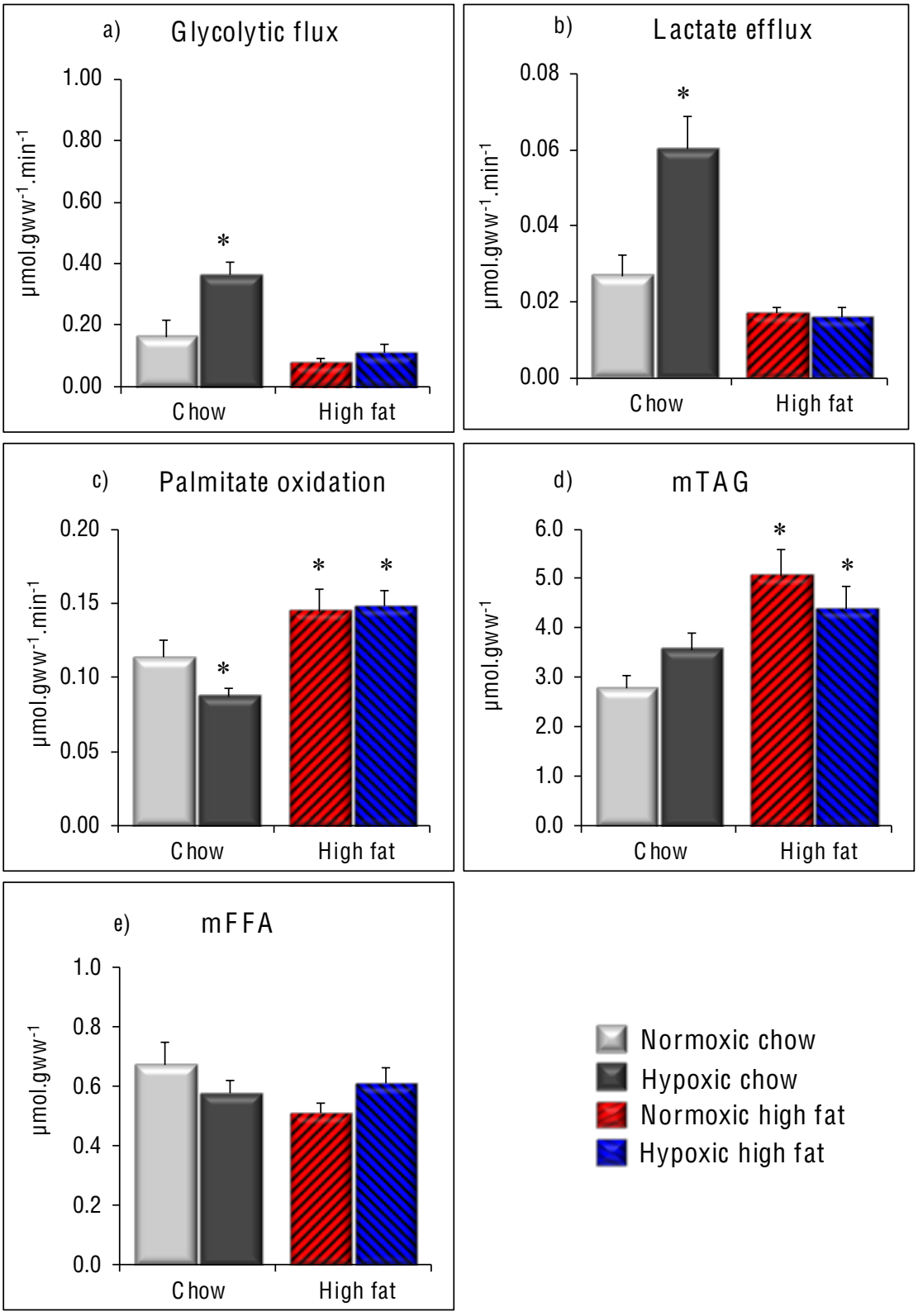

Figure 4.5 Cardiac substrate metabolism: a) Glycolytic flux, b) lactate efflux, c) palmitate oxidation, myocardial d) TAG and e) FFA content in chow and high fat fed mice following 3 weeks of chronic hypoxia. *$p < 0.05$ relative to normoxic chow fed mice. n = 6-8 per group.

4.4.6 Cardiac high-energy phosphate metabolism

Cardiac high energy phosphate metabolism was assessed in the isolated perfused heart by ^{31}P NMR spectroscopy and HPLC. High fat feeding alone did not alter the PCr/ATP ratio, but high fat feeding plus hypoxia reduced the PCr/ATP ratio by 25% ($p < 0.01$) (Figure 4.6). ATP concentration, [ATP] was unchanged in normoxic high fat fed mice, but was decreased by 31% in hearts from hypoxic high fat fed mice ($p < 0.05$). Cardiac phosphocreatine, [PCr] was decreased by high fat feeding by 30% ($p < 0.05$) and 35% ($p < 0.01$) in both normoxic and hypoxic mouse hearts respectively, compared to normoxic chow fed mice, but total creatine, [TCr] was decreased by 38% ($p < 0.05$) only in hypoxic high fat fed. Cytosolic [ADP] was 55% higher in normoxic high fat fed mice, and was increased by 2-fold and 38% in hypoxia compared to normoxic chow and high fat fed mice respectively. High fat feeding decreased ΔG_{ATP} by 3% in both normoxic and hypoxic mouse hearts ($p < 0.05$) (Figure 4.7).

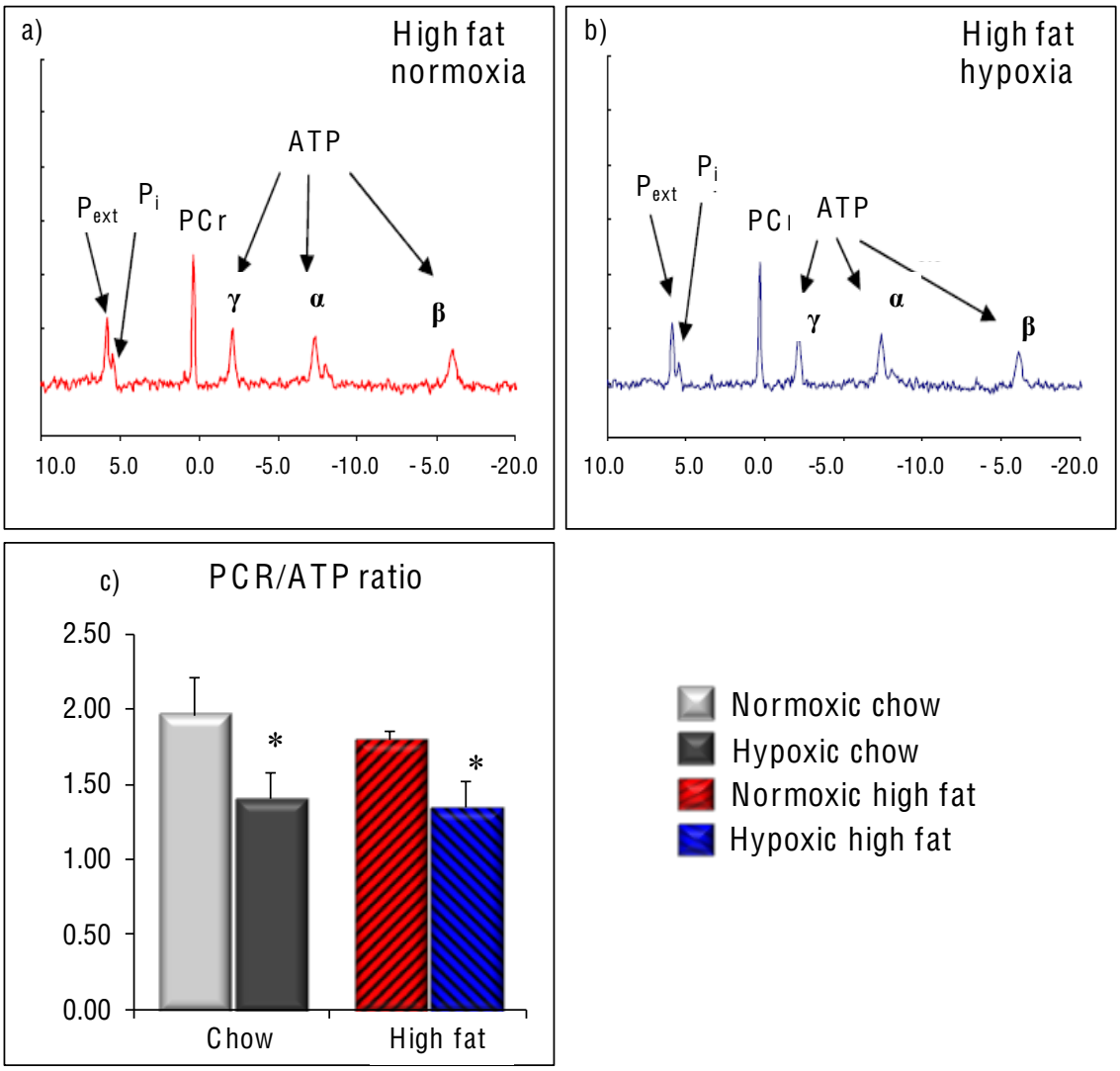

Figure 4.6 Cardiac high-energy phosphate metabolism: Representative MR spectra of a) normoxic and b) hypoxic high fat fed mouse hearts. c) PCr/ATP ratio in chow fed and high fat fed mice following 3 weeks of chronic hypoxia.*$p < 0.05$ relative to normoxic chow fed mice. n = 5-7 per group.

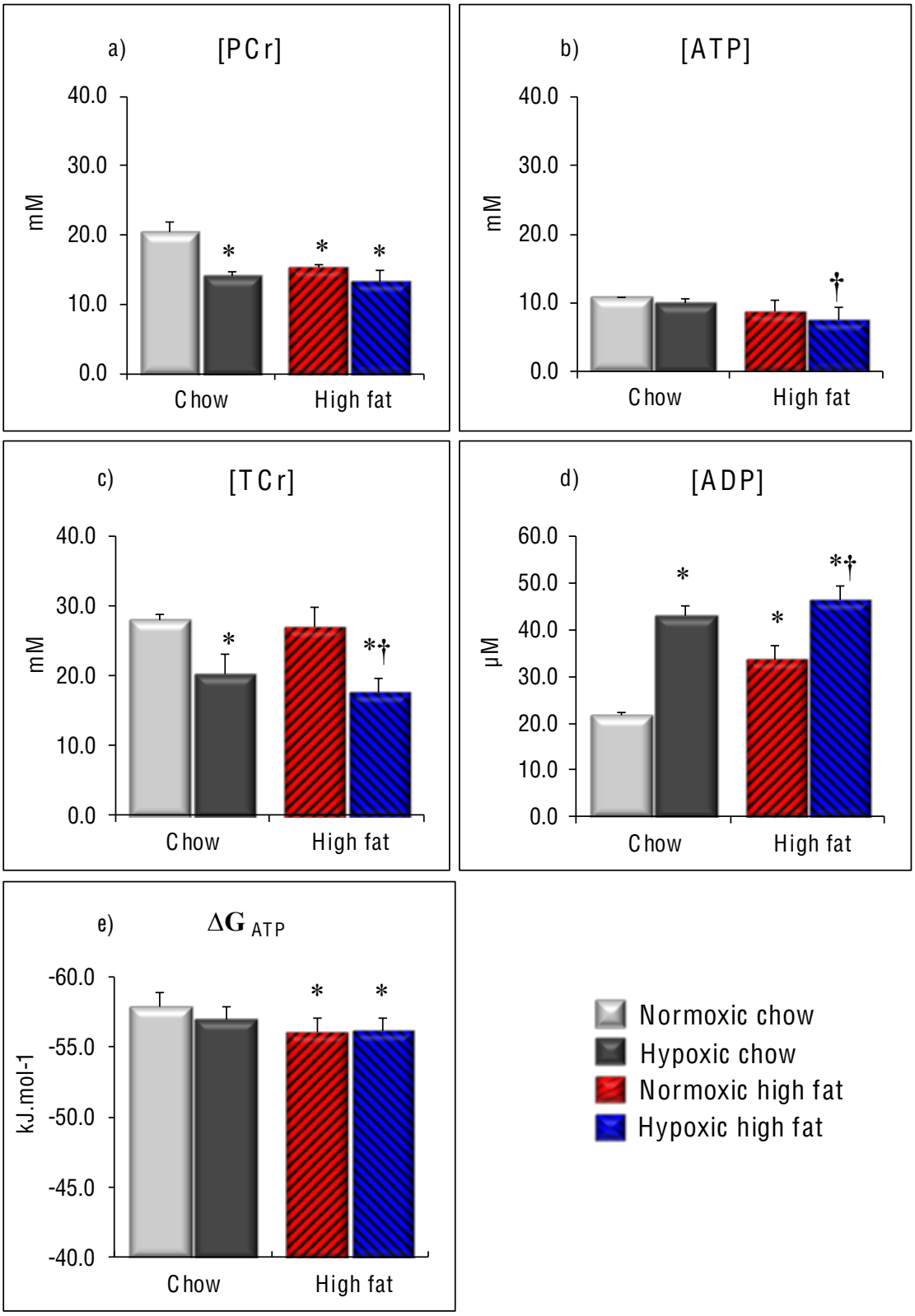

Figure 4.7 Cardiac high energy phosphate metabolism: Concentration of cardiac a) PCr, b) ATP, c) TCr, d) ADP and e) ΔG_{ATP} in chow and high fat fed mice following 3 weeks of chronic hypoxia. *p < 0.05 relative to normoxic chow fed mice. † < 0.05 relative to normoxic high fat fed mice. n= 5-7 per group.

4.4.7 Cardiac molecular profile

Please refer to Appendix 4 for western blot images (where applicable).

4.4.7.1 Hypoxia markers

Hypoxia in chow fed mice increased VEGF mRNA and protein levels, but this effect was absent with high fat feeding (Figure 4.8). SIRT1 protein levels were increased by 27% ($p < 0.05$) and 22% ($p < 0.05$) by high fat feeding in both normoxia and hypoxia respectively (Figure 4.8).

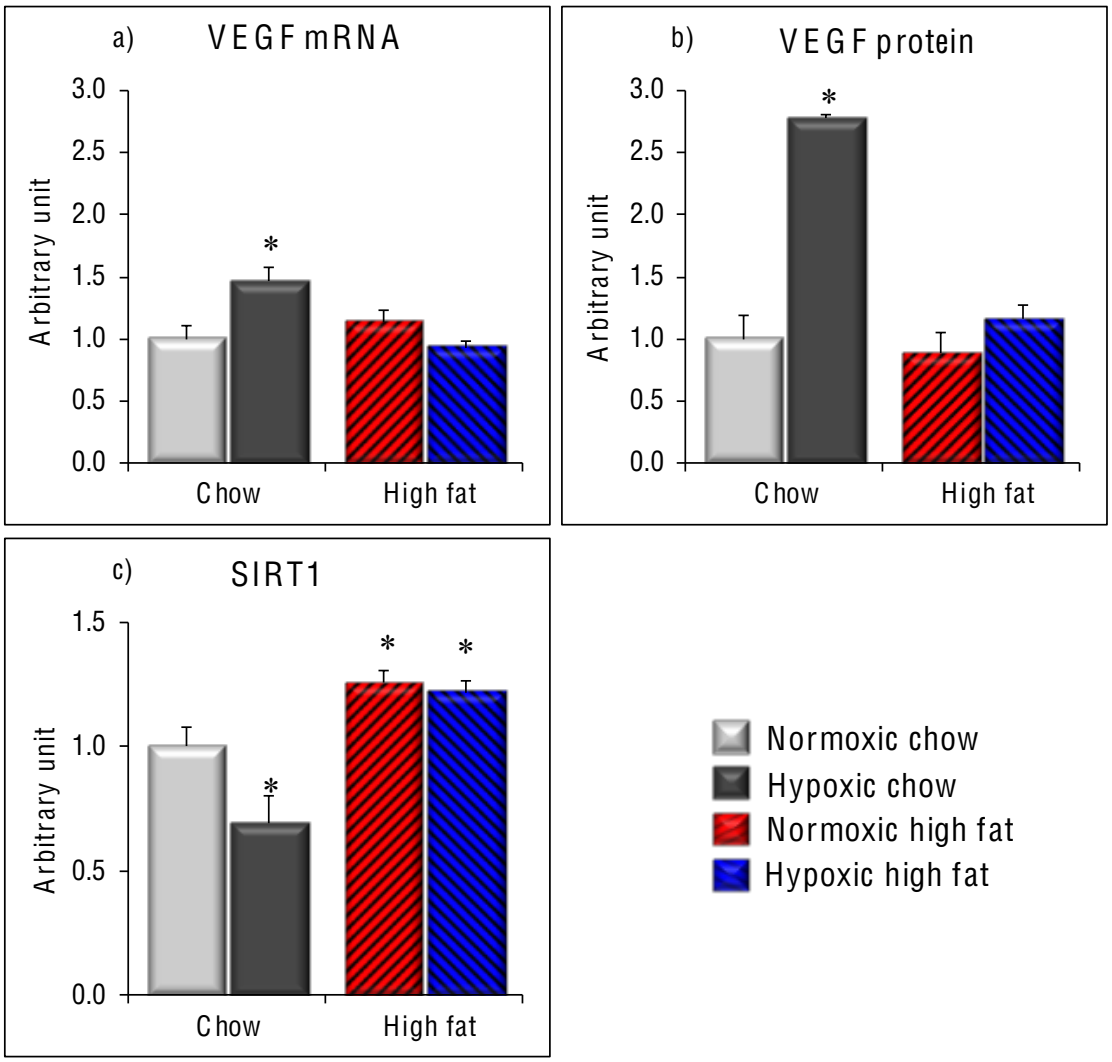

Figure 4.8 Hypoxia markers: Cardiac a) VEGF mRNA expression; protein levels of b) VEGF and c) SIRT1 in chow and high fat fed mice following 3 weeks of chronic hypoxia. mRNA expression in cardiac tissues was normalized to the geometric mean of β-actin (housekeeping gene). *$p < 0.05$ relative to normoxic chow fed mice. n = 5-9 per group.

4.4.7.2 Glucose metabolism

High fat feeding decreased GLUT4 protein levels by 59% ($p < 0.05$) and 64% ($p < 0.05$) under normoxia and hypoxia respectively (Figure 4.9). PDK4 protein levels were unchanged with high fat feeding irrespective of oxygen exposure (Figure 4.9)

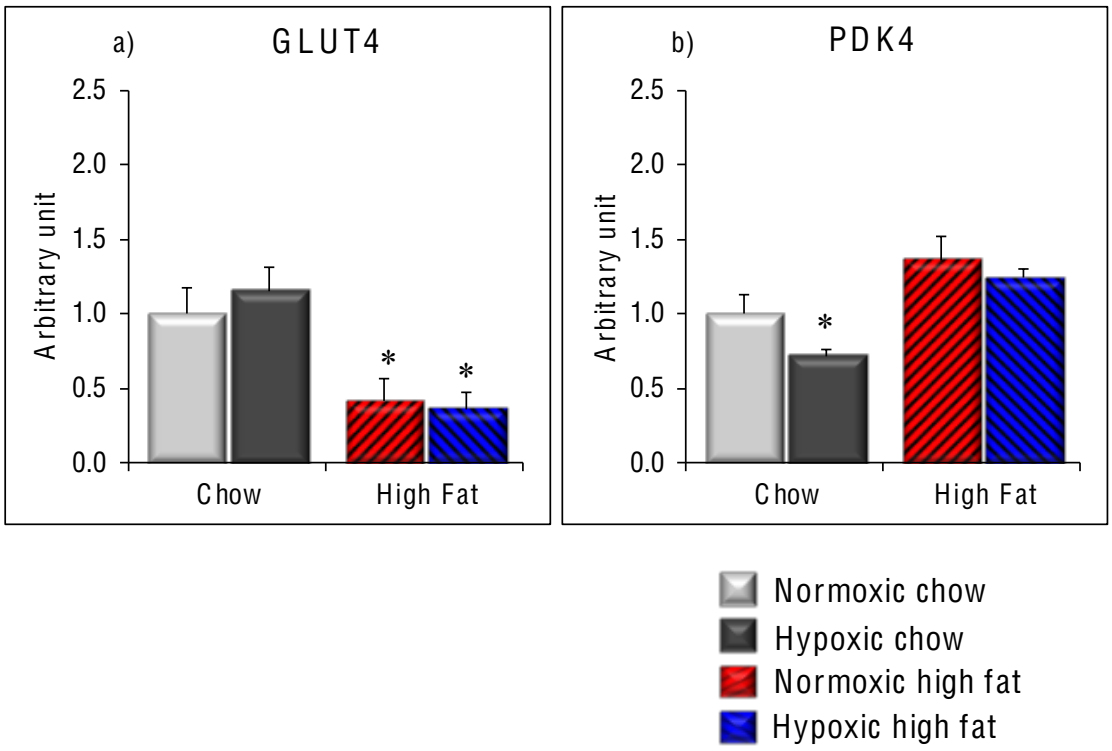

Figure 4.9 Glucose metabolism: Cardiac a) GLUT4 and b) PDK4 protein levels in chow and high fat fed mice following 3 weeks of chronic hypoxia.*$p < 0.05$ relative to normoxic chow fed mice. n = 6-7 per group.

4.4.7.3 Fatty acid metabolism

Protein levels of PPARα downstream targets controlling fatty acid metabolism were all increased under normoxia with no additional effect with hypoxia in high fat fed mouse hearts. In hearts from high fat fed mice, both MCAD mRNA and protein levels were increased 1.5 fold, with a 2-fold increase in UCP3 and MTE1 protein levels ($p < 0.01$) (Figure 4.10).

4.4.7.4 Cardiac PPAR isoforms

High fat feeding increased PPARα mRNA expression 1.5 fold ($p < 0.05$) in both normoxia and hypoxia, over-riding the down-regulation of PPARα activity observed with hypoxia alone (Figure 4.11). RXR protein levels were unaffected by high fat feeding. Expression of PPARβ/δ mRNA and PPARγ mRNA was also unchanged with high fat feeding (Figure 4.11)

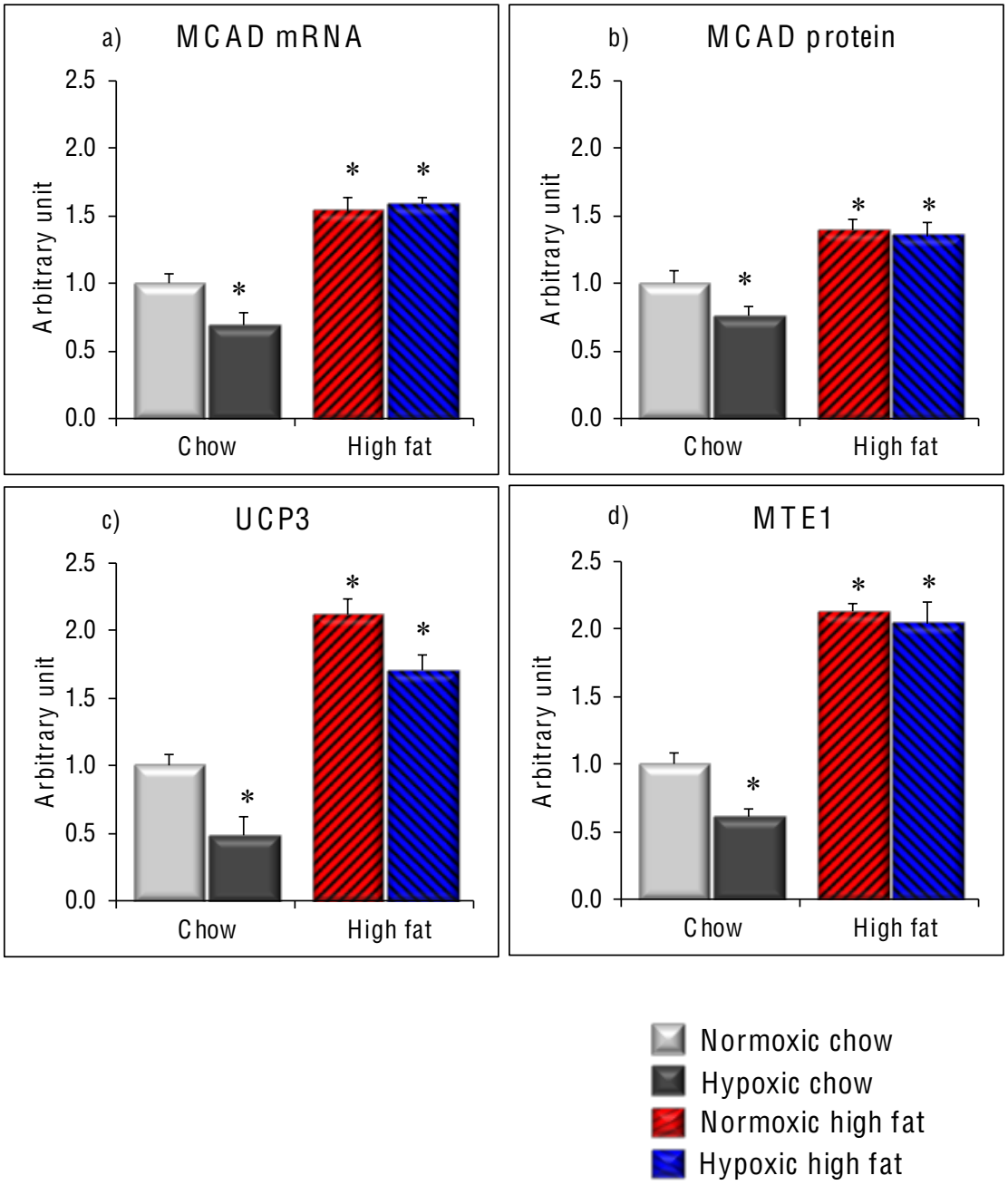

Figure 4.10 Fatty acid metabolism: Cardiac a) MCAD mRNA expression; protein levels of b) MCAD, c) UCP3 and d) MTE1 in chow and high fat fed mice following 3 weeks of chronic hypoxia. mRNA expression in cardiac tissues was normalized to the geometric mean of β-actin (housekeeping gene). *$p < 0.05$ relative to normoxic chow fed mice. n = 6-9 per group.

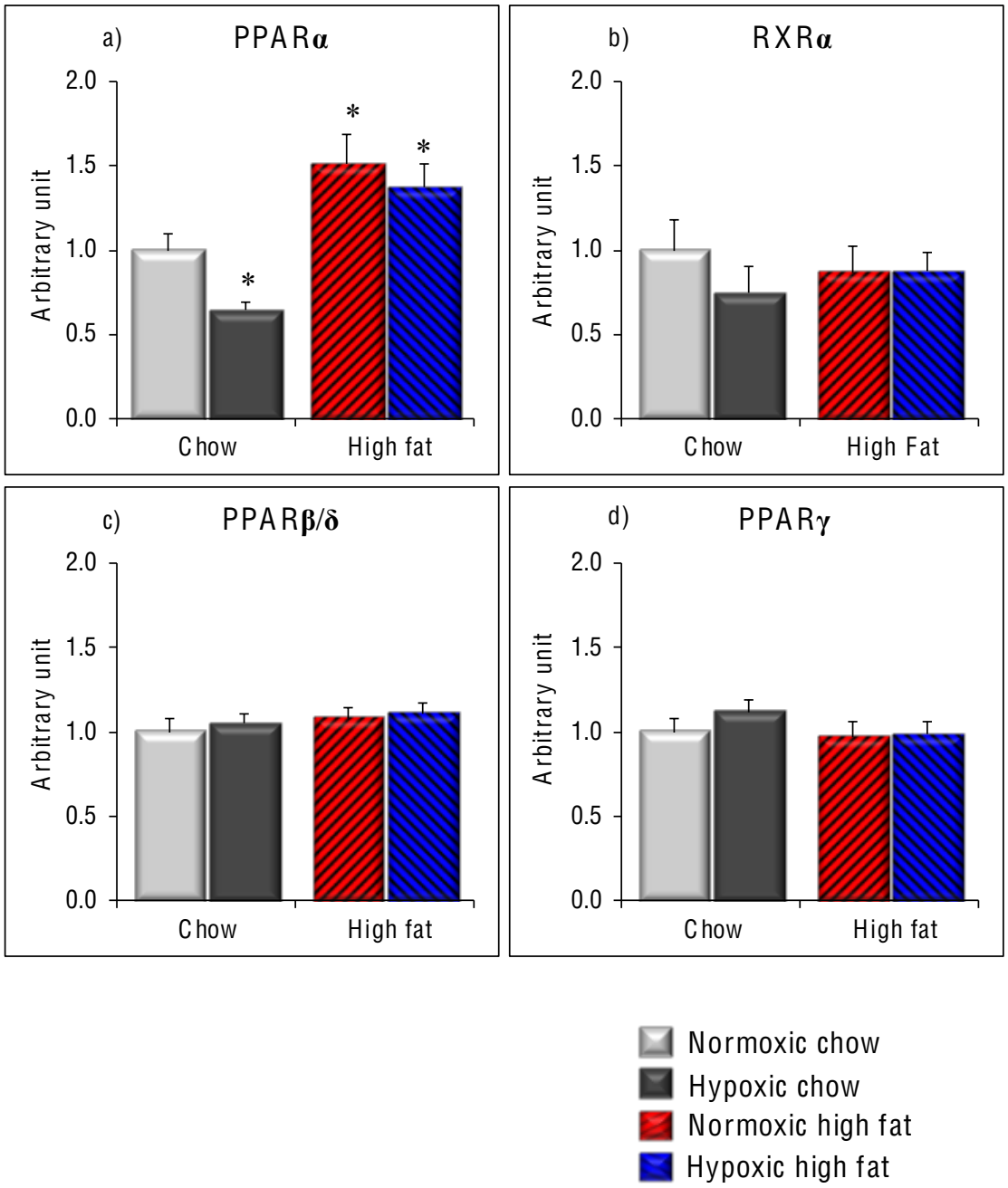

Figure 4.11 Cardiac PPAR isoforms: a) PPARα mRNA expression, b) RXRα protein levels, mRNA expression of c) PPARβ/δ and d) PPARγ in chow and high fat fed mice following 3 weeks of chronic hypoxic housing. mRNA expression in cardiac tissues was normalized to the geometric mean of β-actin (housekeeping gene). *$p < 0.05$ relative to normoxic chow fed mice. n = 6 per group.

4.4.8 **PPARα** regulated proteins in gastrocnemius muscle

Similar to cardiac muscle, hypoxia decreased UCP3 protein levels in gastrocnemius skeletal muscle by 26% ($p < 0.05$) (Figure 4.12). Following high fat feeding, UCP3 levels were double to those of chow fed mice ($p < 0.01$), and were not modified with hypoxia. Skeletal muscle MTE1 protein levels were reduced by 34% in hypoxic chow fed mice ($p < 0.05$), and showed a 71% increase with high fat feeding ($p < 0.01$), but was unaffected by hypoxia. PDK4 was not significantly decreased in skeletal muscle of hypoxic chow fed mice, but was increased by 55% by high fat feeding ($p < 0.05$), irrespective of oxygen exposure (Figure 4.12).

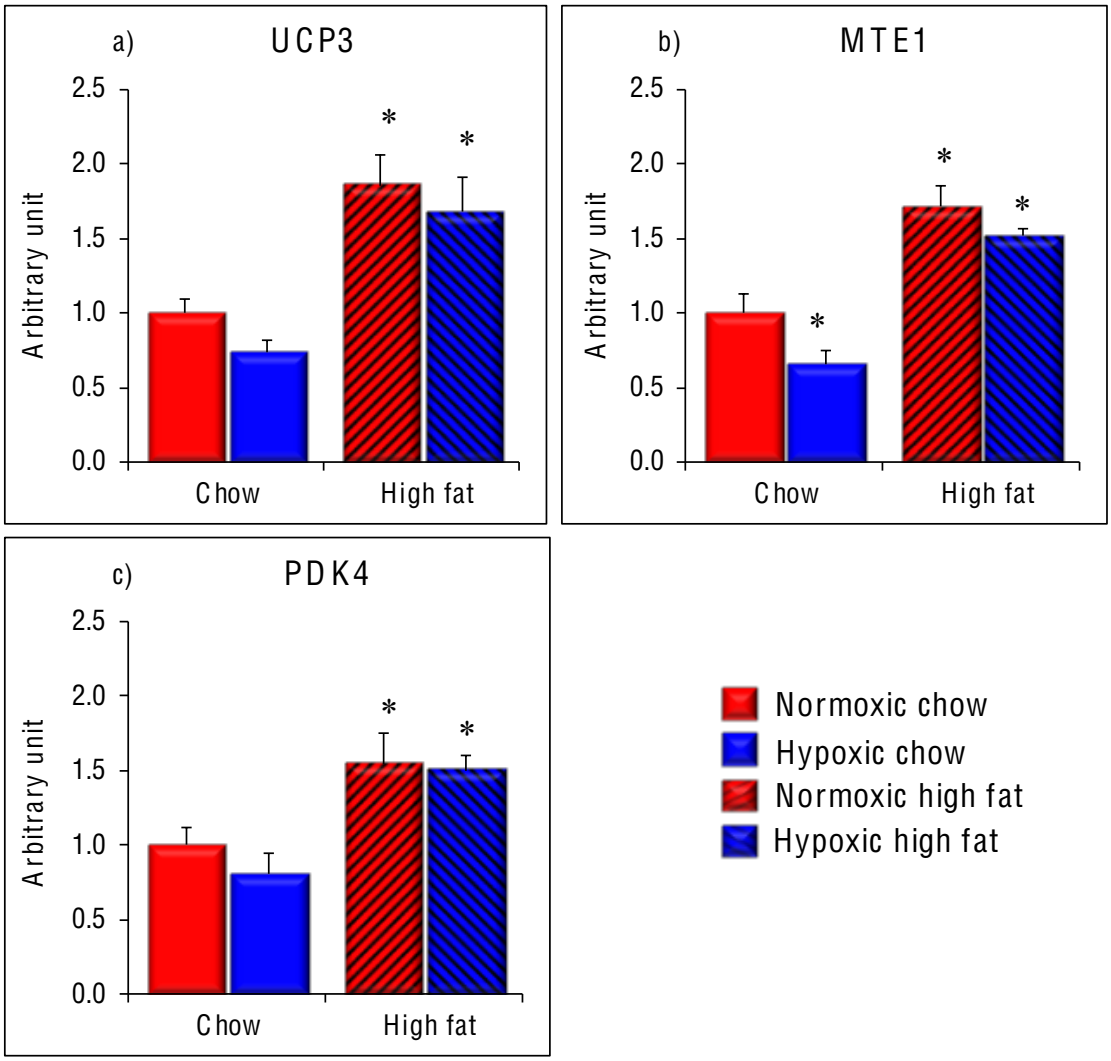

Figure 4.12 **Levels of PPARα regulated proteins in skeletal muscle**: a) UCP3, b) MTE1 and c) PDK4 protein levels in chow and high fat fed mice following 3 weeks of chronic hypoxia. *$p < 0.05$ relative to normoxic chow fed mice. n = 6 per group.

Table 4.2: Summary of results

Data are means ± SEM. *p < 0.05 relative to normoxic wild type mice. †p < 0.05 relative to normoxic high fat fed wild type mice

	CHOW FED				HIGH FAT FED			
	Normoxia	n	Hypoxia	n	Normoxia	n	Hypoxia	n
Hypoxic physiology								
Food consumption (g.food.day^{-1})	2.76 ± 0.06	6	3.04 ± 0.23	5	2.34 ± 0.18	7	2.49 ± 0.24	6
Energy intake (kcal.day^{-1}.gbw^{-1})	0.29 ± 0.04	6	0.30 ± 0.01	5	0.37 ± 0.05*	7	0.39 ± 0.04*	6
Final body weight (g)	32.1 ± 0.60	22	31.3 ± 0.60	16	31.4 ± 1.08	7	28.9 ± 0.79*	6
Cardiac morphology								
LV mass (mg)	131 ± 3.50	22	106 ± 4.70 *	16	140 ± 6.51*	7	117 ± 2.67*†	6
LVmass/body wt ratio (mg.g^{-1})	4.12 ± 0.20	22	3.47 ± 0.10 *	16	4.67 ± 0.40	7	4.07 ± 0.17	6
End diastolic-volume (µl)	64.2 ± 2.80	22	53.5 ± 4.00 *	16	67.0 ± 5.1	7	48.4 ± 2.4*†	6
End systolic-volume (µl)	24.6 ± 1.70	22	21.1 ± 2.80	16	26.4 ± 2.2	7	22.0 ± 1.2	6
Heart rate (bpm)	444 ± 10.0	22	495 ± 25.0	16	430 ± 14	7	496 ± 6.0*†	6
Stroke volume (µl)	39.6 ± 1.80	22	32.4 ± 2.10*	16	40.5 ± 3.9	7	26.5 ± 2.0*†	6
Cardiac output (ml.min^{-1})	17.4 ± 0.70	22	16.1 ± 1.60	16	17.3 ± 1.6	7	13.11 ± 1.00*†	6
Cardiac index (ml.min^{-1}.gbw^{-1})	0.54 ± 0.03	22	0.51 ± 0.04	16	0.55 ± 0.08	7	0.46 ± 0.04*	6
Ejection fraction (%)	61.9 ± 1.90	22	61.1 ± 3.10	16	60.1 ± 2.83	7	54.4 ± 2.33*	6
Plasma metabolites								
Glucose (mM)	9.93 ± 1.11	6	10.78 ± 0.89	6	10.5 ± 0.89	9	11.4 ± 1.03	6
TAG (mM)	2.59 ± 0.65	6	2.89 ± 0.30	6	2.27 ± 0.38	9	3.50 ± 0.47	6
FFA (mM)	0.36 ± 0.07	6	0.36 ± 0.05	6	0.43 ± 0.10	9	0.51 ± 0.12	6
Cardiac substrate metabolism								
Glycolytic flux (µmol.gww^{-1}.min^{-1})	0.16 ± 0.05	6	0.36 ± 0.04*	6	0.08 ± 0.02	6	0.11 ± 0.03	8
Lactate efflux (µmol.gww^{-1}.min^{-1})	0.03 ± 0.01	6	0.06 ± 0.01*	6	0.02 ± 0.002	6	0.02 ± 0.11	8
Palmitate oxidation (µmol.gww^{-1}.min^{-1})	0.12 ± 0.01	6	0.09 ± 0.01*	6	0.14 ± 0.02*	6	0.15 ± 0.01*	8

Table 4.2 (continued)

Cardiac lipid content								
mTAG (μmol.gww^{-1})	2.78 0.25	6	3.63 ± 0.31*	6	5.05 ± 0.54*	7	4.38 ± 0.47*	6
mFFA (μmol.gww^{-1})	0.67 0.08	6	0.57 ± 0.44	6	0.51 ± 0.08	6	0.61 ± 0.12	6
Cardiac high phosphate metabolites								
PCr/ATP ratio	1.96 ± 0.25	5	1.61 ± 0.07*	7	1.79 ± 0.06	5	1.34 ± 0.18*	5
ATP (mM)	10.8 ± 0.11	5	10.0 ± 1.67	7	8.80 ± 1.50	5	7.45 ± 1.90†	5
PCr (mM)	20.4 ± 1.48	5	14.0 ± 0.70*	7	14.2 ± 0.53*	5	13.2 ± 1.72*	5
TCr (mM)	28.0 ± 0.72	5	20.3 ± 2.71*	7	27.0 ± 2.71	5	17.5 ± 2.05*†	5
ADP (μM)	21.7 ± 0.61	5	43.0 ± 2.10*	7	33.6 ± 3.07*	5	46.3 ± 3.29*†	5
ΔG ATP (kJ.mol$^{-1)}$	-57.9 ± 0.87	5	-56.9 ± 0.25	7	-56.1 ± 0.40*	5	-56.1 ± 0.26*	5
Cardiac mRNA expression (arbitrary unit)								
PPARα	1.00 ± 0.10	6	0.64 ± 0.05*	6	1.51 ± 0.17*	6	1.38 ± 0.14*	6
PPARβ/δ	1.00 ± 0.19	6	1.05 ± 0.06	6	1.08 ± 0.06	6	1.11 ± 0.07	6
PPARγ	1.00 ± 0.17	6	1.14± 0.18	6	0.97 ± 0.09	6	0.98 ± 0.08	6
MCAD	1.00 ± 0.07	6	0.67 ± 0.08*	6	1.54 ± 0.11*	6	1.59 ± 0.10*	6
VEGF	1.00 ± 0.10	5	1.46 ± 0.18*	5	1.14 ± 0.09	5	0.95 ± 0.05	5
Cardiac protein levels (arbitrary unit)								
SIRT1	1.00 ± 0.08	9	0.69 ± 0.10*	10	1.27 ± 0.05*	6	1.22 ± 0.06*	6
VEGF	1.00 ± 0.19	8	2.77 0.04	7	0.88 ± 0.17	6	1.15 ± 0.11	6
GLUT4	1.00 ± 0.18	6	1.15 ± 0.16	6	0.41 ± 0.15*	6	0.36 ± 0.11*	6
PDK4	1.00 ± 0.05	6	0.72 ± 0.05*	6	1.36 ± 0.16	7	1.24 ± 0.06	7
MCAD	1.00 ± 0.10	9	0.76 ± 0.07*	9	1.40 ± 0.08*	6	1.35 ± 0.10*	6
UCP3	1.00 ± 0.08	6	0.48 ± 0.14*	6	2.12 ± 0.11*	7	1.75 ± 0.12*	7
MTE1	1.00 ± 0.09	6	0.61 ± 0.06*	6	2.03 ± 0.15*	6	2.04 ± 0.15*	6
RXRα	1.00 ± 0.19	6	0.75 ± 0.17	5	0.86 ± 0.18	6	0.88 ± 0.17	6

Table 4.2 (continued)

Gastrocnemius muscle protein levels (arbitrary unit)								
UCP3	1.00 ± 0.10	6	0.74 ± 0.08*	6	1.86 ± 0.20*	6	1.68 ± 0.23*	6
MTE1	1.00 ± 0.13	6	0.66 ± 0.09*	6	1.71 ± 0.14*	6	1.54 ± 0.06*	6
PDK4	1.00 ± 0.12	6	0.81 ± 0.14	6	1.54 ± 0.20*	6	1.49 ± 0.10*	6

4.5 DISCUSSION

4.5.1 Principal finding

In this study, it was demonstrated that 3-weeks duration of high fat feeding increased PPARα expression and its downstream targets, including MCAD, UCP3, and MTE1. The fall in PPARα expression by hypoxia in chow fed mouse heart was overridden by the PPARα-stimulating effect of high fat feeding. Although the normoxic mouse hearts were able to maintain cardiac function with high fat feeding, this did not occur in high fat fed mice housed in hypoxic conditions. Hearts from these mice had impaired cardiac function, accompanied by increased UCP3, and potentially impaired ATP production. In addition, hypoxic hearts in high fat fed mice were unable to upregulate VEGF, a prominent HIF downstream target at both protein and mRNA levels, which may have exacerbated the maladaptive response to hypoxia. Hence, stimulation of PPARα activity appears to be detrimental to hypoxic adaptation.

4.5.2 High fat feeding stimulated PPARα expression and increased fatty acid metabolism

Fatty acids modulate cardiac metabolism through the transcription factor PPARα [47, 70, 77] and in our study, the 3 weeks duration of high fat feeding increased PPARα expression 1.5-fold, in both normoxic and hypoxic wild type hearts. Other studies have shown that high fat feeding (45% kcal from fat) for 5 weeks did not increase PPARα expression, but increased the transcription of its regulated genes including MCAD, UCP3, MTE1 and PDK1 [219]. In the present study, high fat feeding increased myocardial fatty acid oxidation, MCAD mRNA expression and protein levels by at least 30%, consistent with other high fat feeding studies of similar

duration [220], presumably via PPARα activation. Plasma free fatty acids were not elevated with 3 weeks of high fat feeding, parallel to the unchanged body mass, which suggests that the heart adapted to excess calorie intake by oxidising fatty acids at an increased rate, sufficient to prevent accumulation in plasma. Plasma lipid profile has been shown to be unaffected even with a more sustained high fat feeding, up to 24 weeks [229, 230], and FFAs seem to be only elevated by continuous feeding of a moderately high fat diet (30% kcal from fat) for 14 months [222]. The present findings demonstrated that myocardial TAG content was elevated within 3 weeks of high fat feeding, with no increase in LV dilation or dysfunction with normoxia, consistent with previous findings [220]. Studies using isolated cells or transgenic mice have shown that the ability to synthesise cardiac triglycerides plays a critical role in protection from 'lipotoxicity' by diverting excess fatty acids from cytotoxic pathways [231]. Therefore, the 3 weeks duration of high fat feeding was of sufficient duration to activate PPARα, shifting cardiac metabolism towards fatty metabolism.

Glycolytic flux and net lactate efflux were unaltered by high fat feeding in both normoxic and hypoxic mouse heart, consistent with the short duration of high fat feeding. Wright *et al.* demonstrated that glycolytic rates were decreased by 30% after 2 weeks of high fat diet and declined by a further 10% after 5 weeks of high fat diet [219], parallel to a 55% decrease in cardiac GLUT4 protein levels after 2 weeks of high fat feeding. Here, GLUT4 protein levels were also decreased with high fat feeding in all mouse hearts. Increased lipid delivery to the heart has also been shown to suppress glucose utilisation by inhibiting the PDH complex via enhanced expression of PDK4 [232]. Apart from acute effects of small molecular weight effectors such as high mitochondrial-derived acetyl-CoA/CoA and $NADH/NAD^+$

concentration ratios that are generated by increased rates of fatty acid oxidation, PDK4 expression is also regulated by PPARα [75]. The short duration of high fat feeding in our study did not significantly upregulate PDK4 protein levels; increased PDK4 levels have only been reported after 4 weeks of high fat feeding [219, 232] and in models of overt myocardial insulin resistance, such as in the MHC-PPARα heart [212]. Together with unchanged level of glycolytic and net lactate efflux, the results suggest that cardiac glucose metabolism was normal in this short-term high fat feeding model.

Although all 3 PPAR isoforms have been reported to be involved in lipid metabolism [53], 3 weeks of high fat feeding did not alter the expression of PPARβ/δ nor PPARγ. The expression of PPARγ, in rodent heart is very low compared to PPARα and PPARβ/δ [57] and pharmacological activation of PPARγ by thiazolidinediones (TZD) agonists, did not increase fatty acid oxidation or activate known PPAR target genes when administered to cultured myocytes [77]. PPARβ/δ expression is relatively high in the myocardium [57] and studies suggest overlapping targets and function between PPARα and PPARβ/δ [77]. However, work on cardiac-specific PPARβ/δ overexpressing transgenic mice (MHC-PPARβ/δ) showed that the two receptors have distinct metabolic regulatory programs in the heart [233]. Unlike MHC-PPARα mice, the MHC-PPARβ/δ mice displayed normal survival and have no evidence of myocardial lipid accumulation or cardiac dysfunction, even on a high fat diet. The metabolic changes observed in the present study therefore, appear to be specific to PPARα activation. Moreover, other cardiac proteins under PPARα control, including UCP3 and MTE1, were increased with high fat feeding and these changes were unaffected by hypoxia, indicating that the stimulus acting on PPARα was much

stronger than the opposing downregulation of PPARα by hypoxia. This is consistent with the finding of Belanger *et al.* who demonstrated pharmacological stimulation of PPARα with WY-14,643 has a similar, over-riding effect on PPARα/RXR binding during hypoxia[234].

4.5.3 High fat feeding is detrimental to hypoxic adaptation

Short term high fat feeding in normoxia did not have an effect on cardiac morphology and function, consistent with the findings in both humans [235, 236] and animal models [237]. However, cardiac function was severely impaired in high fat fed mice exposed to chronic hypoxia. Increased MCAD activity correlated positively with oxygen consumption [199] and increased myocardial fatty acid oxidation increased oxygen consumption and decreased cardiac efficiency [238, 239]. Indeed, the exclusive use of fatty acids for β-oxidation requires 11% more oxygen per carbon unit than glucose oxidation alone per ATP molecule produced [21], but this accounts for only a fraction of the 40% increase in oxygen consumption in isolated hearts perfused with > 1 mM fatty acids [198, 240]. The exact mechanism for this is unknown, but has been linked to increased mitochodrial uncoupling during enhanced uptake of free fatty acids in cardiac mucsle cells [241] and high fat feeding, in rat hearts [199]. Here, high fat feeding increased UCP3 levels by 2-fold, irrespective of oxygen exposure. Plasma free fatty acids control UCP3 levels in the heart via activation of PPARα [71, 85], and this study suggests that the increased mitochondrial uncoupling becomes critical and affects function in the hypoxic myocardium, consistent with findings that reported increased UCP3 levels are associated with decreased cardiac efficiency, hydraulic work/O_2 consumption in chronically infarcted rat heart [242]. The increase in fatty acid oxidation and UCP3 protein appears to be an effective strategy to process

excess fatty acids and maintain cardiac function in normoxia, but is ineffective when oxygen availability is limited.

Decreased mitochondrial respiration and ADP/O ratio were observed in rat hearts exposed to hypoxia [200] and high fat feeding alone [199]. In the absence of high fat feeding, hypoxia decreased UPC3 levels, but when this effect is overridden by high fat feeding in hypoxia, the heart suffers from metabolic and functional abnormalities. Increased myocardial uncoupling secondary to elevated free fatty acids may also lead to the reduction in PCr/ATP ratio in our hypoxic mouse heart, mainly as a result of decreased ATP, which was not seen in chow fed mouse hearts. In support of this hypothesis, elevated plasma free fatty acids correlated negatively with cardiac PCr/ATP ratio [243] in diabetic patients. Short duration (5 days) of high fat feeding (75% kcal from fat) decreased myocardial PCr/ATP ratio in humans [235], but did not affect function; therefore, in the chronically hypoxic heart, we suggest that the functional impairment with high fat feeding can be explained by UCP3 mediated reduction in cardiac efficiency.

In addition, the futile cycling of fatty acids between their acyl moieties and the intracellular TAG pool may also decrease cardiac efficiency following increased fatty acid utilisation [30]. Although this mechanism aims to limit the increase in cytosolic concentration of FFAs, it is at the expense of consuming ATP for non-contractile purposes [30, 244]. The FFAs liberated from the TAG pool are required to be reesterified via an ATP-dependent manner to form their respective acyl-CoA moieties for subsequent β-oxidation or reincorporation into the TAG pool. It has been reported that the cycling of fatty acids and TAG contributed to approximately 30% of total cellular energy consumption in rat cardiac myocytes [245].

4.5.4 Uncoupling may also be present in skeletal muscle

From the current investigation, it appears that the molecular mechanisms operating in cardiac muscle were largely conserved in skeletal muscle, and this had significant implication for whole body physiology. High fat feeding (60% kcal from fat) doubled skeletal muscle UCP3 protein levels [246], in agreement with our results and this increase in UPC3 mirrored the increase in cardiac UCP3 levels observed with high fat feeding. Mice provided with the high-fat diet consumed same amount of food in terms of weight, but consumed more calories than their chow fed counterparts, but there was no significant weight gain with high fat fed mice. This may be attributed to whole body mitochondrial uncoupling as skeletal muscle UCP3 protein appeared regulated in a similar way to heart in response to hypoxia and/or modification of PPARα activity. Therefore, evidence from calorific intake and body mass indicated that mitochondrial uncoupling increased as a consequence of high fat feeding.

4.5.5 Impaired HIF signaling with high fat feeding

Diabetic rat hearts [247] failed to upregulate HIF-1α in response to global ischaemia and biopsies obtained from ischaemic heart regions in patients with diabetes have significantly lower HIF protein and mRNA levels than those from non-diabetic patients [248]. Plasma free fatty acids are elevated in diabetic patients [249, 250], however, it is unknown whether HIF activity is blunted in a milder, pre-diabetic model of early dietary induced obesity, achieved by short term high fat feeding. Here, hypoxic high fat fed mice were unable to upregulate cardiac VEGF, a prominent HIF downstream target at both protein and mRNA levels. There is a 40% and 70% decrease in VEGF protein and receptor levels in diabetic and insulin-resistant rat hearts [251]. In humans, decreased VEGF protein and receptor levels were

accompanied by a decreased post-ischaemic vascularisation and hypoxia-induced collateral vessel formation [248, 251]. The work from Chapter 3 has shown that the metabolic adaptive response mediated by PPARα in the heart is potentially HIF-dependent. Although the data is not conclusive, it is apparent from the literature that HIF activation is impaired in pathological conditions associated with chronically elevated plasma free fatty acids. Therefore, a compromised HIF system could potentially further intensify the metabolic abnormalities in hearts with elevated free fatty acids in oxygen-limited conditions.

In summary, the work in this chapter has shown that the heart is unable to adapt to hypoxia when PPARα activity is stimulated via dietary manipulation. High fat feeding for 3 weeks lead to a significant increase in fatty acid oxidation, a response that was mediated via PPARα activation and its downstream targets, including MCAD, UCP3 and MTE1, irrespective of oxygen exposure. Despite an increase in fatty acid oxidation, high fat fed wild type mice exposed to normoxia were able to retain cardiac function. However, mice fed with a high fat diet were intolerant to chronic hypoxia and exhibit severe impairment in cardiac function. The PCr/ATP ratio was reduced in hypoxic high fat fed mouse heart, with decreased ATP, possibly due to the detrimental effect of increased mitochondrial uncoupling during limited oxygen supply and impaired HIF signalling with high fat feeding. Therefore, it appears that the metabolic adaptation to chronic hypoxia can only occur as a result of PPARα downregulation with a subsequent decrease in fatty acid oxidation. Potentially, a further reduction in fatty acid metabolism through PPARα ablation may enhance hypoxic adaption and will be addressed in the next chapter

CHAPTER 5

EFFECT OF CHRONIC HYPOXIA AND HIGH FAT FEEDING IN PPARα NULL MICE

5.1 ABSTRACT

In Chapter 4, increased PPARα expression was found to be detrimental to the hypoxic heart. In this chapter, we examined whether loss of PPARα altered cardiac metabolic and functional changes to hypoxia. PPARα$^{-/-}$ mice were subjected to 3 weeks hypoxia or normoxia, and were fed a high fat diet (55% fat) or chow fed, as controls. *In vivo* cardiac function, cardiac substrate metabolism, and molecular changes were assessed, and compared to wild type controls, isolating the changes that were PPARα-dependent. PPARα$^{-/-}$ mice fed a chow diet had normal cardiac function, but hypoxic housing of PPARα$^{-/-}$ mice reduced cardiac output by 19% ($p < 0.05$), as a result of 18% ($p < 0.05$) and 24% ($p < 0.01$) fall in EDV and stroke volume respectively, relative to normoxic PPARα$^{-/-}$ mice. High fat feeding in PPARα$^{-/-}$ mice decreased cardiac index and ejection fraction by 29% ($p < 0.01$) and 6% ($p < 0.05$) respectively, relative to chow fed PPARα$^{-/-}$ mice. Hypoxia plus high fat feeding exacerbated cardiac dysfunction of PPARα$^{-/-}$ mice, and increased LV mass by 15% ($p < 0.01$) compared to normoxic chow fed PPARα$^{-/-}$ mice. PPARα$^{-/-}$ mice had abnormal cardiac substrate metabolism; glycolytic flux and lactate efflux were 3-fold higher ($p < 0.01$) compared to wild-type controls, while palmitate oxidation was 9% ($p < 0.05$) lower. High fat feeding in PPARα$^{-/-}$ mice had no additional effect on cardiac substrate metabolism over PPARα ablation, irrespective of oxygen supply. PPARα deletion decreased many PPARα downstream targets, without affecting mRNA expression of PPARβ/δ and PPARγ in all PPARα$^{-/-}$ mouse hearts. Cardiac MCAD levels were 40% lower in normoxic PPARα$^{-/-}$ mice compared to normoxic wild type mice, at both mRNA and protein levels and were unchanged by hypoxia and/or high fat feeding. Cardiac UCP3 and MTE1 were at least 50% lower in all PPARα$^{-/-}$ mice compared to wild type mice, irrespective of oxygen exposure or diet. As a result, all PPARα mice lacked the metabolic flexibility for hypoxic adaptation to occur, which impaired cardiac function. In conclusion, hearts of PPARα-deficient mice were intolerant to chronic hypoxia, irrespective of fatty acid supply, reflecting the importance of PPARα regulation in cardiac metabolic adaptation to chronic hypoxia.

5.2 INTRODUCTION

Work in previous chapters suggest that the metabolic adaptation to chronic hypoxia associated with PPARα downregulation was overridden by the PPARα stimulating-effect of high fat, which impaired cardiac function. Since suppressed PPARα expression was associated with cardiac metabolic adaptation to chronic hypoxia, in this chapter, the effect of chronic hypoxia was further examined in PPARα null (PPARα$^{-/-}$) mouse hearts. The PPARα$^{-/-}$ mouse is a general knockout model, which lacks detectable proliferation of peroxisomes in the liver [65]. PPARα$^{-/-}$ mice are viable and live to a normal age, but the hearts of aged PPARα$^{-/-}$ mice show progressive myocardial degeneration with contraction band necrosis, inflammatory infiltrates and fibrosis at 32 weeks of age [252]. PPARα$^{-/-}$ mouse hearts also have decreased protein levels of fatty acid metabolizing enzymes, including VLCAD, MCAD, SCAD, CPT1, mitochondrial trifunctional protein α subunit, and decreased mRNA expression of fatty acid translocase and fatty acid transporter proteins [252, 253]. As a result, PPARα mice have abnormal cardiac substrate utilisation. ^{13}C NMR spectroscopy in isolated perfused hearts revealed that the contribution of fatty acids to oxidative metabolism was 3-fold lower in PPARα$^{-/-}$ mice compared to wild type mice, while glycolytic rates were 1.5 fold higher [254], with a concomitant increase in glucose oxidation [254, 255].

Despite abnormal substrate utilisation, isolated perfused PPARα$^{-/-}$ mouse hearts have normal contractile function [222, 256]. It could be argued that PPARα deletion may improve adaptation to hypoxia and protect the hypoxic heart as the switch to a more oxygen efficient substrate, as observed in Chapter 3, had already occurred in PPARα$^{-/-}$ mouse hearts. In support, increased glucose uptake [222] and glucose

oxidation [213] in PPARα$^{-/-}$ mouse hearts were associated with improved recovery following low-flow [222], or global ischaemia [213]. This protection hypothesis, however, was not supported by Luptak *et al.*, whose study showed that isolated perfused hearts from PPARα$^{-/-}$ mice exhibit greater ATP depletion when subjected to increased workload (induced by raising calcium concentration from 2 to 4 mM), with decreased cardiac function[256]. PPARα$^{-/-}$ mice also have increased susceptibility to injury following myocardial infarction, with 10% larger infarct sizes following 30 minutes of coronary occlusion [257]. Following transverse aortic constriction (TAC), PPARα$^{-/-}$ mice developed greater cardiac hypertrophy, associated with decreased LV contractility and 10% reduction in ejection fraction [258]. Cardiac oxygen supply is potentially involved in these interventions, and therefore, PPARα ablation may be detrimental to chronic hypoxia.

Study aim

To investigate whether loss of PPARα alters hypoxic adaptation, cardiac function and metabolism were assessed in PPARα$^{-/-}$ mice exposed to chronic hypoxia. In an extension of Chapter 4, PPARα$^{-/-}$ mice were also fed a high fat diet and housed in hypoxic conditions, to isolate any changes that were independent of PPARα regulation and further establish the PPARα-driven effect during hypoxic adaptation.

5.3 METHODS

Fourteen month-old male PPARα$^{-/-}$ mice, on EvSv129 background were exposed to 3 weeks of normoxia or hypoxia, and half the mice were fed with a high-fat diet vs. ordinary chow pellets (for diet details, refer to Appendix 5). Mice were a kind gift of Dr Frank J. Gonzalez (National Cancer Institute, Bethesda, MD, USA).

Methods have been described in Chapter 2. Briefly, *in vivo* cardiac morphology and function were measured using multi-slice cardiac MRI. Hearts were excised and perfused in the Langendorff mode. Glycolytic flux and palmitate oxidation rates were measured using ^{3}H-labeled substrates. Following perfusion, hearts were freeze-clamped in liquid nitrogen for further molecular analysis. Whole cell lysates from powdered frozen hearts were used to measure protein levels of MCAD, UCP3, MTE1, GLUT4, PDK4, RXR, and SIRT1. mRNA expression of VEGF, MCAD, PPARα, PPARβ/δ and PPARγ was quantified using qRT-PCR. VEGF protein levels were quantified using ELISA. Cardiac lipids were extracted from freeze clamped tissue using chloroform: methanol solution, for the measurement of myocardial TAG and FFA content.

Whole cell lysates from powdered frozen gastrocnemius were used to measure protein levels of UCP3, MTE1, and PDK4.

5.4 RESULTS 1: EFFECT OF CHRONIC HYPOXIA IN PPARα NULL MICE

Results for normoxic and hypoxic chow fed wild type mice presented in Chapter 3, are shaded in grey to represent the control groups in this chapter.

5.4.1 Hypoxic physiology

PPARα$^{-/-}$ mice were generally smaller in size than wild type mice. Age-matched normoxic PPARα$^{-/-}$ mice weighed on average 29 ± 1g, 9% ($p < 0.05$) lower than their wild type counterparts. Hypoxic housing had no effect on body weight in PPARα$^{-/-}$ mice (Figure 5.1). Chronic hypoxia increased whole blood haemoglobin and haematocrit in PPARα$^{-/-}$ mice in a similar manner to wild type mice, increasing haemoglobin and haematocrit level by 47% and 45% respectively ($p < 0.01$) compared to normoxic PPARα$^{-/-}$ mice ($p < 0.01$) (Figure 5.1).

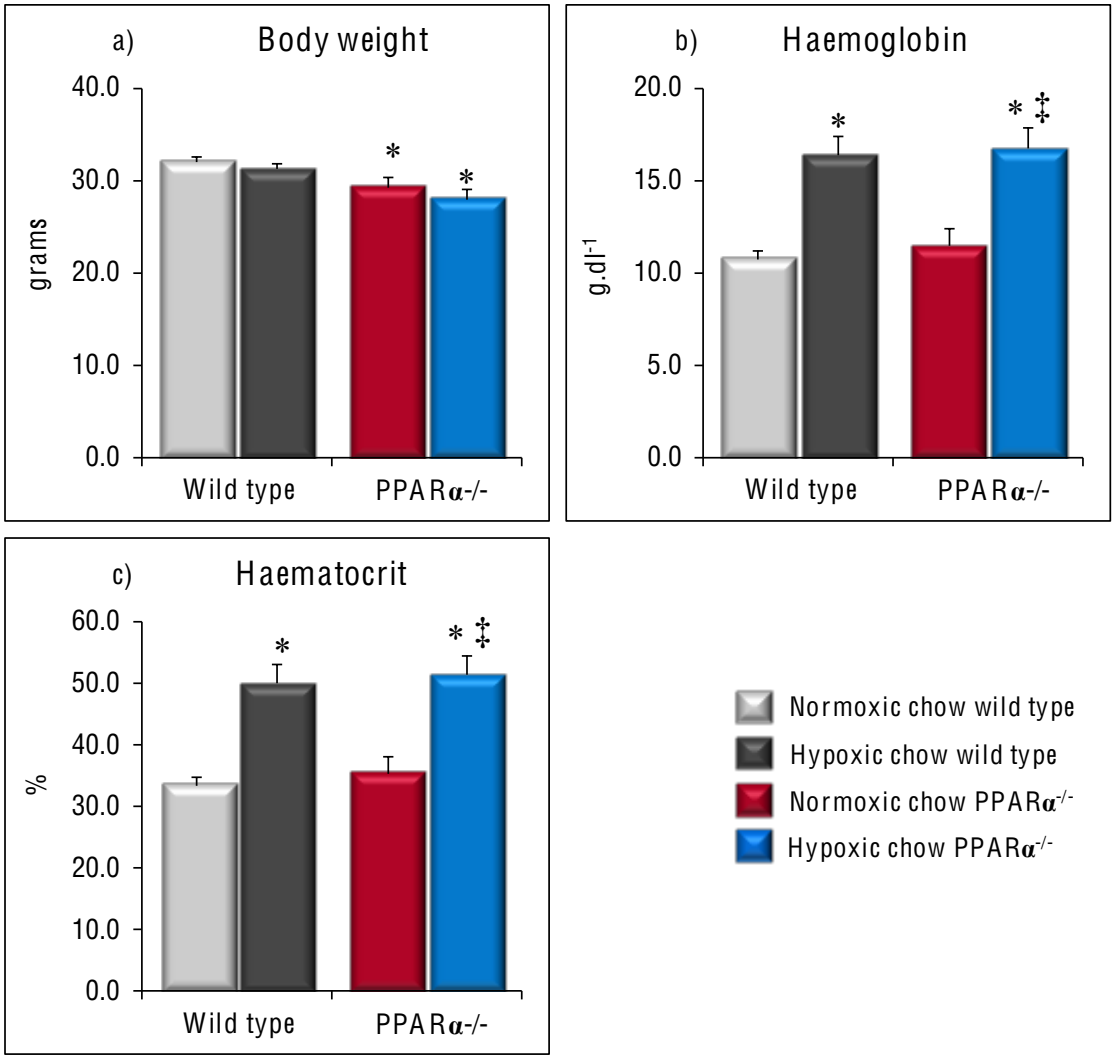

Figure 5.1 Effect of chronic hypoxia on mouse physiology: a) Body weight, b) haemoglobin and c) haematocrit and in wild type and PPARα$^{-/-}$ mice following 3 weeks of chronic hypoxia. *p < 0.05 relative to normoxic wild type mice, ‡ < 0.05 relative to normoxic PPARα$^{-/-}$ mice. n = 6-16 per group.

5.4.2 *In vivo* cardiac morphology

Normoxic PPARα$^{-/-}$ mice had smaller left ventricles, in proportion to their body weights (Figure 5.2). Hypoxia had no additional effect on LV mass in PPARα$^{-/-}$ mice.

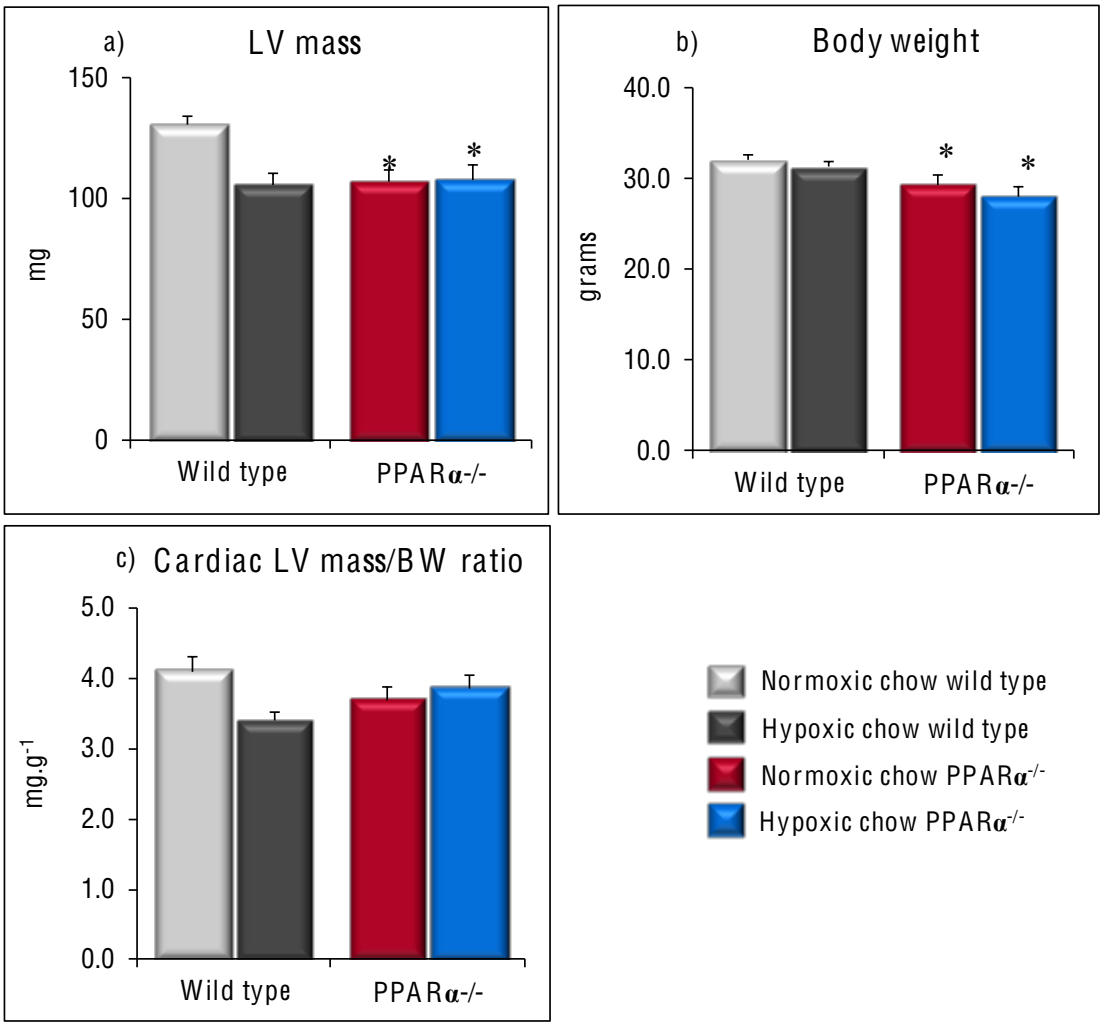

Figure 5.2 Effect of chronic hypoxia on *in vivo* cardiac morphology: a) LV mass, b) body weight c) LV mass / body weight (BW) ratio in wild type and PPARα$^{-/-}$ mice following 3 weeks of chronic hypoxia. *$p < 0.05$ relative to normoxic wild type mice. n = 6-16 per group.

5.4.3 *In vivo* cardiac function

Normoxic PPARα$^{-/-}$ mice fed a chow diet had normal cardiac function (Figure 5.3). However, when housed under hypoxic conditions, PPARα$^{-/-}$ mice on chow diet had 18% lower EDV ($p < 0.05$) compared to normoxic PPARα$^{-/-}$ mice that resulted in a 24% reduction in stroke volume ($p < 0.01$) (Figure 5.3.1). As heart rates were normal, cardiac output was reduced by 19% in hypoxic chow fed PPARα$^{-/-}$ mice ($p < 0.05$) relative to normoxic PPARα$^{-/-}$ mice. Cardiac index and ejection fraction were normal in all chow fed PPARα$^{-/-}$ mice, irrespective of oxygen exposure (Figure 5.3.2).

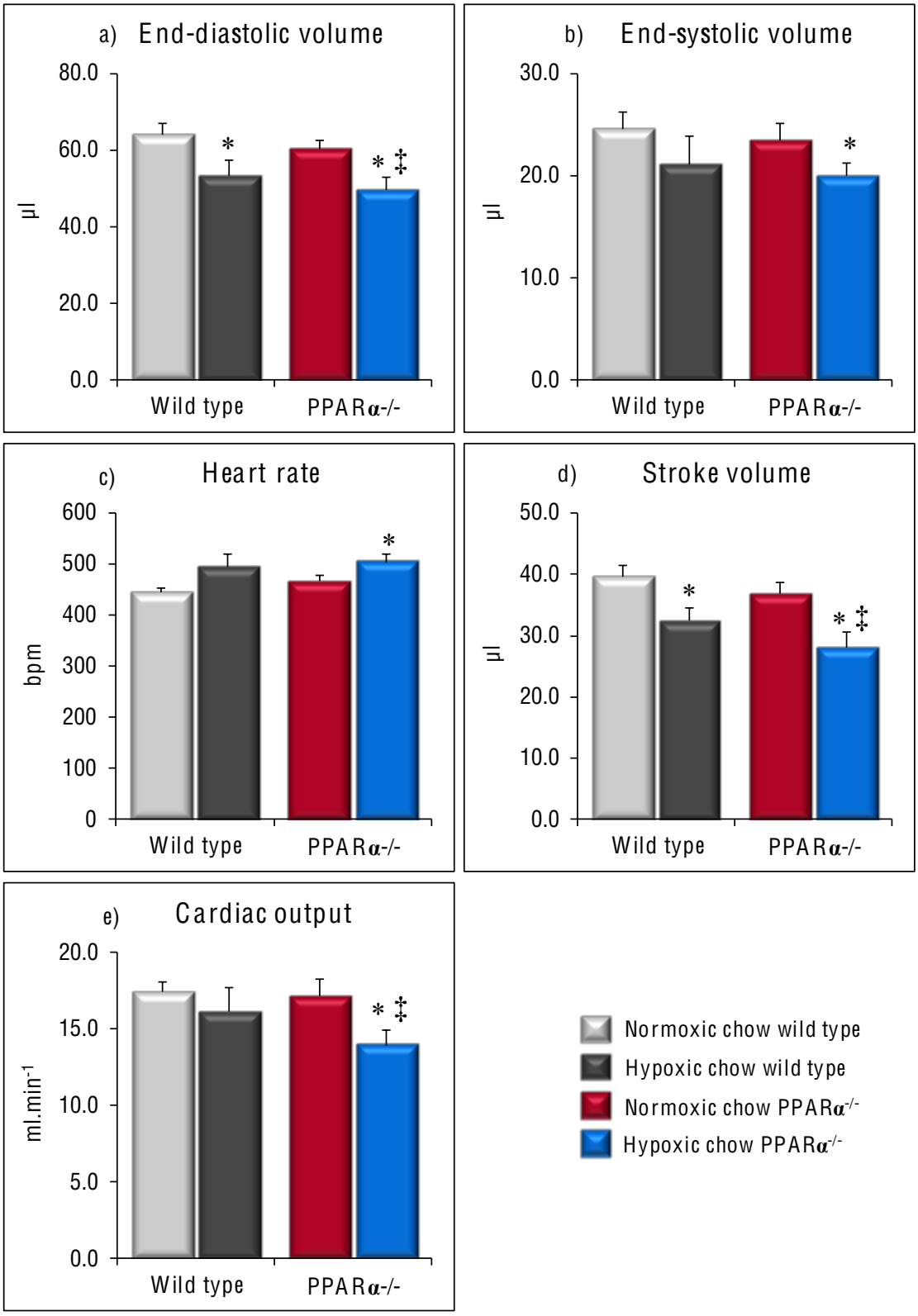

Figure 5.3.1 Effect of chronic hypoxia on *in vivo* cardiac function: a) End-diastolic volume, b) end-systolic volume, c) heart rate, d) stroke volume and e) cardiac output in wild type mice and PPARα$^{-/-}$ mice following 3 weeks of chronic hypoxia *$p < 0.05$ relative to normoxic wild type mice, ‡ $p < 0.05$ relative to normoxic PPARα$^{-/-}$ mice. n = 6-16 per group.

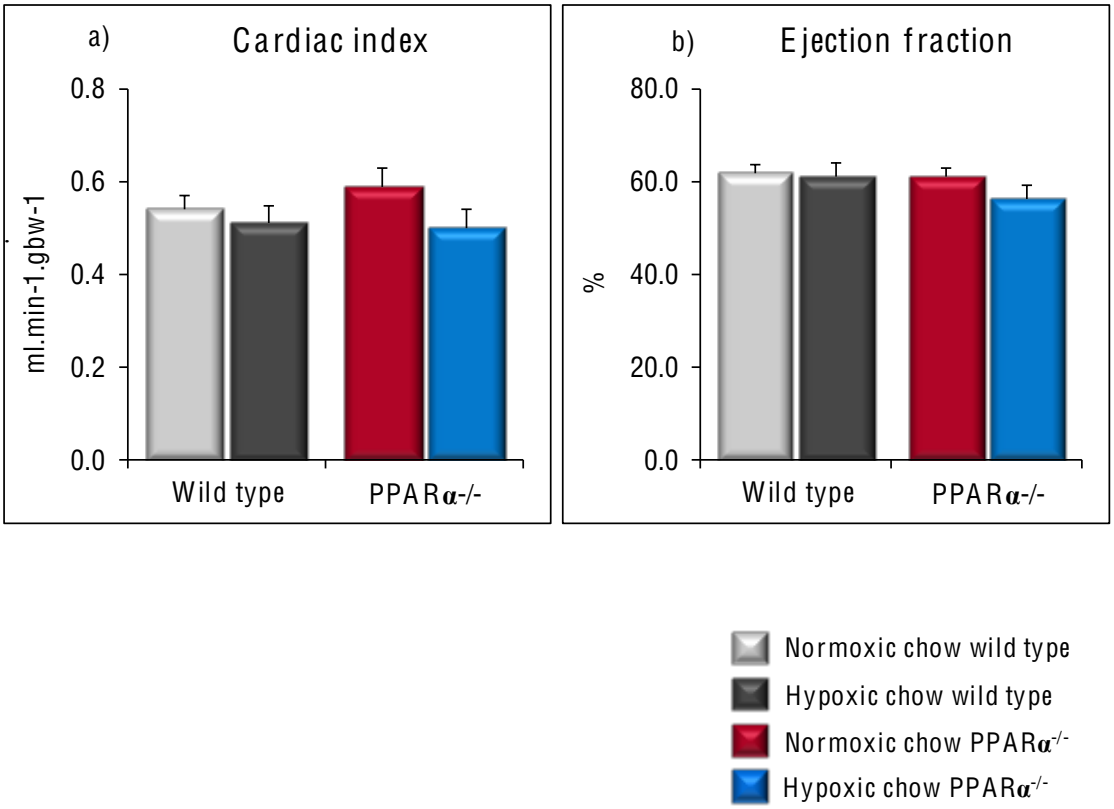

Figure 5.3.2 Effect of chronic hypoxia on *in vivo* cardiac function: a) Cardiac index and b) ejection fraction in wild type and PPARα$^{-/-}$ mice following 3 weeks of chronic hypoxia. n = 6-16 per group.

5.4.4 Cardiac substrate metabolism

PPARα$^{-/-}$ mouse hearts had 3-fold ($p < 0.01$) higher glycolytic rates than normoxic wild type mouse hearts, which were unaltered by hypoxia (Figure 5.4). Stimulation of glycolytic flux with insulin doubled glycolytic rates in both normoxic and hypoxic PPARα$^{-/-}$ mouse hearts, indicating that basal glycolysis was not maximal. Lactate efflux from hypoxic PPARα$^{-/-}$ mouse hearts was 3-fold higher ($p < 0.01$) than normoxic wild type hearts. Cardiac palmitate oxidation in normoxic PPARα$^{-/-}$ mice was 9% lower than wild type mice, and similarly, which was not modified by hypoxia (Figure 5.4).

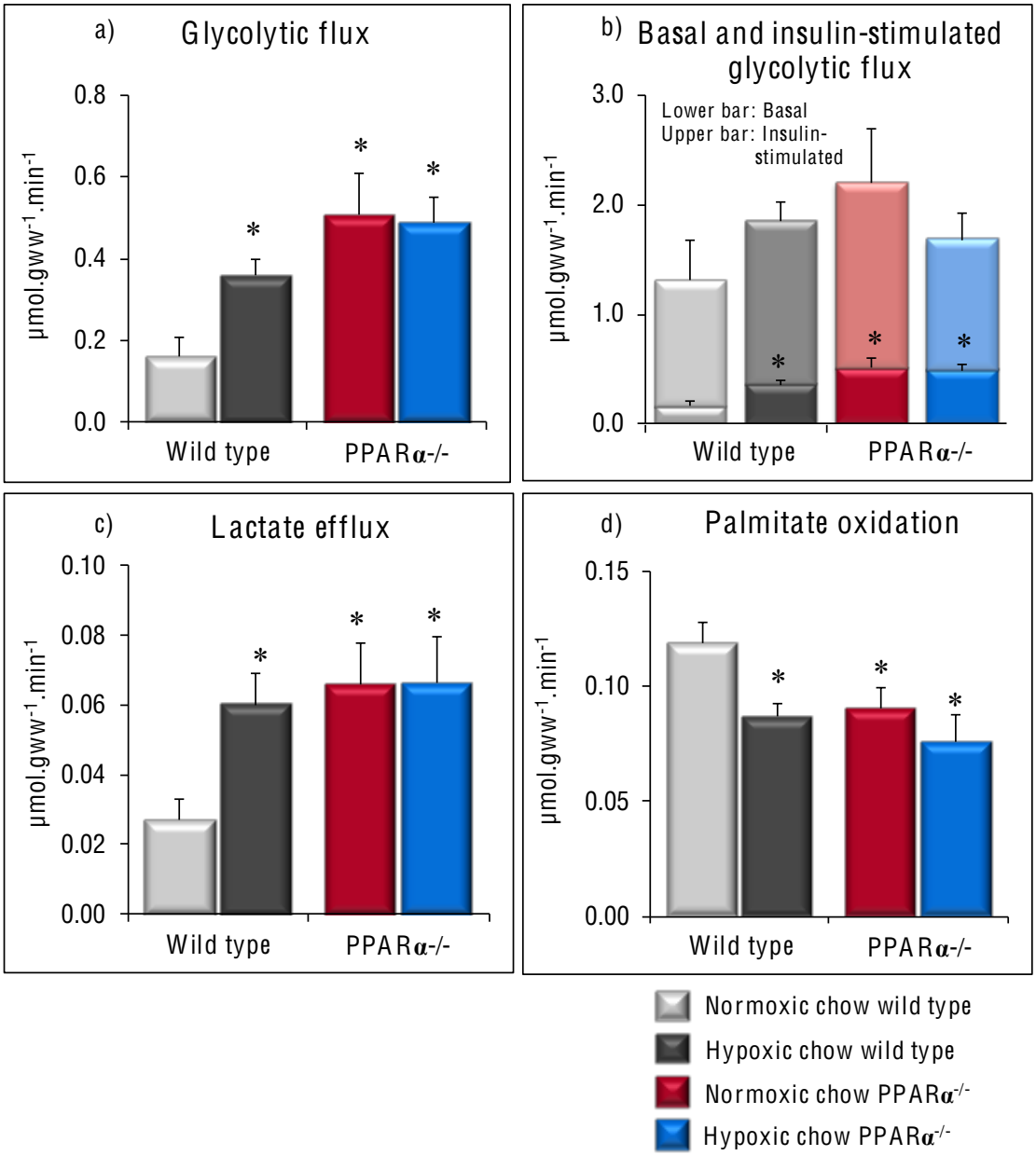

Figure 5.4 Cardiac substrate metabolism: a) Glycolytic flux, b) insulin-stimulated glycolytic flux, c) lactate efflux and d) palmitate oxidation in wild type and PPARα$^{-/-}$ mice following 3 weeks of chronic hypoxia. *p < 0.05 relative to normoxic wild type mice. n = 6-9 per group.

5.4.5 Cardiac triacylglycerol and free fatty acid content

Endogenous myocardial TAG was 40% ($p < 0.05$) higher in all PPARα$^{-/-}$ mouse hearts compared to wild type mouse hearts, irrespective of oxygen exposure while myocardial FFA was normal in all PPARα$^{-/-}$ hearts (Figure 5.5)

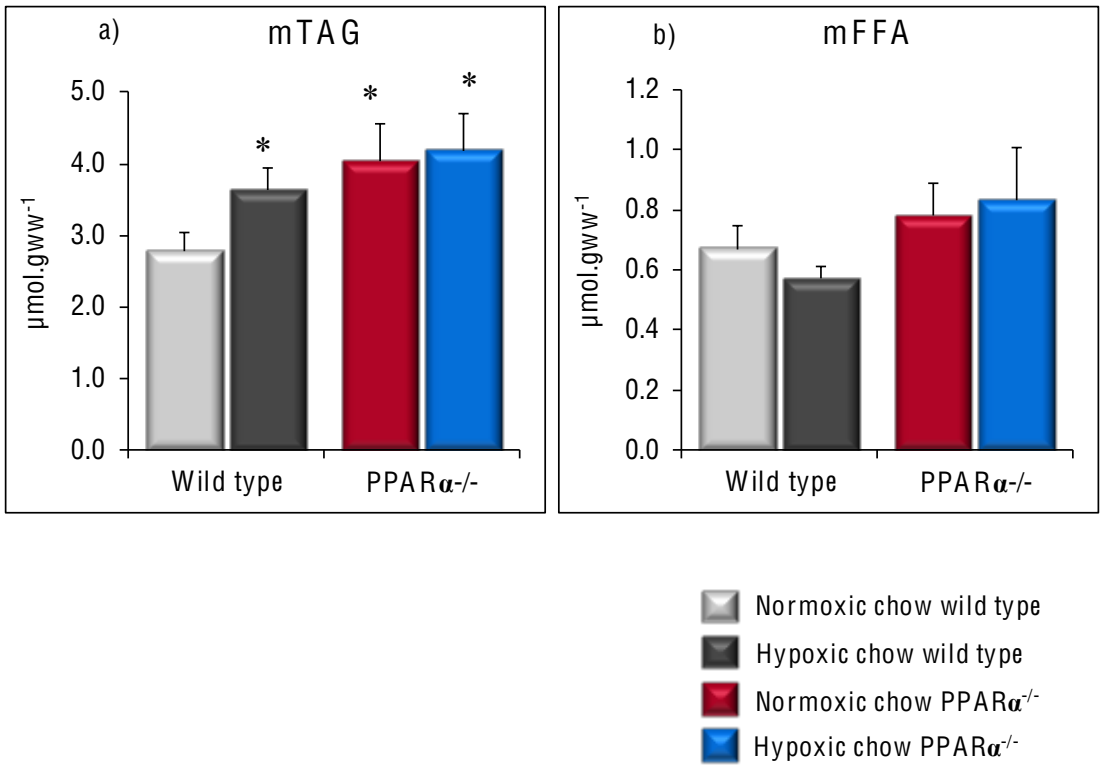

Figure 5.5 Cardiac TAG and FFA content: Myocardial a) TAG (mTAG) and b) FFA (mFFA) in chow fed and high fat fed wild type and PPARα$^{-/-}$ mice following 3 weeks of chronic hypoxia. *$p < 0.05$ relative to normoxic chow fed mice. n= 6 per group.

5.4.6 Cardiac molecular profile

Please refer to Appendix 4 for western blot images (where applicable).

5.4.6.1 Hypoxia markers

Hypoxic housing of PPARα$^{-/-}$ mice increased both cardiac VEGF mRNA expression and protein levels by 40% and 2.4-fold, respectively, relative to normoxic wild type and PPARα$^{-/-}$ mice (Figure 5.6). SIRT1 levels were 30% lower in both normoxic and hypoxic PPARα$^{-/-}$ mouse hearts compared to wild type mice (Figure 5.6).

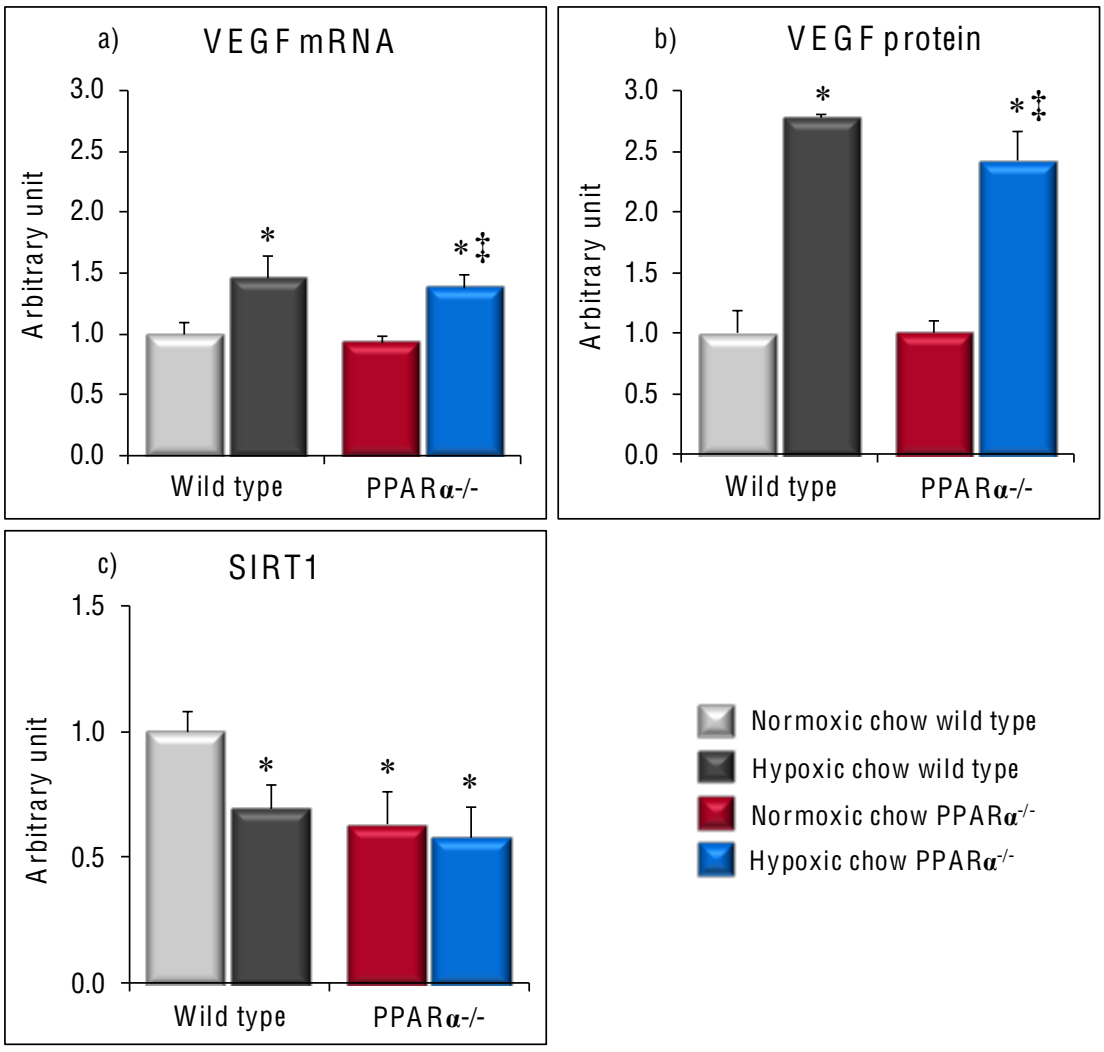

Figure 5.6 Cardiac hypoxia markers: a) VEGF mRNA expression, b) VEGF and c) SIRT1 protein levels in wild type and PPARα$^{-/-}$ mice following 3 weeks of chronic hypoxia. mRNA expression in cardiac tissues was normalized to the geometric mean of β-actin (housekeeping gene). *p < 0.05 relative to normoxic wild type mice, ‡ < 0.05 relative to normoxic PPARα$^{-/-}$ mice. n = 5-7 per group.

5.4.6.2 Mitochondrial proteins

The mitochondrial proteins αKGDH, citrate synthase and PGC1α were not affected by PPARα ablation, irrespective of oxygen supply (Figure 5.7).

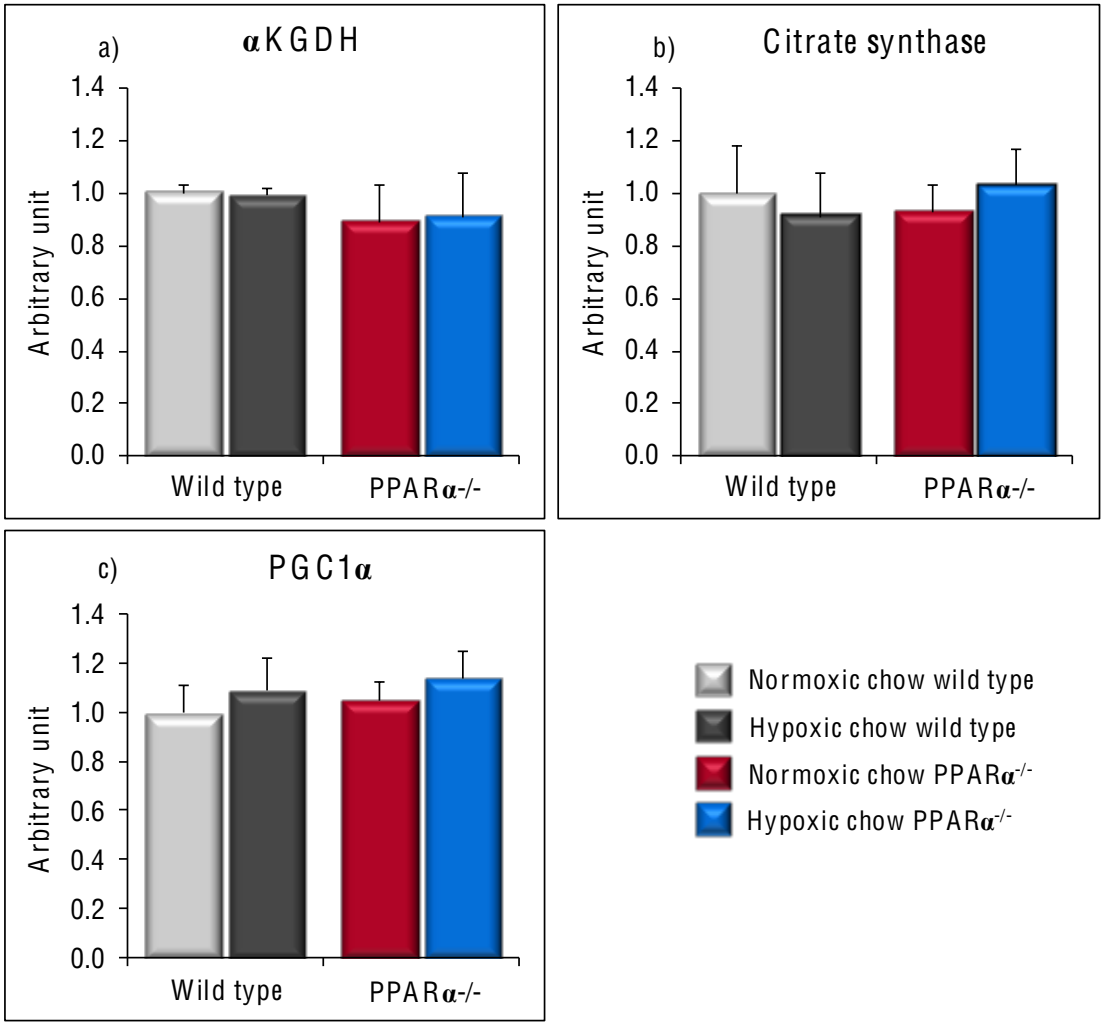

Figure 5.7 Cardiac mitochondrial proteins: a) αKGDH, b) citrate synthase and c) PGC1α protein levels in wild type and PPARα$^{-/-}$ mice following 3 weeks of chronic hypoxia. No statistically significant differences. n = 5 per group.

5.4.6.3 Electron transport chain proteins

Levels of the electron transport chain proteins, complex I, II and IV were normal in PPARα$^{-/-}$ mouse hearts and was not altered by hypoxia (Figure 5.8)

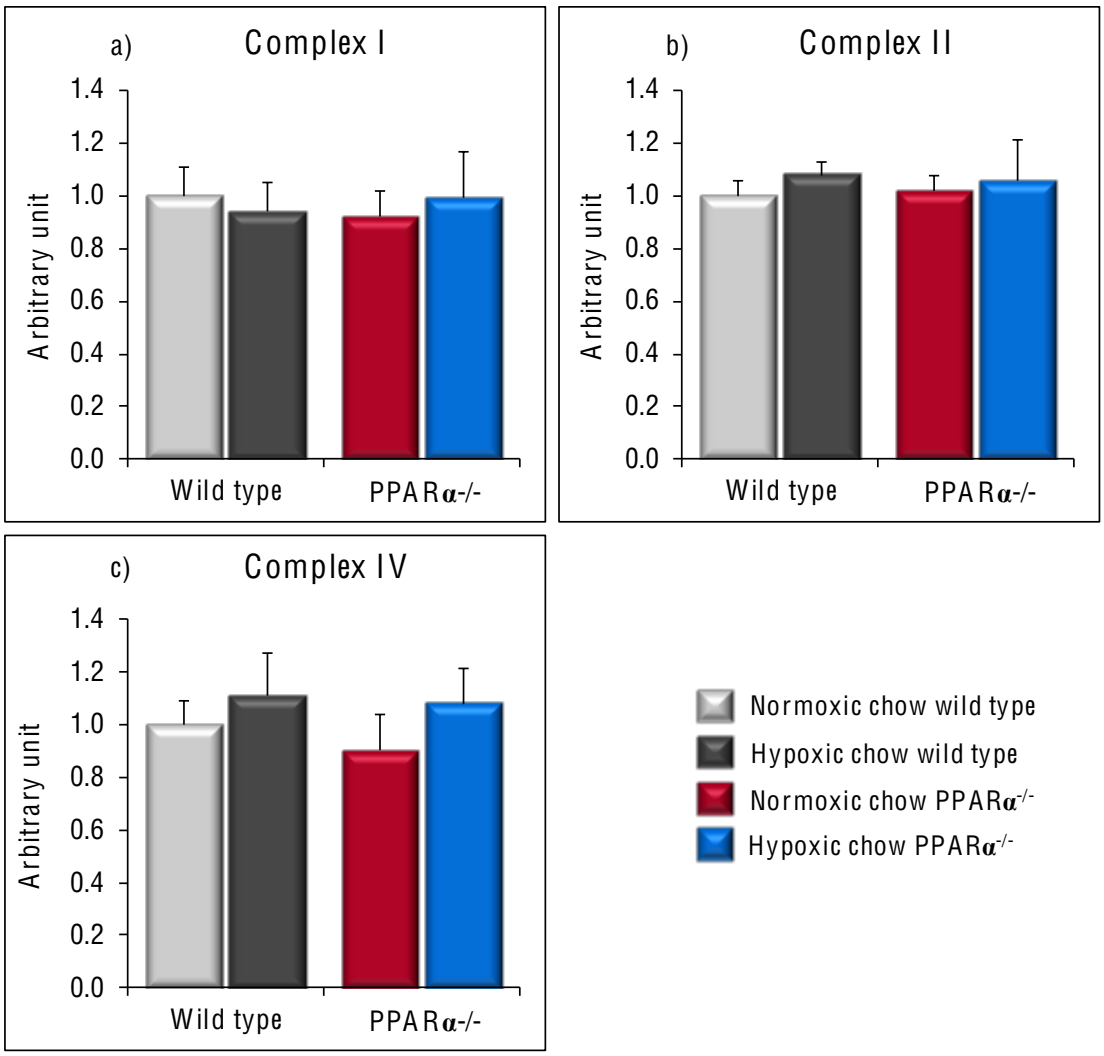

Figure 5.8 Cardiac electron transport chain proteins: a) Complex I, b) Complex II and c) Complex IV protein levels in wild type and PPARα$^{-/-}$ mice following 3 weeks of chronic hypoxia. No statistically significant differences. n = 5-6 per group.

5.4.6.4 Glucose metabolism

Protein levels of GLUT1 and GLUT4 were normal in all PPARα$^{-/-}$ mouse hearts. Cardiac PDK4 protein levels were 40% lower in PPARα$^{-/-}$ mice compared to normoxic wild type mice and was not affected by hypoxia (Figure 5.9). The activities of the glycolytic enzymes, pyruvate kinase and PGK1, were normal in all PPARα$^{-/-}$ mouse hearts.

5.4.6.5 Fatty acid metabolism

PPARα downstream targets were downregulated in all PPARα$^{-/-}$ mouse hearts (Figure 5.10). Cardiac MCAD levels were 40% lower in normoxic PPARα$^{-/-}$ mice compared to normoxic wild type mice, at both mRNA and protein levels, and were unchanged by hypoxia. Similarly, cardiac UCP3 and MTE1 protein levels were at least 50% lower in all PPARα$^{-/-}$ mice compared to wild type mice, irrespective of oxygen exposure.

5.4.6.6 Cardiac PPAR isoforms

PPARα mRNA expression was negligible in all PPARα$^{-/-}$ mouse hearts and was not affected by hypoxia. Protein levels of the PPARα obligate partner, RXRα were normal in PPARα$^{-/-}$ mouse hearts and were not affected by hypoxia. Similarly, PPARβ/δ and PPARγ mRNA expression was normal in all PPARα$^{-/-}$ mouse hearts (Figure 5.11).

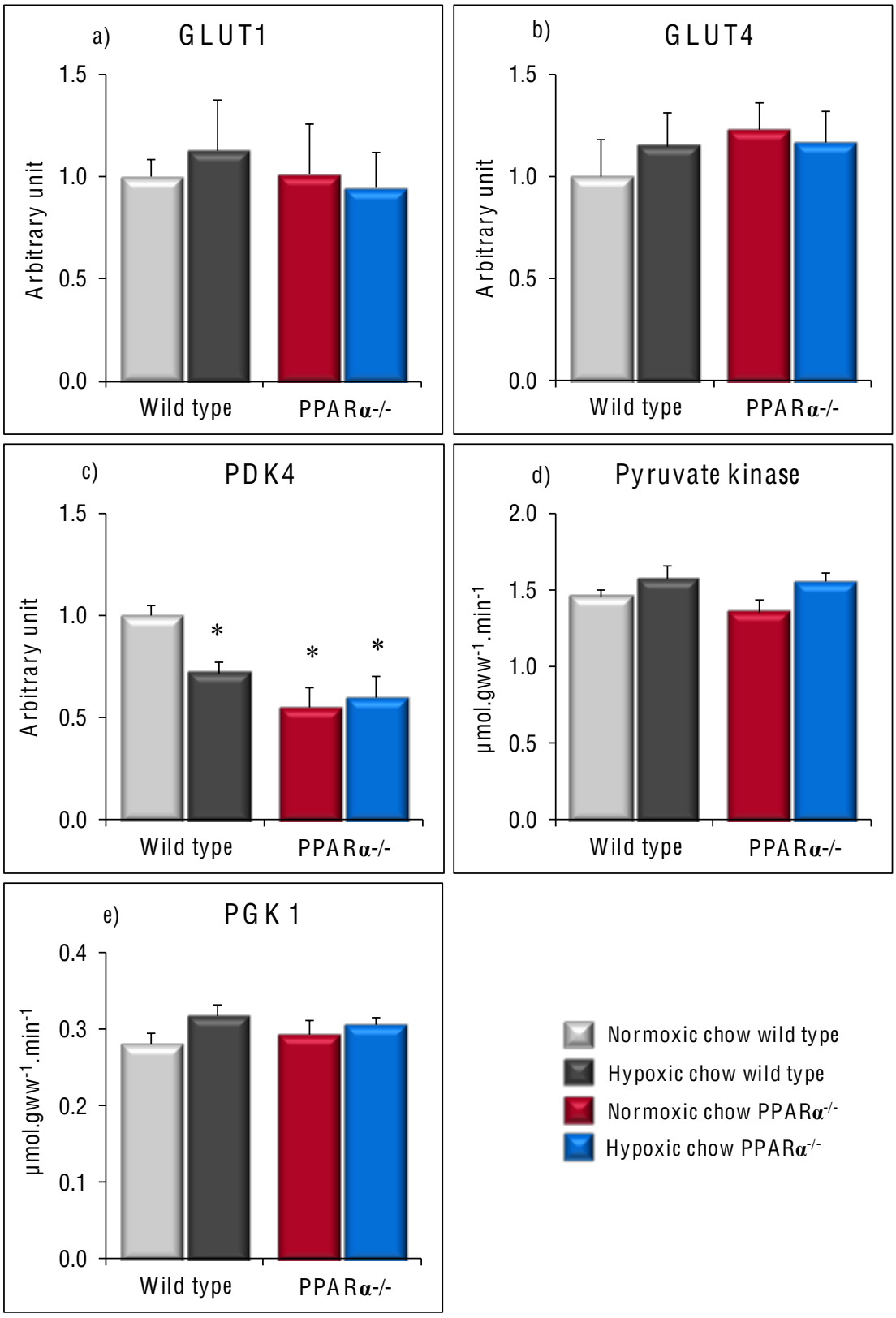

Figure 5.9 Glucose metabolism: Cardiac protein levels of a) GLUT1, b) GLUT4, c) PDK4, and enzyme activities of d) pyruvate kinase and e) PGK1 in wild type and PPARα$^{-/-}$ mice following 3 weeks of chronic hypoxia. *p < 0.05 relative to normoxic wild type mice. n = 5-7 per group.

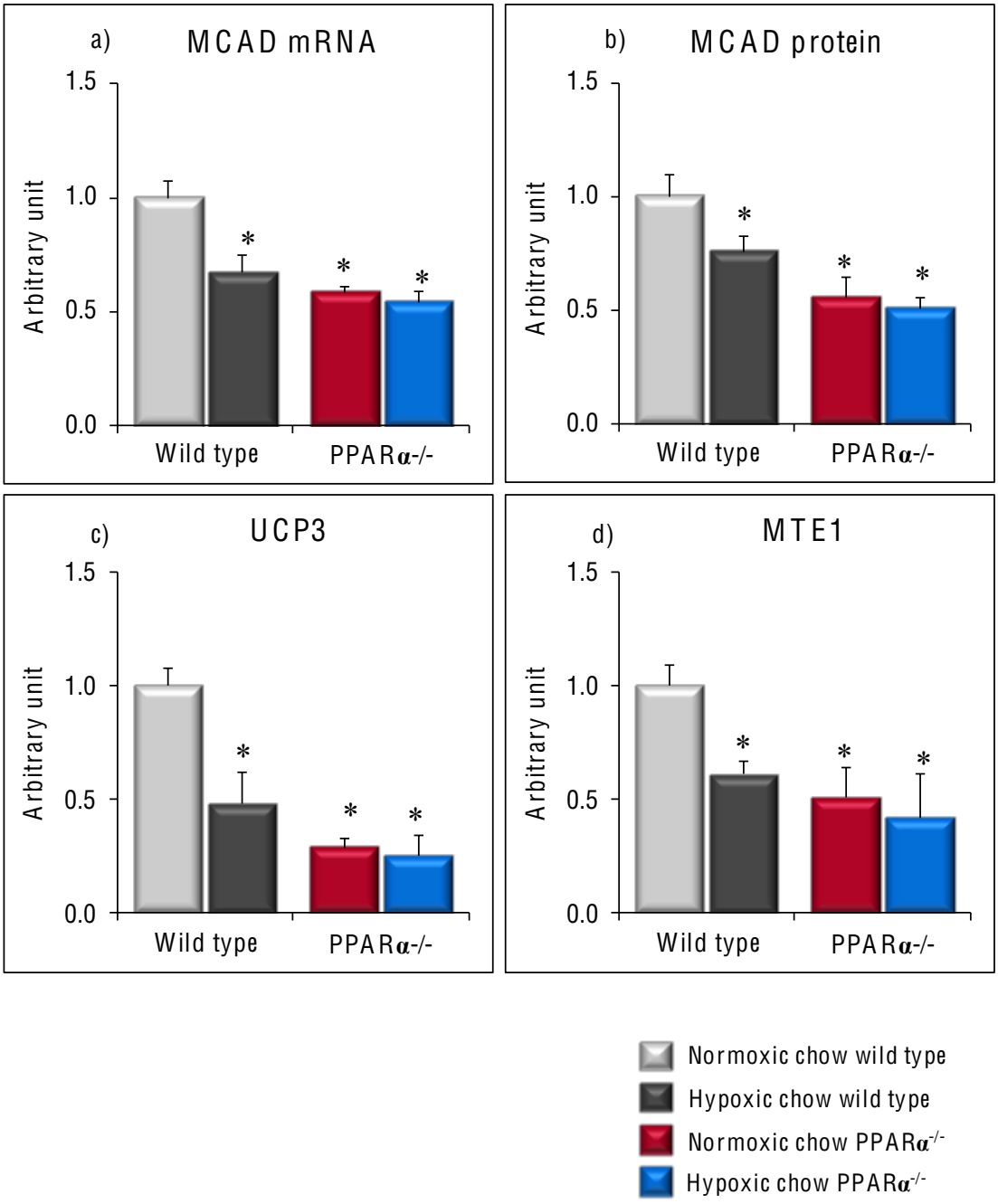

Figure 5.10 Fatty acid metabolism: Cardiac a) MCAD mRNA expression, b) MCAD, c) UCP3 and d) MTE1 protein levels in wild type and PPARα$^{-/-}$ mice following 3 weeks of chronic hypoxia. mRNA expression in cardiac tissues was normalized to the geometric mean of β-actin (housekeeping gene).*$p < 0.05$ relative to normoxic chow fed mice. n = 5-9 per group.

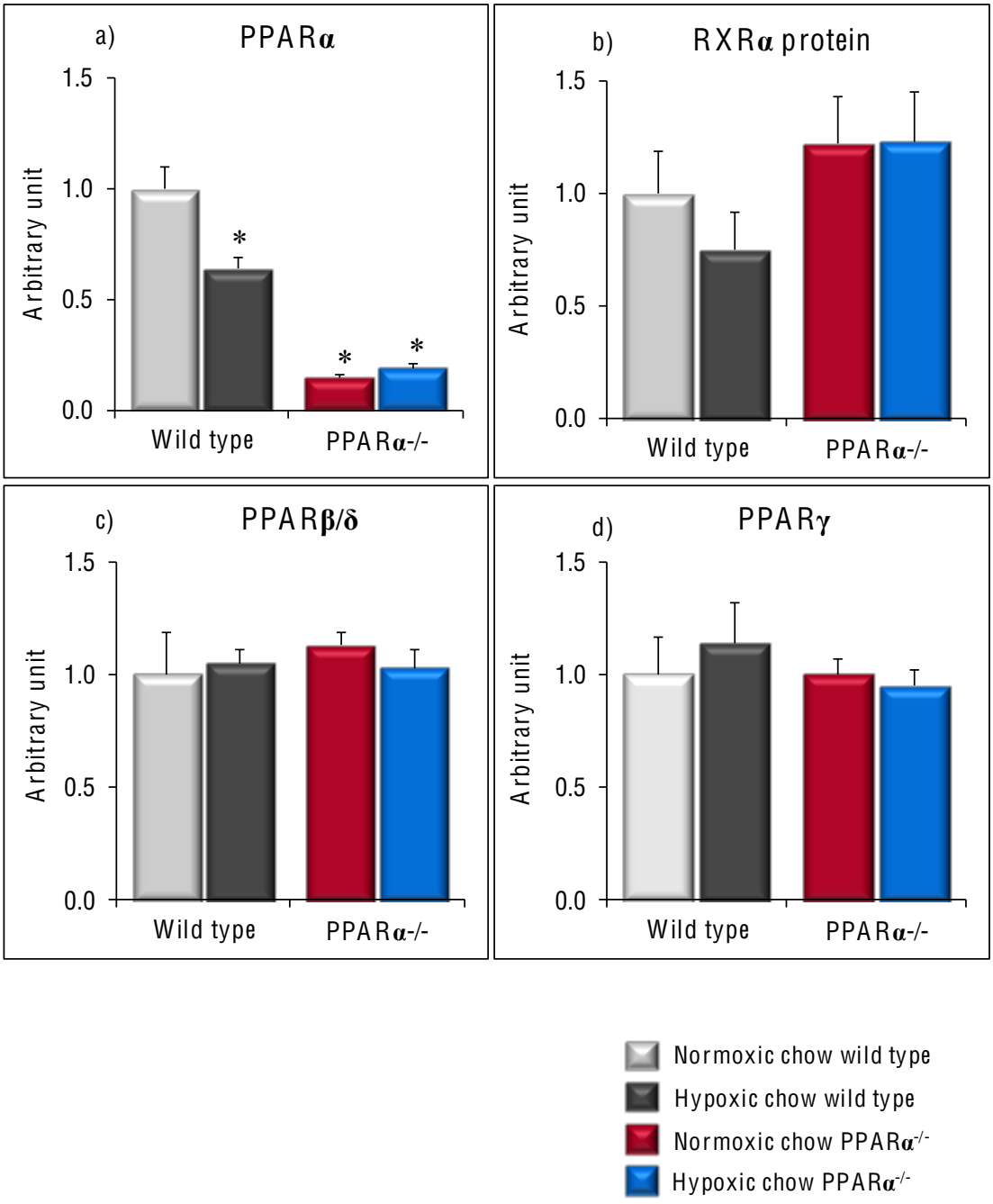

Figure 5.11 Cardiac PPAR isoforms: a) PPARα mRNA expression, b) RXRα protein levels, c) PPARβ/δ and d) PPARγ mRNA expression in wild type and PPARα$^{-/-}$ mice following 3 weeks of chronic hypoxia. mRNA expression in cardiac tissues was normalized to the geometric mean of β-actin (housekeeping gene). *p < 0.05 relative to normoxic wild type mice. n= 6 per group.

5.4.7 **PPARα**-regulated proteins in gastrocnemius muscle

Similar to the heart, deletion of PPARα$^{-/-}$ decreased UCP3 and MTE1 protein levels in gastrocnemius skeletal muscle by 60% ($p < 0.01$) and 45% ($p < 0.05$) respectively, which were not affected by hypoxia (Figure 5.12). Gastrocnemius PDK4 protein levels were normal in all PPARα$^{-/-}$ mice (Figure 5.12).

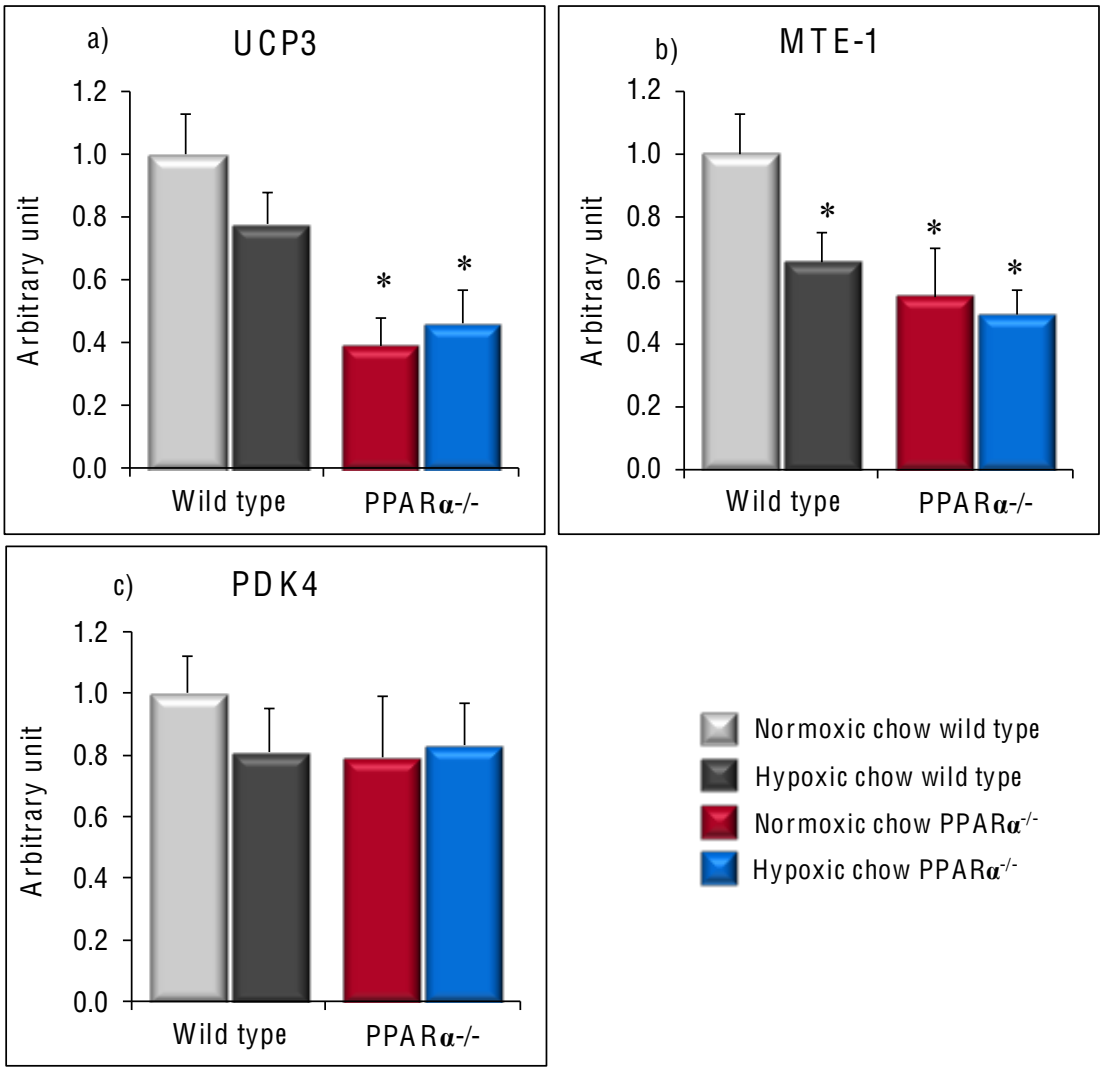

Figure 5.12 PPARα-regulated proteins in skeletal muscle: a) UCP3, b) MTE1 and c) PDK4 protein levels in chow fed and high fat fed wild type and PPARα$^{-/-}$ mice following 3 weeks of chronic hypoxic housing. *$p < 0.05$ relative to normoxic chow fed mice. n = 6 per group.

5.5 RESULTS 2: EFFECT OF HIGH FAT FEEDING IN PPARα NULL MICE

Results presented in this section highlight the changes caused by high fat in PPARα$^{-/-}$ mouse hearts (summarized in Table 5.1). Results for normoxic and hypoxic PPARα$^{-/-}$ mice presented in Section 5.4 are shaded in grey to represent the control groups in this section.

5.5.1 *In vivo* cardiac morphology

High fat feeding did not alter the body weights of PPARα$^{-/-}$ mice, whether hypoxic or normoxic. Hypoxia in high fed PPARα$^{-/-}$ mice resulted in LV hypertrophy, as LV mass was increased by 15% relative to normoxic PPARα$^{-/-}$ mice (Figure 5.13).

5.5.2 *In vivo* cardiac function

Feeding a high fat diet to PPARα$^{-/-}$ mice was deleterious for cardiac function, irrespective of oxygen exposure. Unlike chow fed PPARα$^{-/-}$ mice, stroke volume and cardiac output were reduced by at least 29% ($p < 0.01$) in normoxic high fat fed PPARα$^{-/-}$ mice relative to normoxic chow fed PPARα-/- mice. Chronic hypoxia did not cause an additional reduction in stroke volume and cardiac output over PPARα ablation with high fat feeding (Figure 5.14.1). While chow fed PPARα$^{-/-}$ mice had normal cardiac index and ejection fraction, high fat feeding reduced cardiac index and ejection fraction in all PPARα$^{-/-}$ mice by at least 5%, irrespective of oxygen exposure ($p < 0.05$) (Figure 5.14.2).

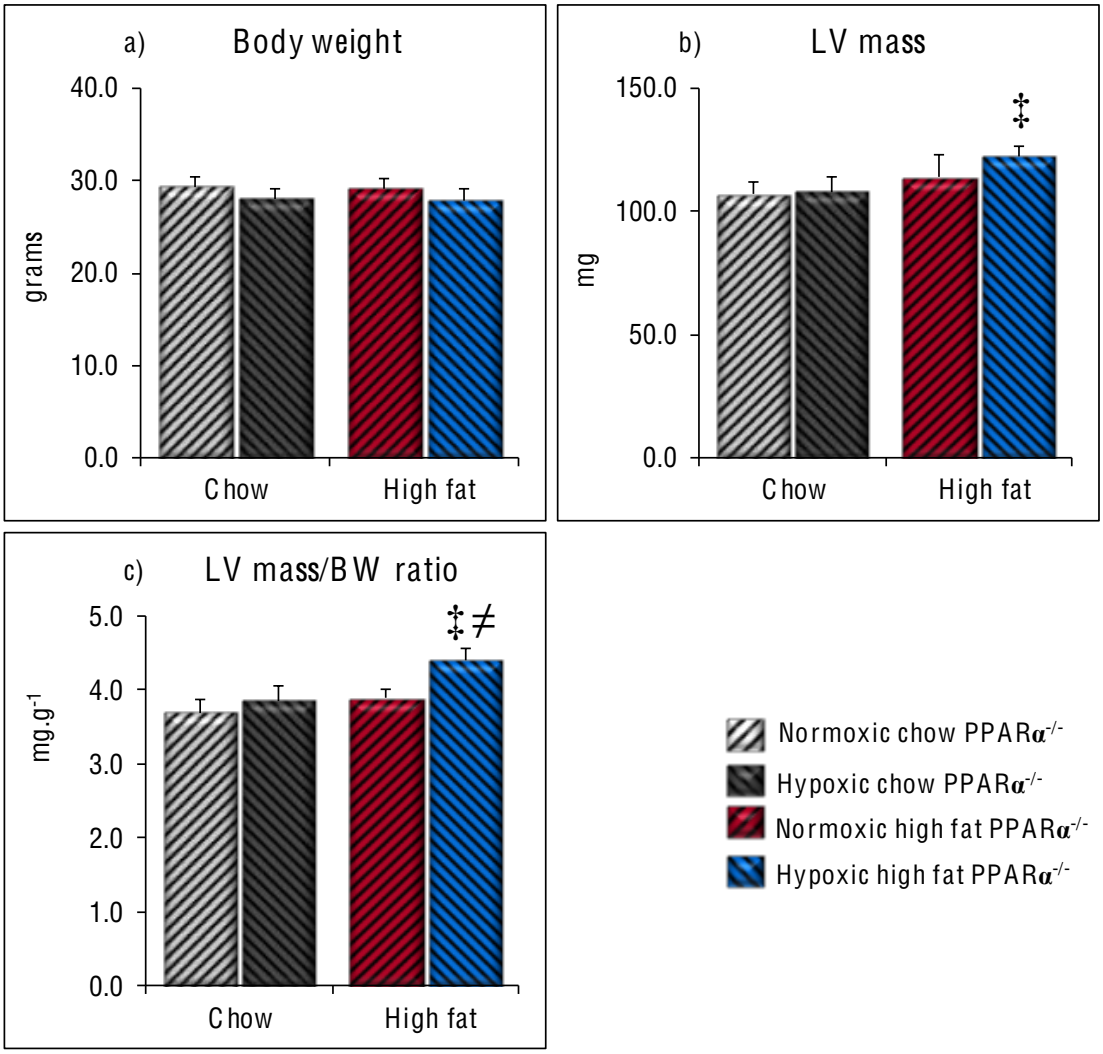

Figure 5.13 Effect of hypoxia and high fat feeding on *in vivo* cardiac morphology: a) LV mass and, b) body weight c) LV mass / body weight (BW) ratio in chow fed and high fat fed PPARα$^{-/-}$ mice following 3 weeks of chronic hypoxia. ‡ < 0.05 relative to normoxic chow fed PPARα$^{-/-}$ mice, ≠ relative to normoxic high fat fed PPARα$^{-/-}$ mice. n = 5-16 per group.

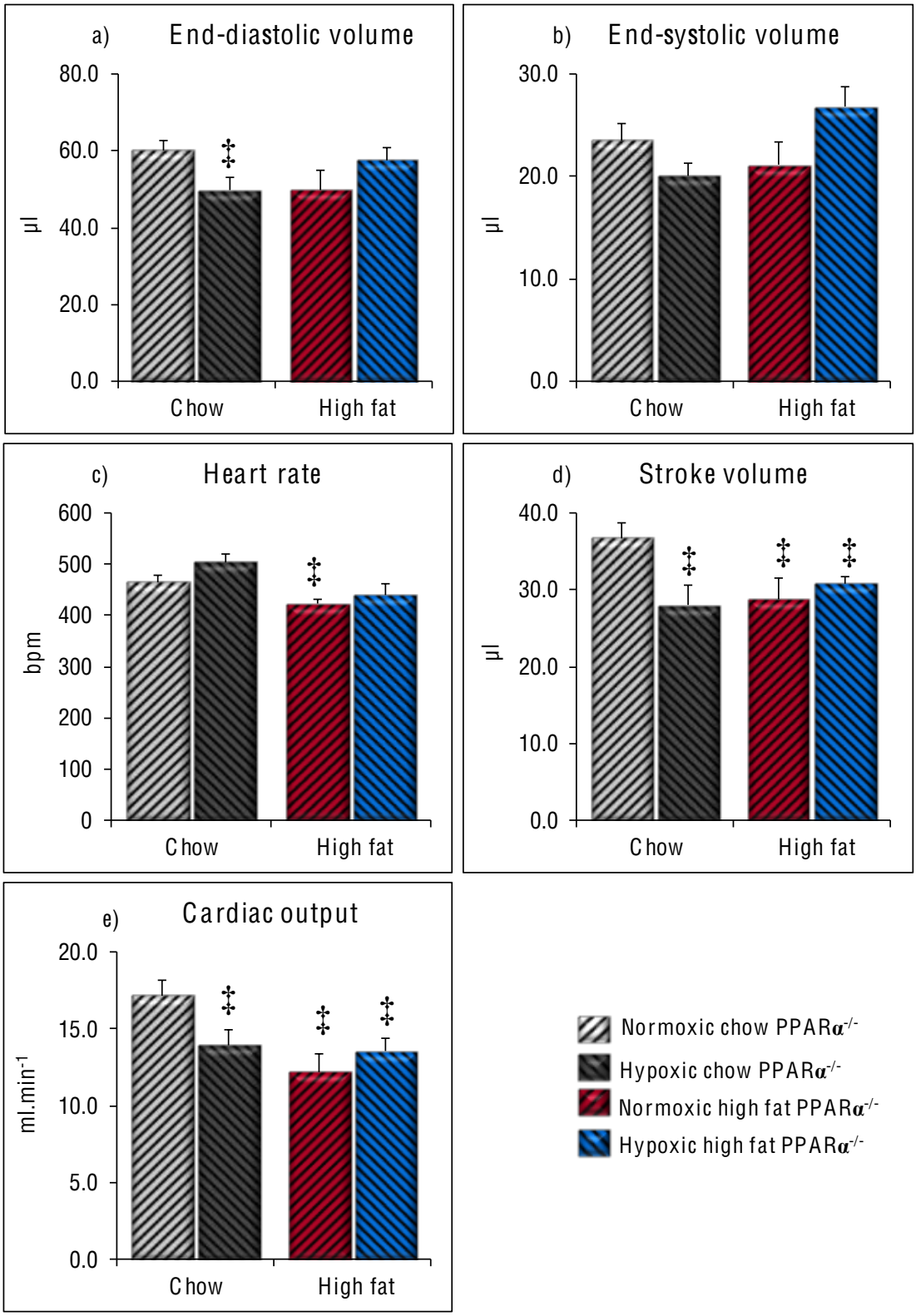

Figure 5.14.1 Effect of hypoxia and high fat feeding on *in vivo* cardiac function: a) End diastolic volume, b) end systolic volume, c) heart rates, d) stroke volume and e) cardiac output in chow fed and high fat fed PPARα$^{-/-}$ mice following 3 weeks of chronic hypoxia. ‡ $p < 0.05$ relative to normoxic chow fed PPARα$^{-/-}$ mice. n = 5-16 per group.

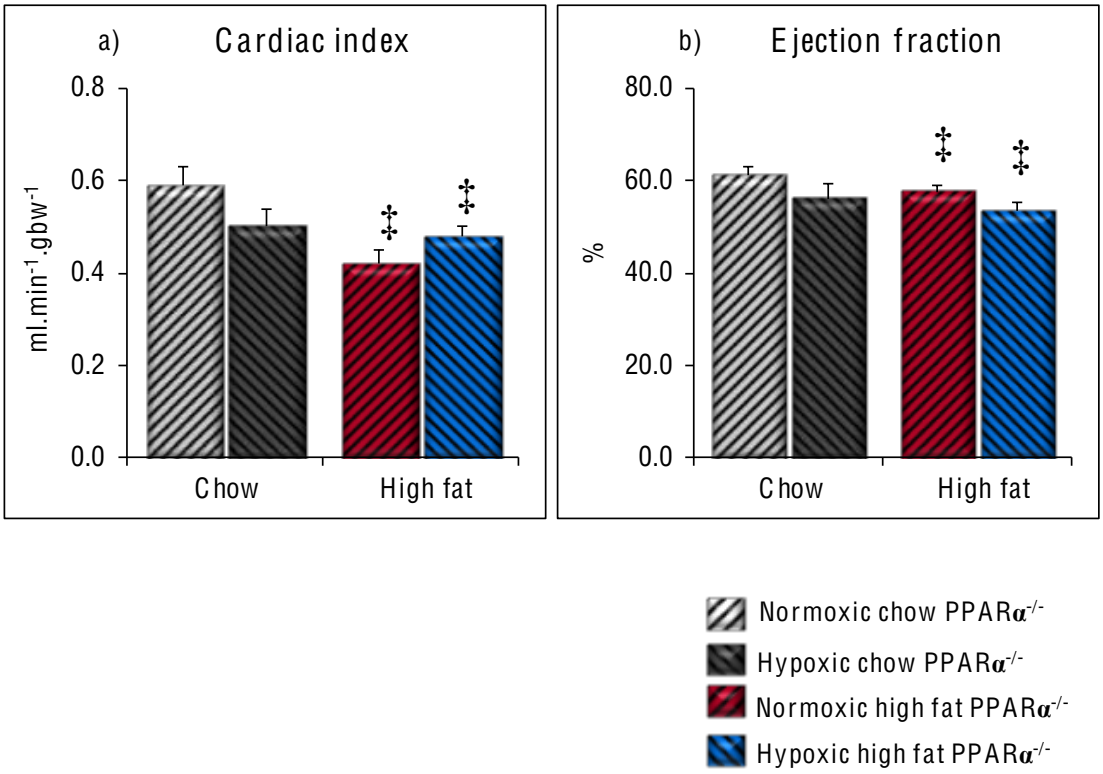

Figure 5.14.2 Effect of hypoxia and high fat feeding on *in vivo* cardiac function: a) Cardiac index and b) ejection fraction in wild type and PPARα$^{-/-}$ mice following 3 weeks of chronic hypoxia. ‡ $p < 0.05$ relative to normoxic chow fed PPARα$^{-/-}$ mice. n = 5-16 per group.

5.5.3 Cardiac substrate metabolism

High fat feeding of PPARα$^{-/-}$ mice did not have additional effects on cardiac substrate metabolism over those of PPARα ablation, as they also exhibit high glycolytic flux and lactate efflux, with low palmitate oxidation (Table 5.1). Myocardial TAG and FFA content also did not change with high fat feeding in PPARα$^{-/-}$ mice (Table 5.1)

5.5.4 Cardiac molecular profile

Please refer to Appendix 4 for western blot images (where applicable).

5.5.4.1 Hypoxia markers

While hypoxia in PPARα$^{-/-}$ mice increased cardiac VEGF mRNA and proteins, high fat feeding during hypoxia prevented the upregulation of cardiac VEGF at mRNA and protein levels (Figure 5.15). SIRT1 protein levels were 30% lower in normoxic and hypoxic PPARα$^{-/-}$ mouse hearts compared to wild type mice (Figure 5.6), but high fat feeding prevented these changes (Figure 5.15).

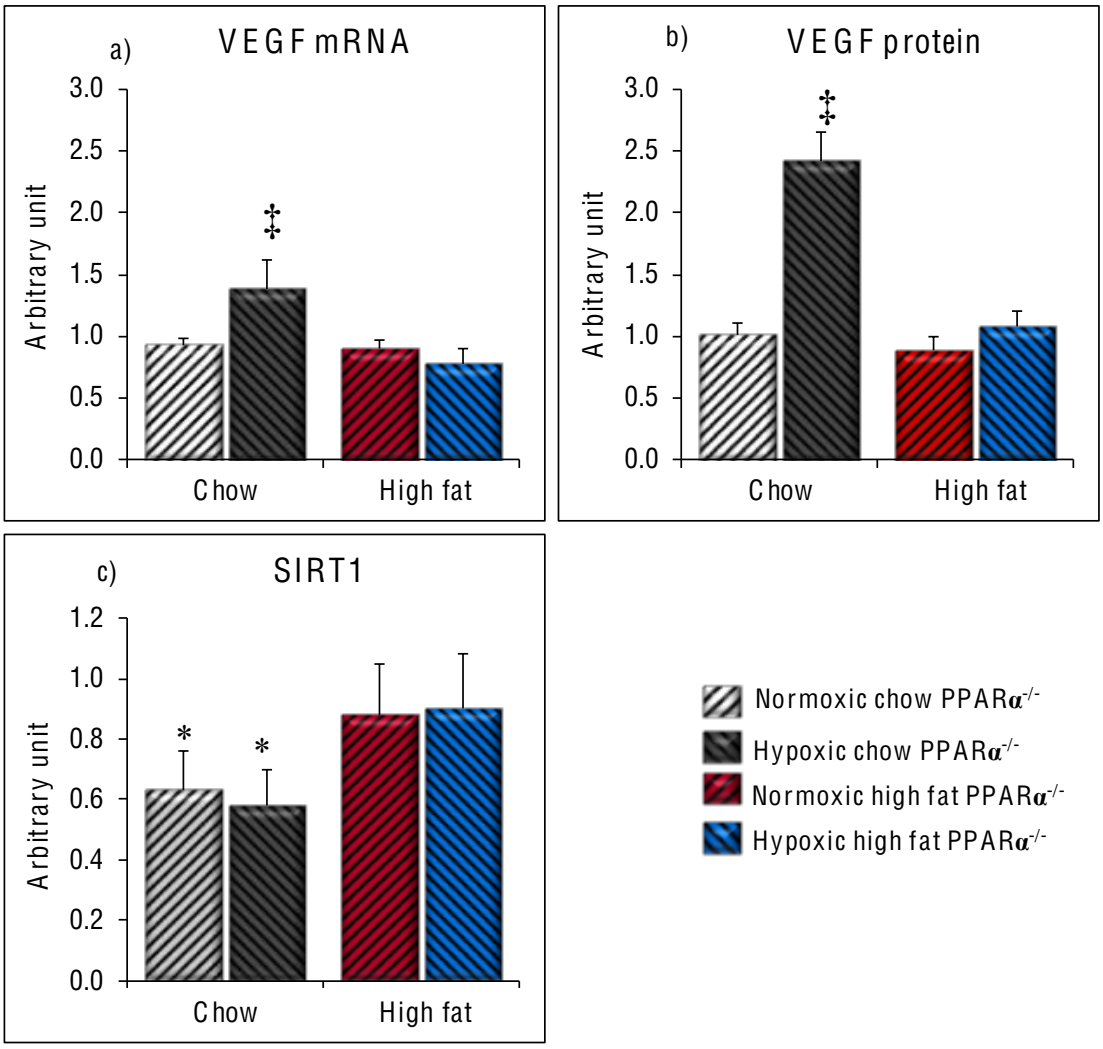

Figure 5.15 Hypoxia markers: Cardiac a) VEGF mRNA expression and b) VEGF protein levels in high fat fed PPARα$^{-/-}$ mice following 3 weeks of chronic hypoxia. *$p < 0.05$ relative to normoxic chow fed wild type mice, ‡$p < 0.05$ relative to normoxic chow fed PPARα$^{-/-}$ mice. n = 5-12 per group.

5.5.4.2 Glucose metabolism

GLUT4 protein levels were normal in all PPARα$^{-/-}$ mouse hearts, irrespective of diet and/or oxygen exposure. Cardiac PDK4 protein was low all PPARα$^{-/-}$ mice despite being on high fat diet (Table 5.1).

5.5.4.3 Fatty acid metabolism

High fat feeding in all PPARα$^{-/-}$ mice did not result in additional effect on cardiac PPARα downstream targets over PPARα ablation. MCAD protein and mRNA were persistently low in all high fat fed PPARα$^{-/-}$ mouse hearts, as with UCP3 and MTE1 protein levels (Table 5.1).

5.5.4.4 Cardiac PPAR isoforms

PPARα mRNA expression was negligible in all PPARα$^{-/-}$ mouse hearts and was not affected by high fat feeding, irrespective of oxygen exposure. The PPARα obligate partner, RXRα was also normal in high fat fed PPARα$^{-/-}$ mouse hearts and was not affected by hypoxia. Similarly, the mRNA expression of PPARβ/δ and PPARγ was normal in all high fat fed PPARα$^{-/-}$ mouse hearts (Table 5.1)

Table 5.1: Summary of results

Data are means ± SEM. *$p < 0.05$ relative to normoxic wild type mice. ‡ $p < 0.05$ relative to normoxic PPARα-/- mice
≠$p < 0.05$ relative to normoxic high fat fed PPARα$^{-/-}$ mice

	CHOW FED				HIGH FAT FED			
	Normoxia	n	Hypoxia	n	Normoxia	n	Hypoxia	n
Cardiac morphology and function								
Final body weight (g)	29.4 ± 0.97*	16	28.0 ± 1.11*	6	29.2 ± 1.64	5	27.9 ± 1.25	5
LV mass (mg)	107 ± 4.62*	16	108 ± 5.94*	6	113 ± 9.46	5	122 ± 3.89‡	5
LVmass/BW ratio (mg.g^{-1})	3.69 ± 0.19	16	3.86 ± 0.19*	6	3.92 ± 0.12	5	4.41 ± 0.15‡≠	5
End-diastolic volume (µl)	60.3 ± 2.47	16	49.7 ± 3.45*‡	6	49.9 ± 4.90	5	57.6 ± 3.34	5
End-systolic volume (µl)	23.5 ± 1.67	16	20.1 ± 1.27	6	21.1 ± 2.28	5	26.8 ± 2.02	5
Heart rate (bpm)	465 ± 12.1	16	503 ± 15.5*	6	423 ± 9.74‡	5	440 ± 20.4	5
Stroke volume (µl)	36.8 ± 1.97	16	27.9 ± 2.57*‡	6	28.8 ± 2.80	5	30.8 ± 2.06‡	5
Cardiac output (ml.min^{-1})	17.2 ± 1.06	16	13.9 ± 1.00*‡	6	12.2 ± 1.16‡	5	13.5 ± 0.83‡	5
Cardiac index (ml.min^{-1}.gbw^{-1})	0.59 ± 0.04	16	0.50 ± 0.04	6	0.42 ± 0.03‡	5	0.48 ± 0.02‡	5
Ejection fraction (%)	61.1 ± 1.98	16	56.2 ± 3.19	6	57.7 ± 1.29‡	5	53.5 ±1.97‡	5
Cardiac substrate metabolism								
Glycolytic flux (µmol.gww.min^{-1})	0.51 ± 0.10*	6	0.49 ± 0.06*	9	0.32 ± 0.04*	6	0.39 ± 0.02*	7
Lactate efflux (µmol.gwwt.min^{-1})	0.07 ± 0.01*	6	0.07 ± 0.01*	9	0.05 ± 0.007*	6	0.05 ± 0.003*	7
Palmitate oxidation (µmol.gww.min^{-1})	0.09 ± 0.02*	9	0.07 ± 0.03*	9	0.06 ± 0.01*	9	0.07 ± 0.01*	9
Cardiac lipid content								
mTAG (µmol.gww^{-1})	4.04 ± 0.52*	6	4.19 ± 0.049*	6	4.09 ± 0.51*	6	4.35 ± 0.46*	6
mFFA (µmol.gww^{-1})	0.78 ± 0.11	6	0.83 ± 0.18	6	0.72 ± 0.12	6	0.85 ± 0.13	6

Table 5.1 (continued)

Cardiac mRNA expression (arbitrary unit)								
PPARα	0.15 ± 0.01*	6	0.19 ± 0.02*	6	0.17 ± 0.02*	6	0.16 ± 0.02*	6
PPARβ/δ	1.13 ± 0.06	6	1.03 ± 0.08	6	1.01 ± 0.08	6	1.11 ± 0.09	6
PPARγ	1.00 ± 0.07	6	0.95 ± 0.07	6	1.04 ± 0.08	6	0.93 ± 0.07	6
MCAD	0.58 ± 0.03*	6	0.54 ± 0.05*	6	0.56 ± 0.04*	6	0.54 ± 0.08*	6
VEGF	0.93 ± 0.05	5	1.38 ± 0.11*‡	5	0.90 ± 0.07	5	0.77 ± 0.06	5
Cardiac protein levels (arbitrary unit)								
SIRT1	0.63 ± 0.13*	12	0.58 ± 0.12*	12	0.88 ± 0.17	6	0.90 ± 0.18	6
VEGF	1.00 ± 0.09	7	2.42 ± 0.24*‡	7	0.88 ± 0.11	8	1.08 ± 0.13	8
GLUT4	1.23 ± 0.13	6	1.17 ± 0.15	6	1.27 ± 0.15	7	1.12 ± 0.19	6
PDK4	0.55 ± 0.10*	6	0.60 ± 0.10*	6	0.61 ± 0.22*	6	0.60 ± 0.08*	6
MCAD	0.56 ± 0.09*	9	0.51 ± 0.05*	9	0.58 ± 0.11*	6	0.53 ± 0.30*	6
UCP3	0.29 ± 0.04*	6	0.25 ± 0.09*	6	0.55 ± 0.14*	5	0.45 ± 0.16*	5
MTE1	0.51 ± 0.13*	6	0.42 ± 0.19*	6	0.43 ± 0.09*	7	0.52 ± 0.12*	6
RXRα	1.22 ± 0.21	6	1.23 ± 0.22	6	1.11 ± 0.14	6	1.22 ± 0.22	6
Gastrocnemius muscle protein levels (arbitrary unit)								
UCP3	0.39 ± 0.09*	6	0.46 ± 0.11*	6	0.62 ± 0.10*	6	0.63 ± 0.11*	6
MTE1	0.55 ± 0.15*	6	0.49 ± 0.08*	6	0.65 ± 0.09*	6	0.64 ± 0.10*	6
PDK4	0.79 ± 0.20	6	0.83 ± 0.14	6	0.74 ± 0.16	6	0.76 ± 0.14	6

5.6 DISCUSSION

Principal finding

In this chapter, it was found that PPARα$^{-/-}$ mouse hearts were intolerant to chronic hypoxia, and the impairment of cardiac function in hypoxic PPARα$^{-/-}$ mice was accompanied by abnormal cardiac metabolism. Normoxic PPARα$^{-/-}$ mouse hearts had low palmitate oxidation and were highly glycolytic, and these changes were able to maintain normal cardiac function. However, insulin stimulation showed that glycolytic rates were not maximal in hypoxic PPARα$^{-/-}$ mouse hearts, and that elevated basal glycolytic rate was insufficient to protect PPARα$^{-/-}$ mice from hypoxia, despite reduced palmitate oxidation. High fat feeding was detrimental to cardiac function in all PPARα$^{-/-}$ mice, even though the hearts were resistant to the metabolic effect of high fat feeding, irrespective of oxygen supply, consistent with the regulatory role of PPARα in cardiac fatty acid metabolism. PPARα downstream targets were low in all PPARα$^{-/-}$ mouse hearts. The collective findings suggest that the loss of metabolic flexibility associated with PPARα deletion is detrimental to cardiac function when subjected to hypoxia and/or high fat feeding.

PPARα deficient mice were metabolically inflexible

Decreased palmitate oxidation rates and MCAD levels in PPARα$^{-/-}$ mouse hearts confirmed the importance of PPARα in the transcriptional control of cardiac fatty acid oxidation capacity [252, 253]. Consequently, hearts from mice lacking PPARα were highly glycolytic, but were sufficient to support normal contractile function, consistent with published functional data on *ex vivo* perfused PPARα$^{-/-}$ mouse hearts [222, 254]. However, PPARα$^{-/-}$ mouse hearts were metabolically inflexible, as cardiac

substrate metabolism was not modified following hypoxia relative to their normoxic counterparts, in association with decreased cardiac output.

The impairment of cardiac function following hypoxia is supported by the intolerance of PPARα$^{-/-}$ hearts to increased workload [254, 256, 258], which have been shown to increase oxygen consumption by 40% at the expense of ATP synthesis [256]. Hearts of PPARα deficient mouse hearts are possibly energy starved[53], as myocardial ATP production from glucose can be outstripped by high functional demands. Indeed, work from this lab has shown that PCr in PPARα$^{-/-}$ mice was decreased due to severe depletion of total creatine [259], supported by the report of decreased creatine levels via metabolic profiling of PPARα$^{-/-}$ mouse hearts [260].

Insulin stimulation revealed that glycolytic rates in all PPARα$^{-/-}$ mouse hearts were not maximal. Indeed, during haemodynamic overload, enhancing glucose uptake by overexpressing GLUT1 corrected the functional defects of PPARα$^{-/-}$ mouse hearts [256]. This is not surprising as PPARα does not appear to have a direct effect on glucose transport and utilisation, demonstrated by unchanged cardiac glycolytic enzymes, GLUT1 and GLUT4 protein levels in PPARα$^{-/-}$ mice, as reported by others [222, 254]. The increase in glycolysis and possibly glucose oxidation [254, 255] in PPARα$^{-/-}$ hearts were most likely occurring secondary to a decrease in fatty acid oxidation [261], and through its control of cardiac PDK4 [75], which was persistently low in all PPARα$^{-/-}$ mouse hearts. Information from lactate efflux suggests that the ratio of lactate production to glucose uptake was lower than wild type mouse hearts, and taken together with reduced PDK4 levels, glucose oxidation rates in PPARα$^{-/-}$ mouse hearts were possibly elevated, as reported by others [213, 254, 255].

Therefore, their inability to suppress glucose oxidation during restricted oxygen supply may confer the maladaptive cardiac phenotype observed. In agreement, a 22% decrease in cardiac efficiency in PPARα$^{-/-}$ mouse hearts subjected to an increased preload of 15mmHg increased myocardial oxygen consumption by 25%, and despite this, glycolytically derived acetyl-CoA and PDH flux remained high in PPARα$^{-/-}$ hearts [262]. Therefore, it appears that PPARα$^{-/-}$ mice lack the metabolic compensatory apparatus for cardiac hypoxic adaptation.

Genetic ablation of PPARα severely depressed cardiac PPARα mRNA expression. Although PPARα expression was not completely abolished, it has been shown that in the heart, targeted disruption [263] of the PPARα gene in PPARα$^{-/-}$ mice results in a non-functional transcript [65, 264]. Mice lacking PPARα have increased accumulation of triglycerides in the myocardium, irrespective of oxygen supply, consistent with the reported lipid accumulation in PPARα$^{-/-}$ mouse hearts [260, 265], but this does not seem to affect cardiac function in normoxic PPARα$^{-/-}$ mice. There was no compensatory increase in PPARβ/δ for the lack of PPARα, as described in the literature [264], suggesting that in hypoxia, PPARβ/δ may act passively, in synchrony with PPARα to regulate fatty acid utilisation as myocardial free fatty acids were unchanged in all PPARα$^{-/-}$ mouse hearts. Further molecular investigation demonstrated that cardiac UCP3 protein levels were low in all PPARα$^{-/-}$ mice, as previously reported [85], confirming UCP3 as a target of PPARα. MTE1, also a PPARα target, operates with UCP3 [93] in controlling fatty acid oxidation and was also decreased in all PPARα$^{-/-}$ hearts. The decrease in UCP3 and MTE1 protein levels were also apparent in skeletal muscle. Although reduced UCP3 appeared to be a beneficial adaptation to hypoxia, it was insufficient to protect PPARα$^{-/-}$ mice from

hypoxia. Therefore, decreased PPARα expression and fatty acid oxidation alone were inadequate to protect the hypoxic heart, and the ability of the heart to upregulate glycolysis was vital for the maintenance of cardiac function.

High fat feeding is detrimental to cardiac function in PPARα$^{-/-}$ mice

High fat feeding was deleterious to all PPARα$^{-/-}$ mouse hearts, irrespective of oxygen exposure. Given that EDV was unchanged with high fat feeding, the reduction in ejection fraction suggests a systolic dysfunction [266], which worsened with hypoxia, indicated by the hypertrophied LV. This severe cardiac phenotype was not observed in chow fed PPARα$^{-/-}$ mice. Metabolically, PPARα$^{-/-}$ mouse hearts were resistant to the normal effects of high fat feeding, as ligand binding did not occur in the absence of PPARα, demonstrated by the unchanged cardiac PPARα mRNA expression with high fat feeding in all PPARα$^{-/-}$ mice. MCAD levels were unaffected by high fat feeding in PPARα$^{-/-}$ mouse hearts, therefore, PPARα$^{-/-}$ mice lost the ability to enhance cardiac fatty acid oxidation in response to increased fatty acid supply, as was observed in fasted PPARα$^{-/-}$ mouse hearts [267].

The ensuing accumulation of intramyocardial triglycerides may have exacerbated cardiac dysfunction in high fat fed PPARα$^{-/-}$ mouse hearts [227, 268, 269]. However, the accumulation of intramyocardial triglyceride was similar in all PPARα$^{-/-}$ mice, and myocardial free fatty acids were unchanged, irrespective of oxygen supply and/or diet. Therefore the effect of high fat diet on cardiac function, in the absence of PPARα, cannot be explained by the routinely measured cardiac metabolic markers as these parameters were not altered compared to chow fed PPARα$^{-/-}$ mice. Deterioration of cardiac function could be attributed to increased vulnerability of PPARα$^{-/-}$ to

oxidative stress [270], that may be exacerbated by high fat feeding. Furthermore, it has been proposed that the pronounced hypertrophic growth response and functional deterioration in PPARα$^{-/-}$ mice subjected to 4 weeks of TAC, compared to sham-operated PPARα$^{-/-}$ mice, were associated with enhanced expression of pro-inflammatory cytokines, such as IL-6, COX-2 and TNF-α, and extracellular matrix remodelling [258]. Finally, it is quite conceivable that loss of PPARα compromised the energy-generating capacity of cardiac muscle [53] and therefore, PPARα$^{-/-}$ mouse hearts were incapable of increased work after imposition of multiple stresses.

Interestingly, high fat feeding in PPARα$^{-/-}$ mice blunted the VEGF response to hypoxia, an effect that was observed with high fat feeding in wild type mice, but not in chow fed PPARα$^{-/-}$ mouse hearts. This may provide an additional explanation for the deterioration of cardiac function with high fat feeding following hypoxia in PPARα$^{-/-}$ mice. Further studies are needed to examine the effect of high fat feeding on HIF activity as there is increasing evidence documenting the detrimental effect of high fat feeding on HIF response[248, 251], and subsequently on cardiac function, as described in Chapter 4. However, the mechanism associated with these changes is unknown. A number of studies have demonstrated a link between SIRT1 and HIF [208, 209, 271]. Activation of PPARα by fasting also activated SIRT1 gene expression in the liver [272], and the protective effects of SIRT1 on cardiac hypertrophy were attenuated in PPARα$^{-/-}$ mice [210]. Therefore, SIRT1 may act as an intermediary regulator between HIF and PPARα during metabolic adaptation to hypoxia. In Chapter 3, it was shown that hypoxia in wild type mice decreased SIRT1 protein levels, consistent with downregulation of PPARα. However, SIRT1 protein levels in PPARα$^{-/-}$ mice were inconsistent. While deletion of PPARα suppressed

cardiac SIRT1 protein levels in all chow fed PPARα$^{-/-}$ mice, high fat feeding did not alter SIRT1 protein levels in PPARα$^{-/-}$ mouse hearts. Therefore, the present study was unable to identify the relationship between PPARα and SIRT1 and their interaction during hypoxic adaptation.

In summary, the work in this chapter has shown that PPARα$^{-/-}$ mouse hearts were intolerant to chronic hypoxia. Innate alteration of cardiac substrate metabolism towards glucose metabolism displayed by the PPARα null mice was inadequate to protect the hearts from hypoxia, and the ability of the heart to upregulate glycolysis was pivotal for the maintenance of cardiac function. The loss of PPARα rendered the hearts metabolically inflexible, preventing adaptation when challenged with hypoxia and/or or high fat feeding, demonstrating that cardiac metabolic adaptation to hypoxia is PPARα-dependent.

CHAPTER 6

REGULATION OF PPARα BY HIF

6.1 ABSTRACT

Work in Chapter 3 demonstrated that the metabolic adaptation associated with decreased PPARα expression preserved *in vivo* cardiac function. Hypoxia in the same hearts increased downstream markers of HIF, cardiac VEGF and PDK1 protein levels 3-fold and 79% respectively. It was postulated that the downregulation of PPARα expression during chronic hypoxia was as a consequence of HIF stabilisation. To test this hypothesis, temporal molecular metabolic changes in HL-1 cardiomyocytes exposed to hypoxia or pharmacological activation of HIF using HIF hydroxylase inhibitors, dimethyloxalylglycine (DMOG), or 2-(1-chloro-4-hydroxyisoquinoline-3-carboxamido) acetic acid (BIC) were investigated. HL-1 cells were either exposed to normoxia, 6, 24, 48 hours of hypoxia (2% O_2) or treated with DMOG for 24 hours or BIC for 24 or 48 hours. After hypoxia or pharmacological stimulation, protein levels of HIF-1α, HIF-2α and their downstream targets were measured. RNA was extracted to quantify the mRNA expression of PPAR isoforms and PPARα downstream targets, including MCAD, UCP3 and PDK4. After 24 hours hypoxia, HIF-1α and HIF-2α protein levels were upregulated 5-fold ($p < 0.01$) and 72% ($p < 0.05$) respectively, which increased the HIF downstream target, VEGF, by 37% ($p < 0.01$). Hypoxia also increased protein levels GLUT1 and PDK1 by 3-fold ($p < 0.01$) and 69% ($p < 0.05$) respectively. In the same hypoxic cells, PPARα expression was reduced by 27% ($p < 0.01$), which decreased its regulated downstream targets including MCAD and UCP3, by 30% ($p < 0.01$). Neither PPARβ/δ nor PPARγ mRNA expression were altered after 24 hours hypoxia. Twenty-four hours treatment of HL-1 cells with BIC upregulated HIF-1α 9-fold and downregulated PPARα and its downstream targets, in a similar manner to hypoxia, which mirrored the observation of the *in vivo* studies. Non-specific HIF activation by DMOG affected all 3 PPAR isoforms. In conclusion, this study demonstrated a HIF-dependent downregulation of PPARα during chronic hypoxia.

6.2 INTRODUCTION

Hypoxia-inducible factor (HIF) is a key modulator of the transcriptional responses to changes in oxygen availability [127, 273]. HIF regulates the expression of multiple genes that control cellular and systemic adaptation to hypoxia, including a switch from oxidative to glycolytic metabolism, and stimulation of oxygen delivery through increased erythropoiesis and angiogenesis [132, 133]. Therefore, HIF target genes include EPO [133, 274], VEGF [134], GLUT1 [135, 136], and PDK1 [137, 138]. There are three known members of the HIF family (HIF-1, HIF-2 and HIF-3), all being α/β heterodimeric proteins [140]. HIF-α subunits are regulated posttranslationally via an oxygen dependent hydroxylation mechanism catalyzed by three HIF-prolyl-4-hydroxylases (named PHD1, PHD2, and PHD3), of which PHD2 and PHD3 are predominantly expressed in the heart [144]. In addition, the function of the HIF-α transactivator domain is inhibited by asparagine hydroxylation catalysed by Factor Inhibiting HIF (FIH) [145]. Both of these hydroxylation reactions are linked to oxygen availability; under normoxia, von Hippel-Lindau protein (pVHL) targets hydroxylated HIF-α for ubiquitination and proteasomal degradation. When oxygen tension is reduced, PHDs and FIHs are inhibited, allowing HIF-α to translocate into the nucleus and dimerise with HIF-β to form functional heterodimeric HIF [127, 140, 275].

In Chapter 3, the decrease in PPARα expression following hypoxia was accompanied by an increase in cardiac VEGF and PDK1 levels, indicating HIF was involved in the hypoxic metabolic adaptation. PPARα/HIF interaction and its subsequent effect on hypoxic adaptation is not well established, and has been studied, with opposite findings in different cells lines. Electrophoretic mobility shift assay (EMSA) analysis

revealed HIF-1α binding to HIF-1 consensus responsive element in the PPARα gene promoter, parallel to HIF-1α nuclear accumulation in intestinal epithelial cells exposed to 7% O_2 for 12 hours, thereby reducing PPARα protein levels by 84% [205]. In contrast, coimmunoprecipitation assay in ovarian cancer cells showed that PPARα formed complexes with HIF-2α, rather than HIF-1α [206]. In rat cardiomyocytes, HIF-1α was involved in hypoxia-induced suppression of fatty acid metabolism by decreasing the DNA binding activity of PPARα/RXR [234], but it has also been suggested that in the same cell type, hypoxia decreased RXR via a HIF-independent mechanism [207]. PHD1-deficient mice, a model with chronic HIF upregulation, have increased PPARα expression in skeletal muscle [276]. Hence there are precedents for a link between the HIF system and PPARα control, although the relationship is unclear.

However, the quantification of HIF in cardiac tissues of perfused hearts has been proven difficult, due to short HIF half-life upon reoxygenation [277] and technical difficulties in maintaining stable oxygen levels during tissue collection. Therefore, an *in vitro* hypoxia model is needed to isolate any HIF-dependent changes, as the hypoxic status of the cardiomyocytes could be maintained throughout harvesting. Consequently, in this chapter, the hypoxic response was investigated in HL-1 cells, a cardiac muscle cell line derived from mouse atrial cardiomyocyte tumour lineage, which has the ability to divide and spontaneously contract while maintaining a differentiated cardiac phenotype [278, 279]. These cells have been used to investigate cardiomyocyte responses to ischaemia-reperfusion [280], insulin resistance [281] and leptin treatment [282], and therefore are a promising *in vitro* model to investigate the mechanistic aspects of cardiac metabolism under physiological and

pathophysiological conditions, such as hypoxia. In addition, HIF signalling can be readily manipulated in HL-1 cells using pharmacological agents [194, 283].

Given that HIF activation is negatively regulated by the PHD and FIH hydroxylases, they have been identified as a crucial target to augment the transcriptional activity of HIF [284, 285]. While oxygen concentration plays a major role in determining the efficiency of PHD- and FIH-catalysed reactions, the sensitivity of both enzymes also depends on its co-substrate, 2-oxoglutarate (2-OG), and co-factor, iron [127, 286]. Therefore, iron chelators, transition metal ions and 2-oxoglutarate analogues are known hypoxia-mimetic agents as they inhibit the HIF hydroxylases, and potently activate the HIF response [170, 285] (Figure 6.1). Here, two different HIF hydroxylase inhibitors were used to stabilise HIF in HL-1 cells (Figure 6.2) – i) dimethyloxalylglycine (DMOG), a cell permeable, competitive inhibitor of 2-oxoglutarate [194, 283] and ii) 2-(1-chloro-4-hydoxyisoquinoline-3-carboxamido) acetic acid, a bicyclic isoquinoline compound (BIC), also known as FG2216, a specific PHD inhibitor [170, 285, 287]. Both inhibitors were synthesised by Kar Kheng Yeoh and Prof. Chris Schofield in the Chemistry Research Laboratory, University of Oxford.

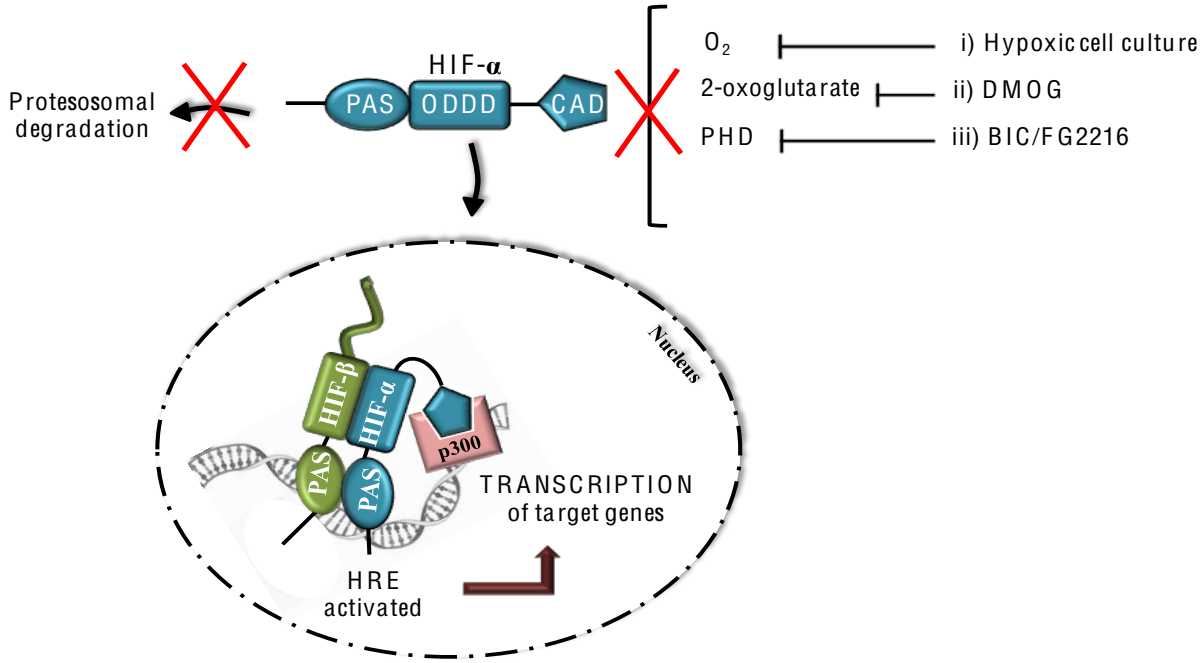

Figure 6.1: Stabilisation of HIF by hypoxia and HIF hydroxylase inhibitors

a) Dimethyloxalylglycine (DMOG)

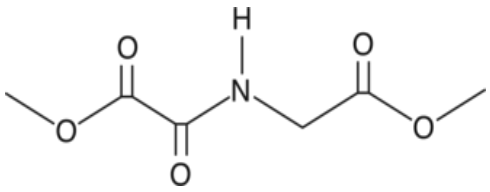

Molecular weight: 175.14

b) 2-(1-chloro-4-hydroxyisoquinoline-3-carboxamido) acetic acid (BIC)

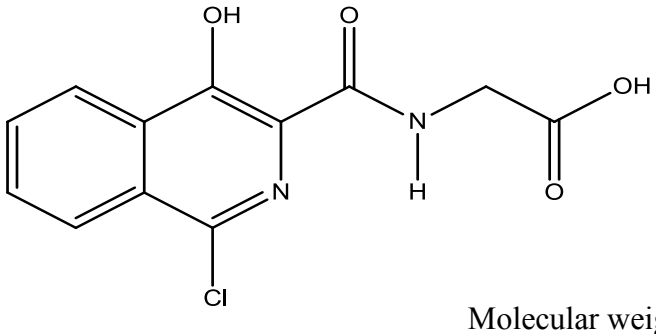

Molecular weight: 280.22

Figure 6.2: Chemical structure of HIF hydroxylase inhibitors, a) DMOG and b) BIC.

Study aim

This chapter describes the effect of HIF stabilisation on the different cardiac PPAR isoforms, aiming to identify HIF as an upstream regulator of PPARα. HL-1 cells were studied over a number of hypoxic time points in order to examine how the relationship between HIF, PPARα and metabolism developed in response to hypoxia.

6.3 METHODS

6.3.1 HL-1 cell culture

HL-1 murine cardiomyocytes were a kind gift from Dr William C. Claycomb (New Orleans, USA). The cells were cultured on 6-well plates precoated with 5 μg/ml fibronectin and 0.02% gelatin, and maintained in Claycomb medium (Sigma, UK). The cells were supplemented with 10% foetal bovine serum (FBS), ascorbic acid (0.3 mM), norepinephrine (0.1 mM), L-glutamine (4 mM) and 1% penicillin-streptomycin and incubated in 5% CO_2 at 37°C and 95% humidity. All experiments were performed on confluent, beating cells.

6.3.2 Hypoxia

To replicate the *in vivo* hypoxia protocol, HL-1 cells were cultured under 2% hypoxia for 6, 24 and 48 hours. Two incubators (Wolf Laboratories, UK) adjustable to different oxygen concentrations by infusion of nitrogen, were used for cell culture. Normoxic cell culture was set at 21% O_2, and hypoxic cell culture was set at 2% O_2 . Experiments were run simultaneously. The oxygen concentration was monitored continuously using an oxygen sensor (Wolf Laboratories, UK).

6.3.3 Pharmacological stabilisation of HIF

Cells were treated with DMOG for 24 hours or BIC for 24 or 48 hours. The toxic effects of the HIF activators have been investigated in our lab on cardiosphere-derived cells (CDCs) [170]. In the DMOG cytotoxicity test, gradient concentrations of 0.1 mM, 0.5 mM, 1 mM and 2 mM were used to treat 5 x 10^5 CDCs for either 24

hours or 4 days. Prolonged DMOG treatment (4 days) and high concentration (2 mM) caused 70-90% cell death. For BIC, lower concentrations of 10 μM, 30 μM, 50 μM or 100 μM were used on CDCs for either 24 hours or 4 days. BIC was not toxic to the cells under any of these conditions. Therefore DMOG was used at a concentration of 1 mM and BIC was used at a concentration of 50 μM, as they served an optimum concentration to upregulate HIF and its target genes without being toxic to the cells [170].

6.3.4 Cell harvest

After hypoxic incubation or drug treatments, cells were aspirated with phosphate buffered saline (PBS) and harvested for measurement of protein levels or mRNA expression. Cell lysates containing protease inhibitors (Roche, UK) were used to measure protein levels of HIF-1α, HIF-2α, GLUT1, PDK1 and SIRT1. RNA was extracted to quantify the mRNA expression of PPARα, PPARβ/δ, PPARγ, MCAD, UCP3, PDK4, and VEGF by qRT-PCR. HL-1 cells were harvested and lysed rapidly to prevent HIF degradation.

6.3.5 Confocal microscopy

HL-1 cells were grown on glass cover-slips in 24-well plates. Following exposure to hypoxia or normoxia for 24 hours, cells were washed with ice-cold PBS with 0.1% Tween and fixed with 4% paraformaldehyde (Sigma, UK) for 10 minutes. For mitochondrial staining, mitotracker dye (1 μl/10 ml serum-free medium) was added to cells prior to fixing. Fixed cells were permeabilized with PBS containing 0.1-0.5% Triton-X100, 2% BSA and 2% FBS for 10 minutes at room temperature and blocked

with PBS containing 2% FBS and 2% BSA for 30 minutes. GLUT1 primary antibody (1:1000 dilution) was added to cover slips and incubated at room temperature for 1 hour. Goat anti-rabbit secondary antibody (1:3500 dilution) was incubated with cover slips at room temperature for 30 minutes. Cover slips were mounted with DAPI VectaShield (Vector laboratories, UK) to stain the nuclei. Images were acquired using a Zeiss LSM510 META confocal microscope (performed by Dr Renata Gomes) and processed using Zeiss LSM image browser software.

6.4 RESULTS

6.4.1 Characterisation of hypoxic HL-1 cells

6.4.1.1 HIF and HIF downstream targets

After 6 hours in culture in 2% O_2, HL-1 cardiomyocytes expressed 8-fold ($p < 0.01$) higher HIF-1α protein levels compared to normoxic cells. HIF-1α protein accumulation significantly decreased over prolonged exposure to hypoxia, but was still 4.5-fold ($p < 0.01$) and 2-fold ($p < 0.01$) higher than in normoxic cells after 24 and 48 hours of hypoxia, respectively (Figure 6.3). Changes in HIF-2α protein levels were less dramatic, with a 2-fold increase ($p < 0.01$) after 6 hours hypoxia and, unlike HIF-1α, were not significantly decreased over the duration of hypoxia. Compared to normoxic HL-1 cells, HIF-2α was 72% ($p < 0.05$) and 40% ($p < 0.05$) higher after 24 and 48 hours hypoxia, respectively (Figure 6.3).

Activation of HIF during hypoxia subsequently upregulated several important HIF regulated genes, including VEGF, GLUT1 and PDK1 (Figure 6.4). VEGF mRNA expression was increased by 40% ($p < 0.01$), 37% ($p < 0.01$) and 2.6- fold ($p < 0.01$) after 6, 24 and 48 hours of hypoxic exposure respectively. The increase in GLUT1 protein levels mimicked the HIF response, peaking at 6 hours with a 2.7 fold ($p < 0.01$) increase and progressively decreased over the hypoxic duration, with 48% ($p < 0.05$) increase after 24 hours of hypoxia and returned to normal level after 48 hours. PDK1 protein levels increased by 81% ($p < 0.01$) and 34% ($p < 0.05$) after 6 and 24 hours hypoxia respectively, but had returned to the normoxic levels after 48 hour of hypoxia (Figure 6.4). The increase in GLUT1 protein levels was confirmed by

confocal microscopy, which revealed an accumulation of GLUT1 protein around the plasma membrane of hypoxic cells exposed to 24 hours hypoxia (Figure 6.5).

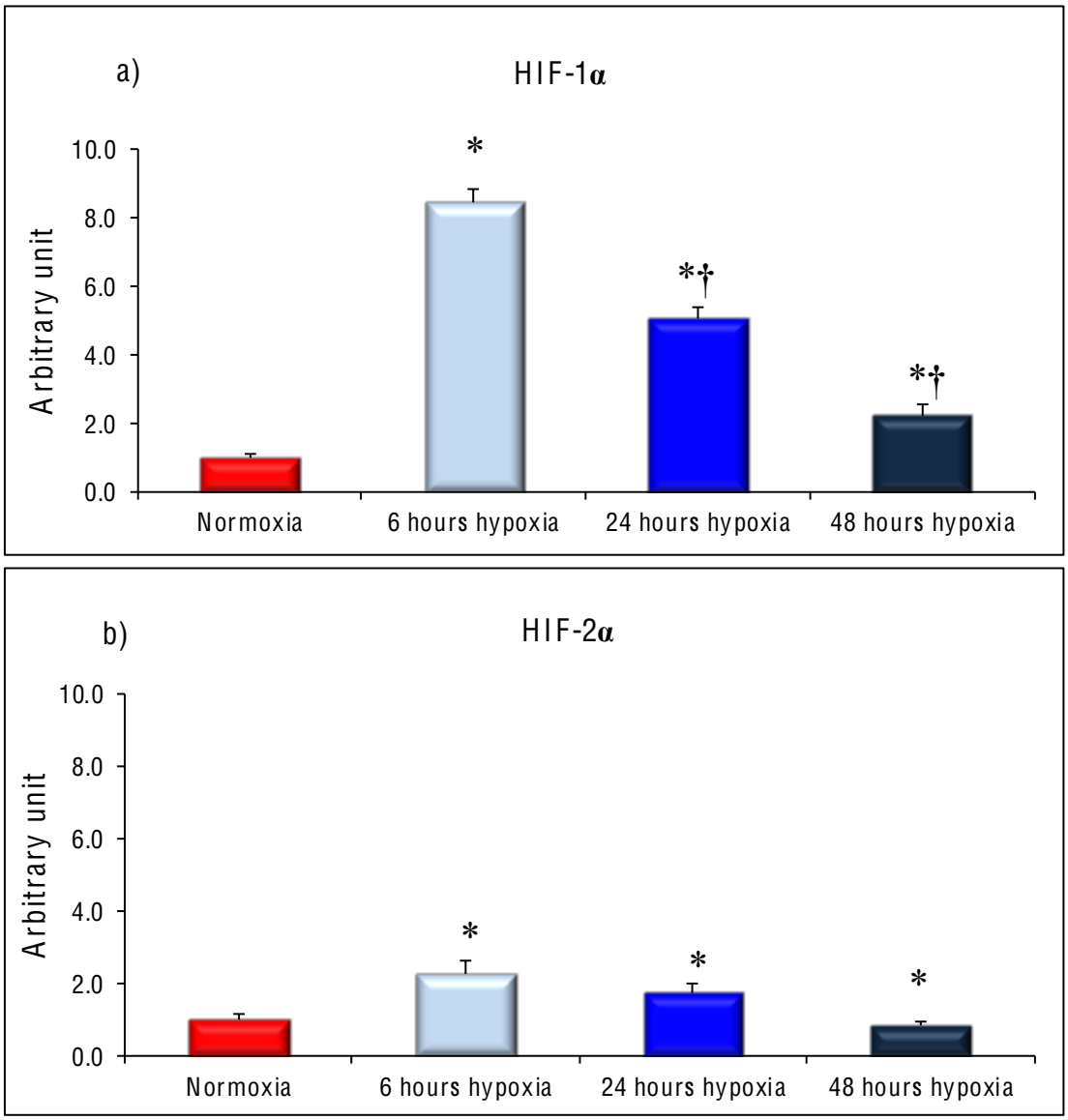

Figure 6.3: a) HIF-1α and b) HIF-2α protein levels in HL-1 cardiomyocytes after 6, 24 and 48 hours hypoxia (2% O_2). *p < 0.05 relative to normoxic HL-1 cardiomyocytes. † < 0.05 relative to 6 and 24 hours hypoxia. n = 5 per group.

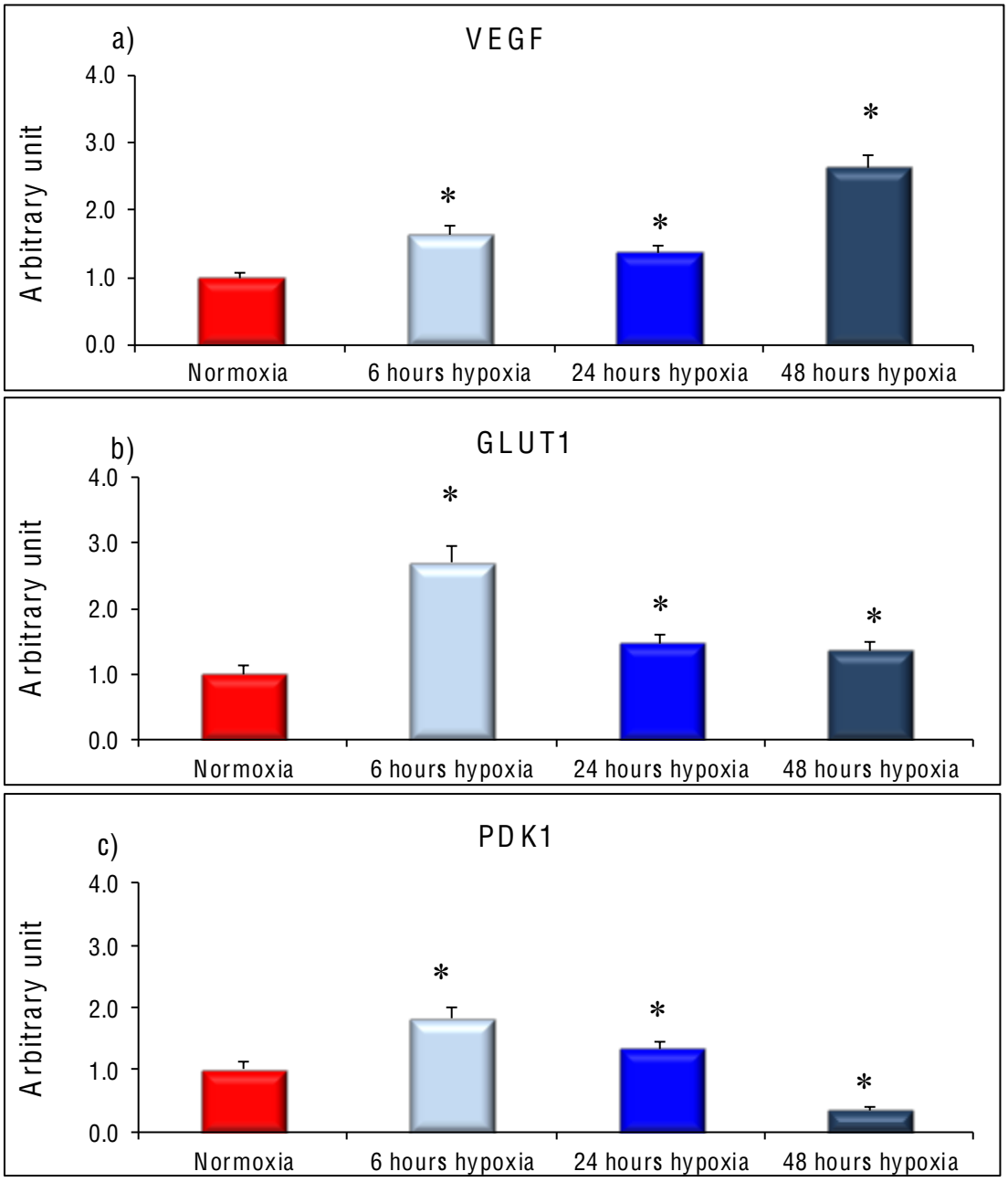

Figure 6.4: a) VEGF mRNA expression, b) GLUT1 and c) PDK1 protein levels in HL-1 cardiomyocytes after 6, 24 and 48 hours hypoxia (2% O_2). mRNA expression in HL-1 cells were normalized to the geometric mean of β-actin (housekeeping gene).*$p < 0.05$ relative to normoxic HL-1 cardiomyocytes. n = 5 per group.

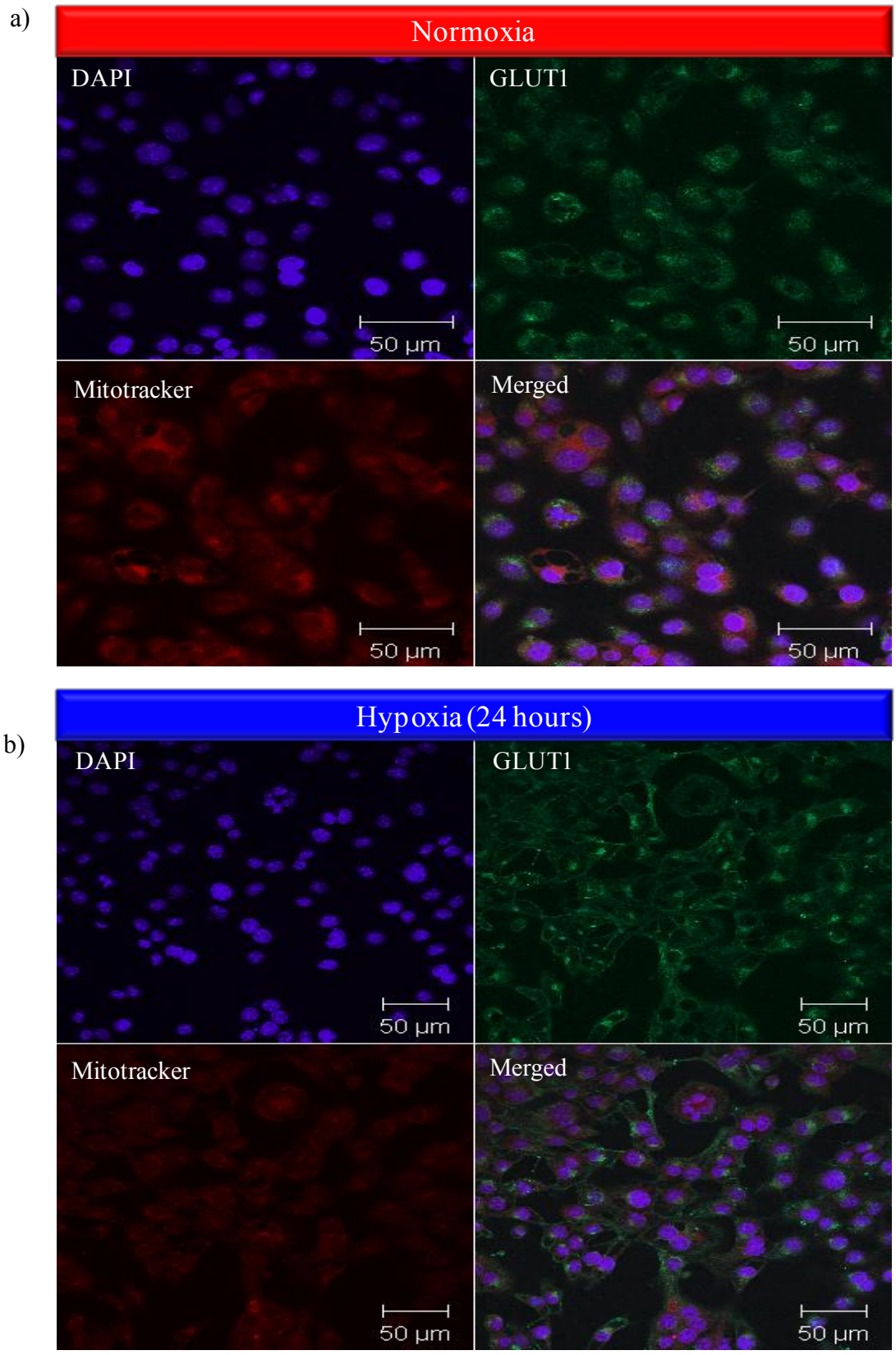

Figure 6.5: Representative confocal microscopy images of HL-1 cardiomyocytes after 24 hours of a) normoxia and b) hypoxia. Cells were stained purple for nuclei with DAPI, green for GLUT1 with Alexa Fluor 488 and red for mitochondria with mitotracker.

6.4.1.2 SIRT1 protein levels

SIRT1 protein levels were unchanged after 6 hours of hypoxia, but were significantly decreased by prolonged hypoxic exposure. SIRT1 protein levels were decreased by 37% ($p < 0.05$) and 41% ($p < 0.01$) after 24 and 48 hours of hypoxia, respectively (Figure 6.6).

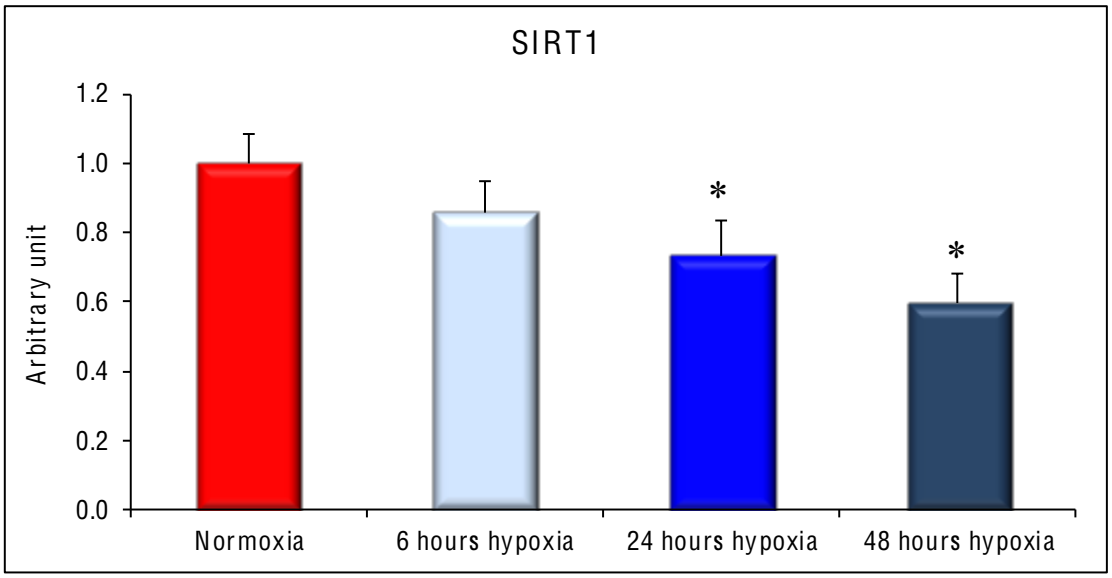

Figure 6.6: SIRT1 protein levels in HL-1 cardiomyocytes after 6, 24 and 48 hours hypoxia (2% O_2). *$p < 0.05$ relative to normoxic HL-1 cardiomyocytes. n = 5 per group.

6.4.2 Effect of HIF activation by HIF hydroxylase inhibitors in HL-1 cells

6.4.2.1 HIF and HIF downstream targets

HL-1 cardiomyocytes incubated with HIF hydroxylase inhibitors, DMOG and BIC, had elevated HIF protein levels (Figure 6.7). After 24 hours of DMOG treatment, HIF-1α protein increased 8.6 fold ($p < 0.01$). BIC upregulated HIF-1α levels 9.4-fold ($p < 0.001$) and 7.4-fold ($p < 0.01$) after 24 and 48 hours treatment respectively. HIF-2α activation was more gradual with DMOG and BIC treatment. DMOG increased HIF-2α protein 2.4-fold ($p < 0.01$) after 24 hours hypoxia, while BIC increased HIF-2α 2.1-fold ($p < 0.05$) and 2.4-fold ($p < 0.01$) after 24 and 48 hours hypoxia, respectively (Figure 6.7).

HIF stabilisation by DMOG subsequently upregulated VEGF mRNA expression, GLUT1 and PDK1 protein levels by 60% ($p < 0.01$), 3-fold ($p < 0.01$) and 85% ($p < 0.01$) respectively after 24 hours (Figure 6.8). BIC increased VEGF, GLUT1, and PDK1 in a similar manner to DMOG treated cells after 24 hours. HL-1 cells treated with BIC for 48 hours further upregulated VEGF mRNA expression 3.7-fold ($p < 0.01$), and increased GLUT1 and PDK1 protein levels 3.2-fold ($p < 0.01$) and 69% ($p < 0.01$) respectively (Figure 6.8).

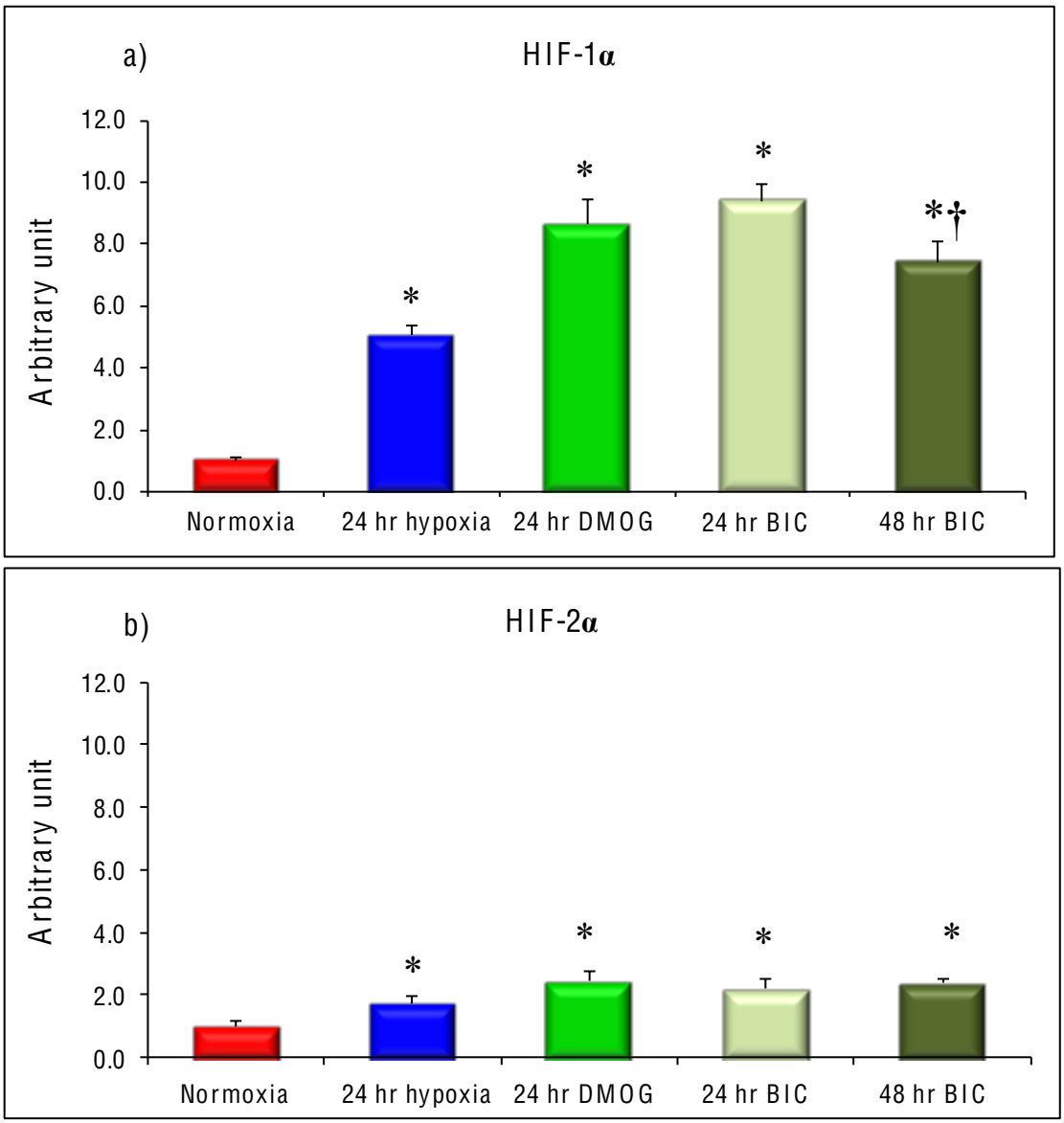

Figure 6.7: a) HIF-1α and b) HIF-2α protein levels in HL-1 cardiomyocytes after 24 hours hypoxia (2% O_2), 24 hours DMOG treatment, or 24 and 48 hours BIC treatment. *$p < 0.05$ relative to normoxic HL-1 cardiomyocytes. †$p < 0.05$ 24 hr BIC vs. 48 hr BIC. n = 5 per group.

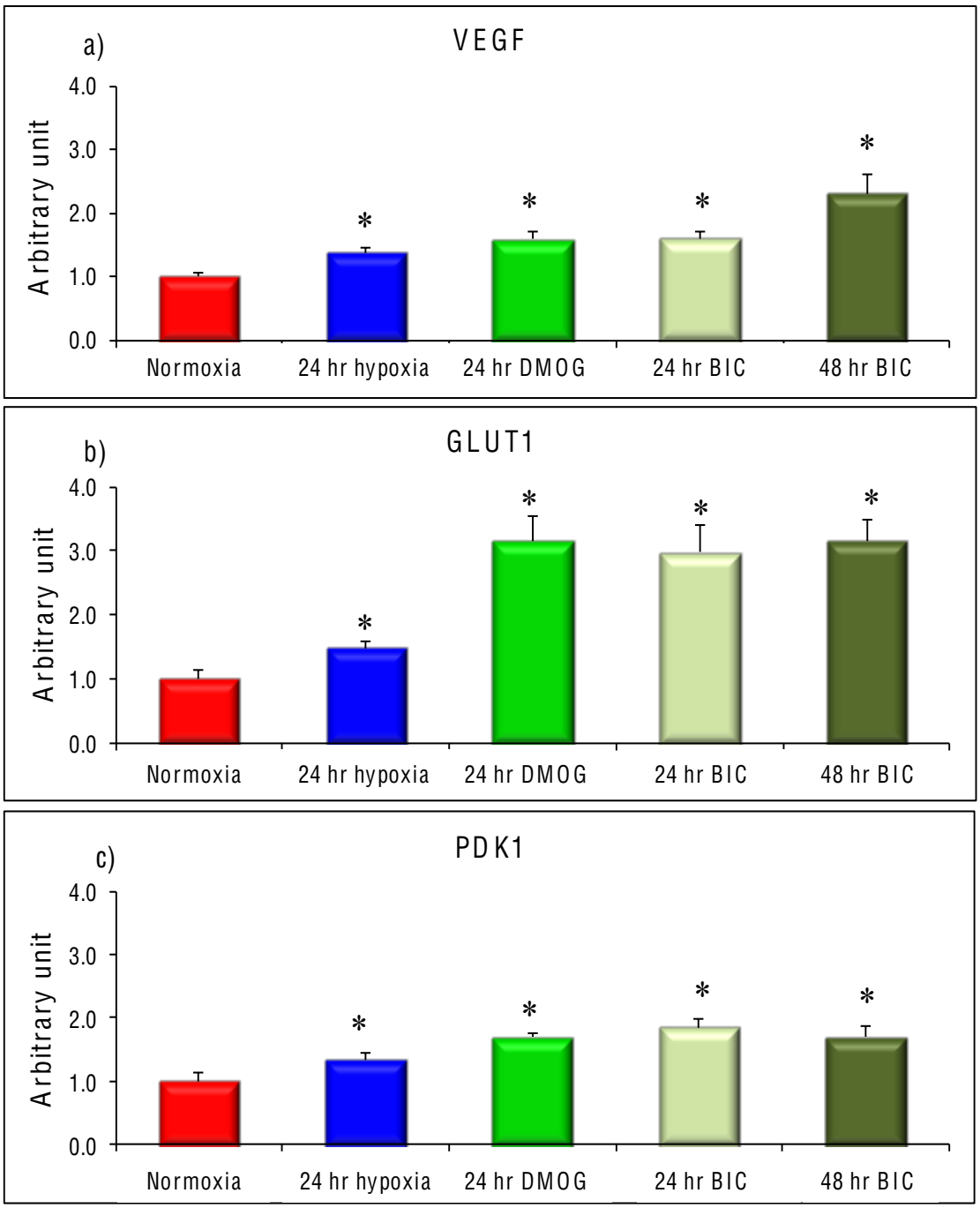

Figure 6.8: a) VEGF mRNA expression, b) GLUT1 and c) PDK1 protein levels in HL-1 cardiomyocytes after 24 hours hypoxia (2% O_2), 24 hours DMOG treatment, or 24 and 48 hours BIC treatment. mRNA expression in HL-1 cells were normalized to the geometric mean of β-actin (housekeeping gene). *$p < 0.05$ relative to normoxic HL-1 cardiomyocytes. n = 5 per group.

6.4.2.2 SIRT1 protein levels

In contrast to hypoxia, pharmacological activation of HIF by both DMOG and BIC did not affect SIRT1 protein levels (Figure 6.9),

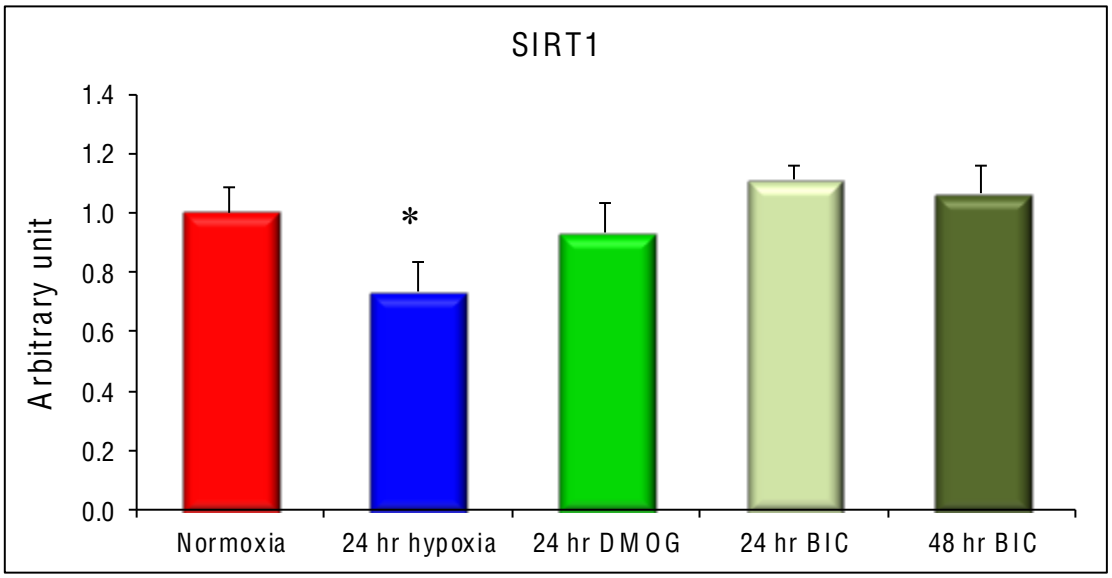

Figure 6.9: SIRT1 protein levels in HL-1 cardiomyocytes after 24 hours hypoxia (2% O_2), 24 hours DMOG treatment, or 24 and 48 hours BIC treatment. *$p < 0.05$ relative to normoxic HL-1 cardiomyocytes. n = 5 per group.

6.4.3 Distribution of PPAR isoforms in HL-1 cells

The mRNA expression of cardiac PPAR isoforms was determined in normoxic, non-treated HL-1 cells. Similar to the intact heart [57], PPARβ/δ was most abundant in HL-1 cells, and was expressed 5-fold higher relative to PPARα expression while PPARγ was the least expressed, with 2% expression relative to PPARα (Figure 6.10).

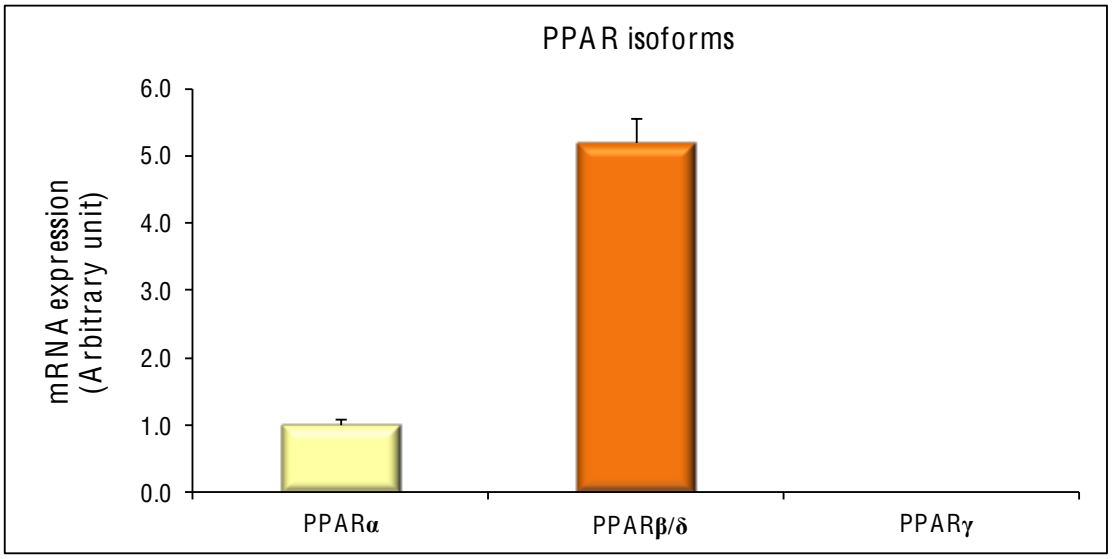

Figure 6.10: Relative mRNA expression of PPARβ/δ, and PPARγ to PPARα in HL-1 normoxic, non-treated HL-1 cardiomyocytes. mRNA expression in HL-1 cells were normalized to the geometric mean of β-actin (housekeeping gene). n = 5 per group.

6.4.4 Effect of HIF activation by hypoxia and HIF hydroxylase inhibitors on PPAR isoforms

HIF stabilisation by both hypoxia and HIF hydroxylase inhibitors resulted in PPARα downregulation in HL-1 cells (Figure 6.11). Relative to normoxic HL-1 cells, hypoxia for 24 and 48 hours decreased PPARα mRNA expression by 23% ($p < 0.01$) and 43% ($p < 0.01$), respectively, while mRNA expression of PPARβ/δ and PPARγ was not altered. Acute hypoxic exposure for 6 hours, however, affected all 3 isoforms; PPARα mRNA expression was decreased by 10% ($p < 0.05$) while PPARβ/δ and PPARγ were increased by 2.4- ($p < 0.01$) and 1.6- ($p < 0.01$) fold respectively.

After 24 hours of DMOG treatment, PPARα expression was decreased by 25% ($p < 0.01$), compared to non-treated, normoxic HL-1 cells (Figure 6.11). DMOG treatment also affected other PPAR isoforms; PPARβ/δ was 81% ($p < 0.01$) higher while PPARγ expression was 36% ($p < 0.01$) lower relative to normoxic, non-treated cells.

BIC treatment of HL-1 cells decreased PPARα expression by 25% ($p < 0.01$) and 31% ($p < 0.01$) after 24 and 48 hours respectively (Figure 6.11). PPARβ/δ expression was not affected by BIC treatment. However, HL-1 cells treated with BIC increased PPARγ expression by 94% ($p < 0.01$) after 24 hours, which then fell by 46% ($p < 0.05$) in the following 24 hours.

6.4.5 Effect of HIF activation by hypoxia and HIF hydroxylase inhibitors on PPARα downstream targets

Relative to normoxic HL-1 cells, MCAD expression was decreased by 31% ($p < 0.01$) and 64% ($p < 0.01$) after 24 and 48 hours hypoxia, respectively, while UCP3 expression was 30% ($p < 0.05$) lower at both hypoxia time point. Acute hypoxic exposure for 6 hours did not alter any PPARα downstream targets (Figure 6.12).

DMOG treatment did not affect any of the PPARα downstream targets. BIC treatment decreased MCAD expression by 17% ($p < 0.01$) and 22% ($p < 0.05$) after 24 and 48 hours respectively, but UCP3 was not significantly decreased. PDK4 mRNA expression was not altered by neither hypoxia nor DMOG and BIC treatments (Figure 6.12).

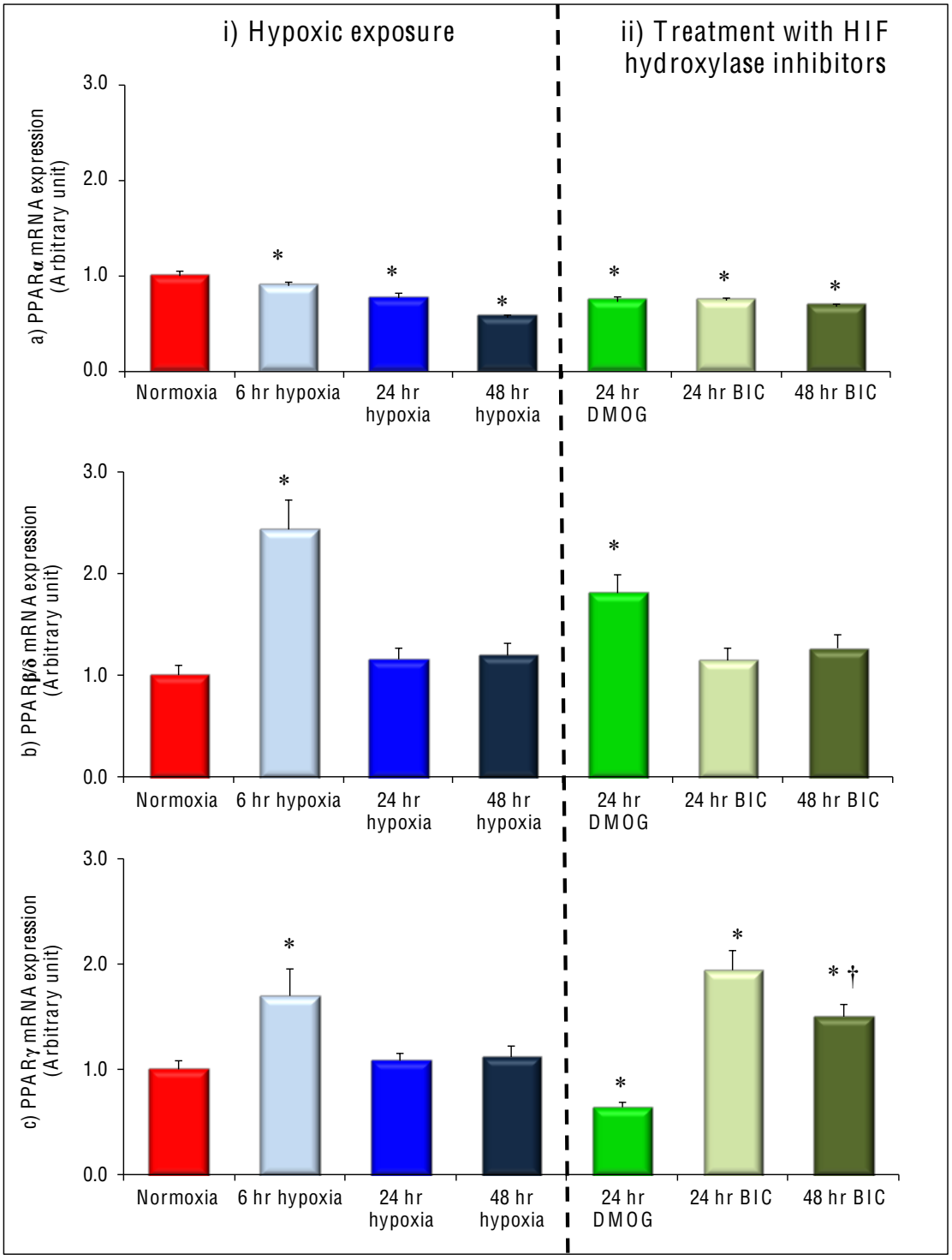

Figure 6.11: a) PPARα, b) PPARβ/δ and c) PPARγ mRNA expression in HL-1 cardiomyocytes after i) 6, 24 or 48 hours hypoxia (2% O_2) or ii) treated with DMOG for 24 hours, or BIC for 24 or 48 hours. mRNA expression in HL-1 cells were normalized to the geometric mean of β-actin (housekeeping gene). *$p < 0.05$ relative to normoxic HL-1 cardiomyocytes. †$p < 0.05$ 24 hr BIC vs. 48 hr BIC. n = 5 per group.

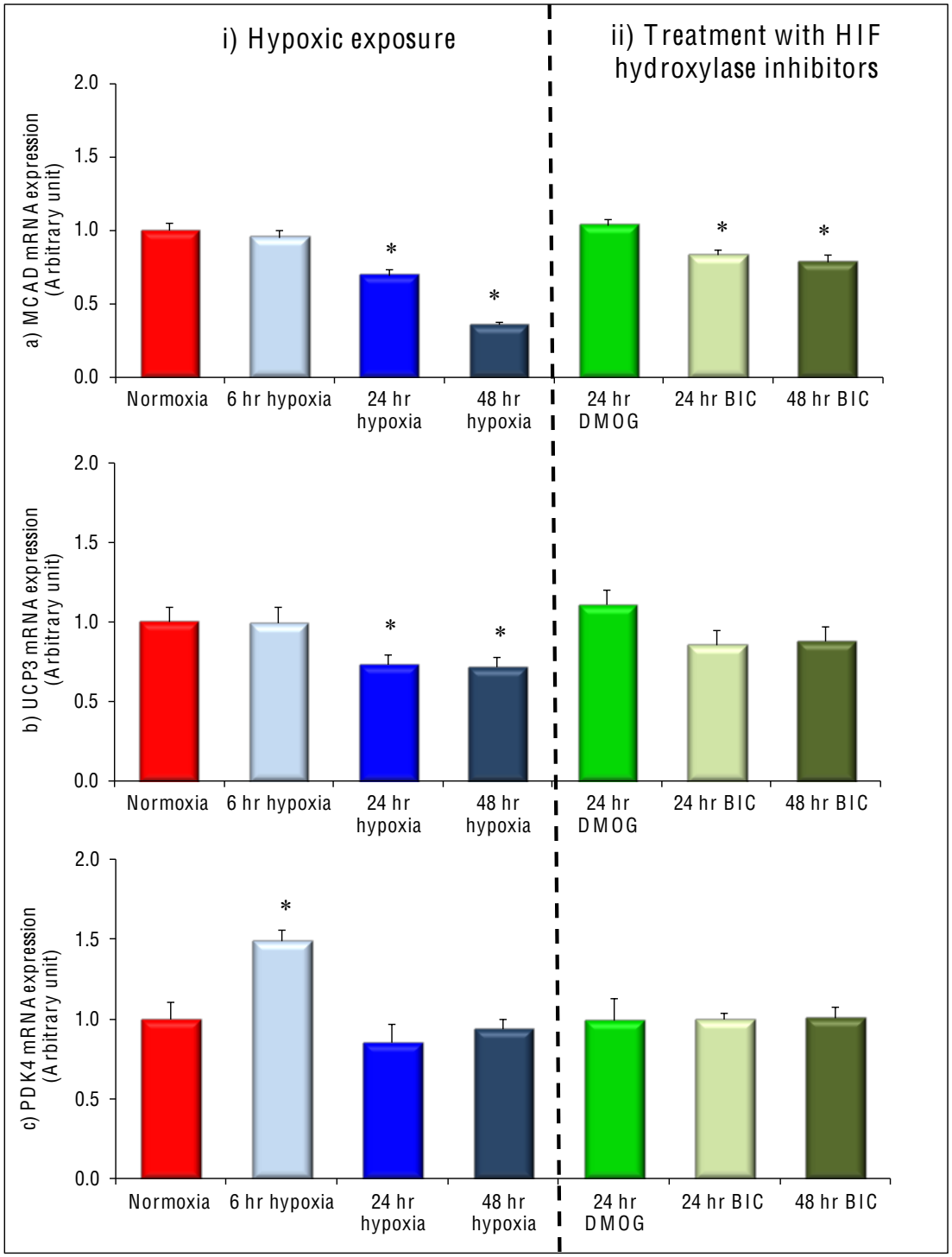

Figure 6.12: a) MCAD, b) UCP3 and c) PDK4 mRNA expression in HL-1 cardiomyocytes after i) 6, 24 or 48 hours hypoxia (2% O_2) or ii) treated with DMOG for 24 hours or BIC for 24 or 48 hours. mRNA expression in HL-1 cells were normalized to the geometric mean of β-actin (housekeeping gene).*$p < 0.05$ relative to normoxic HL-1 cardiomyocytes. n = 5 per group.

6.5 DISCUSSION

Principal findings

This study found that HIF at different stages of hypoxia modulated metabolism in HL-1 cardiomyocytes, indicated by increased GLUT1 and PDK1 protein levels. Hypoxia in HL-1 cardiomyocytes also transcriptionally decreased PPARα expression in a time-dependent manner. Both PPARβ/δ and PPARγ mRNA expression remained unchanged with 24 hours hypoxia in HL-1 cells. In parallel, HIF stabilisation by the specific PHD inhibitor, BIC, decreased PPARα mRNA expression in a similar manner to hypoxic HL-1 cells. HIF stabilisation by both hypoxia and BIC also suppressed MCAD. Taken together, these results suggest HIF as a regulator of PPARα during hypoxia.

HIF stabilisation by hypoxia in HL-1 cells

HL-1 cardiomyocytes have been used in hypoxia studies as they have equivalent responses to adult primary cardiomyocytes in terms of expression of hypoxia inducible genes [152, 279]. In agreement, work in this chapter showed that HIF-1α and HIF-2α proteins accumulated in HL-1 cells over the 48 hours duration of hypoxic exposure. Given that oxygen is the key substrate for HIF hydroxylation, the K_m value for oxygen of the HIF hydroxylases, PHDs in particular, is relatively high (230-250 μM), which is close to atmospheric oxygen concentration [288, 289]. Therefore, a slight reduction in oxygen concentration will inhibit the activity of PHDs, despite other substrates and cofactors being present at adequate levels [288]. It is not surprising, that in HL-1 cells, 2% oxygen increased HIF-1α levels 8-fold after 6 hours. However, the increased of HIF-1α protein levels was more gradual over the duration of hypoxia, decreasing to half after 24 hours. This is in agreement with

previous reports demonstrating a steady decrease in HIF-1α levels during prolonged hypoxia [290, 291], and the degree of HIF-1α protein downregulation varied greatly among cell types (24 – 72 hours, 1% O_2) [292]. The mechanism for the decline in HIF-1α protein levels is not clear, as it is not restricted to changes in local oxygen delivery. It has been proposed that this response could form the basis of a negative feedback regulation, caused by desensitization of HIF by PHD over-activation during chronic hypoxia [293]. However, some report it being independent of the PHD/pVHL pathway [292, 294]. Analysis of HIF-1α mRNA however, did not show any variation in acute or chronic hypoxia and it is believed that this feedback mechanism is necessary to keep HIF-α protein at a sufficient level to confer hypoxic protection [293].

The increase in HIF-2α levels was less dramatic, and did not significantly decrease over the duration of hypoxia, consistent with recently published results highlighting its role during prolonged hypoxia [295, 296]. In intact organs, HIF-1α induction in rat kidney and liver was found to be transient, and disappeared after 3 hours of 8% O_2, whereas HIF-2α expression was sustained for more than 6 hours in all organs studied (heart, lung, liver, kidney, duodenum and cerebrum) [296]. *In vitro*, rapid induction of the HIF-1α protein observed after 4 hours hypoxia (0.5% O_2) in human lung epithelial cells diminished after 6 hours, and fell to baseline levels at 12 hours, while HIF-2α protein remained unchanged from 4 to 12 hours of hypoxia. A similar observation was reported for HeLa and rat derived PC12 cells after 16 hours of 1% O_2 [295], but HIF-2α levels have not been examined over a longer period of hypoxic incubation. Despite strong similarities in amino acid sequence and hypoxia-mechanism of activation [296], targeted disruption of HIF-1α and HIF-2α genes in

mice resulted in different phenotypes, and may explain their distinct physiological roles [297]. While HIF-1α null mice exhibit mid-gestation lethality and severe blood vessel defects and die at approximately embryonal day 11 [298], HIF-2α null mice exhibit embryonic defects associated with abnormal lung maturation, blood vessels impairment, but they sometimes survive postnatally [299, 300].

HIF stabilisation by hypoxia and HIF hydroxylase inhibitors downregulate PPARα expression

Markers of cellular metabolism in HL-1 cells changed dramatically in response to hypoxia. HIF-activation of GLUT1 and PDK1 in HL-1 cells suggested increased glycolytic metabolism, as described by others [135, 137]. Confocal microscopy was used to verify the increase in glucose metabolism, which showed increased GLUT1 at the plasma membrane to facilitate increased glucose uptake during hypoxia [152, 301]. In support of this, the uptake of radiolabelled glucose was increased 2-fold after 8 hours of 1% O_2 in HL-1 cells, with a concomitant decrease in β-oxidation [194]. Parallel to this, in the present study, the expression of PPARα and its downstream target, MCAD, in HL-1 cells decreased with hypoxia, and were further downregulated after 48 hours hypoxia. In agreement, microarray analysis identified a time-dependent downregulation of PPARα (2.1-fold and 8.9-fold decrease) in epithelial cells after 6 and 18 hours of hypoxia, respectively [205]. These authors also reported that the change was specific to PPARα expression and PPARγ remaining unaltered [205]. Here, neither PPARγ nor PPARβ/δ was changed after 24 hours hypoxia in HL-1 cells, and this mirrored the *in vivo* work from Chapter 3.

Transcriptional regulation of the PPARα gene during hypoxia has not been established for the heart. To determine whether PPARα downregulation was conserved in HL-1 cardiomyocytes with specific HIF activation, normoxic HL-1 cells were incubated with HIF hydroxylase inhibitors. Here, 1 mM DMOG significantly inhibited PHD/FIH enzyme activity and upregulated HIF and its regulated genes, as reported by others in HL-1 cells [194] as well as other cell types [285]. BIC potently activated HIF and its regulated genes at a much lower concentration of 50μM. Both DMOG and BIC increased the expression of VEGF, GLUT1 and PDK1, indicating that pharmacological stimulation of HIF in HL-1 cells exhibited a response typical to hypoxia through the HIF-transcription system. Most importantly, the accumulation of both HIF-1α and HIF-2α proteins in DMOG and BIC-treated cells attenuated PPARα mRNA expression, inferring that that regulation of PPARα may be HIF-dependent. Chemical HIF activation by $CoCl_2$ in epithelial cells for 8 hours reportedly decreased PPARα protein by 72%, consistent with the finding of a HIF-1α binding site on the PPARα DNA consensus motif [205]. Therefore, PPARα appears to be regulated by HIF during hypoxic adaptation.

HIF activation by DMOG, however, affected of all 3 isoforms and failed to affect any of the PPARα downstream targets, possibly due to its non-selective inhibition of PHD/FIH. DMOG is a promiscuous 2-oxoglutarate analogue, and may inhibit other 2-oxoglutarate-dependent dioxygenases [302]. For example, DMOG inhibited collagen prolyl-4-hydroxylase and affected collagen synthesis [303], which have been shown to impair lung growth due to the essential role of matrix proteins in the developing lung [304]. DMOG might be associated with other undesired side effects

in cells; however, the side effect of DMOG on substrate metabolism, particularly on cardiac PPAR isoforms, has not been reported.

In contrast, BIC is a small molecule inhibitor, specific for blocking prolyl hydroxylation [285]. BIC, patented by FibroGen Inc.(FG-2116) [305], has been administered to healthy human subjects [306], and in anaemic patients secondary to chronic kidney disease (CKD) in clinical trials [307], due to its high efficacy and oral bioavailability to induce EPO synthesis [308]. *In vitro* stabilisation of HIF using BIC in HL-1 cells downregulated both PPARα and MCAD, and more closely mimicked the hypoxia response at 2% oxygenation. Accordingly, Tian *et al.* found that despite similar levels of upregulated HIF-1α, hypoxia and HIF hydroxylase inhibitors, including DMOG and BIC, had differential sensitivity towards HIF-1α hydroxylation sites [285]. Their *in vitro* study demonstrated that severe oxygen deprivation (0.1% O_2 for 5 hours) and DMOG treatment for a similar duration, completely suppressed asparaginyl hydroxylation, whereas in 1% oxygen, HIF-1α asparaginyl hydroxylation still persisted, as with BIC treatment even at a higher concentration of 1mM [285]. Given that prolyl hydroxylation was equally inhibited by hypoxia and both HIF hydroxylase inhibitors, their finding provided an additional explanation for the similar metabolic response observed between 2% hypoxia and BIC treatment, compared to that of DMOG in our HL-1 cells. However, potent HIF-1α (9-fold) activation by BIC after 24 hours resulted in increased PPARγ expression, which subsided after 48 hours of treatment, in line with a gradual decline of HIF-1α accumulation. It is also not surprising that the 8-fold upregulation of HIF-1α in HL-1 cells by 6 hours hypoxia also affected other PPAR isoforms, as HIF-1α activation in

pathological cardiac hypertrophy has been shown to increase PPARγ expression [204].

In the present study, it is not known whether PPARα interaction was specific to HIF-1α or HIF-2α activation. In addition to the hypoxia study in epithelial cells performed by Naravulla and Colgan, which linked PPARα to HIF-1α [205], genetic manipulation leading to cardiac HIF-1α overexpression in cells [234] and a transgenic mouse model [309] also decreased PPARα expression. However, the prominent role of HIF-2α during prolonged hypoxia [295, 296] should not be discounted. Here, HIF-2α accumulation was sustained between 24 and 48 hours of BIC treatment and PPARα has also been shown to form complexes with HIF-2α in cancer cells [206]. Although HIF-1α accumulation in HL-1 cardiomyocytes declined over prolonged duration of hypoxia, the signal was much higher than normoxia at 48 hours and it is unknown after what duration of hypoxia HIF-1α protein levels would completely disappear. Similarly, we were unable to determine the hypoxic duration in which HIF-2α remained elevated. This served as a limitation to our study as we were restricted by high cell death rate and loss of HL-1 cell viability beyond 48 hours of 2% O_2. For future investigations, genetic manipulation of the HIF-α isoforms by siRNA transfection in HL-1 cardiomyocytes [310] may provide a more promising approach for mechanistic insights.

Effects of HIF stabilisation on SIRT1

A number of studies have demonstrated a link between HIF and SIRT1 during hypoxia [208, 209, 271], implicating SIRT1 as a modulator of hypoxic signalling. SIRT1 may also interact with PPARα, as activation of PPARα by fasting activated

SIRT1 gene expression in the liver [272], and a subsequent study found that protective effects of SIRT1 on cardiac hypertrophy were abrogated in PPARα$^{-/-}$ mice [210]. The independent association of SIRT1 with HIF, and PPARα with SIRT1, suggests that SIRT1 may act as an intermediary regulator between HIF and PPARα during metabolic adaptation to hypoxia. It was found that hypoxic exposure of HL-1 cells decreased SIRT1 proteins in a time-dependent manner. However, HIF activation by BIC or DMOG, did not affect SIRT1 levels. The effect of hypoxia on SIRT1 is controversial, with evidence for their deacetylase activity increasing [209, 271] and decreasing [208] in a range of cell types and mouse tissues under hypoxic conditions. Thus, the role played by SIRT1 in hypoxia is still unclear, perhaps due to differences in the experimental cell culture systems. Moreover, changes in SIRT1 deacetylase activity do not always parallel the protein levels [311], raising the need to measure activity in conjunction with protein levels in the future.

In summary, the major focus of this work was to identify HIF-dependent regulation of PPARα in HL-1 cardiomyocytes, characterizing HIF protein stabilisation by hypoxia and pharmacological inhibition of HIF hydroxylase. The data demonstrated apparent interaction between HIF and PPARα, which orchestrated molecular changes essential for adaption to chronic hypoxia.

CHAPTER 7

GENERAL DISCUSSION

The work from this thesis has extensively examined the cardiac response to physiological hypoxia. This is the first time that the relationship between substrate utilisation, cardiac energetics and function following chronic hypoxia in an intact heart, has been documented. The collective findings demonstrate that PPARα is integral to the physiological cardiac adaptation to hypoxia, which is intricately linked to HIF activity.

One of the most important observations from the work in this thesis was that the downregulation of PPARα was an essential component of cardiac metabolic adaptation to chronic hypoxia (Chapter 3). Consequently, dietary and genetic manipulation of PPARα unveiled the mechanisms by which PPARα exerts its effect on hypoxic adaptation. Ligand activation of PPARα during hypoxia was achieved by high fat feeding (Chapter 4) and conversely, genetic ablation of PPARα (PPARα$^{-/-}$ mice) abolished cardiac PPARα expression following chronic hypoxia (Chapter 5). By combining the metabolic, functional and energetics data from this thesis (Table 7.1) the relationship between PPARα and cardiac adaptation to chronic hypoxia can be deduced.

Table 7.1: Relationship between PPARα and cardiac function, metabolism and energetics

Cardiac parameters	Wild type, chow fed	Wild type, high fat fed		**PPARα$^{-/-}$**, chow fed		**PPARα$^{-/-}$**, high fat fed	
	Hypoxia	Normoxia	Hypoxia	Normoxia	Hypoxia	Normoxia	Hypoxia
PPARα	36% ↓	1.5-fold ↑	1.5-fold ↑	negligible	negligible	negligible	negligible
LV mass/BW ratio	17% ↓	⟺	⟺	⟺	⟺	⟺	19% ⇧
Cardiac output	⟺	⟺	35% ↓	⟺	19% ↓	29% ↓	21% ↓
Ejection fraction	⟺	⟺	9% ↓	⟺	⟺	6% ↓	12% ↓
Glycolytic flux	2.2-fold ↑	⟺	⟺	3.1-fold ↑	3.0-fold ↑	⟺	⟺
Lactate efflux	1.3-fold ↑	⟺	⟺	2.4-fold ↑	2.5-fold ↑	⟺	⟺
Palmitate oxidation	25% ↓	18% ↑	26% ↑	24% ↓	36% ↓	⟺	⟺
PCr/ATP	29% ↓	⟺	25% ↓	(N/D)	(N/D)	(N/D)	(N/D)
ATP	⟺	⟺	31% ↓	(N/D)	(N/D)	(N/D)	(N/D)
PCr	38% ↓	25% ↓	25% ↓	(N/D)	(N/D)	(N/D)	(N/D)
ΔG_{ATP}	⟺	3% ↓	3% ↓	(N/D)	(N/D)	(N/D)	(N/D)

↑ = increase relative to chow fed, normoxic wild type mice

↓ = decrease relative to chow fed, normoxic wild type mice

⟺ = unchanged relative to chow fed, normoxic wild type mice

⇧ = increase relative to chow fed, normoxic PPARα$^{-/-}$ mice

↓ = decrease relative to chow fed, normoxic PPARα$^{-/-}$ mice

⟺ = unchanged relative to chow fed, normoxic PPARα$^{-/-}$ mice

N/D = not determined

7.1 PPARα regulated hypoxic adaptation via its transcriptional role in fatty acid metabolism

PPARα modulates fatty acid metabolism through its transcriptional regulation of genes encoding proteins involved in β-oxidation, including MCAD [53, 312]. In agreement, here it was shown that cardiac palmitate oxidation correlated positively with PPARα mRNA expression (Figure 7.1), with MCAD proteins increasing or decreasing in high fat fed or PPARα$^{-/-}$ mouse hearts respectively, irrespective of oxygen exposure. The functional adaptation following chronic hypoxia was associated with decreased palmitate oxidation, which corresponded to the reduction in PPARα expression and MCAD proteins. However, the stimulus by high fat feeding was much stronger than opposing downregulation of PPARα by hypoxia as observed by Belanger *et al.* [234]. High fat feeding had no adverse effects on cardiac morphology and function under normoxia, consistent with previous reports in humans [236, 313] and mice [220], but stimulation of PPARα during hypoxia prevented the adaptive decrease in fatty acid oxidation, and reduced ejection fraction. Conversely, the inborn suppression of fatty acid metabolism displayed by the PPARα$^{-/-}$ mouse hearts was also maladaptive to hypoxic adaptation (Table 7.1). The loss of PPARα exacerbated the detrimental effect of high fat feeding on cardiac function, irrespective of oxygen supply.

Cardiac PPARβ/δ and PPARγ mRNA expression was not altered by hypoxia in wild type mice, nor by high fat feeding or in PPARα$^{-/-}$ mice, irrespective of oxygen supply, indicating that hypoxic adaptation was specific to the alteration in PPARα expression. Therefore, the work in this thesis has shown that decreased fatty acid oxidation during hypoxia is a PPARα dependent process, beneficial for hypoxic adaptation;

upregulation or deletion of PPARα during hypoxia prevented the heart to metabolically adapt, and impaired cardiac function.

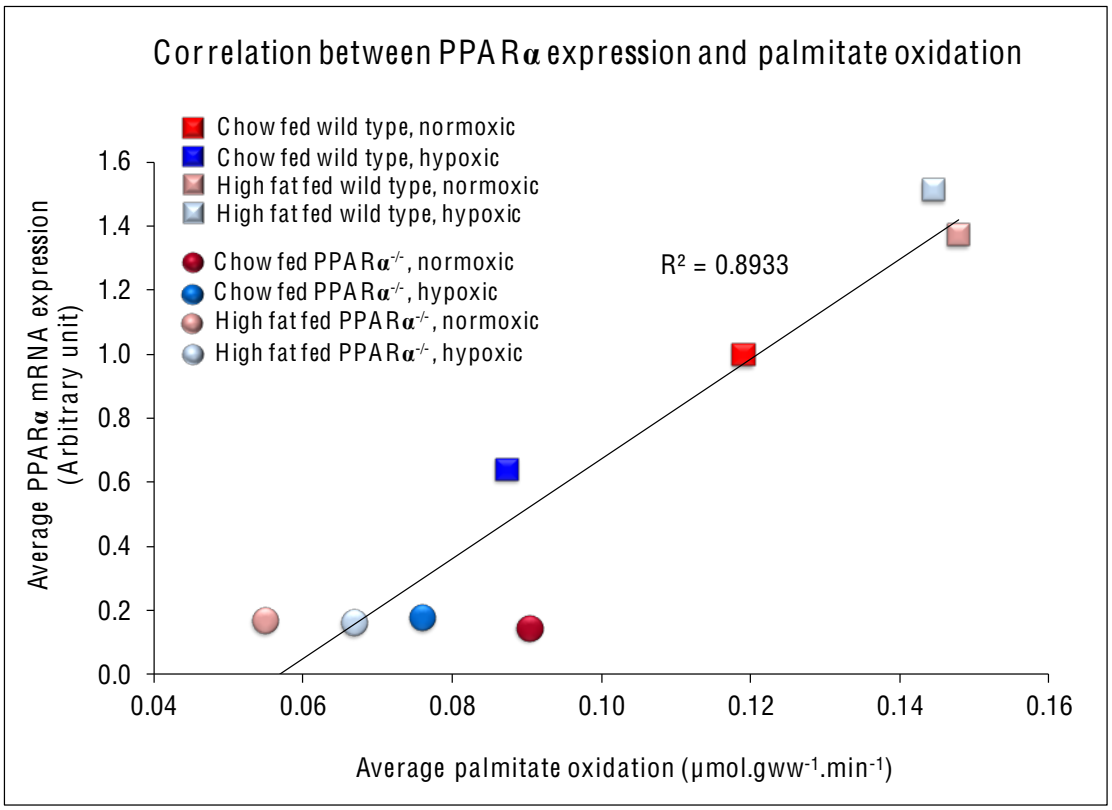

Figure 7.1: Positive correlation between cardiac PPARα expression and palmitate oxidation.

7.2 The ability of the hypoxic heart to upregulate glycolysis was vital for hypoxic adaptation

Glucose is a more oxygen-efficient fuel source than fatty acids, generating 11% more ATP per oxygen atom consumed than fatty acids [21]. The increase in glycolysis and lactate efflux following hypoxia reflects an adaptive shift in cardiac substrate utilisation to a more oxygen-sparing metabolic pathway for energy production [314]. This metabolic adaptation was most likely occurring through HIF–mediated increase in glycolytic metabolism and secondary to the decrease in fatty acid oxidation by

PPARα via the Randle effect [32, 261]. When the hypoxic hearts were forced to upregulate fatty acid oxidation with high fat feeding, they were unable to increase glycolytic rates, which impaired cardiac function. Conversely, the reported increase in glucose uptake in PPARα$^{-/-}$ mouse hearts has been shown to improve the recovery of ischaemic hearts [213, 222]. In contrast, here, it was shown that PPARα$^{-/-}$ mouse hearts were not protected from hypoxia. Although normoxic PPARα$^{-/-}$ mouse hearts displayed a metabolic phenotype identical to wild type mice adapted to hypoxia, their inability to further upregulate glycolysis when oxygen was limited in hypoxia reduced cardiac output (Table 7.1).

It is interesting to note that PPARα may not play a direct role in glucose transport and metabolism following chronic hypoxia. GLUT1 and GLUT4 protein levels were unchanged with hypoxia and were normal in all PPARα$^{-/-}$ mouse hearts, irrespective of oxygen supply. However, PPARα may have an indirect role in glucose and fatty acid balance via its control on cardiac PDK4 [75], confirmed by the PDK4 deficiency in PPARα$^{-/-}$ mice. The role of PDK4 during hypoxic adaptation is not well defined, and we were limited in determining the involvement of PPARα in regulating cardiac PDH flux during limited oxygen supply, as glucose oxidation was not measured. This is an interesting aspect of hypoxic adaptation to be investigated in the future as it will provide a comprehensive overview on the role of PPARα on glucose oxidation, beyond its ability to indirectly upregulate glycolysis by suppressing fatty acid oxidation following hypoxia.

7.3 Metabolic remodelling preserved contractile function by maintaining cellular energetic components of the hypoxic heart

Factors that may lead to cardiac contractile dysfuntion include metabolic abnormalities that result in increased energy consumption, and decreased energy production and transfer, via the phosphocreatine (PCr) and creatine energy shuttle [315]. Here, it was shown that the net effect of the hypoxic metabolic remodelling, associated with decreased fatty acid oxidation and increased reliance on glycolysis, was sufficient to maintain ATP production and myocardial contraction, at the expense of PCr replenishment. Conversely, abnormal cardiac substrate utilisation and metabolic inflexibilities displayed by the hypoxic high fat fed and PPARα$^{-/-}$ mouse hearts resulted in impaired cardiac energetics, and likely contributed to the functional defects in these mice (Table 7.1).

Additionally, it is proposed that the PPARα- mediated decrease in UCP3 and MTE may serve to conserve the inner mitochondrial membrane proton gradient, thereby maintaining mitochondrial efficiency and ATP production during limited oxygen availability. Essop *et al.* [200] showed that the decrease in oxygen consumption in hypoxic rat hearts did not impair mitochondrial efficiency of oxidative phosphorylation, as UCP3 levels decreased, parallel to downregulation of fatty acid oxidation. Cardiac UCP3 and MTE1 were low in all PPARα$^{-/-}$ mice hearts, confirming them as PPARα downstream targets [71, 73]. Subsequently, activation of PPARα with high fat feeding increased UCP3 and MTE1, which appeared to be an effective strategy to process excess fatty acids and maintain cardiac function under normoxia [93, 94]. However, when oxygen availability was limited, increased UCP3-mediated uncoupling via high fat feeding can cause significant ATP wasting, by

limiting the supply of ATP to contractile work [199, 238]. Indeed, PCr/ATP ratio was impaired in hypoxic high fat fed mice, with lower ΔG_{ATP}, mainly as a result of decreased cardiac ATP, an observation which was not seen in hypoxic chow fed mice. Although hypoxia in chow fed mice also decreased PCr/ATP, ΔG_{ATP} was maintained function was not affected. Therefore, in the hypoxic high fat heart, it is possible that the impairment in cardiac function can be explained by UCP3- mediated reduction in cardiac efficiency.

PPARα$^{-/-}$ mouse hearts also lacked the compensatory mechanism to optimize ATP production following hypoxia. Beyond low fatty acid oxidation, PPARα$^{-/-}$ mouse hearts may have a restricted reserve to enhance glycolysis following hypoxia, which may lead to a state of energy starvation [53]. It has been shown that PCr reserve was 41% lower in normoxic PPARα$^{-/-}$ mouse hearts, relative to their wild type counterparts, and was further depleted by 10% during hypoxia [259]. It is feasible that hypoxic PPARα$^{-/-}$ mouse hearts have compromised energy generating capacity as a consequence of their metabolic inflexibility, and PPARα$^{-/-}$ mice were incapable of increased work after imposition of multiple stresses, evident by the apparent LV hypertrophy when challenged with both hypoxia and high fat feeding. In agreement, PPARα$^{-/-}$ mouse hearts were unable to cope with starvation and high temperature stress [252], which was accompanied by decreased energetic status and contractile dysfunction when challenged with high workloads [256] and pronounced hypertrophic growth response and functional deterioration following chronic pressure overload [258].

7.4 **HIF as upstream regulator of PPARα**

Quantification of HIF in cardiac tissues of perfused hearts has proved to be very difficult, due to its short half-life upon reoxygenation [277], together with technical difficulties in maintaining stable oxygen levels during tissue collection. Consequently, HL-1 cardiomyocytes were shown to be a viable *in vitro* model to study HIF/PPARα interaction, as HIF signalling can be readily manipulated and stabilised throughout harvesting. In Chapter 6, it was shown that HIF activation after 24-hours of hypoxic incubation increased VEGF expression in HL-1 cells, and decreased MCAD and UCP3 expression secondary to a fall in PPARα expression, parallel with the *in vivo* findings from Chapter 3 (Figure 7.2). Pharmacological activation of HIF in normoxic HL-1 cells using the specific prolyl hydroxylase inhibitor, BIC [285], induced a metabolic phenotype similar to hypoxic HL-1 cells and mouse hearts, demonstrating a HIF-dependent downregulation of PPARα.

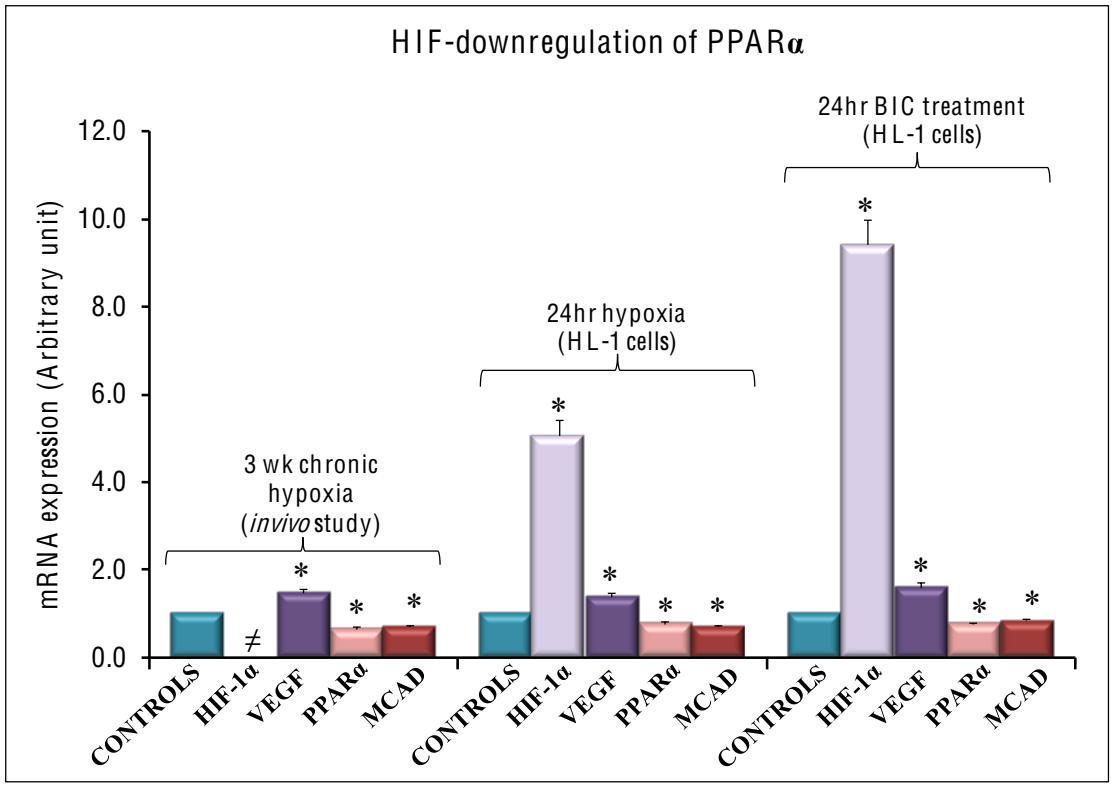

Figure 7.2: Metabolic adaptation following chronic hypoxia *in vivo,* HL-1 cells and BIC-treated HL-1 cells. * $p < 0.05$ compared to respective control. ≠ not determined.

Although the work from Chapter 6 validated the use of HL-1 cardiomyocytes as an *in vitro* model of hypoxia in terms of expression of hypoxia inducible genes, it should be taken into consideration that the metabolism of HL-1 cells are different to *in vivo* metabolism, the former relying heavily on glycolytic metabolism under normoxia [316, 317]. Despite the differences in substrate preference, HL-1 cells were still metabolically remodelled after 8 hours of 1% O_2, and exhibited a 2-fold increase in glucose uptake and a 30% decrease in fatty acid oxidation [194], consistent with reduced PPARα and MCAD expression observed in the present study. That HIF downregulation of PPARα was still conserved in two cardiac systems with distinctive substrate metabolism implies that such mechanism is a pivotal adaptive response to decreased oxygen availability.

Therefore, it may be inferred that the metabolic switch away from fatty acid metabolism during advanced heart failure is potentially a hypoxic response associated with a HIF-dependent downregulation of PPARα.

7.4.1 SIRT1 as intermediary regulator between HIF and PPARα

Given the recent association of SIRT1 with HIF [208, 271], and PPARα with SIRT1 [210, 272], it is possible that SIRT1 may act as an intermediary regulator between PPARα and HIF. In a preliminary attempt to investigate this relationship, SIRT1 protein levels were measured following hypoxic exposure. Hypoxia in wild type mice and HL-1 cells decreased SIRT1 protein levels. In parallel, Lim *et al.* suggested that SIRT1 is a negative regulator of HIF; under normoxia, SIRT1 deacetylates HIF-1α and the repression of HIF signalling is relieved during hypoxia, as SIRT1 activity decreases [208]. In addition, here it was shown that cardiac SIRT1 levels were

increased and decreased in high fat fed and PPARα$^{-/-}$ mice respectively, consistent with PPARα regulatory control of SIRT1 [210, 272]. This suggests the existence of a feedback mechanism during hypoxic adaptation whereby SIRT1, under the control of PPARα, is maintained at low levels following hypoxia, preventing the suppression of HIF. However, further studies are needed to conclusively demonstrate the interaction between SIRT1 with PPARα and HIF.

7.4.2 Detrimental effect of high fat feeding on HIF signalling

The work in this thesis demonstrated that high fat feeding is not only detrimental to cardiac metabolic flexibility via PPARα, but may also have a direct negative effect on HIF signalling. Here, it was shown that VEGF activation was normal following hypoxia in chow fed wild type and PPARα$^{-/-}$ mice, but was blunted following high fat feeding in both hypoxic wild type and PPARα$^{-/-}$ mouse hearts. In ischaemic diabetic hearts, HIF and VEGF activation was impaired in both humans and mice [247, 248, 251]. Plasma free fatty acids are elevated in diabetic patients [250], but a blunted HIF response in a milder, pre-diabetic model achieved by short term high fat feeding following hypoxia is not well defined. The deleterious effect of high fat on HIF signalling may have exacerbated the cardiac functional abnormalities in high fat fed wild type and PPARα$^{-/-}$ mouse hearts following chronic hypoxia, and deserve a more detailed attention in future research.

Conclusion

In summary, the work in this thesis has shown that 3 weeks exposure to 11% hypoxia in healthy mice decreased PPARα expression, and induced a metabolic switch away from fatty acid oxidation towards glycolysis, sufficient to maintain ATP production

and normal contractile function. The disruption of metabolic adaptation via changes in PPARα expression, achieved by high fat feeding and genetic ablation of PPARα, impaired the hypoxic response and resulted in cardiac dysfunction. HIF activation in HL-1 cardiomyocytes decreased PPARα expression, and caused similar molecular changes to mouse hearts adapted to hypoxia, demonstrating a PPARα/HIF interaction. In conclusion, the work in this thesis has demonstrated the pivotal role of HIF-dependent downregulation of PPARα for metabolic adaptation, essential for the maintenance of cardiac function and energetics following chronic physiological hypoxia.

REFERENCES

1. Neubauer, S., *The failing heart--an engine out of fuel*. N Engl J Med, 2007. 356(11): p. 1140-51.
2. Packer, M., *Pathophysiology of chronic heart failure*. Lancet, 1992. 340(8811): p. 88-92.
3. Coronel, R., J.R. de Groot, and J.J. van Lieshout, *Defining heart failure*. Cardiovasc Res, 2001. 50(3): p. 419-22.
4. Katz, A.M., *Pathophysiology of heart failure: identifying targets for pharmacotherapy*. Med Clin North Am, 2003. 87(2): p. 303-16.
5. Francis, J., R.M. Weiss, S.G. Wei, A.K. Johnson, and R.B. Felder, *Progression of heart failure after myocardial infarction in the rat*. Am J Physiol Regul Integr Comp Physiol, 2001. 281(5): p. R1734-45.
6. Chien, K.R., *Stress pathways and heart failure*. Cell, 1999. 98(5): p. 555-8.
7. Packer, M., *Beta-blockade in the management of chronic heart failure. Another step in the conceptual evolution of a neurohormonal model of the disease*. Eur Heart J, 1996. 17 Suppl B: p. 21-3.
8. Packer, M., *New concepts in the pathophysiology of heart failure: beneficial and deleterious interaction of endogenous haemodynamic and neurohormonal mechanisms*. J Intern Med, 1996. 239(4): p. 327-33.
9. Foody, J.M., M.H. Farrell, and H.M. Krumholz, *beta-Blocker therapy in heart failure: scientific review*. Jama, 2002. 287(7): p. 883-9.
10. Pfeffer, M.A., E. Braunwald, L.A. Moye, L. Basta, E.J. Brown, Jr., T.E. Cuddy, B.R. Davis, E.M. Geltman, S. Goldman, G.C. Flaker, and et al., *Effect of captopril on mortality and morbidity in patients with left ventricular dysfunction after myocardial infarction. Results of the survival and ventricular enlargement trial. The SAVE Investigators*. N Engl J Med, 1992. 327(10): p. 669-77.
11. Jessup, M. and S. Brozena, *Heart failure*. N Engl J Med, 2003. 348(20): p. 2007-18.
12. *NHS National Heart failure audit 2008/2009*. Available from: http://www.ic.nhs.uk/webfiles/Services/NCASP/audits%20and%20reports/NHS_National_Heart_Failure_Audit_09_INTERACTIVE.pdf.
13. McMurray, J.J. and M.A. Pfeffer, *Heart failure*. Lancet, 2005. 365(9474): p. 1877-89.
14. Mann, D.L. and M.R. Bristow, *Mechanisms and models in heart failure: the biomechanical model and beyond*. Circulation, 2005. 111(21): p. 2837-49.
15. van Bilsen, M., P.J. Smeets, A.J. Gilde, and G.J. van der Vusse, *Metabolic remodelling of the failing heart: the cardiac burn-out syndrome?* Cardiovasc Res, 2004. 61(2): p. 218-26.
16. van Bilsen, M., F.A. van Nieuwenhoven, and G.J. van der Vusse, *Metabolic remodelling of the failing heart: beneficial or detrimental?* Cardiovasc Res, 2009. 81(3): p. 420-8.
17. Taegtmeyer, H., *Cardiac metabolism as a target for the treatment of heart failure*. Circulation, 2004. 110(8): p. 894-6.
18. Stanley, W.C. and M.P. Chandler, *Energy metabolism in the normal and failing heart: potential for therapeutic interventions*. Heart Fail Rev, 2002. 7(2): p. 115-30.
19. Hardy, C.J., R.G. Weiss, P.A. Bottomley, and G. Gerstenblith, *Altered myocardial high-energy phosphate metabolites in patients with dilated cardiomyopathy*. Am Heart J, 1991. 122(3 Pt 1): p. 795-801.

20. Neubauer, S., M. Horn, T. Pabst, M. Godde, D. Lubke, B. Jilling, D. Hahn, and G. Ertl, *Contributions of 31P-magnetic resonance spectroscopy to the understanding of dilated heart muscle disease*. Eur Heart J, 1995. 16 Suppl O: p. 115-8.
21. Opie, L.H., *Heart physiology: from cell to circulation*. 4th edition ed2004: Lippincott, Williams and Wilkins.
22. Ashrafian, H., M.P. Frenneaux, and L.H. Opie, *Metabolic mechanisms in heart failure*. Circulation, 2007. 116(4): p. 434-48.
23. Stanley, W.C., F.A. Recchia, and G.D. Lopaschuk, *Myocardial substrate metabolism in the normal and failing heart*. Physiol Rev, 2005. 85(3): p. 1093-129.
24. Wisneski, J.A., E.W. Gertz, R.A. Neese, and M. Mayr, *Myocardial metabolism of free fatty acids. Studies with 14C-labeled substrates in humans*. J Clin Invest, 1987. 79(2): p. 359-66.
25. Taegtmeyer, H., *Switching metabolic genes to build a better heart*. Circulation, 2002. 106(16): p. 2043-5.
26. van der Vusse, G.J., M. van Bilsen, and J.F. Glatz, *Cardiac fatty acid uptake and transport in health and disease*. Cardiovasc Res, 2000. 45(2): p. 279-93.
27. Salway, J., *Metabolism at a glance*. 2nd edition ed1999: Blackwell
28. Taegtmeyer, H., L. Golfman, S. Sharma, P. Razeghi, and M. van Arsdall, *Linking gene expression to function: metabolic flexibility in the normal and diseased heart*. Ann N Y Acad Sci, 2004. 1015: p. 202-13.
29. Eaton, S., *Control of mitochondrial beta-oxidation flux*. Prog Lipid Res, 2002. 41(3): p. 197-239.
30. Lopaschuk, G.D., J.R. Ussher, C.D. Folmes, J.S. Jaswal, and W.C. Stanley, *Myocardial fatty acid metabolism in health and disease*. Physiol Rev, 2010. 90(1): p. 207-58.
31. Bing, R.J., A. Siegel, I. Ungar, and M. Gilbert, *Metabolism of the human heart. II. Studies on fat, ketone and amino acid metabolism*. Am J Med, 1954. 16(4): p. 504-15.
32. Randle, P.J., P.B. Garland, C.N. Hales, and E.A. Newsholme, *The glucose fatty-acid cycle. Its role in insulin sensitivity and the metabolic disturbances of diabetes mellitus*. Lancet, 1963. 1: p. 785-9.
33. Abumrad, N., C. Coburn, and A. Ibrahimi, *Membrane proteins implicated in long-chain fatty acid uptake by mammalian cells: CD36, FATP and FABPm*. Biochim Biophys Acta, 1999. 1441(1): p. 4-13.
34. Gibbons, G.F., K. Islam, and R.J. Pease, *Mobilisation of triacylglycerol stores*. Biochim Biophys Acta, 2000. 1483(1): p. 37-57.
35. Lopaschuk, G.D. and R.L. Barr, *Measurements of fatty acid and carbohydrate metabolism in the isolated working rat heart*. Mol Cell Biochem, 1997. 172(1-2): p. 137-47.
36. Hauton, D., M.J. Bennett, and R.D. Evans, *Utilisation of triacylglycerol and non-esterified fatty acid by the working rat heart: myocardial lipid substrate preference*. Biochim Biophys Acta, 2001. 1533(2): p. 99-109.
37. Lopaschuk, G.D., D.D. Belke, J. Gamble, T. Itoi, and B.O. Schonekess, *Regulation of fatty acid oxidation in the mammalian heart in health and disease*. Biochim Biophys Acta, 1994. 1213(3): p. 263-76.
38. Goodwin, G.W., C.S. Taylor, and H. Taegtmeyer, *Regulation of energy metabolism of the heart during acute increase in heart work*. J Biol Chem, 1998. 273(45): p. 29530-9.

39. Paulson, D.J., K.M. Ward, and A.L. Shug, *Malonyl CoA inhibition of carnitine palmityltransferase in rat heart mitochondria*. FEBS Lett, 1984. 176(2): p. 381-4.
40. Osorio, J.C., W.C. Stanley, A. Linke, M. Castellari, Q.N. Diep, A.R. Panchal, T.H. Hintze, G.D. Lopaschuk, and F.A. Recchia, *Impaired myocardial fatty acid oxidation and reduced protein expression of retinoid X receptor-alpha in pacing-induced heart failure*. Circulation, 2002. 106(5): p. 606-12.
41. Zorzano, A., L. Sevilla, M. Camps, C. Becker, J. Meyer, H. Kammermeier, P. Munoz, A. Guma, X. Testar, M. Palacin, J. Blasi, and Y. Fischer, *Regulation of glucose transport, and glucose transporters expression and trafficking in the heart: studies in cardiac myocytes*. Am J Cardiol, 1997. 80(3A): p. 65A-76A.
42. Liao, R., M. Jain, L. Cui, J. D'Agostino, F. Aiello, I. Luptak, S. Ngoy, R.M. Mortensen, and R. Tian, *Cardiac-specific overexpression of GLUT1 prevents the development of heart failure attributable to pressure overload in mice*. Circulation, 2002. 106(16): p. 2125-31.
43. Holman, G.D., L. Lo Leggio, and S.W. Cushman, *Insulin-stimulated GLUT4 glucose transporter recycling. A problem in membrane protein subcellular trafficking through multiple pools*. J Biol Chem, 1994. 269(26): p. 17516-24.
44. Holness, M.J., K. Bulmer, G.F. Gibbons, and M.C. Sugden, *Up-regulation of pyruvate dehydrogenase kinase isoform 4 (PDK4) protein expression in oxidative skeletal muscle does not require the obligatory participation of peroxisome-proliferator-activated receptor alpha (PPARalpha)*. Biochem J, 2002. 366(Pt 3): p. 839-46.
45. Lydell, C.P., A. Chan, R.B. Wambolt, N. Sambandam, H. Parsons, G.P. Bondy, B. Rodrigues, K.M. Popov, R.A. Harris, R.W. Brownsey, and M.F. Allard, *Pyruvate dehydrogenase and the regulation of glucose oxidation in hypertrophied rat hearts*. Cardiovasc Res, 2002. 53(4): p. 841-51.
46. Kersten, S., B. Desvergne, and W. Wahli, *Roles of PPARs in health and disease*. Nature, 2000. 405(6785): p. 421-4.
47. Finck, B.N. and D.P. Kelly, *Peroxisome proliferator-activated receptor alpha (PPARalpha) signaling in the gene regulatory control of energy metabolism in the normal and diseased heart*. J Mol Cell Cardiol, 2002. 34(10): p. 1249-57.
48. Handschin, C. and B.M. Spiegelman, *Peroxisome proliferator-activated receptor gamma coactivator 1 coactivators, energy homeostasis, and metabolism*. Endocr Rev, 2006. 27(7): p. 728-35.
49. Berger, J. and D.E. Moller, *The mechanisms of action of PPARs*. Annu Rev Med, 2002. 53: p. 409-35.
50. Desvergne, B. and W. Wahli, *Peroxisome proliferator-activated receptors: nuclear control of metabolism*. Endocr Rev, 1999. 20(5): p. 649-88.
51. Barger, P.M. and D.P. Kelly, *PPAR signaling in the control of cardiac energy metabolism*. Trends Cardiovasc Med, 2000. 10(6): p. 238-45.
52. Djouadi, F., J.M. Brandt, C.J. Weinheimer, T.C. Leone, F.J. Gonzalez, and D.P. Kelly, *The role of the peroxisome proliferator-activated receptor alpha (PPAR alpha) in the control of cardiac lipid metabolism*. Prostaglandins Leukot Essent Fatty Acids, 1999. 60(5-6): p. 339-43.
53. Madrazo, J.A. and D.P. Kelly, *The PPAR trio: regulators of myocardial energy metabolism in health and disease*. J Mol Cell Cardiol, 2008. 44(6): p. 968-75.

54. Issemann, I. and S. Green, *Activation of a member of the steroid hormone receptor superfamily by peroxisome proliferators*. Nature, 1990. 347(6294): p. 645-50.
55. Dreyer, C., H. Keller, A. Mahfoudi, V. Laudet, G. Krey, and W. Wahli, *Positive regulation of the peroxisomal beta-oxidation pathway by fatty acids through activation of peroxisome proliferator-activated receptors (PPAR)*. Biol Cell, 1993. 77(1): p. 67-76.
56. Escher, P., O. Braissant, S. Basu-Modak, L. Michalik, W. Wahli, and B. Desvergne, *Rat PPARs: quantitative analysis in adult rat tissues and regulation in fasting and refeeding*. Endocrinology, 2001. 142(10): p. 4195-202.
57. Braissant, O., F. Foufelle, C. Scotto, M. Dauca, and W. Wahli, *Differential expression of peroxisome proliferator-activated receptors (PPARs): tissue distribution of PPAR-alpha, -beta, and -gamma in the adult rat*. Endocrinology, 1996. 137(1): p. 354-66.
58. Ferre, P., *The biology of peroxisome proliferator-activated receptors: relationship with lipid metabolism and insulin sensitivity*. Diabetes, 2004. 53 Suppl 1: p. S43-50.
59. Huss, J.M. and D.P. Kelly, *Nuclear receptor signaling and cardiac energetics*. Circ Res, 2004. 95(6): p. 568-78.
60. Mukherjee, R., L. Jow, D. Noonan, and D.P. McDonnell, *Human and rat peroxisome proliferator activated receptors (PPARs) demonstrate similar tissue distribution but different responsiveness to PPAR activators*. J Steroid Biochem Mol Biol, 1994. 51(3-4): p. 157-66.
61. Keller, H., C. Dreyer, J. Medin, A. Mahfoudi, K. Ozato, and W. Wahli, *Fatty acids and retinoids control lipid metabolism through activation of peroxisome proliferator-activated receptor-retinoid X receptor heterodimers*. Proc Natl Acad Sci U S A, 1993. 90(6): p. 2160-4.
62. Forman, B.M., J. Chen, and R.M. Evans, *The peroxisome proliferator-activated receptors: ligands and activators*. Ann N Y Acad Sci, 1996. 804: p. 266-75.
63. Forman, B.M., J. Chen, and R.M. Evans, *Hypolipidemic drugs, polyunsaturated fatty acids, and eicosanoids are ligands for peroxisome proliferator-activated receptors alpha and delta*. Proc Natl Acad Sci U S A, 1997. 94(9): p. 4312-7.
64. Gonzalez, F.J., J.M. Peters, and R.C. Cattley, *Mechanism of action of the nongenotoxic peroxisome proliferators: role of the peroxisome proliferator-activator receptor alpha*. J Natl Cancer Inst, 1998. 90(22): p. 1702-9.
65. Lee, S.S. and F.J. Gonzalez, *Targeted disruption of the peroxisome proliferator-activated receptor alpha gene, PPAR alpha*. Ann N Y Acad Sci, 1996. 804: p. 524-9.
66. Motojima, K., P. Passilly, J.M. Peters, F.J. Gonzalez, and N. Latruffe, *Expression of putative fatty acid transporter genes are regulated by peroxisome proliferator-activated receptor alpha and gamma activators in a tissue- and inducer-specific manner*. J Biol Chem, 1998. 273(27): p. 16710-4.
67. van Bilsen, M., G.J. van der Vusse, A.J. Gilde, M. Lindhout, and K.A. van der Lee, *Peroxisome proliferator-activated receptors: lipid binding proteins controling gene expression*. Mol Cell Biochem, 2002. 239(1-2): p. 131-8.
68. van der Lee, K.A., M.M. Vork, J.E. De Vries, P.H. Willemsen, J.F. Glatz, R.S. Reneman, G.J. Van der Vusse, and M. Van Bilsen, *Long-chain fatty*

acid-induced changes in gene expression in neonatal cardiac myocytes. J Lipid Res, 2000. 41(1): p. 41-7.
69. Brandt, J.M., F. Djouadi, and D.P. Kelly, *Fatty acids activate transcription of the muscle carnitine palmitoyltransferase I gene in cardiac myocytes via the peroxisome proliferator-activated receptor alpha*. J Biol Chem, 1998. 273(37): p. 23786-92.
70. Gulick, T., S. Cresci, T. Caira, D.D. Moore, and D.P. Kelly, *The peroxisome proliferator-activated receptor regulates mitochondrial fatty acid oxidative enzyme gene expression*. Proc Natl Acad Sci U S A, 1994. 91(23): p. 11012-6.
71. Young, M.E., S. Patil, J. Ying, C. Depre, H.S. Ahuja, G.L. Shipley, S.M. Stepkowski, P.J. Davies, and H. Taegtmeyer, *Uncoupling protein 3 transcription is regulated by peroxisome proliferator-activated receptor (alpha) in the adult rodent heart*. Faseb J, 2001. 15(3): p. 833-45.
72. Murray, A.J., R.E. Anderson, G.C. Watson, G.K. Radda, and K. Clarke, *Uncoupling proteins in human heart*. Lancet, 2004. 364(9447): p. 1786-8.
73. Stavinoha, M.A., J.W. RaySpellicy, M.F. Essop, C. Graveleau, E.D. Abel, M.L. Hart-Sailors, H.J. Mersmann, M.S. Bray, and M.E. Young, *Evidence for mitochondrial thioesterase 1 as a peroxisome proliferator-activated receptor-alpha-regulated gene in cardiac and skeletal muscle*. Am J Physiol Endocrinol Metab, 2004. 287(5): p. E888-95.
74. Hoeks, J., M.K. Hesselink, M. van Bilsen, G. Schaart, G.J. van der Vusse, W.H. Saris, and P. Schrauwen, *Differential response of UCP3 to medium versus long chain triacylglycerols; manifestation of a functional adaptation*. FEBS Lett, 2003. 555(3): p. 631-7.
75. Sugden, M.C., K. Bulmer, G.F. Gibbons, and M.J. Holness, *Role of peroxisome proliferator-activated receptor-alpha in the mechanism underlying changes in renal pyruvate dehydrogenase kinase isoform 4 protein expression in starvation and after refeeding*. Arch Biochem Biophys, 2001. 395(2): p. 246-52.
76. Hopkins, T.A., M.C. Sugden, M.J. Holness, R. Kozak, J.R. Dyck, and G.D. Lopaschuk, *Control of cardiac pyruvate dehydrogenase activity in peroxisome proliferator-activated receptor-alpha transgenic mice*. Am J Physiol Heart Circ Physiol, 2003. 285(1): p. H270-6.
77. Gilde, A.J., K.A. van der Lee, P.H. Willemsen, G. Chinetti, F.R. van der Leij, G.J. van der Vusse, B. Staels, and M. van Bilsen, *Peroxisome proliferator-activated receptor (PPAR) alpha and PPARbeta/delta, but not PPARgamma, modulate the expression of genes involved in cardiac lipid metabolism*. Circ Res, 2003. 92(5): p. 518-24.
78. Cheng, L., G. Ding, Q. Qin, Y. Huang, W. Lewis, N. He, R.M. Evans, M.D. Schneider, F.A. Brako, Y. Xiao, Y.E. Chen, and Q. Yang, *Cardiomyocyte-restricted peroxisome proliferator-activated receptor-delta deletion perturbs myocardial fatty acid oxidation and leads to cardiomyopathy*. Nat Med, 2004. 10(11): p. 1245-50.
79. Golfman, L.S., C.R. Wilson, S. Sharma, M. Burgmaier, M.E. Young, P.H. Guthrie, M. Van Arsdall, J.V. Adrogue, K.K. Brown, and H. Taegtmeyer, *Activation of PPARgamma enhances myocardial glucose oxidation and improves contractile function in isolated working hearts of ZDF rats*. Am J Physiol Endocrinol Metab, 2005. 289(2): p. E328-36.
80. Asakawa, M., H. Takano, T. Nagai, H. Uozumi, H. Hasegawa, N. Kubota, T. Saito, Y. Masuda, T. Kadowaki, and I. Komuro, *Peroxisome proliferator-*

activated receptor gamma plays a critical role in inhibition of cardiac hypertrophy in vitro and in vivo. Circulation, 2002. 105(10): p. 1240-6.
81. Tontonoz, P., E. Hu, and B.M. Spiegelman, *Regulation of adipocyte gene expression and differentiation by peroxisome proliferator activated receptor gamma*. Curr Opin Genet Dev, 1995. 5(5): p. 571-6.
82. Guerre-Millo, M., P. Gervois, E. Raspe, L. Madsen, P. Poulain, B. Derudas, J.M. Herbert, D.A. Winegar, T.M. Willson, J.C. Fruchart, R.K. Berge, and B. Staels, *Peroxisome proliferator-activated receptor alpha activators improve insulin sensitivity and reduce adiposity*. J Biol Chem, 2000. 275(22): p. 16638-42.
83. Ding, G., M. Fu, Q. Qin, W. Lewis, H.W. Kim, T. Fukai, M. Bacanamwo, Y.E. Chen, M.D. Schneider, D.J. Mangelsdorf, R.M. Evans, and Q. Yang, *Cardiac peroxisome proliferator-activated receptor gamma is essential in protecting cardiomyocytes from oxidative damage*. Cardiovasc Res, 2007. 76(2): p. 269-79.
84. Hidaka, S., T. Kakuma, H. Yoshimatsu, H. Sakino, S. Fukuchi, and T. Sakata, *Streptozotocin treatment upregulates uncoupling protein 3 expression in the rat heart*. Diabetes, 1999. 48(2): p. 430-5.
85. Murray, A.J., M. Panagia, D. Hauton, G.F. Gibbons, and K. Clarke, *Plasma free fatty acids and peroxisome proliferator-activated receptor alpha in the control of myocardial uncoupling protein levels*. Diabetes, 2005. 54(12): p. 3496-502.
86. Brun, S., M.C. Carmona, T. Mampel, O. Vinas, M. Giralt, R. Iglesias, and F. Villarroya, *Activators of peroxisome proliferator-activated receptor-alpha induce the expression of the uncoupling protein-3 gene in skeletal muscle: a potential mechanism for the lipid intake-dependent activation of uncoupling protein-3 gene expression at birth*. Diabetes, 1999. 48(6): p. 1217-22.
87. Acin, A., M. Rodriguez, H. Rique, E. Canet, J.A. Boutin, and J.P. Galizzi, *Cloning and characterization of the 5' flanking region of the human uncoupling protein 3 (UCP3) gene*. Biochem Biophys Res Commun, 1999. 258(2): p. 278-83.
88. Boss, O., T. Hagen, and B.B. Lowell, *Uncoupling proteins 2 and 3: potential regulators of mitochondrial energy metabolism*. Diabetes, 2000. 49(2): p. 143-56.
89. Rousset, S., M.C. Alves-Guerra, J. Mozo, B. Miroux, A.M. Cassard-Doulcier, F. Bouillaud, and D. Ricquier, *The biology of mitochondrial uncoupling proteins*. Diabetes, 2004. 53 Suppl 1: p. S130-5.
90. Busquets, S., N. Carbo, V. Almendro, M. Figueras, F.J. Lopez-Soriano, and J.M. Argiles, *Hyperlipemia: a role in regulating UCP3 gene expression in skeletal muscle during cancer cachexia?* FEBS Lett, 2001. 505(2): p. 255-8.
91. Echtay, K.S., D. Roussel, J. St-Pierre, M.B. Jekabsons, S. Cadenas, J.A. Stuart, J.A. Harper, S.J. Roebuck, A. Morrison, S. Pickering, J.C. Clapham, and M.D. Brand, *Superoxide activates mitochondrial uncoupling proteins*. Nature, 2002. 415(6867): p. 96-9.
92. Schrauwen, P., J. Hoeks, G. Schaart, E. Kornips, B. Binas, G.J. Van De Vusse, M. Van Bilsen, J.J. Luiken, S.L. Coort, J.F. Glatz, W.H. Saris, and M.K. Hesselink, *Uncoupling protein 3 as a mitochondrial fatty acid anion exporter*. Faseb J, 2003. 17(15): p. 2272-4.
93. Himms-Hagen, J. and M.E. Harper, *Physiological role of UCP3 may be export of fatty acids from mitochondria when fatty acid oxidation*

predominates: an hypothesis. Exp Biol Med (Maywood), 2001. 226(2): p. 78-84.
94. Hunt, M.C. and S.E. Alexson, *The role Acyl-CoA thioesterases play in mediating intracellular lipid metabolism*. Prog Lipid Res, 2002. 41(2): p. 99-130.
95. Gross, R.W., *Purification and characterization of mitochondrial thioesterase from rabbit myocardium and its inhibition by palmitoyl carnitine*. Biochim Biophys Acta, 1984. 802(2): p. 197-202.
96. Garlid, K.D., M. Jaburek, and P. Jezek, *Mechanism of uncoupling protein action*. Biochem Soc Trans, 2001. 29(Pt 6): p. 803-6.
97. Jezek, P., H. Engstova, M. Zackova, A.E. Vercesi, A.D. Costa, P. Arruda, and K.D. Garlid, *Fatty acid cycling mechanism and mitochondrial uncoupling proteins*. Biochim Biophys Acta, 1998. 1365(1-2): p. 319-27.
98. Tonkonogi, M., A. Krook, B. Walsh, and K. Sahlin, *Endurance training increases stimulation of uncoupling of skeletal muscle mitochondria in humans by non-esterified fatty acids: an uncoupling-protein-mediated effect?* Biochem J, 2000. 351 Pt 3: p. 805-10.
99. Pool, P.E. and E.H. Sonnenblick, *The mechanochemistry of cardiac muscle. I. The isometric contraction*. J Gen Physiol, 1967. 50(4): p. 951-65.
100. Neubauer, S., T. Krahe, R. Schindler, M. Horn, H. Hillenbrand, C. Entzeroth, H. Mader, E.P. Kromer, G.A. Riegger, K. Lackner, and et al., *31P magnetic resonance spectroscopy in dilated cardiomyopathy and coronary artery disease. Altered cardiac high-energy phosphate metabolism in heart failure*. Circulation, 1992. 86(6): p. 1810-8.
101. Neubauer, S., M. Horn, M. Cramer, K. Harre, J.B. Newell, W. Peters, T. Pabst, G. Ertl, D. Hahn, J.S. Ingwall, and K. Kochsiek, *Myocardial phosphocreatine-to-ATP ratio is a predictor of mortality in patients with dilated cardiomyopathy*. Circulation, 1997. 96(7): p. 2190-6.
102. Rajabi, M., C. Kassiotis, P. Razeghi, and H. Taegtmeyer, *Return to the fetal gene program protects the stressed heart: a strong hypothesis*. Heart Fail Rev, 2007. 12(3-4): p. 331-43.
103. Sack, M.N., T.A. Rader, S. Park, J. Bastin, S.A. McCune, and D.P. Kelly, *Fatty acid oxidation enzyme gene expression is downregulated in the failing heart*. Circulation, 1996. 94(11): p. 2837-42.
104. Razeghi, P., M.E. Young, J.L. Alcorn, C.S. Moravec, O.H. Frazier, and H. Taegtmeyer, *Metabolic gene expression in fetal and failing human heart*. Circulation, 2001. 104(24): p. 2923-31.
105. Barger, P.M. and D.P. Kelly, *Fatty acid utilization in the hypertrophied and failing heart: molecular regulatory mechanisms*. Am J Med Sci, 1999. 318(1): p. 36-42.
106. Bing, R.J., *Myocardial metabolism*. Circulation, 1955. 12(4): p. 635-47.
107. Bishop, S.P. and R.A. Altschuld, *Increased glycolytic metabolism in cardiac hypertrophy and congestive failure*. Am J Physiol, 1970. 218(1): p. 153-9.
108. Paolisso, G., A. Gambardella, D. Galzerano, A. D'Amore, P. Rubino, M. Verza, P. Teasuro, M. Varricchio, and F. D'Onofrio, *Total-body and myocardial substrate oxidation in congestive heart failure*. Metabolism, 1994. 43(2): p. 174-9.
109. Taylor, M., T.R. Wallhaus, T.R. Degrado, D.C. Russell, P. Stanko, R.J. Nickles, and C.K. Stone, *An evaluation of myocardial fatty acid and glucose*

uptake using PET with [18F]fluoro-6-thia-heptadecanoic acid and [18F]FDG in Patients with Congestive Heart Failure. J Nucl Med, 2001. 42(1): p. 55-62.
110. Davila-Roman, V.G., G. Vedala, P. Herrero, L. de las Fuentes, J.G. Rogers, D.P. Kelly, and R.J. Gropler, *Altered myocardial fatty acid and glucose metabolism in idiopathic dilated cardiomyopathy*. J Am Coll Cardiol, 2002. 40(2): p. 271-7.
111. Chandler, M.P., J. Kerner, H. Huang, E. Vazquez, A. Reszko, W.Z. Martini, C.L. Hoppel, M. Imai, S. Rastogi, H.N. Sabbah, and W.C. Stanley, *Moderate severity heart failure does not involve a downregulation of myocardial fatty acid oxidation*. Am J Physiol Heart Circ Physiol, 2004. 287(4): p. H1538-43.
112. Lei, B., V. Lionetti, M.E. Young, M.P. Chandler, C. d'Agostino, E. Kang, M. Altarejos, K. Matsuo, T.H. Hintze, W.C. Stanley, and F.A. Recchia, *Paradoxical downregulation of the glucose oxidation pathway despite enhanced flux in severe heart failure*. J Mol Cell Cardiol, 2004. 36(4): p. 567-76.
113. Remondino, A., N. Rosenblatt-Velin, C. Montessuit, I. Tardy, I. Papageorgiou, P.A. Dorsaz, M. Jorge-Costa, and R. Lerch, *Altered expression of proteins of metabolic regulation during remodeling of the left ventricle after myocardial infarction*. J Mol Cell Cardiol, 2000. 32(11): p. 2025-34.
114. Huss, J.M. and D.P. Kelly, *Mitochondrial energy metabolism in heart failure: a question of balance*. J Clin Invest, 2005. 115(3): p. 547-55.
115. Karbowska, J., Z. Kochan, and R.T. Smolenski, *Peroxisome proliferator-activated receptor alpha is downregulated in the failing human heart*. Cell Mol Biol Lett, 2003. 8(1): p. 49-53.
116. Razeghi, P., T.J. Myers, O.H. Frazier, and H. Taegtmeyer, *Reverse remodeling of the failing human heart with mechanical unloading. Emerging concepts and unanswered questions*. Cardiology, 2002. 98(4): p. 167-74.
117. Giordano, F.J., *Oxygen, oxidative stress, hypoxia, and heart failure*. J Clin Invest, 2005. 115(3): p. 500-8.
118. Murray, A.J., L.M. Edwards, and K. Clarke, *Mitochondria and heart failure*. Curr Opin Clin Nutr Metab Care, 2007. 10(6): p. 704-11.
119. Ostadal, B., I. Ostadalova, and N.S. Dhalla, *Development of cardiac sensitivity to oxygen deficiency: comparative and ontogenetic aspects*. Physiol Rev, 1999. 79(3): p. 635-59.
120. Essop, M.F., *Cardiac metabolic adaptations in response to chronic hypoxia*. J Physiol, 2007. 584(Pt 3): p. 715-26.
121. Kolar, F. and B. Ostadal, *Molecular mechanisms of cardiac protection by adaptation to chronic hypoxia*. Physiol Res, 2004. 53 Suppl 1: p. S3-13.
122. Grifka, R.G., *Cyanotic congenital heart disease with increased pulmonary blood flow*. Pediatr Clin North Am, 1999. 46(2): p. 405-25.
123. Budev, M.M., A.C. Arroliga, H.P. Wiedemann, and R.A. Matthay, *Cor pulmonale: an overview*. Semin Respir Crit Care Med, 2003. 24(3): p. 233-44.
124. Ware, J.A. and M. Simons, *Angiogenesis in ischemic heart disease*. Nat Med, 1997. 3(2): p. 158-64.
125. Semenza, G.L., *Hypoxia-inducible factor 1: regulator of mitochondrial metabolism and mediator of ischemic preconditioning*. Biochim Biophys Acta, 2011. 1813(7): p. 1263-8.
126. Ratcliffe, P.J., *From erythropoietin to oxygen: hypoxia-inducible factor hydroxylases and the hypoxia signal pathway*. Blood Purif, 2002. 20(5): p. 445-50.

127. Schofield, C.J. and P.J. Ratcliffe, *Oxygen sensing by HIF hydroxylases*. Nat Rev Mol Cell Biol, 2004. 5(5): p. 343-54.
128. Semenza, G.L., *Life with oxygen*. Science, 2007. 318(5847): p. 62-4.
129. Semenza, G.L., *Regulation of oxygen homeostasis by hypoxia-inducible factor 1*. Physiology (Bethesda), 2009. 24: p. 97-106.
130. Ratcliffe, P.J., J.F. O'Rourke, P.H. Maxwell, and C.W. Pugh, *Oxygen sensing, hypoxia-inducible factor-1 and the regulation of mammalian gene expression*. J Exp Biol, 1998. 201(Pt 8): p. 1153-62.
131. Semenza, G.L., P.H. Roth, H.M. Fang, and G.L. Wang, *Transcriptional regulation of genes encoding glycolytic enzymes by hypoxia-inducible factor 1*. J Biol Chem, 1994. 269(38): p. 23757-63.
132. Forsythe, J.A., B.H. Jiang, N.V. Iyer, F. Agani, S.W. Leung, R.D. Koos, and G.L. Semenza, *Activation of vascular endothelial growth factor gene transcription by hypoxia-inducible factor 1*. Mol Cell Biol, 1996. 16(9): p. 4604-13.
133. Wang, G.L. and G.L. Semenza, *Purification and characterization of hypoxia-inducible factor 1*. J Biol Chem, 1995. 270(3): p. 1230-7.
134. Levy, A.P., N.S. Levy, S. Wegner, and M.A. Goldberg, *Transcriptional regulation of the rat vascular endothelial growth factor gene by hypoxia*. J Biol Chem, 1995. 270(22): p. 13333-40.
135. Chen, C., N. Pore, A. Behrooz, F. Ismail-Beigi, and A. Maity, *Regulation of glut1 mRNA by hypoxia-inducible factor-1. Interaction between H-ras and hypoxia*. J Biol Chem, 2001. 276(12): p. 9519-25.
136. Ebert, B.L., J.D. Firth, and P.J. Ratcliffe, *Hypoxia and mitochondrial inhibitors regulate expression of glucose transporter-1 via distinct Cis-acting sequences*. J Biol Chem, 1995. 270(49): p. 29083-9.
137. Papandreou, I., R.A. Cairns, L. Fontana, A.L. Lim, and N.C. Denko, *HIF-1 mediates adaptation to hypoxia by actively downregulating mitochondrial oxygen consumption*. Cell Metab, 2006. 3(3): p. 187-97.
138. Kim, J.W., I. Tchernyshyov, G.L. Semenza, and C.V. Dang, *HIF-1-mediated expression of pyruvate dehydrogenase kinase: a metabolic switch required for cellular adaptation to hypoxia*. Cell Metab, 2006. 3(3): p. 177-85.
139. Semenza, G.L., *Oxygen sensing, homeostasis, and disease*. N Engl J Med, 2011. 365(6): p. 537-47.
140. Kaelin, W.G., Jr. and P.J. Ratcliffe, *Oxygen sensing by metazoans: the central role of the HIF hydroxylase pathway*. Mol Cell, 2008. 30(4): p. 393-402.
141. Stroka, D.M., T. Burkhardt, I. Desbaillets, R.H. Wenger, D.A. Neil, C. Bauer, M. Gassmann, and D. Candinas, *HIF-1 is expressed in normoxic tissue and displays an organ-specific regulation under systemic hypoxia*. Faseb J, 2001. 15(13): p. 2445-53.
142. Wiesener, M.S., P.M. Munchenhagen, I. Berger, N.V. Morgan, J. Roigas, A. Schwiertz, J.S. Jurgensen, G. Gruber, P.H. Maxwell, S.A. Loning, U. Frei, E.R. Maher, H.J. Grone, and K.U. Eckardt, *Constitutive activation of hypoxia-inducible genes related to overexpression of hypoxia-inducible factor-1alpha in clear cell renal carcinomas*. Cancer Res, 2001. 61(13): p. 5215-22.
143. Heidbreder, M., F. Frohlich, O. Johren, A. Dendorfer, F. Qadri, and P. Dominiak, *Hypoxia rapidly activates HIF-3alpha mRNA expression*. Faseb J, 2003. 17(11): p. 1541-3.
144. Willam, C., P.H. Maxwell, L. Nichols, C. Lygate, Y.M. Tian, W. Bernhardt, M. Wiesener, P.J. Ratcliffe, K.U. Eckardt, and C.W. Pugh, *HIF prolyl*

hydroxylases in the rat; organ distribution and changes in expression following hypoxia and coronary artery ligation. J Mol Cell Cardiol, 2006. 41(1): p. 68-77.
145. Chowdhury, R., A. Hardy, and C.J. Schofield, *The human oxygen sensing machinery and its manipulation*. Chem Soc Rev, 2008. 37(7): p. 1308-19.
146. Adrogue, J.V., S. Sharma, K. Ngumbela, M.F. Essop, and H. Taegtmeyer, *Acclimatization to chronic hypobaric hypoxia is associated with a differential transcriptional profile between the right and left ventricle*. Mol Cell Biochem, 2005. 278(1-2): p. 71-8.
147. Daneshrad, Z., M.P. Garcia-Riera, M. Verdys, and A. Rossi, *Differential responses to chronic hypoxia and dietary restriction of aerobic capacity and enzyme levels in the rat myocardium*. Mol Cell Biochem, 2000. 210(1-2): p. 159-66.
148. Ngumbela, K.C., M.N. Sack, and M.F. Essop, *Counter-regulatory effects of incremental hypoxia on the transcription of a cardiac fatty acid oxidation enzyme-encoding gene*. Mol Cell Biochem, 2003. 250(1-2): p. 151-8.
149. Sharma, S., H. Taegtmeyer, J. Adrogue, P. Razeghi, S. Sen, K. Ngumbela, and M.F. Essop, *Dynamic changes of gene expression in hypoxia-induced right ventricular hypertrophy*. Am J Physiol Heart Circ Physiol, 2004. 286(3): p. H1185-92.
150. Sivitz, W.I., D.D. Lund, B. Yorek, M. Grover-McKay, and P.G. Schmid, *Pretranslational regulation of two cardiac glucose transporters in rats exposed to hypobaric hypoxia*. Am J Physiol, 1992. 263(3 Pt 1): p. E562-9.
151. Hurford, W.E., G. Crosby, H.W. Strauss, R. Jones, and E. Lowenstein, *Ventricular performance and glucose uptake in rats during chronic hypobaric hypoxia*. J Nucl Med, 1990. 31(8): p. 1344-51.
152. Chaudary, N., Z. Naydenova, I. Shuralyova, and I.R. Coe, *Hypoxia regulates the adenosine transporter, mENT1, in the murine cardiomyocyte cell line, HL-1*. Cardiovasc Res, 2004. 61(4): p. 780-8.
153. Holden, J.E., C.K. Stone, C.M. Clark, W.D. Brown, R.J. Nickles, C. Stanley, and P.W. Hochachka, *Enhanced cardiac metabolism of plasma glucose in high-altitude natives: adaptation against chronic hypoxia*. J Appl Physiol, 1995. 79(1): p. 222-8.
154. Razeghi, P., M.E. Young, S. Abbasi, and H. Taegtmeyer, *Hypoxia in vivo decreases peroxisome proliferator-activated receptor alpha-regulated gene expression in rat heart*. Biochem Biophys Res Commun, 2001. 287(1): p. 5-10.
155. Kennedy, S.L., W.C. Stanley, A.R. Panchal, and R.S. Mazzeo, *Alterations in enzymes involved in fat metabolism after acute and chronic altitude exposure*. J Appl Physiol, 2001. 90(1): p. 17-22.
156. Bass, A., M. Stejskalova, B. Ostadal, and M. Samanek, *Differences between atrial and ventricular energy-supplying enzymes in five mammalian species*. Physiol Res, 1993. 42(1): p. 1-6.
157. Hochachka, P.W., C.M. Clark, J.E. Holden, C. Stanley, K. Ugurbil, and R.S. Menon, *31P magnetic resonance spectroscopy of the Sherpa heart: a phosphocreatine/adenosine triphosphate signature of metabolic defense against hypobaric hypoxia*. Proc Natl Acad Sci U S A, 1996. 93(3): p. 1215-20.
158. Holloway, C., L. Cochlin, I. Codreanu, E. Bloch, M. Fatemian, C. Szmigielski, H. Atherton, L. Heather, J. Francis, S. Neubauer, P. Robbins, H.

Montgomery, and K. Clarke, *Normobaric hypoxia impairs human cardiac energetics*. Faseb J, 2011. 25(9): p. 3130-5.
159. Holloway, C.J., H.E. Montgomery, A.J. Murray, L.E. Cochlin, I. Codreanu, N. Hopwood, A.W. Johnson, O.J. Rider, D.Z. Levett, D.J. Tyler, J.M. Francis, S. Neubauer, M.P. Grocott, and K. Clarke, *Cardiac response to hypobaric hypoxia: persistent changes in cardiac mass, function, and energy metabolism after a trek to Mt. Everest Base Camp*. Faseb J, 2011. 25(2): p. 792-6.
160. Calmettes, G., V. Deschodt-Arsac, G. Gouspillou, S. Miraux, B. Muller, J.M. Franconi, E. Thiaudiere, and P. Diolez, *Improved energy supply regulation in chronic hypoxic mouse counteracts hypoxia-induced altered cardiac energetics*. PLoS One, 2010. 5(2): p. e9306.
161. Calmettes, G., V. Deschodt-Arsac, E. Thiaudiere, B. Muller, and P. Diolez, *Modular control analysis of effects of chronic hypoxia on mouse heart*. Am J Physiol Regul Integr Comp Physiol, 2008. 295(6): p. R1891-7.
162. Shyu, K.G., J.Y. Liou, B.W. Wang, W.J. Fang, and H. Chang, *Carvedilol prevents cardiac hypertrophy and overexpression of hypoxia-inducible factor-1alpha and vascular endothelial growth factor in pressure-overloaded rat heart*. J Biomed Sci, 2005. 12(2): p. 409-20.
163. Moslehi, J., Y.A. Minamishima, J. Shi, D. Neuberg, D.M. Charytan, R.F. Padera, S. Signoretti, R. Liao, and W.G. Kaelin, Jr., *Loss of hypoxia-inducible factor prolyl hydroxylase activity in cardiomyocytes phenocopies ischemic cardiomyopathy*. Circulation, 2010. 122(10): p. 1004-16.
164. Huang, Y., R.P. Hickey, J.L. Yeh, D. Liu, A. Dadak, L.H. Young, R.S. Johnson, and F.J. Giordano, *Cardiac myocyte-specific HIF-1alpha deletion alters vascularization, energy availability, calcium flux, and contractility in the normoxic heart*. Faseb J, 2004. 18(10): p. 1138-40.
165. Brusselmans, K., V. Compernolle, M. Tjwa, M.S. Wiesener, P.H. Maxwell, D. Collen, and P. Carmeliet, *Heterozygous deficiency of hypoxia-inducible factor-2alpha protects mice against pulmonary hypertension and right ventricular dysfunction during prolonged hypoxia*. J Clin Invest, 2003. 111(10): p. 1519-27.
166. Stuckey, D.J., C.A. Carr, P. Camelliti, D.J. Tyler, K.E. Davies, and K. Clarke, *In vivo MRI characterization of progressive cardiac dysfunction in the mdx mouse model of muscular dystrophy*. PLoS One, 2012. 7(1): p. e28569.
167. Ten Hove, M. and S. Neubauer, *MR spectroscopy in heart failure--clinical and experimental findings*. Heart Fail Rev, 2007. 12(1): p. 48-57.
168. Lowry, O.H., N.J. Rosebrough, A.L. Farr, and R.J. Randall, *Protein measurement with the Folin phenol reagent*. J Biol Chem, 1951. 193(1): p. 265-75.
169. Neubauer, S. and J.S. Ingwall, *Verapamil attenuates ATP depletion during hypoxia: 31P NMR studies of the isolated rat heart*. J Mol Cell Cardiol, 1989. 21(11): p. 1163-78.
170. Tan, S.C., C.A. Carr, K.K. Yeoh, C.J. Schofield, K.E. Davies, and K. Clarke, *Identification of valid housekeeping genes for quantitative RT-PCR analysis of cardiosphere-derived cells preconditioned under hypoxia or with prolyl-4-hydroxylase inhibitors*. Mol Biol Rep, 2012. 39(4): p. 4857-67.
171. Livak, K.J. and T.D. Schmittgen, *Analysis of relative gene expression data using real-time quantitative PCR and the 2(-Delta Delta C(T)) Method*. Methods, 2001. 25(4): p. 402-8.

172. Allard, M.F., B.O. Schonekess, S.L. Henning, D.R. English, and G.D. Lopaschuk, *Contribution of oxidative metabolism and glycolysis to ATP production in hypertrophied hearts*. Am J Physiol, 1994. 267(2 Pt 2): p. H742-50.
173. Heather, L.C., M.A. Cole, C.A. Lygate, R.D. Evans, D.J. Stuckey, A.J. Murray, S. Neubauer, and K. Clarke, *Fatty acid transporter levels and palmitate oxidation rate correlate with ejection fraction in the infarcted rat heart*. Cardiovasc Res, 2006. 72(3): p. 430-7.
174. Razeghi, P., M.E. Young, J. Ying, C. Depre, I.P. Uray, J. Kolesar, G.L. Shipley, C.S. Moravec, P.J. Davies, O.H. Frazier, and H. Taegtmeyer, *Downregulation of metabolic gene expression in failing human heart before and after mechanical unloading*. Cardiology, 2002. 97(4): p. 203-9.
175. Bachmanov, A.A., D.R. Reed, G.K. Beauchamp, and M.G. Tordoff, *Food intake, water intake, and drinking spout side preference of 28 mouse strains*. Behav Genet, 2002. 32(6): p. 435-43.
176. Chacko, V.P., F. Aresta, S.M. Chacko, and R.G. Weiss, *MRI/MRS assessment of in vivo murine cardiac metabolism, morphology, and function at physiological heart rates*. Am J Physiol Heart Circ Physiol, 2000. 279(5): p. H2218-24.
177. Hoppeler, H. and M. Vogt, *Muscle tissue adaptations to hypoxia*. J Exp Biol, 2001. 204(Pt 18): p. 3133-9.
178. MacDougall, J.D., H.J. Green, J.R. Sutton, G. Coates, A. Cymerman, P. Young, and C.S. Houston, *Operation Everest II: structural adaptations in skeletal muscle in response to extreme simulated altitude*. Acta Physiol Scand, 1991. 142(3): p. 421-7.
179. Deveci, D., J.M. Marshall, and S. Egginton, *Chronic hypoxia induces prolonged angiogenesis in skeletal muscles of rat*. Exp Physiol, 2002. 87(3): p. 287-91.
180. Rose, M.S., C.S. Houston, C.S. Fulco, G. Coates, J.R. Sutton, and A. Cymerman, *Operation Everest. II: Nutrition and body composition*. J Appl Physiol, 1988. 65(6): p. 2545-51.
181. Westerterp, K.R., E.P. Meijer, M. Rubbens, P. Robach, and J.P. Richalet, *Operation Everest III: energy and water balance*. Pflugers Arch, 2000. 439(4): p. 483-8.
182. Westerterp-Plantenga, M.S., K.R. Westerterp, M. Rubbens, C.R. Verwegen, J.P. Richelet, and B. Gardette, *Appetite at "high altitude" [Operation Everest III (Comex-'97)]: a simulated ascent of Mount Everest*. J Appl Physiol, 1999. 87(1): p. 391-9.
183. McClelland, G.B., P.W. Hochachka, and J.M. Weber, *Effect of high-altitude acclimation on NEFA turnover and lipid utilization during exercise in rats*. Am J Physiol, 1999. 277(6 Pt 1): p. E1095-102.
184. McClelland, G.B. and G.A. Brooks, *Changes in MCT 1, MCT 4, and LDH expression are tissue specific in rats after long-term hypobaric hypoxia*. J Appl Physiol, 2002. 92(4): p. 1573-84.
185. Hislop, A. and L. Reid, *New findings in pulmonary arteries of rats with hypoxia-induced pulmonary hypertension*. Br J Exp Pathol, 1976. 57(5): p. 542-54.
186. Reeves, J.T., B.M. Groves, J.R. Sutton, P.D. Wagner, A. Cymerman, M.K. Malconian, P.B. Rock, P.M. Young, and C.S. Houston, *Operation Everest II:*

preservation of cardiac function at extreme altitude. J Appl Physiol, 1987. 63(2): p. 531-9.
187. Clark, D.R. and P. Smith, *Capillary density and muscle fibre size in the hearts of rats subjected to stimulated high altitude*. Cardiovasc Res, 1978. 12(10): p. 578-84.
188. Levy, A.P., N.S. Levy, J. Loscalzo, A. Calderone, N. Takahashi, K.T. Yeo, G. Koren, W.S. Colucci, and M.A. Goldberg, *Regulation of vascular endothelial growth factor in cardiac myocytes*. Circ Res, 1995. 76(5): p. 758-66.
189. Fujita, Y., K. Ishino, K. Nakanishi, Y. Fujii, M. Kawada, and S. Sano, *Age-dependent vulnerability to ischemia-reperfusion injury of cyanotic myocardium in a chronic hypoxic rat model*. Acta Med Okayama, 2009. 63(5): p. 237-42.
190. Bartsch, P. and J.S. Gibbs, *Effect of altitude on the heart and the lungs*. Circulation, 2007. 116(19): p. 2191-202.
191. Simonson, T.S., Y. Yang, C.D. Huff, H. Yun, G. Qin, D.J. Witherspoon, Z. Bai, F.R. Lorenzo, J. Xing, L.B. Jorde, J.T. Prchal, and R. Ge, *Genetic evidence for high-altitude adaptation in Tibet*. Science, 2010. 329(5987): p. 72-5.
192. Banke, N.H., A.R. Wende, T.C. Leone, J.M. O'Donnell, E.D. Abel, D.P. Kelly, and E.D. Lewandowski, *Preferential oxidation of triacylglyceride-derived fatty acids in heart is augmented by the nuclear receptor PPARalpha*. Circ Res, 2010. 107(2): p. 233-41.
193. Semenza, G.L., B.H. Jiang, S.W. Leung, R. Passantino, J.P. Concordet, P. Maire, and A. Giallongo, *Hypoxia response elements in the aldolase A, enolase 1, and lactate dehydrogenase A gene promoters contain essential binding sites for hypoxia-inducible factor 1*. J Biol Chem, 1996. 271(51): p. 32529-37.
194. Perman, J.C., P. Bostrom, M. Lindbom, U. Lidberg, M. StAhlman, D. Hagg, H. Lindskog, M. Scharin Tang, E. Omerovic, L. Mattsson Hulten, A. Jeppsson, P. Petursson, J. Herlitz, G. Olivecrona, D.K. Strickland, K. Ekroos, S.O. Olofsson, and J. Boren, *The VLDL receptor promotes lipotoxicity and increases mortality in mice following an acute myocardial infarction*. J Clin Invest, 2011. 121(7): p. 2625-40.
195. Seagroves, T.N., H.E. Ryan, H. Lu, B.G. Wouters, M. Knapp, P. Thibault, K. Laderoute, and R.S. Johnson, *Transcription factor HIF-1 is a necessary mediator of the pasteur effect in mammalian cells*. Mol Cell Biol, 2001. 21(10): p. 3436-44.
196. Semenza, G.L., *Transcriptional regulation of gene expression: mechanisms and pathophysiology*. Hum Mutat, 1994. 3(3): p. 180-99.
197. Mu, J., J.T. Brozinick, Jr., O. Valladares, M. Bucan, and M.J. Birnbaum, *A role for AMP-activated protein kinase in contraction- and hypoxia-regulated glucose transport in skeletal muscle*. Mol Cell, 2001. 7(5): p. 1085-94.
198. Boardman, N., A.D. Hafstad, T.S. Larsen, D.L. Severson, and E. Aasum, *Increased O2 cost of basal metabolism and excitation-contraction coupling in hearts from type 2 diabetic mice*. Am J Physiol Heart Circ Physiol, 2009. 296(5): p. H1373-9.
199. Cole, M.A., A.J. Murray, L.E. Cochlin, L.C. Heather, S. McAleese, N.S. Knight, E. Sutton, A.A. Jamil, N. Parassol, and K. Clarke, *A high fat diet increases mitochondrial fatty acid oxidation and uncoupling to decrease efficiency in rat heart*. Basic Res Cardiol, 2011. 106(3): p. 447-57.

200. Essop, M.F., P. Razeghi, C. McLeod, M.E. Young, H. Taegtmeyer, and M.N. Sack, *Hypoxia-induced decrease of UCP3 gene expression in rat heart parallels metabolic gene switching but fails to affect mitochondrial respiratory coupling*. Biochem Biophys Res Commun, 2004. 314(2): p. 561-4.
201. Heather, L.C., M.A. Cole, J.J. Tan, L.J. Ambrose, S. Pope, A.H. Abd-Jamil, E.E. Carter, M.S. Dodd, K.K. Yeoh, C.J. Schofield, and K. Clarke, *Metabolic adaptation to chronic hypoxia in cardiac mitochondria*. Basic Res Cardiol, 2012. 107(3): p. 268.
202. Green, H.J., J.R. Sutton, A. Cymerman, P.M. Young, and C.S. Houston, *Operation Everest II: adaptations in human skeletal muscle*. J Appl Physiol, 1989. 66(5): p. 2454-61.
203. Cervos Navarro, J., R.C. Kunas, S. Sampaolo, and U. Mansmann, *Heart mitochondria in rats submitted to chronic hypoxia*. Histol Histopathol, 1999. 14(4): p. 1045-52.
204. Krishnan, J., M. Suter, R. Windak, T. Krebs, A. Felley, C. Montessuit, M. Tokarska-Schlattner, E. Aasum, A. Bogdanova, E. Perriard, J.C. Perriard, T. Larsen, T. Pedrazzini, and W. Krek, *Activation of a HIF1alpha-PPARgamma axis underlies the integration of glycolytic and lipid anabolic pathways in pathologic cardiac hypertrophy*. Cell Metab, 2009. 9(6): p. 512-24.
205. Narravula, S. and S.P. Colgan, *Hypoxia-inducible factor 1-mediated inhibition of peroxisome proliferator-activated receptor alpha expression during hypoxia*. J Immunol, 2001. 166(12): p. 7543-8.
206. Tuller, E.R., C.T. Beavers, J.R. Lou, M.A. Ihnat, D.M. Benbrook, and W.Q. Ding, *Docosahexaenoic acid inhibits superoxide dismutase 1 gene transcription in human cancer cells: the involvement of peroxisome proliferator-activated receptor alpha and hypoxia-inducible factor-2alpha signaling*. Mol Pharmacol, 2009. 76(3): p. 588-95.
207. Huss, J.M., F.H. Levy, and D.P. Kelly, *Hypoxia inhibits the peroxisome proliferator-activated receptor alpha/retinoid X receptor gene regulatory pathway in cardiac myocytes: a mechanism for O2-dependent modulation of mitochondrial fatty acid oxidation*. J Biol Chem, 2001. 276(29): p. 27605-12.
208. Lim, J.H., Y.M. Lee, Y.S. Chun, J. Chen, J.E. Kim, and J.W. Park, *Sirtuin 1 modulates cellular responses to hypoxia by deacetylating hypoxia-inducible factor 1alpha*. Mol Cell, 2010. 38(6): p. 864-78.
209. Dioum, E.M., R. Chen, M.S. Alexander, Q. Zhang, R.T. Hogg, R.D. Gerard, and J.A. Garcia, *Regulation of hypoxia-inducible factor 2alpha signaling by the stress-responsive deacetylase sirtuin 1*. Science, 2009. 324(5932): p. 1289-93.
210. Planavila, A., R. Iglesias, M. Giralt, and F. Villarroya, *Sirt1 acts in association with PPARalpha to protect the heart from hypertrophy, metabolic dysregulation, and inflammation*. Cardiovasc Res, 2011. 90(2): p. 276-84.
211. Finck, B.N., X. Han, M. Courtois, F. Aimond, J.M. Nerbonne, A. Kovacs, R.W. Gross, and D.P. Kelly, *A critical role for PPARalpha-mediated lipotoxicity in the pathogenesis of diabetic cardiomyopathy: modulation by dietary fat content*. Proc Natl Acad Sci U S A, 2003. 100(3): p. 1226-31.
212. Finck, B.N., J.J. Lehman, T.C. Leone, M.J. Welch, M.J. Bennett, A. Kovacs, X. Han, R.W. Gross, R. Kozak, G.D. Lopaschuk, and D.P. Kelly, *The cardiac phenotype induced by PPARalpha overexpression mimics that caused by diabetes mellitus*. J Clin Invest, 2002. 109(1): p. 121-30.

213. Sambandam, N., D. Morabito, C. Wagg, B.N. Finck, D.P. Kelly, and G.D. Lopaschuk, *Chronic activation of PPARalpha is detrimental to cardiac recovery after ischemia*. Am J Physiol Heart Circ Physiol, 2006. 290(1): p. H87-95.
214. Young, M.E., F.A. Laws, G.W. Goodwin, and H. Taegtmeyer, *Reactivation of peroxisome proliferator-activated receptor alpha is associated with contractile dysfunction in hypertrophied rat heart*. J Biol Chem, 2001. 276(48): p. 44390-5.
215. Rupp, H. and R. Vetter, *Sarcoplasmic reticulum function and carnitine palmitoyltransferase-1 inhibition during progression of heart failure*. Br J Pharmacol, 2000. 131(8): p. 1748-56.
216. Lionetti, V., A. Linke, M.P. Chandler, M.E. Young, M.S. Penn, S. Gupte, C. d'Agostino, T.H. Hintze, W.C. Stanley, and F.A. Recchia, *Carnitine palmitoyl transferase-I inhibition prevents ventricular remodeling and delays decompensation in pacing-induced heart failure*. Cardiovasc Res, 2005. 66(3): p. 454-61.
217. Fragasso, G., A. Palloshi, P. Puccetti, C. Silipigni, A. Rossodivita, M. Pala, G. Calori, O. Alfieri, and A. Margonato, *A randomized clinical trial of trimetazidine, a partial free fatty acid oxidation inhibitor, in patients with heart failure*. J Am Coll Cardiol, 2006. 48(5): p. 992-8.
218. Morgan, E.E., J.H. Rennison, M.E. Young, T.A. McElfresh, T.A. Kung, K.Y. Tserng, B.D. Hoit, W.C. Stanley, and M.P. Chandler, *Effects of chronic activation of peroxisome proliferator-activated receptor-alpha or high-fat feeding in a rat infarct model of heart failure*. Am J Physiol Heart Circ Physiol, 2006. 290(5): p. H1899-904.
219. Wright, J.J., J. Kim, J. Buchanan, S. Boudina, S. Sena, K. Bakirtzi, O. Ilkun, H.A. Theobald, R.C. Cooksey, K.V. Kandror, and E.D. Abel, *Mechanisms for increased myocardial fatty acid utilization following short-term high-fat feeding*. Cardiovasc Res, 2009. 82(2): p. 351-60.
220. Zhang, L., J.R. Ussher, T. Oka, V.J. Cadete, C. Wagg, and G.D. Lopaschuk, *Cardiac diacylglycerol accumulation in high fat-fed mice is associated with impaired insulin-stimulated glucose oxidation*. Cardiovasc Res, 2011. 89(1): p. 148-56.
221. Wilson, C.R., M.K. Tran, K.L. Salazar, M.E. Young, and H. Taegtmeyer, *Western diet, but not high fat diet, causes derangements of fatty acid metabolism and contractile dysfunction in the heart of Wistar rats*. Biochem J, 2007. 406(3): p. 457-67.
222. Panagia, M., G.F. Gibbons, G.K. Radda, and K. Clarke, *PPAR-alpha activation required for decreased glucose uptake and increased susceptibility to injury during ischemia*. Am J Physiol Heart Circ Physiol, 2005. 288(6): p. H2677-83.
223. Chess, D.J., B. Lei, B.D. Hoit, A.M. Azimzadeh, and W.C. Stanley, *Effects of a high saturated fat diet on cardiac hypertrophy and dysfunction in response to pressure overload*. J Card Fail, 2008. 14(1): p. 82-8.
224. Christopher, B.A., H.M. Huang, J.M. Berthiaume, T.A. McElfresh, X. Chen, C.M. Croniger, R.F. Muzic, Jr., and M.P. Chandler, *Myocardial insulin resistance induced by high fat feeding in heart failure is associated with preserved contractile function*. Am J Physiol Heart Circ Physiol, 2010. 299(6): p. H1917-27.

225. Rennison, J.H., T.A. McElfresh, X. Chen, V.R. Anand, B.D. Hoit, C.L. Hoppel, and M.P. Chandler, *Prolonged exposure to high dietary lipids is not associated with lipotoxicity in heart failure*. J Mol Cell Cardiol, 2009. 46(6): p. 883-90.
226. Pilz, S., H. Scharnagl, B. Tiran, B. Wellnitz, U. Seelhorst, B.O. Boehm, and W. Marz, *Elevated plasma free fatty acids predict sudden cardiac death: a 6.85-year follow-up of 3315 patients after coronary angiography*. Eur Heart J, 2007. 28(22): p. 2763-9.
227. Unger, R.H. and L. Orci, *Lipotoxic diseases of nonadipose tissues in obesity*. Int J Obes Relat Metab Disord, 2000. 24 Suppl 4: p. S28-32.
228. Raher, M.J., H.B. Thibault, E.S. Buys, D. Kuruppu, N. Shimizu, A.L. Brownell, S.L. Blake, J. Rieusset, M. Kaneki, G. Derumeaux, M.H. Picard, K.D. Bloch, and M. Scherrer-Crosbie, *A short duration of high-fat diet induces insulin resistance and predisposes to adverse left ventricular remodeling after pressure overload*. Am J Physiol Heart Circ Physiol, 2008. 295(6): p. H2495-502.
229. Medrikova, D., Z.M. Jilkova, K. Bardova, P. Janovska, M. Rossmeisl, and J. Kopecky, *Sex differences during the course of diet-induced obesity in mice: adipose tissue expandability and glycemic control*. Int J Obes (Lond), 2011.
230. Preitner, F., N. Mody, T.E. Graham, O.D. Peroni, and B.B. Kahn, *Long-term Fenretinide treatment prevents high-fat diet-induced obesity, insulin resistance, and hepatic steatosis*. Am J Physiol Endocrinol Metab, 2009. 297(6): p. E1420-9.
231. Listenberger, L.L., X. Han, S.E. Lewis, S. Cases, R.V. Farese, Jr., D.S. Ory, and J.E. Schaffer, *Triglyceride accumulation protects against fatty acid-induced lipotoxicity*. Proc Natl Acad Sci U S A, 2003. 100(6): p. 3077-82.
232. Holness, M.J., A. Kraus, R.A. Harris, and M.C. Sugden, *Targeted upregulation of pyruvate dehydrogenase kinase (PDK)-4 in slow-twitch skeletal muscle underlies the stable modification of the regulatory characteristics of PDK induced by high-fat feeding*. Diabetes, 2000. 49(5): p. 775-81.
233. Burkart, E.M., N. Sambandam, X. Han, R.W. Gross, M. Courtois, C.M. Gierasch, K. Shoghi, M.J. Welch, and D.P. Kelly, *Nuclear receptors PPARbeta/delta and PPARalpha direct distinct metabolic regulatory programs in the mouse heart*. J Clin Invest, 2007. 117(12): p. 3930-9.
234. Belanger, A.J., Z. Luo, K.A. Vincent, G.Y. Akita, S.H. Cheng, R.J. Gregory, and C. Jiang, *Hypoxia-inducible factor 1 mediates hypoxia-induced cardiomyocyte lipid accumulation by reducing the DNA binding activity of peroxisome proliferator-activated receptor alpha/retinoid X receptor*. Biochem Biophys Res Commun, 2007. 364(3): p. 567-72.
235. Holloway, C.J., L.E. Cochlin, Y. Emmanuel, A. Murray, I. Codreanu, L.M. Edwards, C. Szmigielski, D.J. Tyler, N.S. Knight, B.K. Saxby, B. Lambert, C. Thompson, S. Neubauer, and K. Clarke, *A high-fat diet impairs cardiac high-energy phosphate metabolism and cognitive function in healthy human subjects*. Am J Clin Nutr, 2011. 93(4): p. 748-55.
236. Edwards, L.M., A.J. Murray, C.J. Holloway, E.E. Carter, G.J. Kemp, I. Codreanu, H. Brooker, D.J. Tyler, P.A. Robbins, and K. Clarke, *Short-term consumption of a high-fat diet impairs whole-body efficiency and cognitive function in sedentary men*. Faseb J, 2011. 25(3): p. 1088-96.

237. Zhang, L., J.R. Ussher, T. Oka, V.J. Cadete, C. Wagg, and G.D. Lopaschuk, *Cardiac diacylglycerol accumulation in high fat-fed mice is associated with impaired insulin-stimulated glucose oxidation*. Cardiovasc Res, 2010. 89(1): p. 148-56.
238. How, O.J., E. Aasum, S. Kunnathu, D.L. Severson, E.S. Myhre, and T.S. Larsen, *Influence of substrate supply on cardiac efficiency, as measured by pressure-volume analysis in ex vivo mouse hearts*. Am J Physiol Heart Circ Physiol, 2005. 288(6): p. H2979-85.
239. Mjos, O.D., *Effect of free fatty acids on myocardial function and oxygen consumption in intact dogs*. J Clin Invest, 1971. 50(7): p. 1386-9.
240. Challoner, D.R. and D. Steinberg, *Effect of free fatty acid on the oxygen consumption of perfused rat heart*. Am J Physiol, 1966. 210(2): p. 280-6.
241. Ray, J., F. Noll, J. Daut, and P.J. Hanley, *Long-chain fatty acids increase basal metabolism and depolarize mitochondria in cardiac muscle cells*. Am J Physiol Heart Circ Physiol, 2002. 282(4): p. H1495-501.
242. Murray, A.J., M.A. Cole, C.A. Lygate, C.A. Carr, D.J. Stuckey, S.E. Little, S. Neubauer, and K. Clarke, *Increased mitochondrial uncoupling proteins, respiratory uncoupling and decreased efficiency in the chronically infarcted rat heart*. J Mol Cell Cardiol, 2008. 44(4): p. 694-700.
243. Scheuermann-Freestone, M., P.L. Madsen, D. Manners, A.M. Blamire, R.E. Buckingham, P. Styles, G.K. Radda, S. Neubauer, and K. Clarke, *Abnormal cardiac and skeletal muscle energy metabolism in patients with type 2 diabetes*. Circulation, 2003. 107(24): p. 3040-6.
244. Saddik, M. and G.D. Lopaschuk, *Myocardial triglyceride turnover during reperfusion of isolated rat hearts subjected to a transient period of global ischemia*. J Biol Chem, 1992. 267(6): p. 3825-31.
245. Myrmel, T., K. Forsdahl, and T.S. Larsen, *Triacylglycerol metabolism in hypoxic, glucose-deprived rat cardiomyocytes*. J Mol Cell Cardiol, 1992. 24(8): p. 855-68.
246. Chou, C.J., M.C. Cha, D.W. Jung, C.N. Boozer, S.A. Hashim, and F.X. Pi-Sunyer, *High-fat diet feeding elevates skeletal muscle uncoupling protein 3 levels but not its activity in rats*. Obes Res, 2001. 9(5): p. 313-9.
247. Marfella, R., M. D'Amico, C. Di Filippo, E. Piegari, F. Nappo, K. Esposito, L. Berrino, F. Rossi, and D. Giugliano, *Myocardial infarction in diabetic rats: role of hyperglycaemia on infarct size and early expression of hypoxia-inducible factor 1*. Diabetologia, 2002. 45(8): p. 1172-81.
248. Marfella, R., K. Esposito, F. Nappo, M. Siniscalchi, F.C. Sasso, M. Portoghese, M.P. Di Marino, A. Baldi, S. Cuzzocrea, C. Di Filippo, G. Barboso, F. Baldi, F. Rossi, M. D'Amico, and D. Giugliano, *Expression of angiogenic factors during acute coronary syndromes in human type 2 diabetes*. Diabetes, 2004. 53(9): p. 2383-91.
249. How, O.J., E. Aasum, D.L. Severson, W.Y. Chan, M.F. Essop, and T.S. Larsen, *Increased myocardial oxygen consumption reduces cardiac efficiency in diabetic mice*. Diabetes, 2006. 55(2): p. 466-73.
250. Larsen, T.S. and E. Aasum, *Metabolic (in)flexibility of the diabetic heart*. Cardiovasc Drugs Ther, 2008. 22(2): p. 91-5.
251. Chou, E., I. Suzuma, K.J. Way, D. Opland, A.C. Clermont, K. Naruse, K. Suzuma, N.L. Bowling, C.J. Vlahos, L.P. Aiello, and G.L. King, *Decreased cardiac expression of vascular endothelial growth factor and its receptors in*

insulin-resistant and diabetic States: a possible explanation for impaired collateral formation in cardiac tissue. Circulation, 2002. 105(3): p. 373-9.
252. Watanabe, K., H. Fujii, T. Takahashi, M. Kodama, Y. Aizawa, Y. Ohta, T. Ono, G. Hasegawa, M. Naito, T. Nakajima, Y. Kamijo, F.J. Gonzalez, and T. Aoyama, *Constitutive regulation of cardiac fatty acid metabolism through peroxisome proliferator-activated receptor alpha associated with age-dependent cardiac toxicity*. J Biol Chem, 2000. 275(29): p. 22293-9.
253. Aoyama, T., J.M. Peters, N. Iritani, T. Nakajima, K. Furihata, T. Hashimoto, and F.J. Gonzalez, *Altered constitutive expression of fatty acid-metabolizing enzymes in mice lacking the peroxisome proliferator-activated receptor alpha (PPARalpha)*. J Biol Chem, 1998. 273(10): p. 5678-84.
254. Campbell, F.M., R. Kozak, A. Wagner, J.Y. Altarejos, J.R. Dyck, D.D. Belke, D.L. Severson, D.P. Kelly, and G.D. Lopaschuk, *A role for peroxisome proliferator-activated receptor alpha (PPARalpha) in the control of cardiac malonyl-CoA levels: reduced fatty acid oxidation rates and increased glucose oxidation rates in the hearts of mice lacking PPARalpha are associated with higher concentrations of malonyl-CoA and reduced expression of malonyl-CoA decarboxylase*. J Biol Chem, 2002. 277(6): p. 4098-103.
255. Hafstad, A.D., A.M. Khalid, M. Hagve, T. Lund, T.S. Larsen, D.L. Severson, K. Clarke, R.K. Berge, and E. Aasum, *Cardiac peroxisome proliferator-activated receptor-alpha activation causes increased fatty acid oxidation, reducing efficiency and post-ischaemic functional loss*. Cardiovasc Res, 2009. 83(3): p. 519-26.
256. Luptak, I., J.A. Balschi, Y. Xing, T.C. Leone, D.P. Kelly, and R. Tian, *Decreased contractile and metabolic reserve in peroxisome proliferator-activated receptor-alpha-null hearts can be rescued by increasing glucose transport and utilization*. Circulation, 2005. 112(15): p. 2339-46.
257. Yue, T.L., W. Bao, B.M. Jucker, J.L. Gu, A.M. Romanic, P.J. Brown, J. Cui, D.T. Thudium, R. Boyce, C.L. Burns-Kurtis, R.C. Mirabile, K. Aravindhan, and E.H. Ohlstein, *Activation of peroxisome proliferator-activated receptor-alpha protects the heart from ischemia/reperfusion injury*. Circulation, 2003. 108(19): p. 2393-9.
258. Smeets, P.J., B.E. Teunissen, P.H. Willemsen, F.A. van Nieuwenhoven, A.E. Brouns, B.J. Janssen, J.P. Cleutjens, B. Staels, G.J. van der Vusse, and M. van Bilsen, *Cardiac hypertrophy is enhanced in PPAR alpha-/- mice in response to chronic pressure overload*. Cardiovasc Res, 2008. 78(1): p. 79-89.
259. Gildea, O., *The role of PPARα in adaptation to hypoxia*, 2012, Biochemistry Part II Project, University of Oxford.
260. Atherton, H.J., N.J. Bailey, W. Zhang, J. Taylor, H. Major, J. Shockcor, K. Clarke, and J.L. Griffin, *A combined 1H-NMR spectroscopy- and mass spectrometry-based metabolomic study of the PPAR-alpha null mutant mouse defines profound systemic changes in metabolism linked to the metabolic syndrome*. Physiol Genomics, 2006. 27(2): p. 178-86.
261. Randle, P.J., *Regulatory interactions between lipids and carbohydrates: the glucose fatty acid cycle after 35 years*. Diabetes Metab Rev, 1998. 14(4): p. 263-83.
262. Gelinas, R., F. Labarthe, B. Bouchard, J. Mc Duff, G. Charron, M.E. Young, and C. Des Rosiers, *Alterations in carbohydrate metabolism and its regulation in PPARalpha null mouse hearts*. Am J Physiol Heart Circ Physiol, 2008. 294(4): p. H1571-80.

263. Lee, S.S., T. Pineau, J. Drago, E.J. Lee, J.W. Owens, D.L. Kroetz, P.M. Fernandez-Salguero, H. Westphal, and F.J. Gonzalez, *Targeted disruption of the alpha isoform of the peroxisome proliferator-activated receptor gene in mice results in abolishment of the pleiotropic effects of peroxisome proliferators*. Mol Cell Biol, 1995. 15(6): p. 3012-22.
264. Muoio, D.M., P.S. MacLean, D.B. Lang, S. Li, J.A. Houmard, J.M. Way, D.A. Winegar, J.C. Corton, G.L. Dohm, and W.E. Kraus, *Fatty acid homeostasis and induction of lipid regulatory genes in skeletal muscles of peroxisome proliferator-activated receptor (PPAR) alpha knock-out mice. Evidence for compensatory regulation by PPAR delta*. J Biol Chem, 2002. 277(29): p. 26089-97.
265. Djouadi, F., C.J. Weinheimer, J.E. Saffitz, C. Pitchford, J. Bastin, F.J. Gonzalez, and D.P. Kelly, *A gender-related defect in lipid metabolism and glucose homeostasis in peroxisome proliferator- activated receptor alpha-deficient mice*. J Clin Invest, 1998. 102(6): p. 1083-91.
266. Lorell, B.H. and B.A. Carabello, *Left ventricular hypertrophy: pathogenesis, detection, and prognosis*. Circulation, 2000. 102(4): p. 470-9.
267. Leone, T.C., C.J. Weinheimer, and D.P. Kelly, *A critical role for the peroxisome proliferator-activated receptor alpha (PPARalpha) in the cellular fasting response: the PPARalpha-null mouse as a model of fatty acid oxidation disorders*. Proc Natl Acad Sci U S A, 1999. 96(13): p. 7473-8.
268. Zhou, Y.T., P. Grayburn, A. Karim, M. Shimabukuro, M. Higa, D. Baetens, L. Orci, and R.H. Unger, *Lipotoxic heart disease in obese rats: implications for human obesity*. Proc Natl Acad Sci U S A, 2000. 97(4): p. 1784-9.
269. Sharma, S., J.V. Adrogue, L. Golfman, I. Uray, J. Lemm, K. Youker, G.P. Noon, O.H. Frazier, and H. Taegtmeyer, *Intramyocardial lipid accumulation in the failing human heart resembles the lipotoxic rat heart*. Faseb J, 2004. 18(14): p. 1692-700.
270. Guellich, A., T. Damy, Y. Lecarpentier, M. Conti, V. Claes, J.L. Samuel, J. Quillard, J.L. Hebert, T. Pineau, and C. Coirault, *Role of oxidative stress in cardiac dysfunction of PPARalpha-/- mice*. Am J Physiol Heart Circ Physiol, 2007. 293(1): p. H93-H102.
271. Chen, R., E.M. Dioum, R.T. Hogg, R.D. Gerard, and J.A. Garcia, *Hypoxia increases sirtuin 1 expression in a hypoxia-inducible factor-dependent manner*. J Biol Chem, 2011. 286(16): p. 13869-78.
272. Hayashida, S., A. Arimoto, Y. Kuramoto, T. Kozako, S. Honda, H. Shimeno, and S. Soeda, *Fasting promotes the expression of SIRT1, an NAD+ -dependent protein deacetylase, via activation of PPARalpha in mice*. Mol Cell Biochem, 2010. 339(1-2): p. 285-92.
273. Semenza, G.L., *HIF-1 and mechanisms of hypoxia sensing*. Curr Opin Cell Biol, 2001. 13(2): p. 167-71.
274. Semenza, G.L., *Involvement of oxygen-sensing pathways in physiologic and pathologic erythropoiesis*. Blood, 2009. 114(10): p. 2015-9.
275. Semenza, G.L., *Transcriptional regulation by hypoxia-inducible factor 1 molecular mechanisms of oxygen homeostasis*. Trends Cardiovasc Med, 1996. 6(5): p. 151-7.
276. Aragones, J., M. Schneider, K. Van Geyte, P. Fraisl, T. Dresselaers, M. Mazzone, R. Dirkx, S. Zacchigna, H. Lemieux, N.H. Jeoung, D. Lambrechts, T. Bishop, P. Lafuste, A. Diez-Juan, S.K. Harten, P. Van Noten, K. De Bock, C. Willam, M. Tjwa, A. Grosfeld, R. Navet, L. Moons, T. Vandendriessche,

C. Deroose, B. Wijeyekoon, J. Nuyts, B. Jordan, R. Silasi-Mansat, F. Lupu, M. Dewerchin, C. Pugh, P. Salmon, L. Mortelmans, B. Gallez, F. Gorus, J. Buyse, F. Sluse, R.A. Harris, E. Gnaiger, P. Hespel, P. Van Hecke, F. Schuit, P. Van Veldhoven, P. Ratcliffe, M. Baes, P. Maxwell, and P. Carmeliet, *Deficiency or inhibition of oxygen sensor Phd1 induces hypoxia tolerance by reprogramming basal metabolism*. Nat Genet, 2008. 40(2): p. 170-80.

277. Jewell, U.R., I. Kvietikova, A. Scheid, C. Bauer, R.H. Wenger, and M. Gassmann, *Induction of HIF-1alpha in response to hypoxia is instantaneous*. Faseb J, 2001. 15(7): p. 1312-4.
278. Claycomb, W.C., N.A. Lanson, Jr., B.S. Stallworth, D.B. Egeland, J.B. Delcarpio, A. Bahinski, and N.J. Izzo, Jr., *HL-1 cells: a cardiac muscle cell line that contracts and retains phenotypic characteristics of the adult cardiomyocyte*. Proc Natl Acad Sci U S A, 1998. 95(6): p. 2979-84.
279. White, S.M., P.E. Constantin, and W.C. Claycomb, *Cardiac physiology at the cellular level: use of cultured HL-1 cardiomyocytes for studies of cardiac muscle cell structure and function*. Am J Physiol Heart Circ Physiol, 2004. 286(3): p. H823-9.
280. Barba, I., L. Chavarria, M. Ruiz-Meana, M. Mirabet, E. Agullo, and D. Garcia-Dorado, *Effect of intracellular lipid droplets on cytosolic Ca2+ and cell death during ischaemia-reperfusion injury in cardiomyocytes*. J Physiol, 2009. 587(Pt 6): p. 1331-41.
281. Alfarano, C., L. Sartiani, C. Nediani, E. Mannucci, A. Mugelli, E. Cerbai, and L. Raimondi, *Functional coupling of angiotensin II type 1 receptor with insulin resistance of energy substrate uptakes in immortalized cardiomyocytes (HL-1 cells)*. Br J Pharmacol, 2008. 153(5): p. 907-14.
282. Palanivel, R., M. Eguchi, I. Shuralyova, I. Coe, and G. Sweeney, *Distinct effects of short- and long-term leptin treatment on glucose and fatty acid uptake and metabolism in HL-1 cardiomyocytes*. Metabolism, 2006. 55(8): p. 1067-75.
283. Natarajan, A., S. Samadian, and S. Clark, *Coronary artery bypass surgery in elderly people*. Postgrad Med J, 2007. 83(977): p. 154-8.
284. Fraisl, P., J. Aragones, and P. Carmeliet, *Inhibition of oxygen sensors as a therapeutic strategy for ischaemic and inflammatory disease*. Nat Rev Drug Discov, 2009. 8(2): p. 139-52.
285. Tian, Y.M., K.K. Yeoh, M.K. Lee, T. Eriksson, B.M. Kessler, H.B. Kramer, M.J. Edelmann, C. Willam, C.W. Pugh, C.J. Schofield, and P.J. Ratcliffe, *Differential sensitivity of hypoxia inducible factor hydroxylation sites to hypoxia and hydroxylase inhibitors*. J Biol Chem, 2011. 286(15): p. 13041-51.
286. Epstein, A.C., J.M. Gleadle, L.A. McNeill, K.S. Hewitson, J. O'Rourke, D.R. Mole, M. Mukherji, E. Metzen, M.I. Wilson, A. Dhanda, Y.M. Tian, N. Masson, D.L. Hamilton, P. Jaakkola, R. Barstead, J. Hodgkin, P.H. Maxwell, C.W. Pugh, C.J. Schofield, and P.J. Ratcliffe, *C. elegans EGL-9 and mammalian homologs define a family of dioxygenases that regulate HIF by prolyl hydroxylation*. Cell, 2001. 107(1): p. 43-54.
287. Bernhardt, W.M., M.S. Wiesener, P. Scigalla, J. Chou, R.E. Schmieder, V. Gunzler, and K.U. Eckardt, *Inhibition of prolyl hydroxylases increases erythropoietin production in ESRD*. J Am Soc Nephrol, 2010. 21(12): p. 2151-6.

288. Hirsila, M., P. Koivunen, V. Gunzler, K.I. Kivirikko, and J. Myllyharju, *Characterization of the human prolyl 4-hydroxylases that modify the hypoxia-inducible factor*. J Biol Chem, 2003. 278(33): p. 30772-80.
289. Koivunen, P., M. Hirsila, K.I. Kivirikko, and J. Myllyharju, *The length of peptide substrates has a marked effect on hydroxylation by the hypoxia-inducible factor prolyl 4-hydroxylases*. J Biol Chem, 2006. 281(39): p. 28712-20.
290. Graven, K.K., D. Bellur, B.D. Klahn, S.L. Lowrey, and E. Amberger, *HIF-2alpha regulates glyceraldehyde-3-phosphate dehydrogenase expression in endothelial cells*. Biochim Biophys Acta, 2003. 1626(1-3): p. 10-8.
291. Stiehl, D.P., R. Wirthner, J. Koditz, P. Spielmann, G. Camenisch, and R.H. Wenger, *Increased prolyl 4-hydroxylase domain proteins compensate for decreased oxygen levels. Evidence for an autoregulatory oxygen-sensing system*. J Biol Chem, 2006. 281(33): p. 23482-91.
292. Kong, X., B. Alvarez-Castelao, Z. Lin, J.G. Castano, and J. Caro, *Constitutive/hypoxic degradation of HIF-alpha proteins by the proteasome is independent of von Hippel Lindau protein ubiquitylation and the transactivation activity of the protein*. J Biol Chem, 2007. 282(21): p. 15498-505.
293. Ginouves, A., K. Ilc, N. Macias, J. Pouyssegur, and E. Berra, *PHDs overactivation during chronic hypoxia "desensitizes" HIFalpha and protects cells from necrosis*. Proc Natl Acad Sci U S A, 2008. 105(12): p. 4745-50.
294. Demidenko, Z.N., A. Rapisarda, M. Garayoa, P. Giannakakou, G. Melillo, and M.V. Blagosklonny, *Accumulation of hypoxia-inducible factor-1alpha is limited by transcription-dependent depletion*. Oncogene, 2005. 24(30): p. 4829-38.
295. Bracken, C.P., A.O. Fedele, S. Linke, W. Balrak, K. Lisy, M.L. Whitelaw, and D.J. Peet, *Cell-specific regulation of hypoxia-inducible factor (HIF)-1alpha and HIF-2alpha stabilization and transactivation in a graded oxygen environment*. J Biol Chem, 2006. 281(32): p. 22575-85.
296. Wiesener, M.S., J.S. Jurgensen, C. Rosenberger, C.K. Scholze, J.H. Horstrup, C. Warnecke, S. Mandriota, I. Bechmann, U.A. Frei, C.W. Pugh, P.J. Ratcliffe, S. Bachmann, P.H. Maxwell, and K.U. Eckardt, *Widespread hypoxia-inducible expression of HIF-2alpha in distinct cell populations of different organs*. Faseb J, 2003. 17(2): p. 271-3.
297. Raval, R.R., K.W. Lau, M.G. Tran, H.M. Sowter, S.J. Mandriota, J.L. Li, C.W. Pugh, P.H. Maxwell, A.L. Harris, and P.J. Ratcliffe, *Contrasting properties of hypoxia-inducible factor 1 (HIF-1) and HIF-2 in von Hippel-Lindau-associated renal cell carcinoma*. Mol Cell Biol, 2005. 25(13): p. 5675-86.
298. Iyer, N.V., L.E. Kotch, F. Agani, S.W. Leung, E. Laughner, R.H. Wenger, M. Gassmann, J.D. Gearhart, A.M. Lawler, A.Y. Yu, and G.L. Semenza, *Cellular and developmental control of O2 homeostasis by hypoxia-inducible factor 1 alpha*. Genes Dev, 1998. 12(2): p. 149-62.
299. Compernolle, V., K. Brusselmans, T. Acker, P. Hoet, M. Tjwa, H. Beck, S. Plaisance, Y. Dor, E. Keshet, F. Lupu, B. Nemery, M. Dewerchin, P. Van Veldhoven, K. Plate, L. Moons, D. Collen, and P. Carmeliet, *Loss of HIF-2alpha and inhibition of VEGF impair fetal lung maturation, whereas treatment with VEGF prevents fatal respiratory distress in premature mice*. Nat Med, 2002. 8(7): p. 702-10.

300. Peng, J., L. Zhang, L. Drysdale, and G.H. Fong, *The transcription factor EPAS-1/hypoxia-inducible factor 2alpha plays an important role in vascular remodeling*. Proc Natl Acad Sci U S A, 2000. 97(15): p. 8386-91.
301. Behrooz, A. and F. Ismail-Beigi, *Dual control of glut1 glucose transporter gene expression by hypoxia and by inhibition of oxidative phosphorylation*. J Biol Chem, 1997. 272(9): p. 5555-62.
302. Elvidge, G.P., L. Glenny, R.J. Appelhoff, P.J. Ratcliffe, J. Ragoussis, and J.M. Gleadle, *Concordant regulation of gene expression by hypoxia and 2-oxoglutarate-dependent dioxygenase inhibition: the role of HIF-1alpha, HIF-2alpha, and other pathways*. J Biol Chem, 2006. 281(22): p. 15215-26.
303. Asikainen, T.M. and C.W. White, *HIF stabilizing agents: shotgun or scalpel?* Am J Physiol Lung Cell Mol Physiol, 2007. 293(3): p. L555-6.
304. Groenman, F.A., M. Rutter, J. Wang, I. Caniggia, D. Tibboel, and M. Post, *Effect of chemical stabilizers of hypoxia-inducible factors on early lung development*. Am J Physiol Lung Cell Mol Physiol, 2007. 293(3): p. L557-67.
305. *Fibrogen Anemia Clinical Studies*. Available from: www.fibrogen.com/Anemia_Clinical_Studies.
306. Urquilla P, F.A., Oksanen S, Leigh S, Turtle E, Flippin L, Brenner M, Muthukrishnan E, Fourney P, Lin A, Yeowell D, Molineaux C, *Upregulation of endogenous EPO in healthy subjects by inhibition of HIF-PH [Abstract]*. J Am Soc Nephrol, 2004. 15: p. 546A.
307. Wiecek A, P.G., Ignacy W, Schmidt R, Neumayer HH, Scigalla P, Urquilla P, *Pharmacological stabilization of HIF increases hemoglobin concentration in anemic patients with chronic kidney disease [Abstract]*. Nephrol Dial Transplant, 2005. 195.
308. Hsieh, M.M., N.S. Linde, A. Wynter, M. Metzger, C. Wong, I. Langsetmo, A. Lin, R. Smith, G.P. Rodgers, R.E. Donahue, S.J. Klaus, and J.F. Tisdale, *HIF prolyl hydroxylase inhibition results in endogenous erythropoietin induction, erythrocytosis, and modest fetal hemoglobin expression in rhesus macaques*. Blood, 2007. 110(6): p. 2140-7.
309. Holscher, M., K. Schafer, S. Krull, K. Farhat, A. Hesse, M. Silter, Y. Lin, B.J. Pichler, P. Thistlethwaite, A. El-Armouche, L.S. Maier, D.M. Katschinski, and A. Zieseniss, *Unfavourable consequences of chronic cardiac HIF-1alpha stabilization*. Cardiovasc Res, 2012. 94(1): p. 77-86.
310. Czibik, G., J. Sagave, V. Martinov, B. Ishaq, M. Sohl, I. Sefland, H. Carlsen, F. Farnebo, R. Blomhoff, and G. Valen, *Cardioprotection by hypoxia-inducible factor 1 alpha transfection in skeletal muscle is dependent on haem oxygenase activity in mice*. Cardiovasc Res, 2009. 82(1): p. 107-14.
311. Gurd, B.J., Y. Yoshida, J.T. McFarlan, G.P. Holloway, C.D. Moyes, G.J. Heigenhauser, L. Spriet, and A. Bonen, *Nuclear SIRT1 activity, but not protein content, regulates mitochondrial biogenesis in rat and human skeletal muscle*. Am J Physiol Regul Integr Comp Physiol, 2011. 301(1): p. R67-75.
312. Gilde, A.J. and M. Van Bilsen, *Peroxisome proliferator-activated receptors (PPARS): regulators of gene expression in heart and skeletal muscle*. Acta Physiol Scand, 2003. 178(4): p. 425-34.
313. Holloway, G.P., C.J. Chou, J. Lally, T. Stellingwerff, A.C. Maher, O. Gavrilova, M. Haluzik, H. Alkhateeb, M.L. Reitman, and A. Bonen, *Increasing skeletal muscle fatty acid transport protein 1 (FATP1) targets fatty acids to oxidation and does not predispose mice to diet-induced insulin resistance*. Diabetologia, 2011. 54(6): p. 1457-67.

314. Opie, L.H. and O.L. Bricknell, *Role of glycolytic flux in effect of glucose in decreasing fatty-acid-induced release of lactate dehydrogenase from isolated coronary ligated rat heart*. Cardiovasc Res, 1979. 13(12): p. 693-702.
315. Ventura-Clapier, R., A. Garnier, and V. Veksler, *Energy metabolism in heart failure*. J Physiol, 2004. 555(Pt 1): p. 1-13.
316. Monge, C., N. Beraud, K. Tepp, S. Pelloux, S. Chahboun, T. Kaambre, L. Kadaja, M. Roosimaa, A. Piirsoo, Y. Tourneur, A.V. Kuznetsov, V. Saks, and E. Seppet, *Comparative analysis of the bioenergetics of adult cardiomyocytes and nonbeating HL-1 cells: respiratory chain activities, glycolytic enzyme profiles, and metabolic fluxes*. Can J Physiol Pharmacol, 2009. 87(4): p. 318-26.
317. Eimre, M., K. Paju, S. Pelloux, N. Beraud, M. Roosimaa, L. Kadaja, M. Gruno, N. Peet, E. Orlova, R. Remmelkoor, A. Piirsoo, V. Saks, and E. Seppet, *Distinct organization of energy metabolism in HL-1 cardiac cell line and cardiomyocytes*. Biochim Biophys Acta, 2008. 1777(6): p. 514-24.
318. Huss, J.M., I.P. Torra, B. Staels, V. Giguere, and D.P. Kelly, *Estrogen-related receptor alpha directs peroxisome proliferator-activated receptor alpha signaling in the transcriptional control of energy metabolism in cardiac and skeletal muscle*. Mol Cell Biol, 2004. 24(20): p. 9079-91.

APPENDICES

APPENDIX 1 – BUFFER COMPOSITIONS

Elisa Lysis buffer

25 mM tris-HCl
0.5 mM EDTA
150 mM NaCl
1% Triton X

Krebs Henseleit Buffer

118 mM sodium chloride
3.7 mM potassium chloride
1.2 mM magnesium sulphate (heptahydrate)
1.97mM calcium chloride (dihydrate)
0.5 mM EDTA disodium salt
25 mM sodium hydrogen carbonate
11 mM glucose

Palmitate and albumin containing KH buffer

Due to the hydrophobic nature of fatty acids, palmitate was prebound to albumin to allow solubility in the KH buffer. The palmitate potassium salt was soluble at 60^{o}C and was added slowly to warmed, filtered, albumin-containing KH buffer. When palmitate oxidation rates were measured, the ^{3}H-palmitate was prebound to albumin by adding to the buffer with the non-radioactive palmitate. As 1 mM palmitate contained 1 mM potassium, the concentration of KCl in the KH buffer was reduced to compensate. Free calcium concentrations were checked and adjusted to 1.85 mM prior to each experiment, to compensate for decreased free calcium due to binding to albumin and EDTA. When glycolytic rates were measured, the ^{3}H-glucose was added to the palmitate-containing KH buffer immediately prior to the experiment.

Immunoblotting agents

Lysis buffer

75 mM tris-HCl pH 6.8
3.8% SDS (w/v)
4 M urea
20% glycerol (v/v)
0.1% triton (v/v)

Laemmli loading buffer

187.5 mM tris-HCl
6% SDS (w/v)
30% glycerol (v/v)
0.003% bromophenol blue (w/v)
pH 6.8

SDS transfer buffer

48 mM tris
39 mM glycine
0.0375% SDS (w/v)
20% methanol (v/v)

TBS-Tween

0.9% NaCl (w/v)
10 mM tris-base
0.05% Tween (v/v) Sigma, USA
pH 7.4

APPENDIX 2 – PRIMARY ANTIBODIES FOR IMMUNOBLOTTING

Primary antibody	Primary antibody supplier	Dilution	Secondary antibody	Dilution
PGC1α	Santa Cruz, CA, USA	1:500	Goat anti-rabbit	1:3500
Citrate synthase	Alpha Diagnostics	1:1000	Goat anti-rabbit	1:3500
αKGDH	Santa Cruz, CA, USA	1:1000	Goat anti-rabbit	1:3500
GLUT1	Abcam, UK	1:1000	Goat anti-rabbit	1:2000
GLUT4	Gift: Dr G. Holman, University of Bath, UK	1:4000	Goat anti-rabbit	1:2000
PDK1	Cell Signalling technology	1:3000	Goat anti-rabbit	1:3500
PDK4	Abgent, UK	1:500	Goat anti-rabbit	1:3500
MCAD	Santa Cruz, CA, USA	1:500	Donkey anti-goat	1:3500
UCP3	Abcam, UK	1:2500	Goat anti-rabbit	1:3500
MTE1	Gift: Dr Stefan Alexson, Karolinska Institutet, Stockholm, Sweden	1:2000	Goat anti-rabbit	1:3500
RXRα	Santa Cruz, UK	1:1000	Goat anti-rabbit	1:3500
HIF-**1α**	Novus Biologicals	1:2000	Goat anti-rabbit	1:2000
HIF-**2α**	Novus Biologicals	1:500	Goat anti-rabbit	1:1000
SIRT1	Abcam, UK	1:2000	Goat anti-mouse	1:3500

APPENDIX 3 – PRIMER SEQUENCES

Gene	Forward and Reverse primer (**5'to 3'**)	NCBI Reference Sequence number
***PPARα**	ACTACGGAGTTCACGCATGTG	NM_011144.6
	TTGTCGTACACCAGCTTCAGC	
PPARβ/δ	TCGGGCTTCCACTACGG	NM_011145.3
	ACTGACACTTGTTGCGGTTCT	
PPARγ	GCCCTTTGGTGACTTTATGG	NM_011146.3
	CAGCAGGTTGTCTTGGATGT	
MCAD	ACTGACGCCGTTCAGATTTT	NM_007382.4
	GCTTAGTTACACGAGGGTGATG	
UCP3	GGATGCCTACAGAACCATCG	NM_009464.3
	CGTAGGTCACCATCTCAGCA	
PDK4	ACCGCATTTCTACTCGGATG	NM_013743.2
	GGGTTTCCCGTCTTTGAGTC	
VEGF	CAGGCTGCTGTAACGATGAA	NM_009505.4
	GCATTCACATCTGCTGTGCT	
BETA-ACTIN	GATCTGGCACCACACCTTCT	NM_007393.3
	GGGGTGTTGAAGGTCTCAAA	

*Primer sequence provided by Dr Daniel P. Kelly [318]

APPENDIX 4 – WESTERN BLOT IMAGES

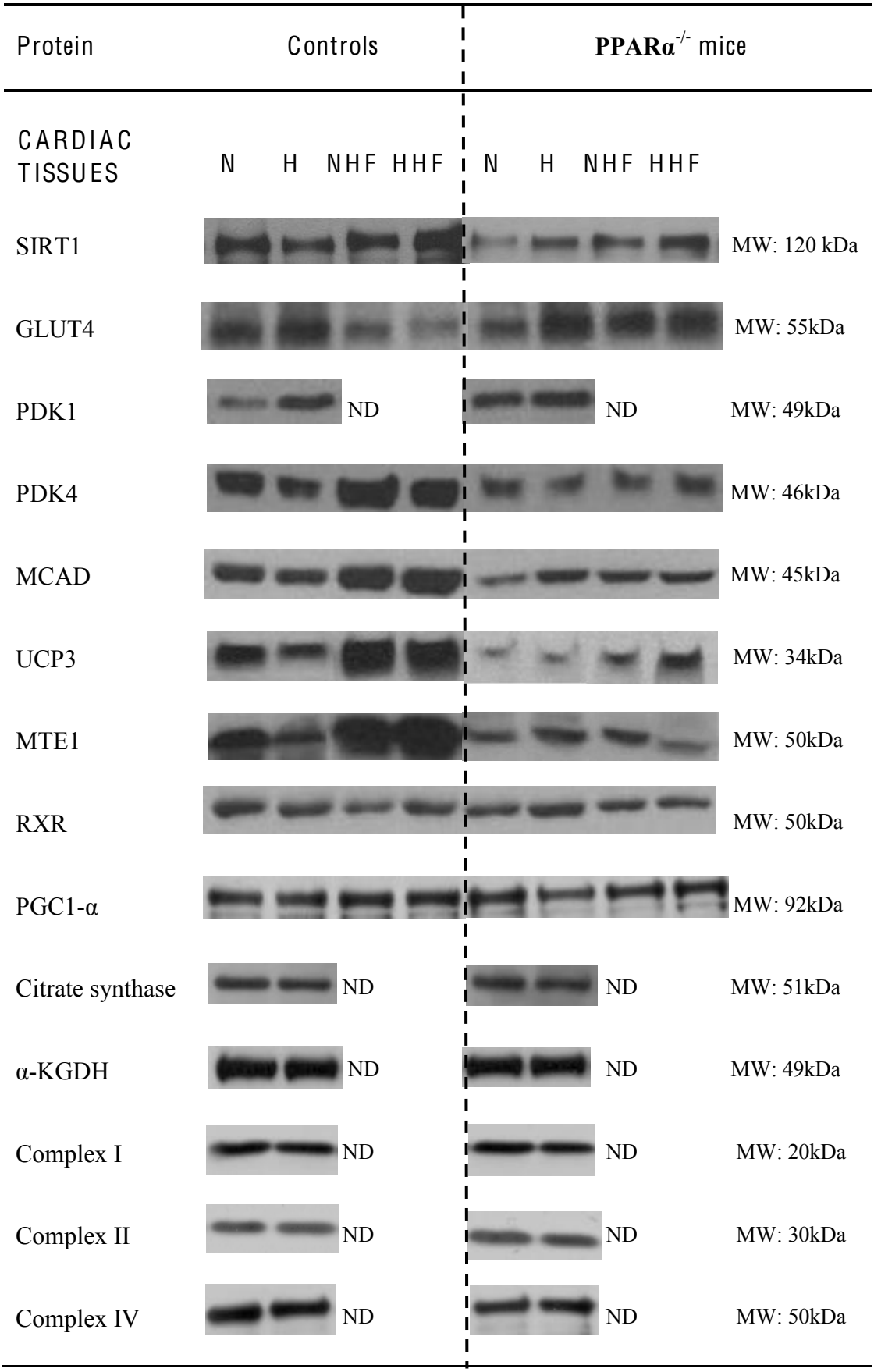

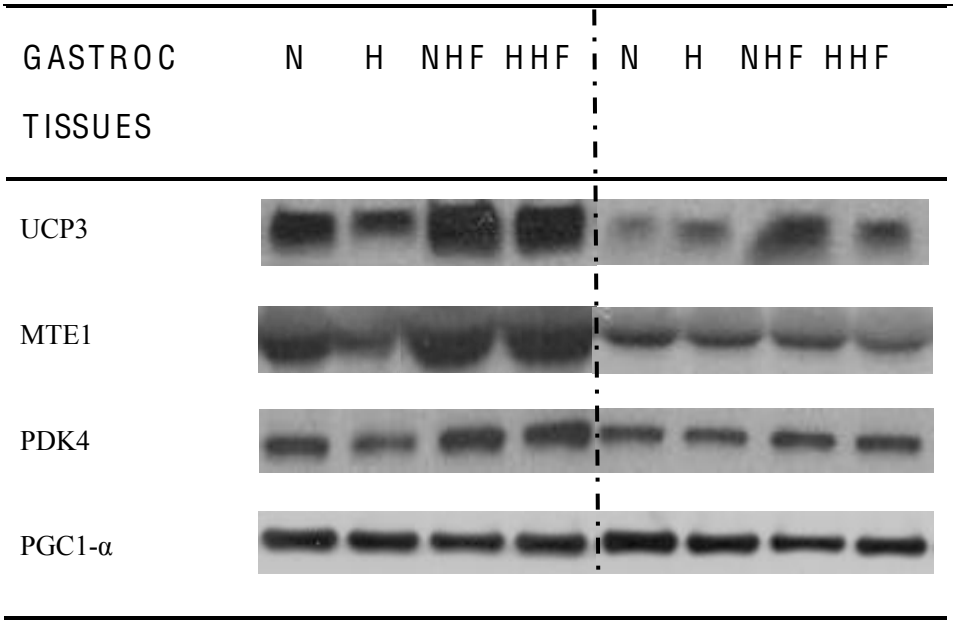

N = normoxia

H = hypoxia

NHF = high fat, normoxia

HHF = high fat, hypoxia

ND = not determined

MW = molecular weight

APPENDIX 5 – DIET COMPOSITION

Diet	Energy density (kcal/g)	Macronutrient (% total energy)		
		Fat	Protein	Carbohydrate
Chow	3.3	7.5	17.5	75
High fat	5.1	55	29	16

APPENDIX 6 – LIST OF PUBLICATIONS

Cole, M.A., A.J. Murray, L.E. Cochlin, L.C. Heather, S. McAleese, N.S. Knight, E. Sutton, A.A. Jamil, N. Parassol, and K. Clarke, *A high fat diet increases mitochondrial fatty acid oxidation and uncoupling to decrease efficiency in rat heart*. Basic Res Cardiol, 2011. 106(3): p. 447-57.

Heather, L.C., M.A. Cole, J.J. Tan, L.J. Ambrose, S. Pope, A.H. Abd-Jamil, E.E. Carter, M.S. Dodd, K.K. Yeoh, C.J. Schofield, and K. Clarke, *Metabolic adaptation to chronic hypoxia in cardiac mitochondria*. Basic Res Cardiol, 2012. 107(3): p. 268.